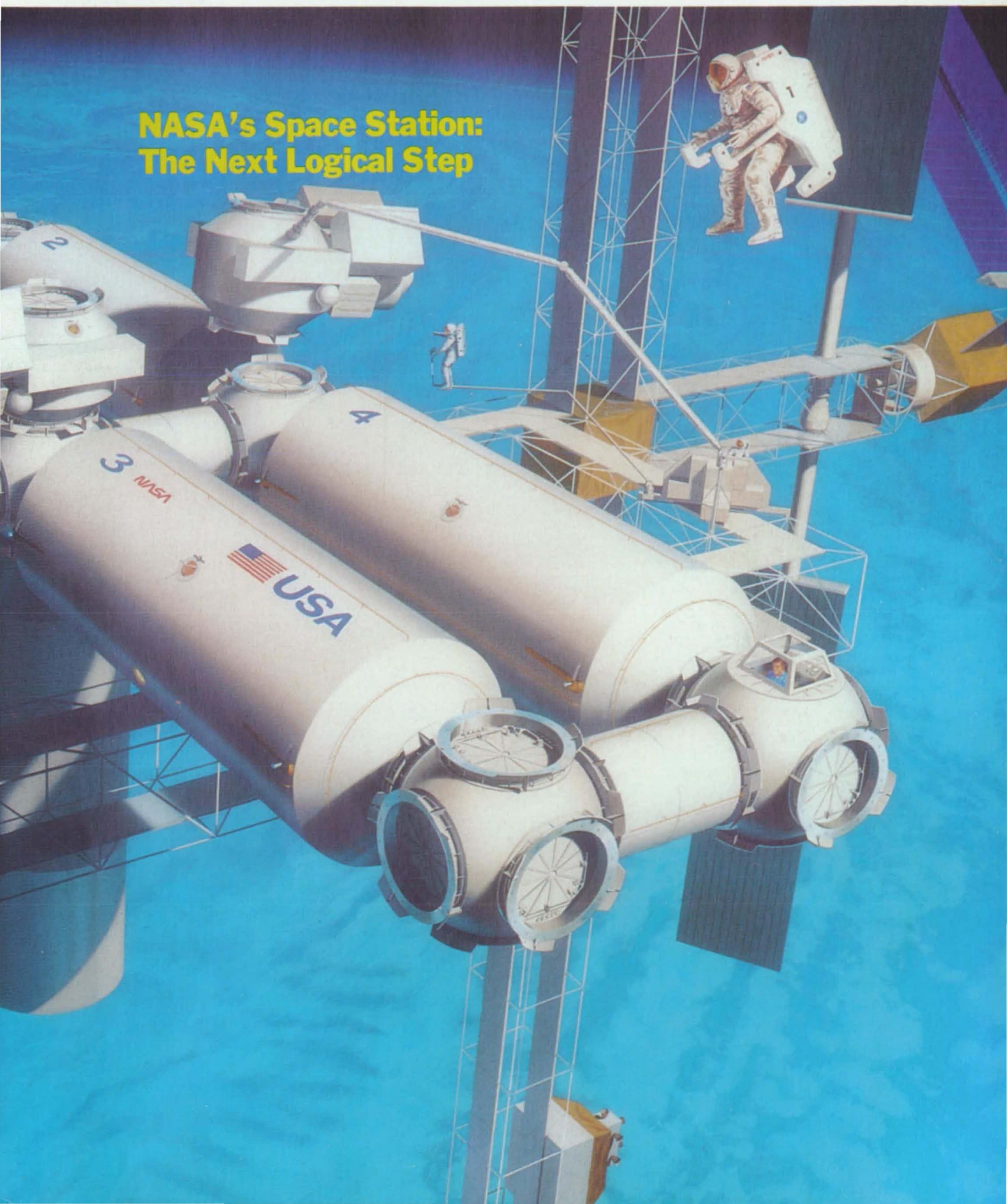


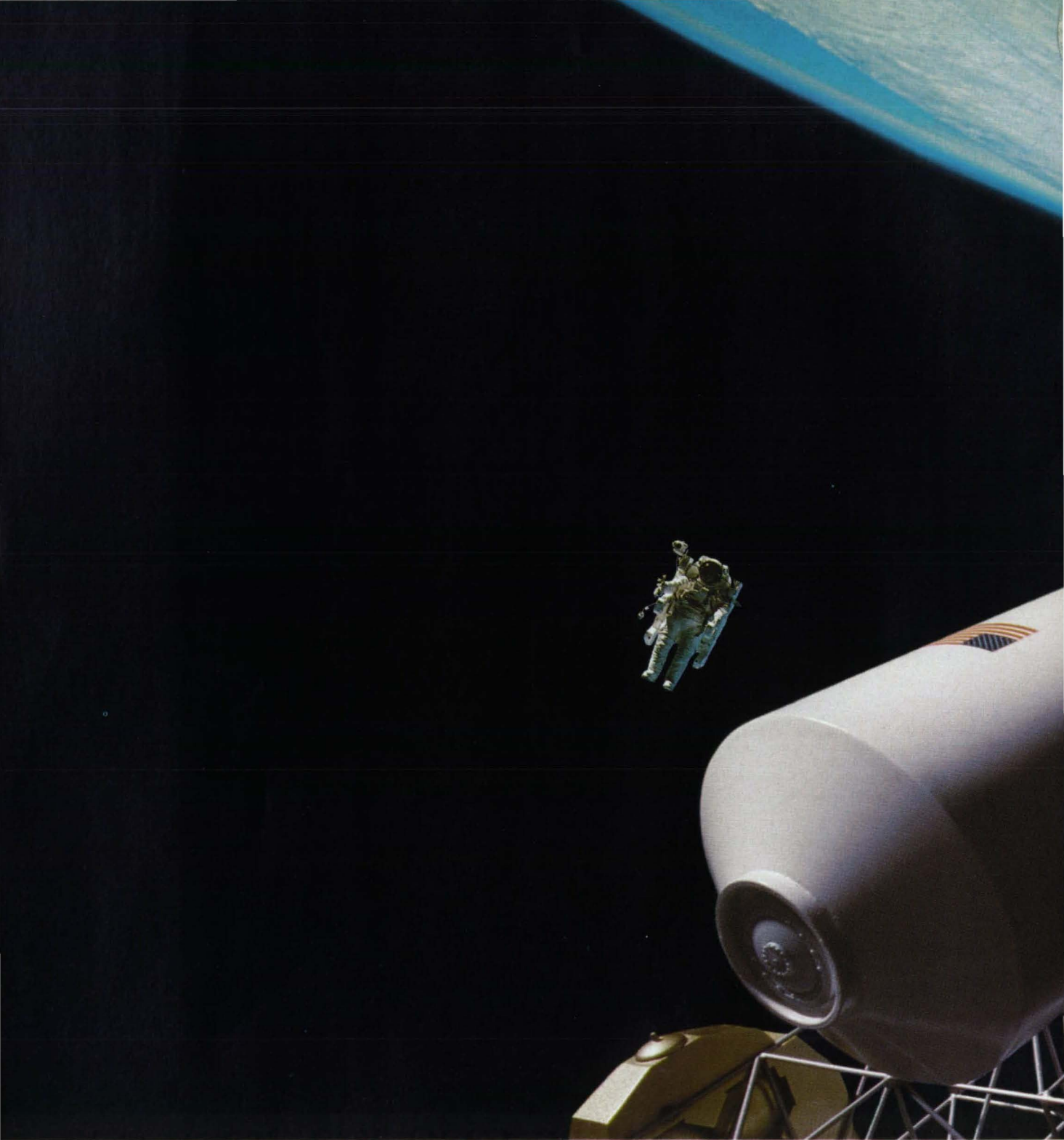
NASA Tech Briefs

National Aeronautics and
Space Administration

October 1987
Volume 11 Number 9

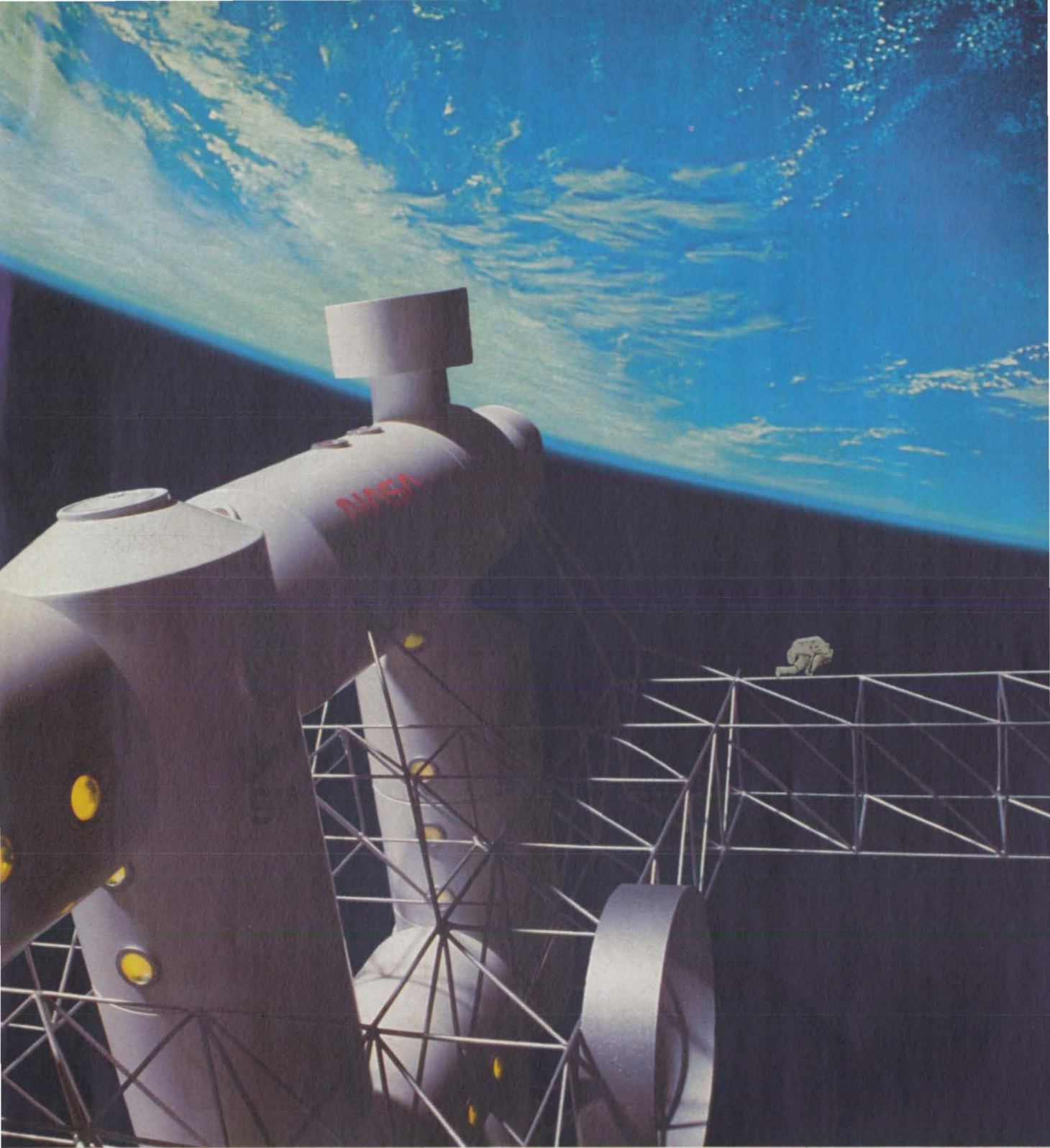
NASA's Space Station: The Next Logical Step





SOME OF THE BEST IDEAS SEEM TO COME OUT OF NOWHERE.

You might not think of space as a hotbed of scientific inquiry. But what space lacks — gravity, vibrations and an atmosphere — is precisely what makes it a superb place for research, a place to look out to the universe, back toward Mother Earth, or inside to perform tasks to be performed in the space station itself. ● That's why the NASA and companies such as Martin Marietta are designing a space station to be placed in orbit and manned by teams of scientists and technicians in the mid-1990s. ● From a point 300 miles in space, the station will be a laboratory, a



astronomy and astrophysical observatory, an assembly and manufacturing center, a satellite repair and servicing station, and a staging base for missions — both manned and unmanned — to the deeper regions of the universe. ● Martin Marietta is proud to head one of the teams that is designing the space station's modules, where astronauts will work and live over the next 20 years. ● At Martin Marietta, we apply the same creative intelligence to space technology that we bring to systems and products in defense, electronics, communications, energy, information management and materials. ● Technology that will help a lot of good ideas get off the ground.

MASTERMINDING TOMORROW'S TECHNOLOGIES














MARTIN MARIETTA

6801 ROCKLEDGE DRIVE, BETHESDA, MARYLAND 20817

SPECIAL FEATURES

Smart Robot Hands on the Ladder of Evolution	16
Mission Accomplished	109

TECHNICAL SECTION

 New Product Ideas	20
 NASA TU Services	22
 Electronic Components and Circuits	24
 Electronic Systems	42
 Physical Sciences	50
 Materials	58
 Computer Programs	66
 Mechanics	70
 Machinery	88
 Fabrication Technology	96
 Mathematics and Information Sciences	103
 Life Sciences	105
 Subject Index	106



A NASA-developed wing design featuring drooping extensions on the outboard leading edges could help reduce the number of aviation accidents caused by stalling and spinning. After extensive studies at NASA's Langley Research Center, the design is now being put to the test on a new lightweight airplane. See Mission Accomplished, page 109.

DEPARTMENTS

ON THE COVER—An artist's conception of the pressurized modules and work nodes for NASA's Space Station. For more information about the Space Station work packages, see *Editorial Notebook* on page 10. (Photo courtesy McDonnell Douglas Astronautics Company)

Editorial Notebook	10
Advertiser's Index	108

At NASA's Jet Propulsion Laboratory, smart robot hands are being developed for use in space and on earth. Built-in microprocessors are the smart hands' secret, processing sensor-derived information to increase autonomy and enhance feedback response. Dr. Antal K. Bejczy's story about JPL's smart hands begins on page 16.



This document was prepared under the sponsorship of the National Aeronautics and Space Administration. Neither Associated Business Publications Co., nor anyone acting on behalf of Associated Business Publications Co., nor the United States Government nor any person acting on behalf of the United States Government assumes any liability resulting from the use of the information contained in this document, or warrants that such use will be free from privately owned rights. The U.S. Government does not endorse any commercial product, process, or activity identified in this publication.

NASA Tech Briefs, ISSN 0145-319X, USPS 750-070, copyright © 1987 in U.S., is published monthly except July/August and November/December (10x per year) by Associated Business Publications Co., 41 E. 42nd St., New York, NY 10017-5391. The copyrighted information does not include the individual Tech Briefs which are supplied by NASA. Editorial, sales, production and circulation offices at 41 E. 42nd Street, New York, NY 10017-5391. Subscriptions for non-qualified subscribers in the U.S., Panama Canal Zone, and Puerto Rico, \$75.00 for 1 year, \$125.00 for 2 years, \$200 for 3 years. Single copies \$15.00. Remit by check, draft, postal or express orders. Other remittances at sender's risk. Address all communications for subscriptions or circulation to NASA Tech Briefs, 41 E. 42nd Street, New York, NY 10017-5391. Second-class postage paid at New York, NY and additional mailing offices.

POSTMASTER: please send address changes to NASA Tech Briefs, 41 E. 42nd Street, Suite 921, New York, NY 10017-5391.

Data-Control Systems hands you a new PCM Decommutator with a unique remote display.



The DCS Model 5011 has given "state of the art" new meaning with this latest generation of microprocessor-controlled PCM Decommutators. Among its advances: a handheld terminal which is a remote word selector, enabling the operator to monitor information while moving around the test site.

Other advances: operational capability up to 10 MBPS NRZ, combined with storage of programmed formats and a six-line, 40-character-per-line plasma display. In addition, the 5011's four-mode synchronization method includes a VERIFY mode



to confirm the correct pattern before entering the LOCK mode.

And, the DCS 5011 offers a decommutator, an integral bit synchronizer, a PCM simulator and a remote display in one powerful unit.

The new Model 5011 Bus structured PCM Decommutator... another innovative product by DCS, employing the latest in DSP, PLA and LCA technology. For information, contact us at one of the addresses below.

Quanta Systems Corporation Data-Control Systems

1455 Research Boulevard
Rockville, MD 20850
(301) 279-8798
TWX (710) 828-9785

8295 Westminster Ave., Suite 150
Westminster, CA 92683
(714) 894-4471
TWX (910) 596-1802

CompuDyne Defense Electronics Group



Now available with integral color console

TI's Explorer II is number one in symbolic processing performance.

At the heart of the world's most powerful symbolic processing workstation is one of the most complex integrated circuits ever built. Texas Instruments Explorer Lisp microprocessor is the world's first chip designed specifically for artificial intelligence applications, and the only one in production today. A product of TI's world-leading semiconductor technology, the Lisp chip is fabricated in 1.2 micron CMOS and integrates more than a half-million transistors.

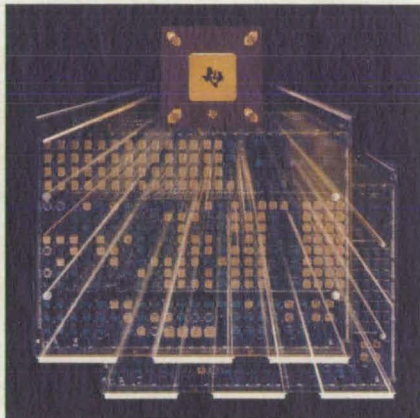
With this new chip for its engine, the Explorer II gives developers what they need most – more power to be more productive. In fact, customer tests confirm that Explorer II delivers more than twice the symbolic processing power of its closest competitor.

A software environment that maximizes developer productivity.

The Explorer II combines a comprehensive set of power tools and thousands of application building blocks in a tightly integrated environment. The result is a powerful software development capability that is far superior to conventional systems. And only TI provides source code for all system software.

By automatically managing many lower-level details, Explorer systems let developers focus on the conceptual level of problems. For example, Explorer's dynamic data type processing provides developers the flexibility to address complex, dynamic problems by eliminating the need to explicitly declare data types

◀ Pictured left: Explorer II, the world's most powerful symbolic processing workstation, is the first in its class to offer an integral color monitor.



Based on the world's first AI microprocessor, the Explorer II delivers more than twice the performance of its closest competitor.

in advance. Unlike conventional systems, Explorer's hardware architecture executes dynamic type checking without compromising performance.

TI's Temporal Garbage Collection system operates invisibly so you can create large programs without repeatedly pausing for memory reorganization as is required by conventional computers. In addition, the new Adaptive Training Facility automatically customizes memory arrangement to your activities. This boosts system performance by reducing disk paging by as much as a factor of four.

Explorer II stands out without standing alone.

Like other Explorer family members, the Explorer II is carefully designed to protect your hardware and software investment. Explorer systems can be easily upgraded to Explorer II with a field-installable processor upgrade. And

applications software runs on both Explorer and Explorer II without modification.

The Explorer LX systems let you combine symbolic and conventional processing by providing both Lisp and UNIX® environments in a single multiprocessor system. And of course, all Explorers interface smoothly with existing networks using industry-standard networking and communications facilities.

Catalyst for expanding delivery options.

The Explorer Lisp chip's unsurpassed performance and level of integration promise to open up new approaches to the delivery of symbolic processing applications. TI plans to use this chip in future delivery vehicles and in co-processors for other computers.

Customer solutions that are second to none.

Texas Instruments is committed to helping you realize the full potential of your Explorer. From powerful symbolic processing systems to expert system development tools to extensive Knowledge Engineering services, TI offers the most complete package of products and services in the AI marketplace today. Together, these make Explorer computers the standout choice of symbolic processing workstations.

For more information about TI's Explorer family products, please call toll-free, 1-800-527-3500.

AmAlox 68

High Density Alumina Ceramic

- Mechanical stability to near 3000°F.
- High resistance to corrosion and oxidation
- Extreme wear resistance
- Hardness is 91.5 Rockwell A
- Compressive strength is 400,000-450,000 psi
- Part tolerance can be held to 0.0001 inch
- Out performs conventional and electronic grade ceramics in wear applications 5 to 10 times
- Precision and complex parts manufactured to your specifications in prototype to production quantities
- Applications include: piston caps/rings; exhaust port/manifold/cylinder liners; blades, vanes, shrouds, rotors, water pump seals, and valve train components

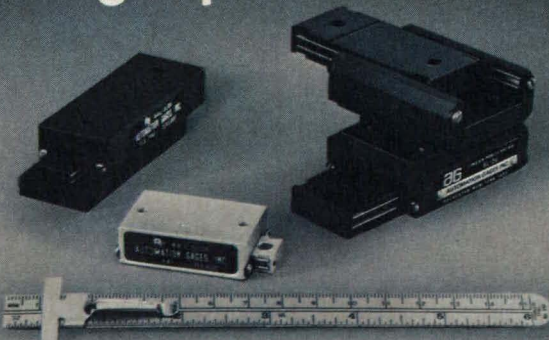


am 
Astro Met Associates, Inc.

9974 SPRINGFIELD PIKE
CINCINNATI, OHIO 45215
513-772-1242
Telex (23) 29-5526

Circle Reader Action No. 484

small in size... big in performance



Series J and K Ball Slides from AG provide smooth, precise operation in a compact size. The J series is all aluminum for lightweight applications. For medium weight applications, the K series is constructed of either steel and iron or all iron. Both models feature AG's unique patented pre-load adjusting wedge that eliminates all backlash and play. Whether your application calls for the Series J, the smallest of all, or Series K, the versatile intermediate model, you can rely on AG Ball Slides for optimum performance.


AG **AUTOMATION GAGES**
850 Hudson Avenue, Rochester, N.Y. 14621
Phone (716) 544-0400

To order, or for information, call Automation Gages at 800-922-0329. In New York State call 716-544-0400.

Call For Area Distributors Nearest You Dept. 242
Circle Reader Action No. 453

NASA Tech Briefs

National Aeronautics and
Space Administration

ABP 

NASA Tech Briefs:

Published by **Associated Business Publications**
Editor-in-Chief **Bill Schnirring**
Publisher **Thomas H. King**
Associate Publisher **Frank Nothhaft**
Associate Publisher **Robin J. DuCharme**
Managing Editor **R. J. Laer**
Associate Editor **Leo D. Kluger**
Associate Editor **Joseph T. Pramberger**
Technical Advisor **Dr. Robert E. Waterman**
Production Manager **Rita Nothhaft**
Traffic Manager **James E. Cobb**
Circulation Director **Anita Weissman**
Controller **Neil B. Rose**
Awards Manager **Evelyn Mars**
Reader Service Manager **Arlene Berrios**

Technical Staff:

Briefs prepared for National Aeronautics and Space Administration by **Logical Technical Services Corp.**, NY, NY
Technical/Managing Editor **Ted Sellinsky**
Art Director **Ernest Gillespie**
Administrator **Elizabeth Texeira**
Chief Copy Editor **Lorne Bullen**
Staff Editors **James Boyd, Larry Grunberger, Jordan Randjelovich, George Watson**
Graphics . . . **Israel Gonzalez, Luis Martinez, Huburn Proffitt**
Editorial & Production **Beatriz Flores, Bill Little, Frank Ponce, Ivonne Valdes**

NASA:

NASA Tech Briefs are provided by the National Aeronautics and Space Administration, Technology Utilization Division, Washington, DC:
Administrator **Dr. James C. Fletcher**
Assistant Administrator for Commercial Programs **Lawrence F. Herbolshelmer (Act)**
Director Technology Utilization Division . . . **Henry J. Clarks**
Publications Manager **Leonard A. Ault**

Associated Business Publications

41 East 42nd Street, Suite 921
New York, NY 10017-5391
(212) 490-3999

President **Bill Schnirring**
Executive Vice President **Frank Nothhaft**
Vice President Marketing **Mark J. Seltman**
Vice President **John K. Abely**

Advertising:

New York Office: (212) 490-3999

Sales Manager **Robin DuCharme**
Account Executive (Mid-Atlantic) **Dick Soule**
Account Executive (Midwest) **Michelle Schmitz**
Account Executives (Eastern MA, NH, ME, RI) . . . **Lee Arpin**
at (617) 899-5613; **Bill Doucette** at (617) 278-7792
Account Executive (Western MA, CT, VT) . . . **George Watts**
at (413) 596-4747
Advertising Assistant **Erving Dockery, Jr.**

California Office: (415) 831-9620

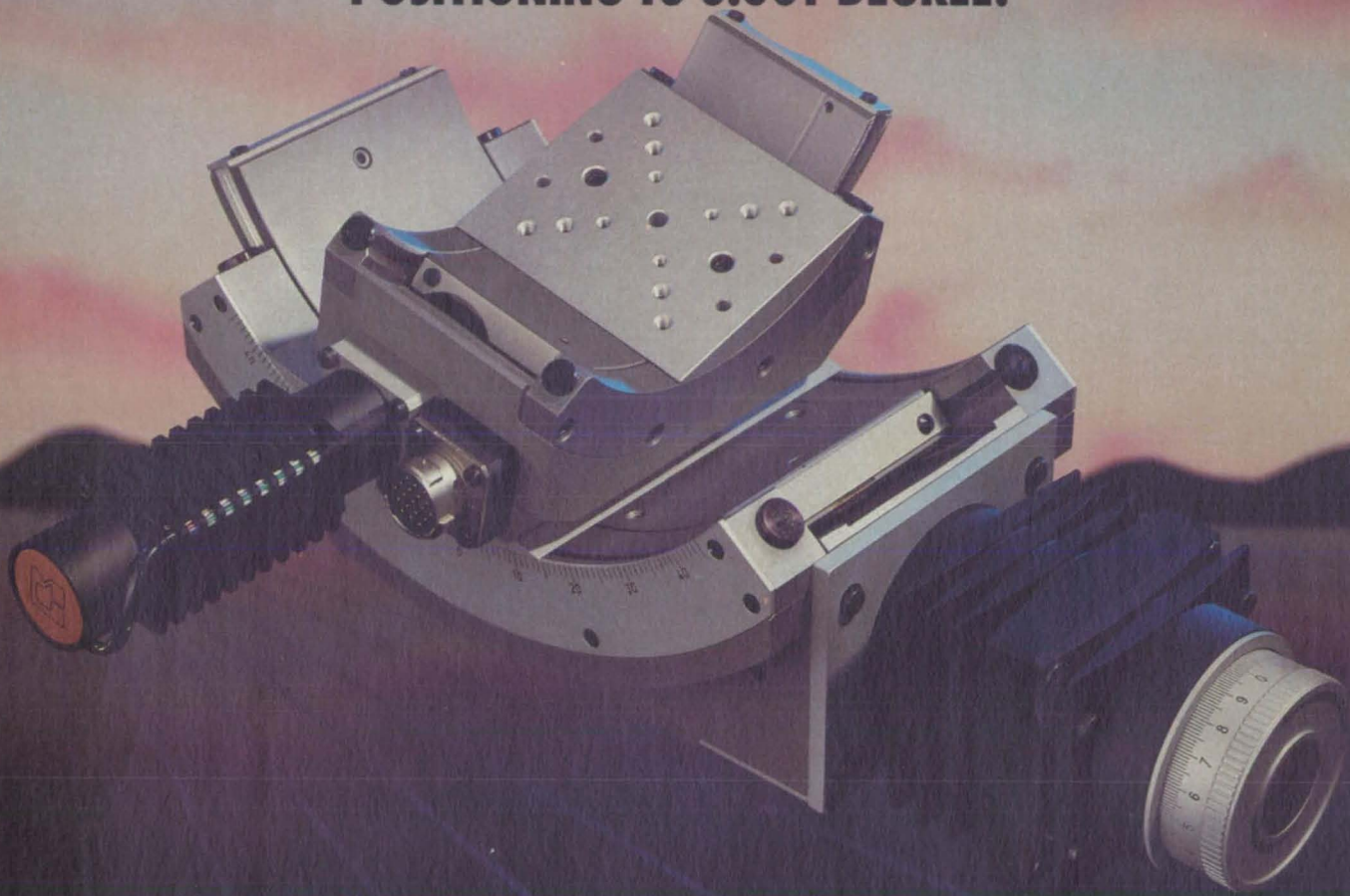
Western Regional Manager **Larry Goldstein**

NTBM-Research Center

Project Director **Mark J. Seltman**
Account Supervisor **Lourdes Del Valle**

THE KLINGER ARGUMENT AGAINST COMPROMISE:

ONLY WE OFFER A CHOICE OF GONIOMETRIC CRADLES THAT PROVIDE POSITIONING TO 0.001 DEGREE.



Our unique BG series goniometric cradles make difficult positioning tasks simple. Designed with the center of rotation external to its body, each of these stages provides unobstructed motion over 90 degrees.

Cradles can be paired to provide orthogonal rotation about a common point or used in conjunction with other Klinger components to form multi-axis positioning systems. All cradles can be manually operated or motor-driven for automated applications.

Standard resolutions are 0.01 or 0.001 degree with load capacities to 100 lbs. All units can be equipped with an incremental encoder for position verification. Other options include homing, vacuum and clean

room preparation.

A full range of sizes is available. Chances are that we have the size that's right for you.

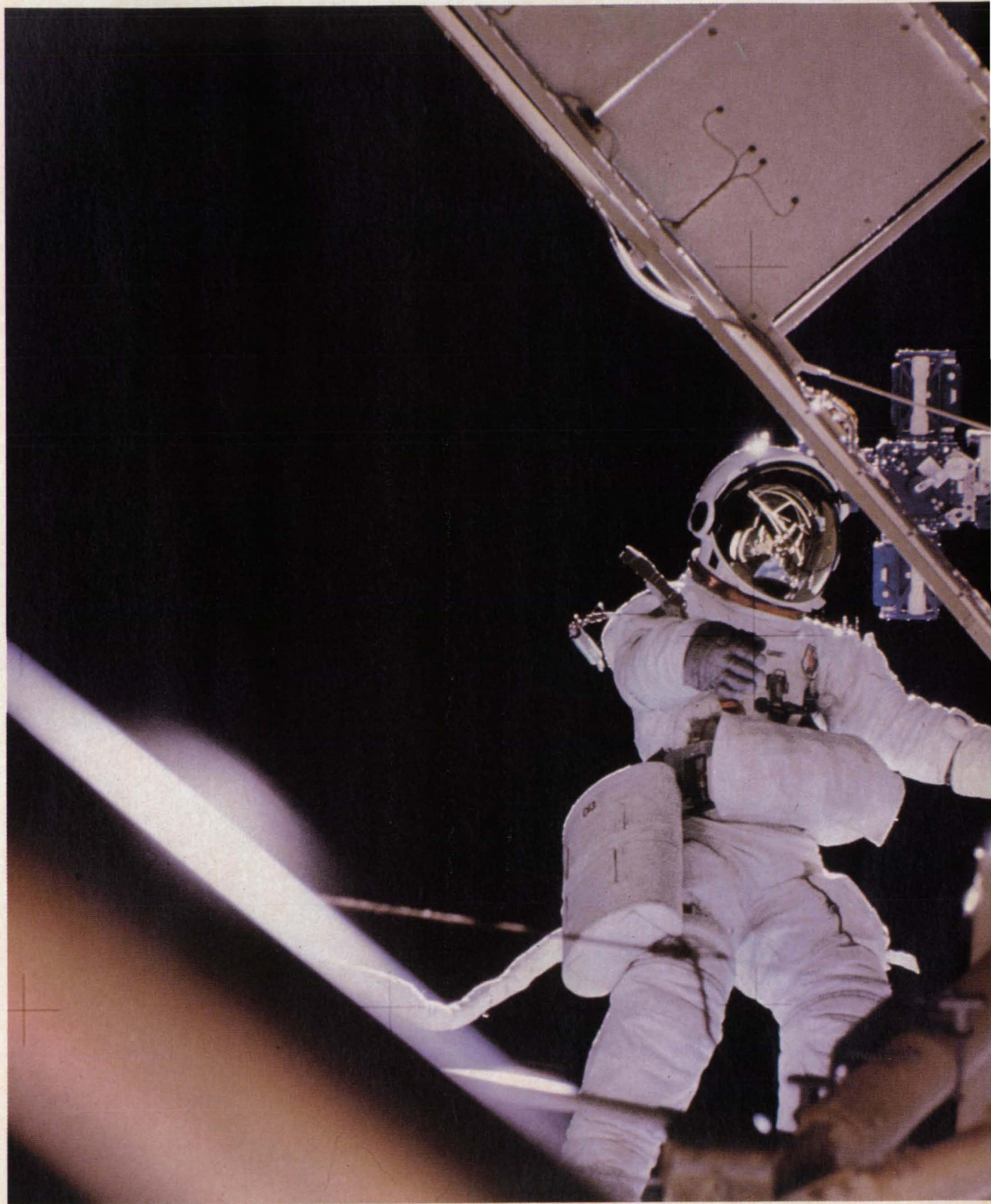
Don't compromise. The best is always a bargain. Klinger standards of engineering and manufacturing, as exemplified by our goniometric cradles, have made us the world leader in micropositioning systems. Get our free 212-page micropositioning handbook for complete specifications on these and thousands of other components.

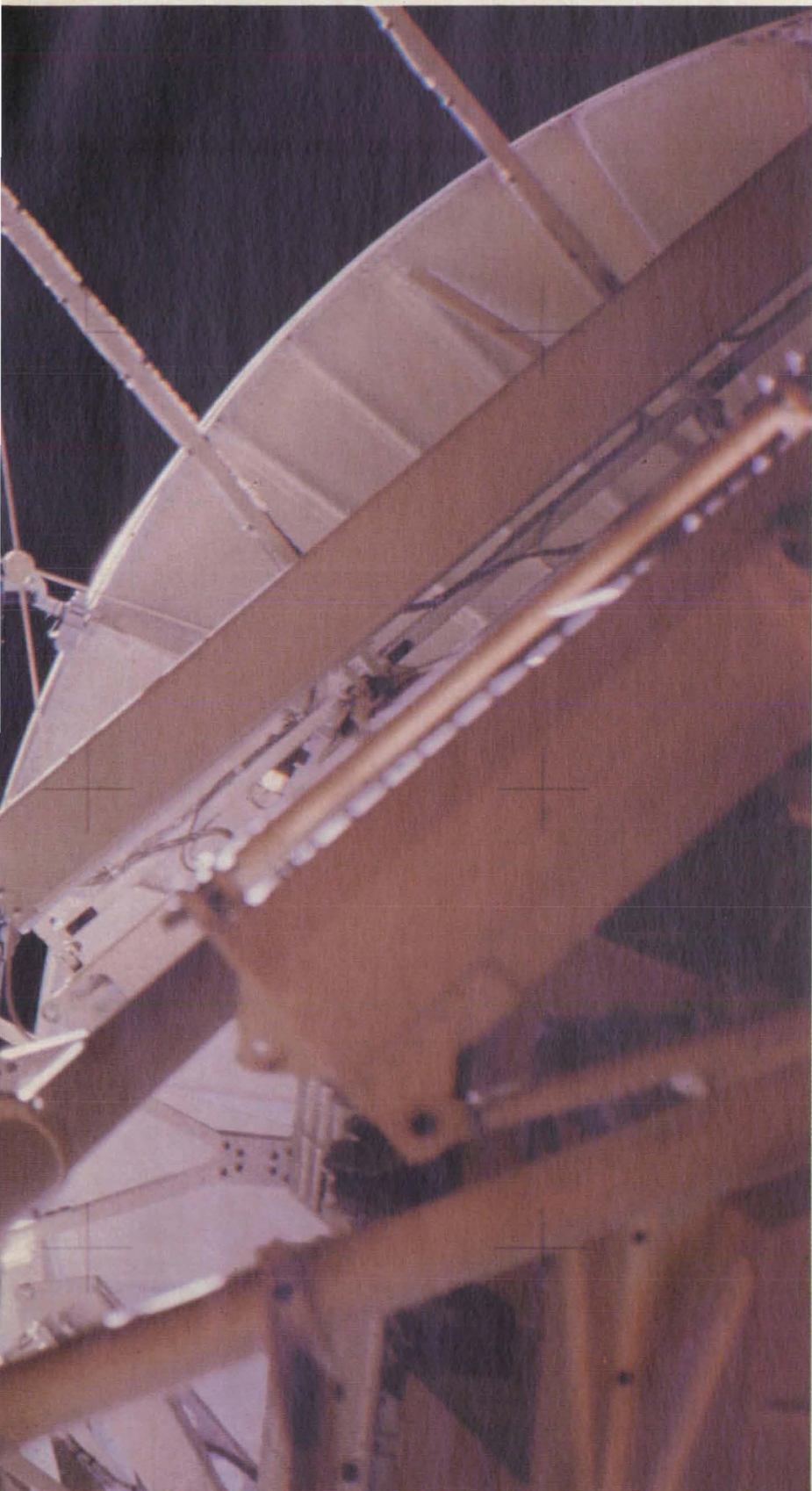
Write or phone Klinger Scientific Corporation, 110-20 Jamaica Avenue, Richmond Hill, NY 11418. (718) 846-3700.

KLINGER SCIENTIFIC



Worldwide Network to Meet Your Needs • **France:** Micro Controle, Evry, (tel.) 64979898 • **England:** Micro Controle, Newbury, (tel.) 44/635521757 • **Italy:** Nachel, Italia, Milano, (tel.) 02/9233315 • **West Germany:** Spindler & Hoyer, Göttingen, (tel.) 49/0/551/69350 • **Belgium:** Micro Controle, Bruxelles • **Switzerland:** G.M.P.S.A., Lausanne, (tel.) 46/21/33/3328 • **Sweden:** Martinsson & Co., Hagersten, (tel.) 08/744 03/00 • **Japan:** Hakuto Co. Ltd., Tokyo, (tel.) 03/341/2611 • **Canada:** Optikon Corp. Ltd., Waterloo, Ontario, (tel.) 519/885/2551 • **Taiwan ROC:** Pan-Co International Ltd., Taipei, (tel.) 886-2/3914642 • **Korea:** Sam Joong Corp., Seoul, (tel.) 82-2/5480732 or 33.





Skylab.

It was a house in space.

It had rooms and our guys
lived up there.

It amazes us still.

When we go back
with the Space Station,
you can bank on two things.

We'll build bigger.

And we'll take a long lease.

The companies of United
Technologies are working
together to make the
Space Station a reality.
Life-support systems from
Hamilton Standard, advanced
materials from Sikorsky, data
management by Norden
and inspiration from above.

 **UNITED
TECHNOLOGIES**

SPACE STATION . . . OUR BEACHHEAD INTO TOMORROW



As I write this editorial, the cream of American aerospace manufacturers are competing for four major space station packages. I know one sure and certain winner. America.

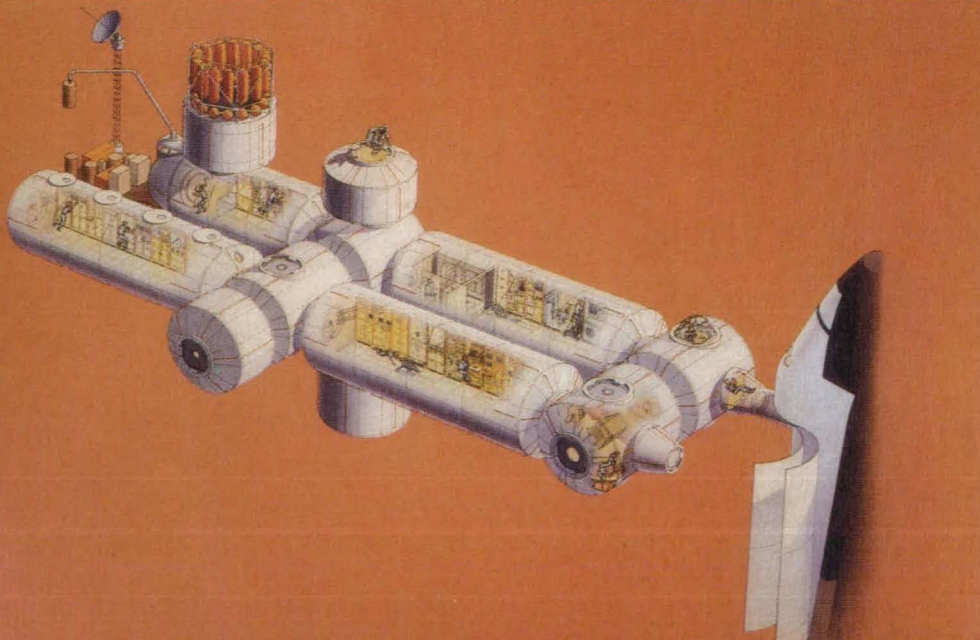
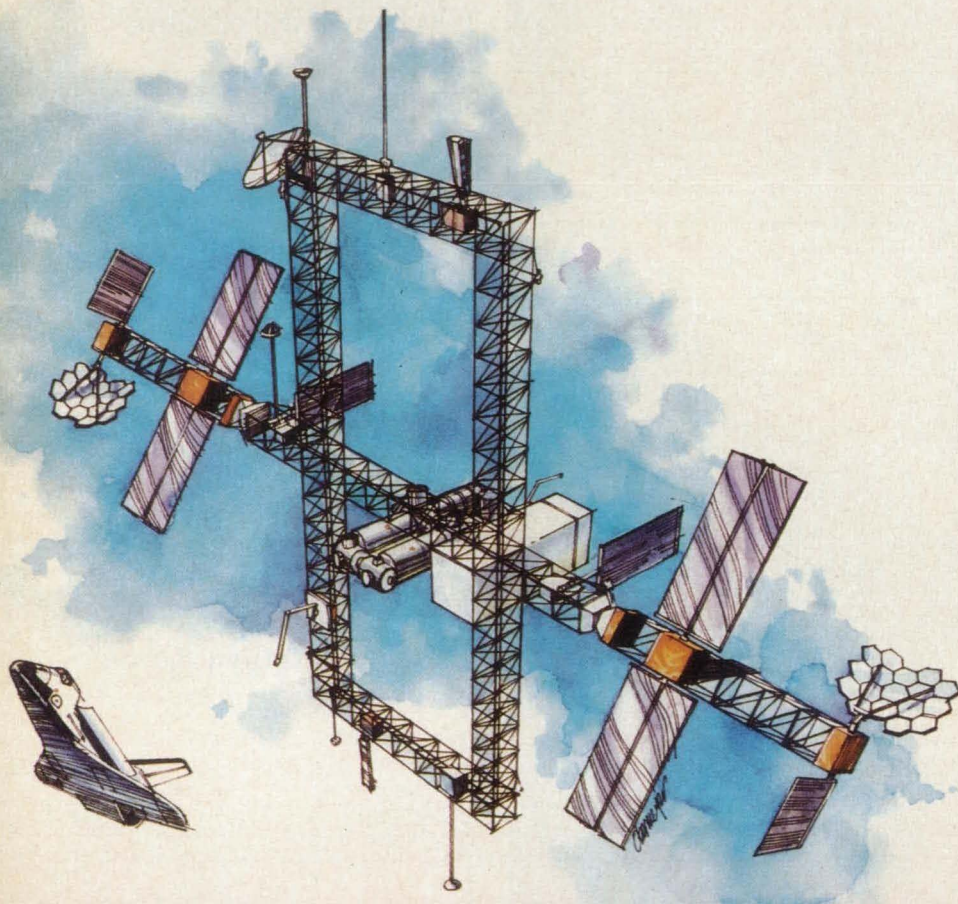
I've been interested in space exploration since I was old enough to read. Space isn't the last frontier, it's the only frontier. This ball of dirt and water we live on is home, but that doesn't mean we're not destined to leave home. If Darwin was right and the first coelacanth hadn't left home, we'd all still be sucking mud on the bottom of the Indian Ocean.

On this Editorial Notebook page, I've chosen to share with you a few thoughts on the space station from a number of people working towards its reality.

"The space station program logically represents the next evolutionary step beyond the space shuttle in the development of our nation's manned space flight capability. A continuously-staffed platform in earth orbit will enhance exploration and utilization of space, serving as a research center in fields such as astronomy, astrophysics, materials and the life sciences. It will serve as a maintenance depot for in-orbit repairs and upgrades and, as a launch pad, will provide a cost-effective gateway for missions to the moon and planets. Also, the space station will enhance relations with America's partners in the program—Europe, Japan, and Canada—and will commit our country to continued international competitiveness in space, rather than concede manned space flight leadership to the Soviets." —Richard M.

Top: A McDonnell Douglas rendering of space station after two years of definition and preliminary design.

Bottom: This Martin Marietta conception of space station depicts the astronauts' living quarters (upper right), U.S. laboratory (lower right), European Space Agency laboratory (lower left), and Japanese laboratory (upper left).



$\mu\Omega$

THREE DIMENSIONAL

1 Ensure dry circuit conditions with a 20 mV clamp.

Keithley's new Model 580 Micro-ohmmeter combines three performance features no other single micro-ohmmeter has. For example, in its Dry Circuit Test mode, the Model 580 ensures that the open circuit test voltage never exceeds 20 mV. This is important, since too high a test voltage can puncture oxides or films on contacts.

2 Measure bonding resistances and more with selectable waveforms.

For bonding applications, the Model 580 has 10 micro-ohm sensitivity, an optional battery pack, and multiple test leads. With pulsed test current, the 580 automatically compensates for thermals, and for temperature-sensitive components, these pulses can be triggered individually. For tests on inductive components, DC current is available.

3 Interface to your computer with the IEEE-488 option.

Use the Model 580 as a stand-alone instrument or select the optional analog output and IEEE-488 bus interface and use it in a computer-based system. All front panel features are programmable.

Like other Keithley instruments, it has relative zeroing, autoranging, and digital calibration, making measurements faster and more convenient.

For a brochure or demonstration of the new Model 580 Micro-ohmmeter, call your local Keithley representative or the Product Information Center at the address below.



Instruments Division
Keithley Instruments, Inc.
28775 Aurora Road
Cleveland, Ohio 44139
(216) 248-0400

KEITHLEY

Davis, President, Martin Marietta Manned Space Systems

"We need the space station for the United States and its partners to develop the technology foothold established by Apollo and the space shuttle into a permanent manned presence. Man in space supported by substantial electrical power can explore the heavens and earth. The onboard laboratories can develop new medicines and materials to benefit all mankind."

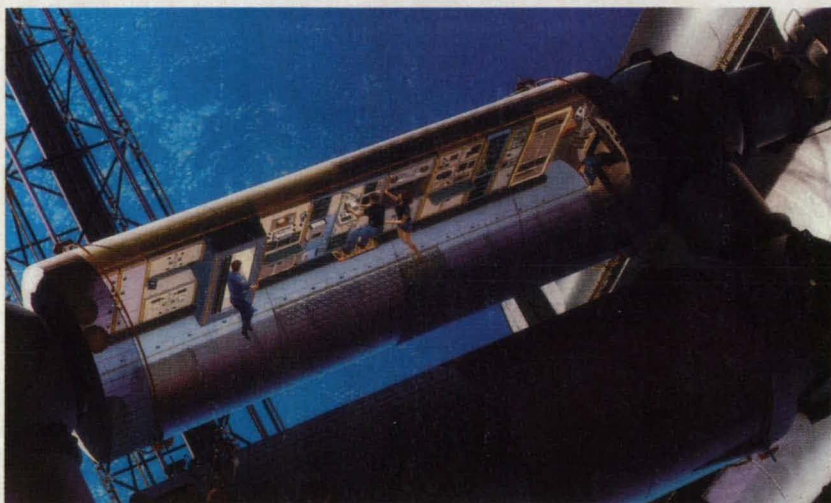
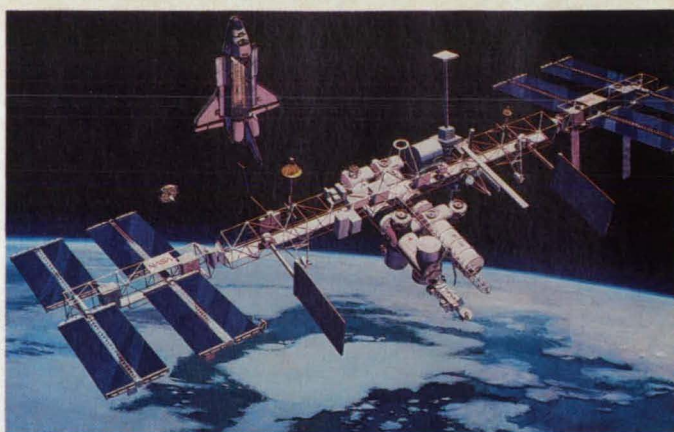
—George J. Hallinan, Space Station Power Program Director, Rocketdyne Division of Rockwell International Corporation

"Man must and will explore the universe. A space station in near-Earth orbit is the first vital step for missions to other planets. Such missions will require large payloads, probably too large for a launch from Earth. By using the space station as an assembly area and jumping off point, we can escape the handicap of Earth's gravity.

A space station—and the capability it affords for exploration—should be viewed in the same way as the voyage and discoveries of Columbus, which quite literally transformed the world well beyond what anyone could have predicted."—Dr. Albert W. Weinrich,

Top: Rockwell International's proposed space station design features a horizontal truss to which the laboratory, habitation modules, and solar panels are attached.

Bottom: A space shuttle docks at a port connecting two of the space station's common modules in this Boeing Aerospace artistic conception.



YOU CAN'T DO THIS WITH A GREASE GUN!

It's easy

WITH TUFOIL LIGHTNING GREASE

OEMS-
YOUR SERVICE MEN
WILL LOVE IT.



Machines work better when you can put a wee dab in the right place.

Recent tests by a major U.S. Government Lab show a surface friction of .029 for their steel on steel 4-ball test using TUFOIL (teflon on teflon is .04). Confirmation is coming in from all over the world. OEMs specify TUFOIL products for astonishing improvements in performance in all types of machines.

TUFOIL for Engines™
TUFOIL Lubit-8™
TUFOIL Gun-Coat™
TUFOIL Compu-Lube™



TUFOIL is the "transistor of lubrication"™ . . . no other lubricant even comes close.

1-800-922-0075

Fluoramics, Inc.
103 Pleasant Avenue
Upper Saddle River, N.J. 07458

CALL FOR PRICES

TUFOIL is a TM of Fluoramics, Inc.
TEFLON is a TM of duPont
©1987 Fluoramics, Inc.

For additional technical information, see NASA Tech Briefs from Nov./Dec. 1986 to date.

Program Manager, RCA Government Communications Systems Division

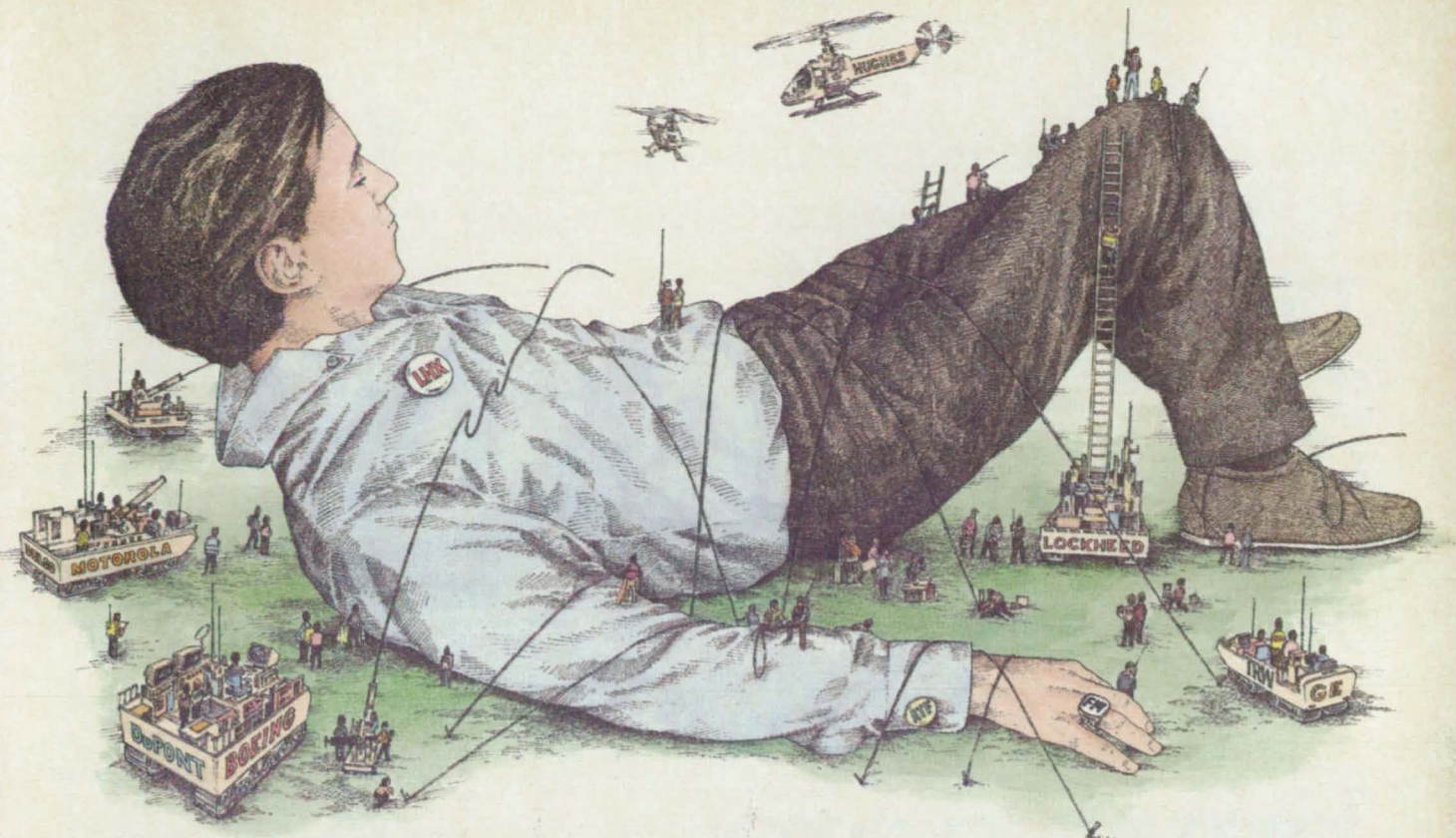
"Space station will speed the process of American invention and discovery. It will provide American businesses with a permanent space-based center of operation to carry out the long term research necessary to pioneer the industrial space frontier."
—Robert W. Hager, Vice President and Program Manager, Boeing Aerospace Company

"Our country's space program has kept America on the leading edge of science and technology. This leadership forms the basis for America's freedom and strength. At a time when our ability to compete is questioned, our country needs space station."

—Sanford N. McDonnell, Chairman and Chief Executive Officer, McDonnell Douglas Corporation

To paraphrase the credit card company, "The American Space Station . . . don't leave home without it." □

Brie Schaeffer



Some development projects are so big they can only be managed with Teamwork.

Creating embedded software systems can be a gigantic challenge. But now there's a way to manage the process, lower costs, improve productivity, and keep your team competitive.

How? With a product called Teamwork® for computer-aided software engineering (CASE).

The Teamwork environment is specifically designed for large scale, complex systems development projects. It provides modules for structured analysis, real-time modeling, information modeling, and structured design. And it has an open data base that allows you to interface your own application tools.

Teamwork is a registered trademark of Cadre Technologies Inc.

Teamwork is being used by many leading companies like Grumman, Rockwell, DuPont, Litton, HP, Delco, Motorola, General Dynamics, and Westinghouse for their most sophisticated projects. And it's helping many of these users meet stringent DoD-2167 requirements.

No wonder Teamwork is the number one workstation-based CASE tool on the market. It was the first to support real-time modeling. First to support all workstation environments. First with data base sharing for workstation users. And it has the most advanced user interface of any CASE tool on the market, making it extremely easy to learn and use.

Today, Teamwork runs on all leading workstations, including Apollo, DEC, Hewlett Packard, IBM and Sun. There's even a PC member of Teamwork. So regardless of your hardware preference—today or tomorrow—Teamwork can work for you. And grow with you.

You've heard all the claims about productivity from CASE tool vendors. Now talk to the people who can deliver it today.

Teamwork, from Cadre. No matter how big the challenge, it can give your team the competitive edge.

Cadre Technologies, Inc.,
222 Richmond St., Providence, RI 02903
(401) 351-CASE **CADRE**

teamwork®

Winning teams depend on it.

In Europe, for the name of the local Cadre distributor, call 41 • 22 • 692424

Circle Reader Action No. 300

Plain talk on why more and more workstation buyers are turning to HP.



They're turning for good reason.

HP offers more capability in workstations than ever before.

Namely, an entire family of high-performance workstations that thrive in multivendor environments. They support industry standards in networking, graphics, the UNIX operating system, the X Window System, and a variety of languages.

It means this. HP workstations fit your computing environment. And grow with you instead of growing obsolete.

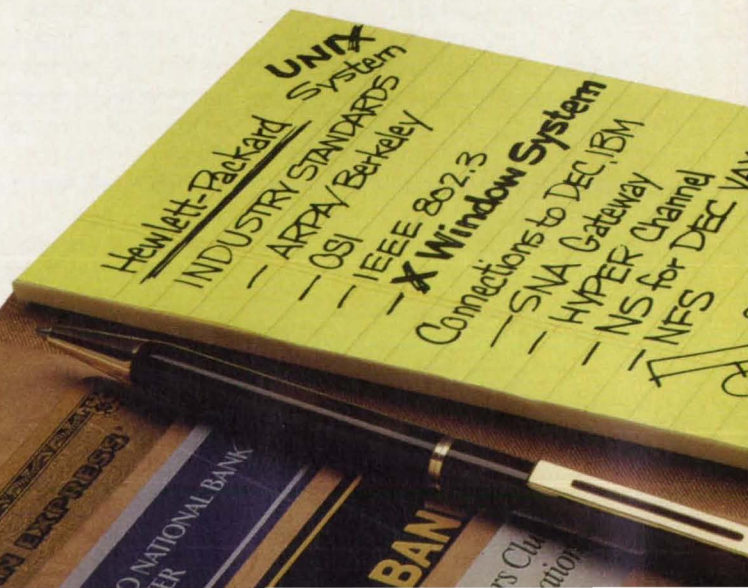
Need applications software? No problem. You have your choice of world-class HP solutions in CAE/CAD, microprocessor development, PCB test, and more. For special applications, we offer over 1,000 software

Brake assembly data courtesy of SDRC
Automobile data courtesy of Chrysler Motors

UNIX is a registered trademark of AT&T in the U.S. and other countries

HYPERchannel is a trademark of Network Systems Corp.

NFS is a trademark of Sun Microsystems



packages from our third parties. So either way, you're covered.

Our new family of 32-bit machines is complete, and gives excellent value from low end to high. Which means you can choose the right workstation, while getting the most from your investment. Our Model 318M, starting at \$4,990, sets new standards in entry-level price/performance. And the Models 330, 350, and 825 provide the power for your toughest technical applications.



Want extraordinary speed and resolution in 2D and 3D graphics? You'll find it on our entire family. One good example: the new Model 825SRX Precision Architecture Super-workstation. It combines 8 MIP computation power with interactive solid rendering graphics.

Something else you should know. The HP family is modular.



And works with an extensive line of HP input and storage devices, monitors, printers, and plotters. So you can get a complete system, supported as a system, from one source.

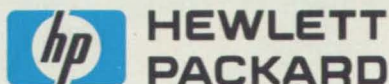
Speaking of the source, HP delivers unsurpassed service and support, with a proven reputation for minimizing your overall cost of ownership.

Plus, no one anticipates your future needs like HP. Our vision of distributed computing ensures that we will satisfy your application requirements tomorrow as well as we do today.

Consider HP workstations now. See for yourself why more and more companies are turning to HP. Questions? Call your local HP sales office listed in the telephone directory white pages.

Tap HP's DATA-LINE for complete facts...instantly!

For on-line information 24 hours a day, use your computer, modem, and HP's DATA-LINE. Dial 1-800-367-7646 (300 or 1200 baud, 7 bits even parity, 1 stop bit). In Colorado, call 1-800-523-1724.



Circle Reader Action No. 416

*we never
stop
asking*

What if...

Smart the

The human hand can be regarded as one of the major determining factors of human evolution. Together with the human brain and binocular vision, the hand enabled man to make and use tools, and to explore, manipulate and change his physical environment. In the evolution of robotic machines intended to replace or extend human activities, smart robot hands play a similar major determining role.

Designed for application on an Orbiting Maneuvering Vehicle (OMV), the first JPL hand was tested at Marshall Space Flight Center (MSFC) on the 3-meter wide Proto-Flight Manipulator Arm. The JPL-OMV smart hand is a one-d.o.f. gripper with intermeshing jaws consisting of parallel plates with a V groove center section. Thus, the claws can mechanically lock on square or cylindrical objects in two-d.o.f. The jaws can travel on a linear path while gripping, and their maximum opening at the tip is 6.5 cm. Each jaw has a built-in load cell to measure gripping force in the range of one to 600 Newtons. The jaws are driven by a DC motor via opposing lead screws. Double slides, supported at both ends for compactness and stiffness, guide the jaws' motion. Each slide is on a sepa-

rate hardened and ground steel rod. A channel built into the drive system's frame gives additional guidance. The entire smart hand mechanism mounts to the robot arm wrist through a six-d.o.f. strain gauge load cell system by which the three interaction forces (F_x , F_y , F_z) and moments (M_x , M_y , M_z) with the environment are measured in the range of 120 Newtons and 70 Newton-Meters (figures 1, 2 and 5).

Self contained in sensor data acquisition, data processing and motor control, the JPL-OMV smart hand has three built-in microprocessors (Motorola MC68701 and MC68705 units), as shown in figure 3. Thus, the command interface, force-moment and position feedback to the remote support equipment require only a single full duplex RS-232 link. The distri-

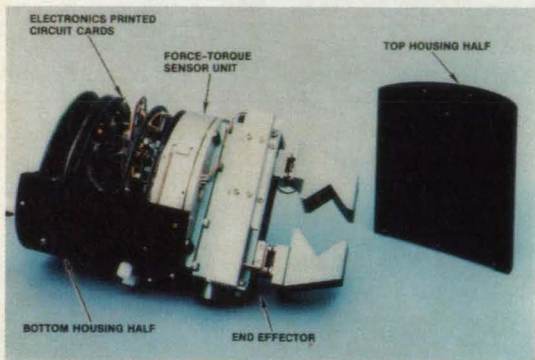


Figure 1

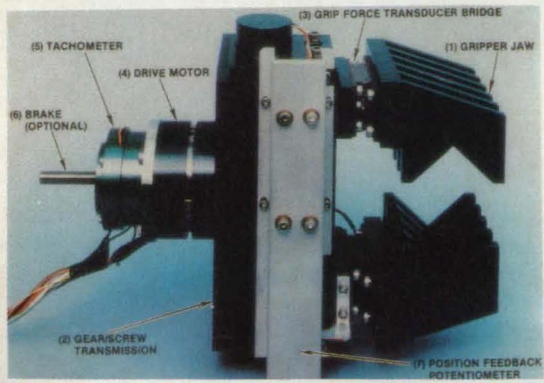
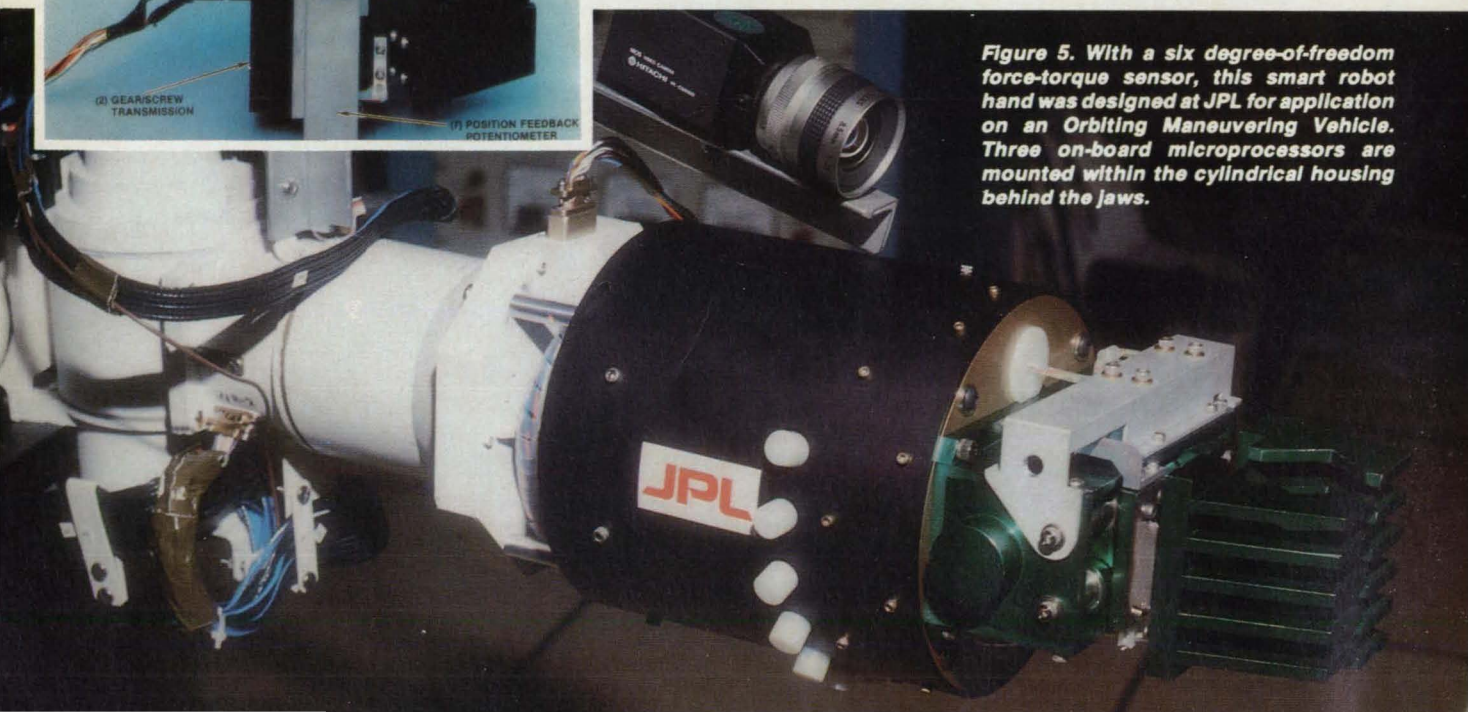


Figure 2

Figure 5. With a six degree-of-freedom force-torque sensor, this smart robot hand was designed at JPL for application on an Orbiting Maneuvering Vehicle. Three on-board microprocessors are mounted within the cylindrical housing behind the jaws.



Robot Hands on Ladder of Evolution

buted microprocessors' architecture in the hand uses advanced integrated circuits, including hybrid and high level multifunctional packages, thereby minimizing the chip counts. Custom designed circular and annular printed circuit cards support the hand's controller ICs. Seven slip rings interface the local electronic circuits with the central electronics. Four are used for power transmission, two for bidirectional data communication, and the seventh for system ground.

Power for the motor and electronics comes from a support chassis that also houses a National Semiconductor 32016 microprocessor and a Parallax graphics processor for high level control and real-time force-moment graphics display. A control box (figure 4) is used to operate the hand, setting the gripper control mode, changing the give force, rate and position, and adjusting operating parameters such as force and rate limits. This gripper can handle fragile objects with a gentle grasp force of from one to five Newtons, or hold a tool with a firm grip of up to 600 Newtons.

Force and torque gripper control takes place in the hand itself, using a microprocessor for motor control. Commands from the control box are sent to the motor controller via a serial link and the com-

(continued on the next page)

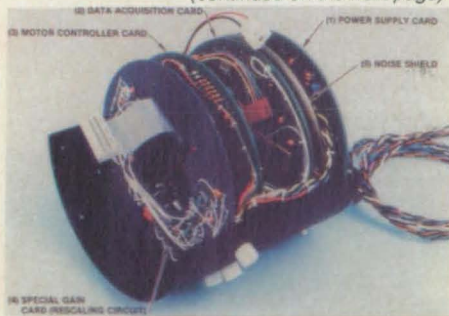
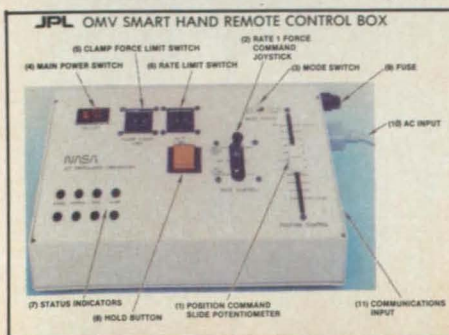


Figure 4



The only smart hands in space today are the hands of the astronauts. Smart robot hands are, however, being created at several research institutions. The term "smart robot hand" refers to the human analogy which reveals that the hand is both a powerful and delicate mechanism as well as a sensory instrument through which information is received and transmitted. Its function is manipulation. The function of the arm is to position and orient the hand. It also acts as a mechanical connection and power and sensing transmission link between the hand and the main body of a person. The full functional meaning of the arm rests in the hand.

Future operations in space such as construction and assembly, satellite servicing and refueling, and planetary exploration involving robotic machines motivated a smart robot hand design and development effort at the Jet Propulsion Laboratory (JPL) to enhance remote manipulation capabilities in both teleoperator and robotic modes of control.

An initial JPL design study subdivided the robot hand design requirements into four major areas: 1) mechanism and mechanical performance; 2) sensing and data handling; 3) control, and 4) man-machine interface for decision and control. The study concluded that the development of dexterous and possibly anthropomorphic hands in a master-slave control configuration would be desirable and technically feasible.

Analysis of space assembly, servicing and repair tasks to be performed by remote manipulators also lead to the conclusion that an evolutionary approach to the design and development of space robot hands can generate important and needed capability increases. First generation smart hands at JPL have one-degree-of-freedom (d.o.f.) parallel-claw end effectors. Equipped with six-d.o.f. force-torque balance and built-in one d.o.f. grasp force sensors, the hands are controllable in position, rate and grasp force. Three smart hands of this category

By Dr. Antal K. Bejczy,
Senior Research
Scientist and
Technical Manager of
the Telerobot
Research Program,
Jet Propulsion Laboratory



Dr. Bejczy has managed advanced teleoperator development efforts at JPL since 1974. Prior to his 1969 arrival at JPL, Dr. Bejczy spent three years at the California Institute of Technology as a postdoctoral NATO Senior Research Fellow in Electrical Engineering and Applied Sciences. Dr. Bejczy is the author or coauthor of over 80 papers on robotics and advanced teleoperation, has two U.S. patents in robot sensing, and over 20 NASA Tech Briefs awards. He serves as editorial board member for several technical journals on robotics. Dr. Bejczy was General Chairman of the 1986 IEEE International Conference on Robotics and Automation, and serves as the President of the IEEE Council on Robotics and Automation for 1987. □

were developed at JPL's Telerobot Research Program. These prototypes differ in their end effector size and drive mechanisms, claw shapes, local electronics, and subsystem interface instrumentation (see sidebar text).

JPL's smart hands represent only the beginning of the evolutionary trail. Future plans include the addition of electro-optical proximity and tactile sensing capabilities. Used in close-up work, optical sensors beam infrared light at the object of interest. Reflections from the object's surface are triangulated to provide depth information. Tactile sensitivity will give robot hands abilities similar to those of human skin, with its sensitivity to touch. Improvements in pattern recognition will enable smart hands to perform the most human-like feat of all: identifying and picking specific pieces from a bin filled with similar parts.

The trend to develop smarter robot hands challenges mechanical design and sensor technology. Hands such as those at JPL were inconceivable just a few years ago, due to the bulk of the local controlling electronics. As circuit size continues to shrink, smart hands will get brighter, bringing increased benefits both in space and on earth. □

munication processor. On this same route, force, moment and position information is continuously sent to the support chassis for graphic display on a TV monitor. The forces and moments measured by the six-d.o.f. strain gauge force-moment sensor assembly are represented as bar graphs in a star configuration which suggests a perspective view of the Cartesian reference frame of the gripper. Jaw opening and clamping force are represented by vertical bars on the left side of the graphics display. Software provides for two display adjustments: taking away unwanted load bias (like gravity) and scaling the display bars by specifying the force and moment level corresponding to a full bar-graph display.

Designed to fit medium size industrial robot arms such as the PUMA 560, the se-

cond smart hand developed at JPL is used for research in hybrid motion and force modes of control. The hand has three parts: a jaw mechanism, sensors and local electronics. Powered by a DC torque motor through gears and recirculating ball spindles, the parallel jaw gripper mechanism moves on rails and is supported by linear bearings to minimize friction. Each jaw subassembly consists of three parts: a moving support, a grasp force sensor operating in the range of one to 150 Newtons, and an interchangeable jaw tip. As seen in the photo to the upper left of the previous page, V-shaped grooves contour the inner surface of the jaws in two perpendicular directions, assuring a friction-independent, mechanically firm grasp. This permits the gripper to mechanically lock on

rectangular or cylindrical objects in two directions with two-d.o.f. constraints or to connect to a tool head with three-d.o.f. constraints.

Behind the base of the jaws is a six-axis force-moment sensor with a dynamic range of 75 Newtons and 20 Newton-meters for reading the three orthogonal forces and moments induced by the robot hand's interaction with the environment. This sensor consists of a Maltese cross-like structure instrumented with strain gauges. Strain gauge readings from this sensor are acquired by the local microprocessor, formatted, and transmitted to the central control computer. There, control programs are executed and sensor data are sent to a remote control station.

Local electronics for the second hand are housed in a shell attached to the force-moment sensor and connected to the robot wrist. In it are two custom printed circuit boards, one for the digital and one for the analog input/output electronics. The digital electronics are based on an Intel 8097 microprocessor with a high number of built-in functions that permit effective management of the real-time multi-tasking environment. The local software system consists of a background process for message analysis and message generation, and an interrupt driven routine for the real-time functions of the controller. The microprocessor clock generates an interrupt every two milliseconds. Presently, three separate grasp control loops are implemented; position, rate and force controls. When in force control mode, the controller maintains a preset grasp force until the central control computer issues a different command.

Also under development at JPL is a third robot hand, a modified version of the first two units (photo below). Under development for the Goddard Space Flight Center's Flight Telerobotic Servicer ground test facility, this hand will fit a large size industrial robot like the PUMA 760. Weighing about 3 kilograms, it will be able to manipulate heavier, more massive objects.

These three smart hand units represent only the beginning of the evolutionary trail. Future development plans include the addition of electro-optical proximity and tactile sensing capabilities. Other smart hand designs on the drawing board have multiple articulated fingers with miniaturized local electronics for sensor data handling and control. □

Designed to fit a large robot arm, this smart hand is under development at NASA's JPL.



CAN YOU AFFORD NOT TO MONITOR YOUR COMPOSITE CURES?



OUT IN THE FIELD IS NO PLACE TO HAVE PROBLEMS WITH YOUR COMPOSITES!

THE EUMETRIC® SYSTEM II

MICRODIELECTROMETER monitors composite processing in real time—before, during, and after cure.

All resins and composites are not created equal. They vary from supplier to supplier and batch to batch. Don't lose control! Inspect the quality of your incoming material with the System II. **Inhibitors and initiators can change cure rates.** If you don't monitor the cure you won't know if your cure times are right. Optimize your cure cycles with the System II.

Measurements can be made in liquids or solids—as small as a drop or as large as an entire part: in ovens, autoclaves, presses, molds, or dies.

The System II helps make quality products for aerospace, electronics and chemical applications—Let it help you too!

Write or call us today to receive complete information on the Eumetric® System II Microdielectrometer.

micromet instruments, inc.

The Leader in Dielectric Instrumentation

21 Erie Street, Cambridge, MA 02139
(617) 497-4330

Last Chance To Pre-Register At Special Rates!

SPACE

TECHNOLOGY
COMMERCE &
COMMUNICATIONS

November 17-20, 1987

George R. Brown Convention Center
Houston, Texas USA



Co-Sponsored by:
THE SPACE FOUNDATION

The Event

SPACE: Technology, Commerce & Communications will address the critical business issues associated with re-establishing access to space, and to provide a forum in which organizations engaged in government, commercial or research ventures can do business or establish new business relationships.

The Conference

The conference will offer attendees a realistic assessment of today's industry and an insight into the factors that influence the direction of future programs. Sessions will examine the risks, the profit potential, the technology and the steps necessary to encourage and sustain a viable business environment. Sessions include:

Tuesday, November 17

- AA-1 How Government and Industry Worldwide will Re-Establish Access to Space
- AA-2 Transition from Public to Private Sector
- AA-3 Current and Future Launch Services: Technology Overview
- AA-4 Commercial Policy Positions Re: ELV Industry
- AA-5 Advanced Launch Systems
- EU-28 Commercial Space Project Management
- RS-11 Commercialization of Remote Sensing Data

Wednesday, November 18

- AA-8 Keynote Session — Cohen
- AA-9 NASA Center Directors Panel
- AA-6 Space Stations and Industrial Platforms
- EU-34 Entrepreneurs in Space
- EU-30 Venture Capital Fair
- EU-27 Commercial Space Roundtable
- RS-8 Remote Sensing Technology
- RS-9 International Barriers to Remote Sensing
- IS-22 Computer and Communication Systems
- IS-23 Information Systems: Data Collection and Analysis
- IS-24 Information Systems: Modeling and Simulation

Thursday, November 19

- AA-0 Keynote Session — Anderson
- LN-26 Return to the Moon
- LN-27 Venture to Mars
- EU-33 Multi-Vendor Presentation: Research in Space
- AA-7 Re-Establishing Access to Space: Legal and Insurance Issues

- RS-11 Commercialization of Remote Sensing Data
 - SC-18 Satellite Communications: Technology, Applications
 - SC-20 Satellite Communications: Cost Reduction, Insurance, etc.
 - SC-21 Satellite Communications: Legal Issues
 - RB-1 Robotics
 - AI-25 Artificial Intelligence
- Friday, November 20**
- EU-31 End User Issues: Financing, Legal, Insurance
 - MP-12 Materials Processing: Current Applications
 - MP-13 Materials Processing: Future Capabilities/Technologies
 - TT-15 Technology Transfer: Spinoffs

Partial Speaker List

- Mr. Robert Anderson, *Chairman and Chief Executive Officer, Rockwell International Corporation*
- Mr. Shigemichi Sonoyama, *Vice President, National Space Development Agency of Japan (NASDA)*
- Mr. Richard Brackeen, *President, Martin Marietta Commercial Titan Systems*
- Dr. Aaron Cohen, *Director, NASA-Johnson Space Center*
- Dr. John W. Townsend, Jr., *Director, NASA-Goddard Space Flight Center*
- Mr. Pierre Bescond, *President, SPOT Image Corp.*
- Dr. Maxime Faget, *President and Chief Executive Officer, Space Industries*
- Mr. Lawrence Herbolzheimer, *Acting Administrator for Commercial Programs, NASA*
- Mr. Andrew Stofan, *Associate Administrator for Space Station, NASA*
- Professor Ernesto Vallerani, *General Manager, Aeritalia Space Systems Group*
- Mr. Bruce L. Crockett, *President, COMSAT World Systems Division*
- Mr. Courtney Stadd, *Director, Office of Commercial Space Transportation, U.S. Department of Transportation*
- Dr. Frederick Henderson III, *President, GEOSAT Committee, Inc.*
- Mr. Alain Gaubert, *Executive Manager, PROSPACE*
- Dr. Peter Kleber, *Project Manager, Industrialization of Space, DFVLR*
- Mr. Peter Tambosi, *VP-Aerospace, Banque Nationale de Paris*
- Dr. Paul Chu, *Director, Space Vacuum Epitaxy Center, University of Houston*
- Mr. Ian Pryke, *Head, Washington Office, European Space Agency*
- Dr. Joseph Allen, *Executive Vice President, Space Industries*
- Mr. Donald Langreich, *Manager, Commercial Space Projects, General Electric Company*
- Mr. Richard Jacobson, *President, SPACEHAB*
- Mr. Charles Gunn, *Director of Unmanned Launch Vehicles and Upper Stages, Office of Space Flight, NASA*
- Dr. Robert Rosen, *Deputy Associate Administrator for Aeronautics & Space Technology, NASA*
- Mr. Grier Rachlin, *Partner, Heron, Burchette, Ruckert & Rothwell*
- Dr. Peter E. Glaser, *Vice President, Advanced Technology, Arthur D. Little Inc.*
- Dr. Franco Bevilacqua, *Advanced Studies Manager, Aeritalia Space Systems Group*

- Mr. James Thompson, *Director, NASA-Marshall Flight Center*
- Mr. Paul Holloway, *Deputy Director, NASA-Langley Research Center*
- Mr. Christopher Trump, *VP, SPAR Aerospace Eng. Giuseppe Viriglio, Program Director, Aeritalia Space Systems Group*
- Mr. Byron Lichtenberg, *President, Payload Systems Inc.*
- Mr. Owen Garratt, *President, EFFORT, Inc.*
- Mr. Peter Wood, *Senior Vice President, ERC International*
- Mr. David O. Wicks, Jr., *President, Criterion Investments*
- Mr. Ian Parker, *Editor-in-Chief, SPACE Magazine*
- Mr. Gary Miglicco, *Partner, Peat, Marwick & Mitchell*
- Dr. Alex Ignatiev, *Associate Director for Development, Space Vacuum Epitaxy Center, University of Houston*
- Dr. David Norton, *Director, Space and Technology Research Center, HARC*
- Mr. Jean-Luc Bessis, *President, Service Argos Inc.*

The Exhibits

(Exhibits open November 18)

Some of the organizations exhibiting include:
NASA, National Space Development Agency of Japan (NASDA), Aeritalia, Lockheed Missiles & Space Company, Martin Marietta Manned Space Systems, Martin Marietta Denver Aerospace, General Dynamics, Ford Aerospace & Communications, McDonnell Douglas, Hercules Aerospace Company, Rockwell International Space Transportation Systems Division, Rockwell International Space Station Systems Division, Belgian Science Policy Office, IBM, Digital Equipment Corporation, Xerox Corporation, Morton Thiokol, Inc., SPOT Image Corporation, Thomson Electron Tubes and Devices Corp., Strategic Software Planning Corp., SPACEHAB, Teledyne Rodney Metals, Pilkington Electro Optics Inc., Vellox Corp., Eaton Corporation — Consolidated Controls, International Signal & Control Group, Tracor, Inc., Space Industries Partnership, Welcom Software Technology Corporation, Houston International Teletop, SPACE Magazine, PROSPACE, Fike Metal Products Division, W.L. Gore & Associates, Space Vacuum Epitaxy Center, Cincinnati Electronics Corp., Institute for Technology Development, Aerospace America, John M. Cockerham & Associates, Inc., Space Policy, Satellite Communications Magazine, Diversified Information Services, Inc., Digital Image Inc., NASA-JSC Life Sciences Project Division, Rocketdyne, Sun Microsystems, DSET Laboratories, Dynamic Engineering, NASA-Medical Operations Branch, MASSCOMP and others.

**RETURN THIS FORM TODAY!
OR CALL (617) 292-6480**

Return this form to: Registration Dept.
SPACE: Technology Commerce & Communications
c/o T.F. Associates, 79 Milk St., Suite 1108,
Boston, MA 02109 Telex: 951417, Ref. TFAS

Yes, preregister me at the discount rate of \$395.00 (government/institution rate \$345.00) for SPACE and send me more detailed conference information and hotel data with my confirmation and invoice.

My company may wish to exhibit. Please send exhibit information.

Name _____
Title _____
Company _____
Address _____
City _____ State _____ Zip _____
Country _____ Tel. _____ Telex: _____

NTB1087

New Product Ideas

New Product Ideas are just a few of the many innovations described in this issue of *NASA Tech Briefs* and having promising commercial applications. Each is discussed further on the referenced page in the appropriate

section in this issue. If you are interested in developing a product from these or other NASA innovations, you can receive further technical information by requesting the TSP referenced at the end of the full-

length article or by writing the Technology Utilization Office of the sponsoring NASA center (see page 22). NASA's patent-licensing program to encourage commercial development is described on page 22.

Implantable, Ingestible Electronic Thermometer

A small quartz-crystal-controlled oscillator is swallowed or surgically implanted to provide continuous monitoring of a patient's internal temperature. The fre-

quency of the oscillator varies with temperature. A receiver placed nearby measures the oscillator frequency, and the temperature is inferred from the previously determined variation of frequency with temperature. (See page 34).

Bismaleimide Copolymer Matrix Resins

Graphite composites prepared from a 1:1 copolymer of two new bismaleimides have mechanical properties superior to those prepared from other bismaleimide-type resins. In addition, the composite mixtures of the two resins exhibit better handling, processing, and thermal properties than the individual resins. The new composites are stronger than those made of epoxy and could replace metal in some structural applications. (See page 60).

Gamma-Ray Fuel Gauges for Airplanes

Studies with a weak Am^{241} 59.5-keV radiation source indicate that it is possible to monitor continuously the fuel quantity in aircraft tanks to an accuracy of better than 1 percent. The operation of a nuclear gauge is based on the attenuation of gamma rays passing through the matter. Presently used capacitance gauges are vulnerable to errors because of microbial growth and other contaminants in the fuel tanks. It is estimated that the new system, including a microprocessor and associated display devices, can be assembled at a cost of less than \$10,000 per fuel tank. (See page 74).

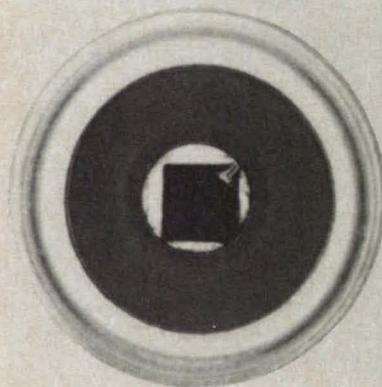
Single-Axis Acoustic Levitator With Rotation Control

An acoustic levitator with rotation control handles liquid and solid specimens as dense as steel. Conventional acoustic levitators that rotate samples in a controlled manner require three acoustic drivers in a chamber. This unit requires only one driver and a circularly symmetrical reflector. In experiments, solid spheres have been rotated as fast as 50 revolutions per second. (See page 96).

Ceramic Adhesive for High Temperatures

An adhesive consisting of a base material of fused silica and a bonding agent of magnesium phosphate can be used in aerospace, metallurgical, ceramic, electronic, and other applications. This easy-to-use adhesive successfully replaces an earlier silicone-rubber adhesive that could not withstand temperatures above 550 °F (228 °C). (See page 100).

EG&G's New HFD Silicon Detector Meets the Challenge of SPEED and GAIN but Beats the Alternative on COST.



- Speed: 16 ns rise time
- Gain: 5×10^4 V/W
- Voltage: -15V, $\pm 5V$
- Temperature and voltage stable
- Ideal for laser rangefinders, short link communications, and analytical instruments.



Available from stock



EG&G PHOTON DEVICES

35 Congress Street, Salem, MA 01970

Telephone: (617) 745-3200 TELEX: 6817405 EGGSA UW

IT'S SIMPLE...

Every single channel adjustment, from bias and record currents to replay equalization, is fully automatic—to IRIG Standards—with the simple push of a button.

WHAT DOES THAT MEAN TO YOU?

First of all, no other recorder in Storehorse's class lets you automatically calibrate and equalize up to 42 Channels. (In fact, most require you add an extra cabinet to even get 42 channels). So you save an incredible amount of time. (As much as 16 man-hours to calibrate other recorders). What would you rather do—set up tests, or run them? What's more, automatic equalization guarantees optimal record and replay characteristics—even from machine to machine. You get flat frequency response and correct phase performance on every replay.

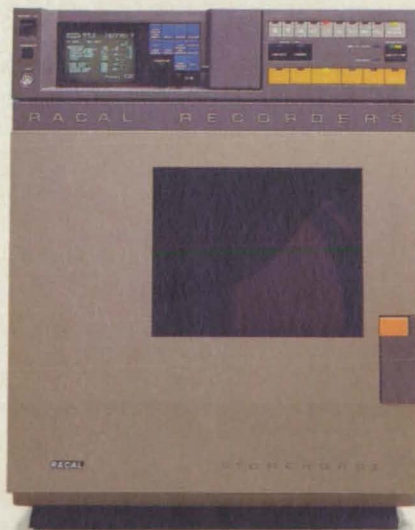
ADVANCED MONITORING AND METERING.

Storehorse's onboard Video Display Unit displays machine and tape status as well as problem diagnostics—automatically! And it lets you easily monitor input and output signals on all tracks simultaneously.

IEEE 488 AND RS232 INTERFACES—STANDARD.

The others can offer IEEE 488 and RS232 but only after you add the extra cost interfaces.

And that's not all...To find out how the Storehorse can make your tasks faster and easier, just give Shirley at Racal a call, or circle the reader service number below. It's just that simple...



Can Your Instrumentation Tape Recorder Reliably Calibrate And Equalize 42 Channels In 6 Minutes?

The Storehorse Can...

RACAL

Racal Recorders, Inc.
4 Goodyear Street, Irvine, CA 92718 USA
Telephone: (714) 380 0900
Outside Calif. Toll Free: (800) 847 1226
Telex: 170777



HOW YOU CAN BENEFIT FROM NASA'S TECHNOLOGY UTILIZATION SERVICES

If you're a regular reader of TECH BRIEFS, then you're already making use of one of the low- and no-cost services provided by NASA's Technology Utilization (TU) Network. But a TECH BRIEFS subscription represents only a fraction of the technical information and applications/engineering services offered by the TU Network as a whole. In fact, when all of the components of NASA's Technology Utilization Network are considered, TECH BRIEFS represents the proverbial tip of the iceberg. We've outlined below NASA's TU Network—named the participants, described their services, and listed the individuals you can contact for more information relating to your specific needs. We encourage you to make use of the information, access, and applications services offered by NASA's Technology Utilization Network.

How You Can Utilize NASA's Industrial Applications Centers—A nationwide network offering a broad range of technical services, including computerized access to over 100 million documents worldwide.

You can contact NASA's network of Industrial Applications Centers (IACs) for assistance in solving a specific technical problem or meeting your information needs. The "user friendly" IACs are staffed by technology transfer experts who provide computerized information retrieval from one of the world's largest banks of technical data. Nearly 500 computerized data bases, ranging from NASA's own data base to Chemical Abstracts and INSPEC, are accessible through the nine IACs located throughout the nation. The IACs also offer technical consultation services and/or linkage with other experts in the field. You can obtain more information about these services by calling or writing the nearest IAC. User fees are charged for IAC information services.

Aerospace Research Applications Center (ARAC)

Indianapolis Center for Advanced Research
611 N. Capitol Avenue
Indianapolis, IN 46204
Dr. F. Timothy Janis, Director
(317) 262-5036

Central Industrial Applications Center/NASA (CIAC)

Southeastern Oklahoma State U.
Station A, Box 2584
Durant, OK 74701
Dickie Deel, Acting Director
(405) 924-6822

North Carolina Science and Technology Research Center (NC/STRC)

Post Office Box 12235

Research Triangle Park, NC 27709

J. Graves Vann, Jr., Director
(919) 549-0671

NASA Industrial Applications Ctr.

823 William Pitt Union
University of Pittsburgh
Pittsburgh, PA 15260
Paul A. McWilliams, Exec. Director
(412) 648-7000

NASA/Southern Technology Applications Center

P. O. Box 24, Progress Ctr., One Progress Blvd.
Alachua, FL 32615
J. Ronald Thornton, Director
(904) 462-3913
(800) 354-4832 (FL only)
(800) 225-0308 (toll-free US)

NASA/UK Technology Applications Center

University of Kentucky
109 Kinthead Hall
Lexington, KY 40506-0057
William R. Strong, Director
(606) 257-6322

NERAC, Inc.

One Technology Drive
Tolland, CT 06084
Daniel U. Wilde, President
(203) 872-7000

Technology Application Center (TAC)

University of New Mexico
Albuquerque, NM 87131
Stanley A. Morain, Director
(505) 277-3622

NASA Industrial Applications Center (WESRAC)

University of Southern California
Research Annex
3716 South Hope Street,
Room 200
Los Angeles, CA 90007
Radford G. King, Acting Director
(213) 743-8988
(800) 642-2872 (CA only)
(800) 872-7477 (toll-free US)

NASA/SU Industrial Applications Center

Southern University Department of Computer Science
Baton Rouge, LA 70813
John Hubbell, Director
(504) 771-2060

If you represent a public sector organization with a particular need, you can contact NASA's Application Team for technology matching and problem solving assistance. Staffed by professional engineers from a variety of disciplines, the Application Team works with public sector organizations to identify and solve critical problems with existing NASA technology. **Technology Application Team, Research Triangle Institute, P.O. Box 12194, Research Triangle Park, NC 27709. Doris Rouse, Director, (919) 541-6980**

How You Can Access Technology Transfer Services At NASA Field Centers: Technology Utilization Officers & Patent Counsels—Each NASA Field Center has a Technology Utilization Officer (TUO) and a Patent Counsel to facilitate technology transfer between NASA and the private sector.

If you need further information about new technologies presented in NASA Tech Briefs, request the Technical Support Package (TSP). If a TSP is not available, you can contact the Technology Utilization Officer at the NASA Field Center that sponsored the research. He can arrange for assistance in applying the technology by putting you in touch with the people who developed it. If you want information about the patent status of a technology or are interested in licensing a NASA invention, contact the Patent Counsel at the NASA Field Center that sponsored the research. Refer to the NASA reference number at the end of the Tech Brief.

Ames Research Ctr. Moffett Field, CA 94035

Technology Utilization
Officer: *Laurance Milov*
Mail Code 223-3
(415) 694-6370

Patent Counsel:
Darrell G. Brekke
Mail Code 200-11
(415) 694-5104

Lewis Research Center 21000 Brookpark Road Cleveland, OH 44135

Technology Utilization
Officer: *Daniel G. Soltis*
Mail Stop 7-3
(216) 433-5567

Patent Counsel:
Gene E. Shook
Mail Code 301-6
(216) 433-5753

National Space Technology Labs.

NSTL Station, MS 39529
Technology Utilization
Officer: *Robert M. Barlow*
Code GA-00
(601) 688-1929

John F. Kennedy Space Center

Kennedy Space Center, FL 32899

Technology Utilization
Officer: *Thomas M. Hammond*
Mail Stop PT-TPO-A
(305) 867-3017

Patent Counsel:
James O. Harrell
Mail Code PT-PAT
(305) 867-2544

Langley Research Ctr. Hampton, VA 23665

Technology Utilization
Officer: *John Samos*
Mail Stop 139A
(804) 865-3281

Patent Counsel:
George F. Helfrich
Mail Code 279
(804) 865-3725

Goddard Space Flight Center Greenbelt, MD 20771

Technology Utilization
Officer: *Donald S. Friedman*
Mail Code 702
(301) 286-6242

Patent Counsel:
John O. Tresansky
Mail Code 204
(301) 286-7351

Jet Propulsion Lab. 4800 Oak Grove Drive Pasadena CA 91109

Technology Utilization
Mgr.: *Norman L. Chalfin*
Mail Stop 156-211
(818) 354-2240

NASA Resident
Technology Utilization
Officer: *Gordon S. Chapman*
Mail Stop 180-801
(818) 354-4849

Patent Counsel:
Paul F. McCaul
Mail Code 180-801
(818) 354-2734

George C. Marshall Space Flight Center Marshall Space Flight Center, AL 35812

Technology Utilization
Officer: *Ismail Akbay*
Code AT01
(205) 544-2223

Patent Counsel:
Leon D. Wofford, Jr.
Mail Code CC01
(205) 544-0024

Lyndon B. Johnson Space Center Houston, TX 77058

Technology Utilization
Officer: *Dean C. Glenn*
Mail Code EA4
(713) 483-3809

Patent Counsel:
Edward K. Fein
Mail Code AL3
(713) 483-4871

NASA Headquarters Washington, D.C. 20546

Technology Utilization
Officer: *Leonard A. Ault*
Code IU
(202) 453-1920

Assistant General
Counsel for Patent
Matters: *Robert F. Kempf*, Code GP
(202) 453-2424

A Shortcut To Software: COSMIC®—For software developed by the U.S. government contact COSMIC, NASA's Computer Software Management and Information Center. New and updated programs are announced in the Computer Programs section. COSMIC publishes an annual software catalog. For more information call or write: **COSMIC®** University of Georgia, 382 East Broad Street, Athens, GA 30602 *John A. Gibson, Dir.*, (404) 542-3265

If You Have a Question . . . NASA Scientific & Technical Information Facility can answer questions about NASA's Technology Utilization Network and its services and documents. The STI staff supplies documents and provides referrals. Call, write or use the feedback card in this issue to contact: **NASA Scientific and Technical Information Facility**, Technology Utilization Office, P.O. Box 8757, Baltimore, MD 21240-0757. *Walter M. Heiland, Manager*, (301) 859-5300, Ext. 242, 243

VisionLab II. The Vision To Understand The Unknown.

VisionLab II breaks the time barrier, with more real-time image processing features. And it breaks the price barrier, with big system performance on an economical, compatible microcomputer system.



Image analysis

New from 3M Comtal, VisionLab II's advanced design delivers exceptional true color, 60Hz, flicker-free performance, plus:

- Real-time continuous roam and zoom.
- Near real-time region of interest processing, spatial processing, convolutions, histograms and filtering.



Contrast enhancement

- A unique separate video bus, with an image-transfer rate of 36MPixels/second.
- Standard configuration of four 512 x 512 x 8-bit memory planes,

plus 640 x 512 x 1-bit overlay for graphics and icons.

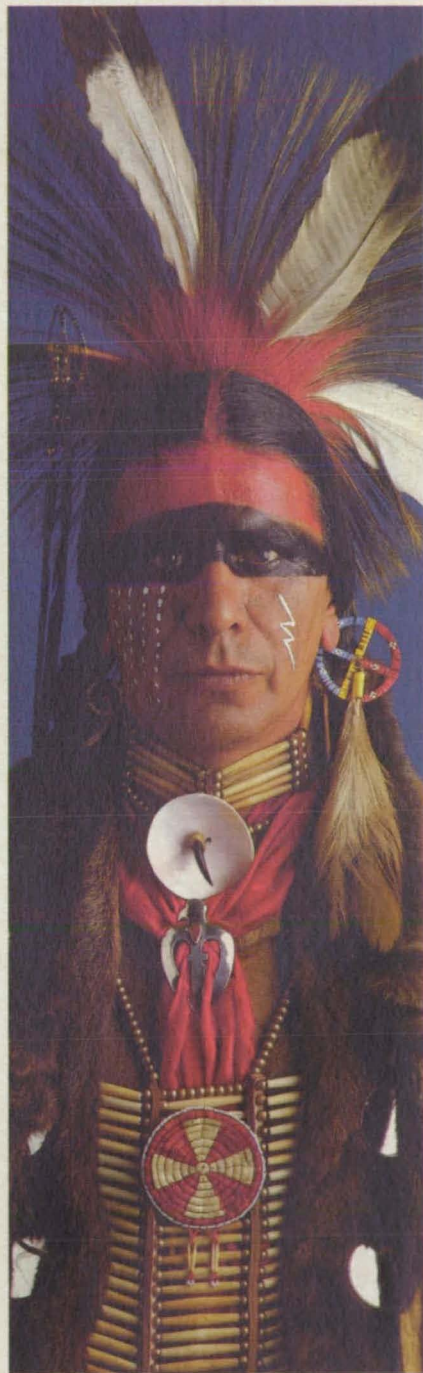
- Dynamic allocation for RGB true color operation, YMCK four color operation, or 1024 x 1024 x 8-bit, with real-time continuous zoom and overview.
- Standard and non-standard video inputs including RS170/330, NTSC and TTL.
- Genloc, with up to four programmable video inputs.
- Standard real-time data capture and optional real-time true color capture.



Zoom and pseudocolor

- Real-time spatial data compression, variable windowing, aspect ratio correction and contrast and gamma correction.

Plus much more. VisionLab II has the power and the performance to revolutionize how you utilize digital imaging. It's the kind of breakthrough you'd expect from 3M Comtal, pioneers in a New World of image processing technology.



VisionLab II

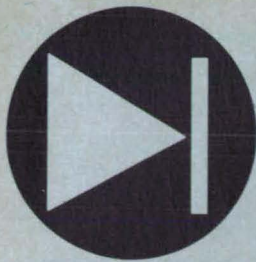
Expanding the Powers of Perception

3M Comtal

For information call today:
(800) 423-4166 • CA: (818) 441-1900

Circle Reader Action No. 319

3M



Electronic Components & Circuits

Hardware, Techniques, and Processes

- 24 Improved Flux-Gate Magnetometer
- 28 Self-Stabilizing Storage Loops for Magnetic-Bubble Memories
- 30 Diode Structure for Microwave and Infrared Applications

- 32 High-Voltage Switch Containing (DI)³ Devices
- 34 Implantable, Ingestible Electronic Thermometer
- 34 Waveguide-Horn-to-Waveguide Transition Assembly
- 36 Diffraction Analysis of Antennas With Mesh Surface

Books and Reports

- 40 Analysis of a Four-Reflector S/X-Band Antenna

Improved Flux-Gate Magnetometer

A simplified circuit drives heading indicator and senses the magnetic field of the Earth.

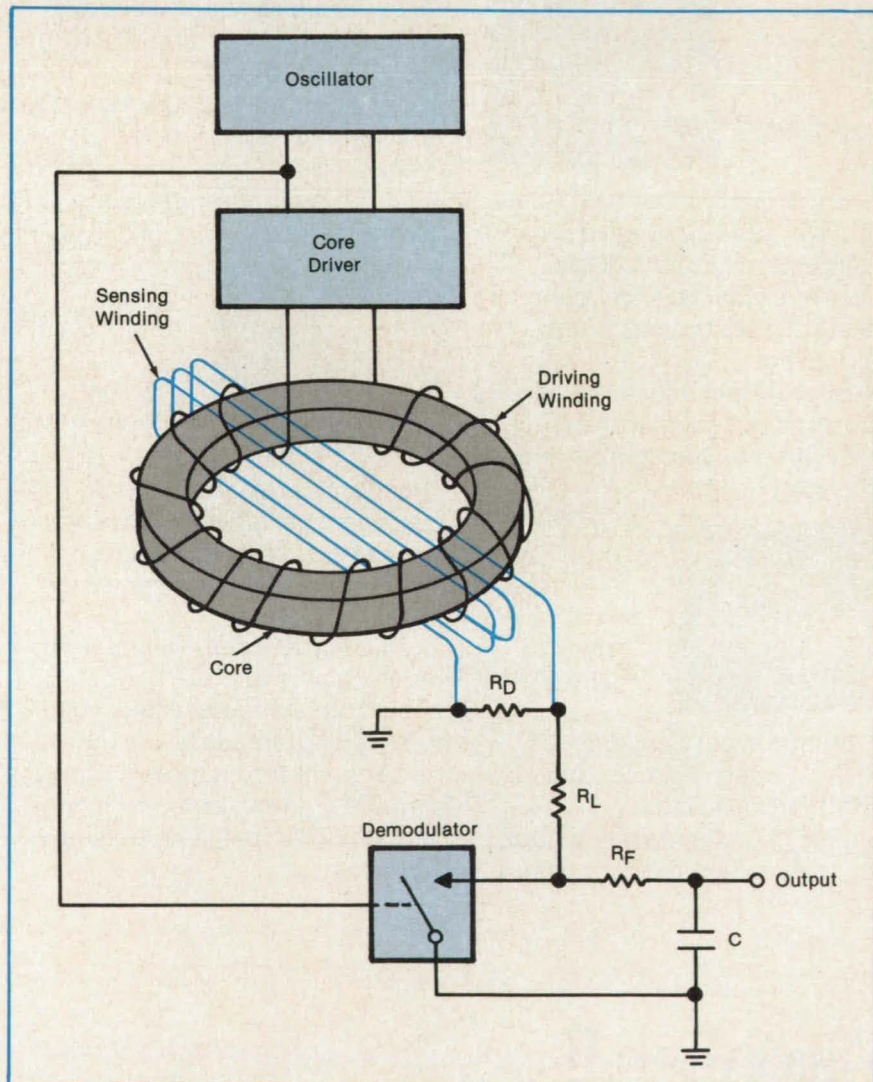
Langley Research Center, Hampton, Virginia

An unusually simple flux-gate magnetometer (see figure), which will supply a digital readout of the magnetic heading of a vehicle, has been developed to drive a heading indicator, or to supply heading information to an autopilot or to other navigational instruments. An important feature is that the core is driven into saturation in one direction only by the alternating drive voltage, which swings from zero to one polarity and back rather than from positive to negative and back as in other systems. Since only one core saturation occurs during each cycle of the driving frequency, the resulting signal from the sensing winding is predominantly at the same frequency as that of the driving voltage rather than at its second harmonic.

The square-wave voltage from the oscillator (a commercially available integrated circuit) is applied to the driving winding of the core by the core driver, which is simply a power amplifier that produces sufficient current to saturate the core and isolates the core winding from the oscillator so that the square wave from the oscillator is not distorted by the loading effect of the core winding. The demodulator is a bilateral switch — a commercially available integrated switching circuit that clamps the output of the sensing winding to ground during half of each cycle of drive voltage.

A current-limiting resistor, R_L , is placed in series with the sensing winding so that only a small current need be switched by the demodulator. Since the signal voltage from the sensing winding has predominantly the same frequency as that of the driving voltage, the demodulator may be controlled by the oscillator voltage without need for a frequency doubler. The damping resistor, R_D , is connected in parallel with the sensing winding, and its value is adjusted to damp out most of the transient oscillations of the signal pulses without materially reducing the amplitude of the original pulse.

The frequency of the oscillator may be increased in order to reduce the "dead time" between pulses and to increase the



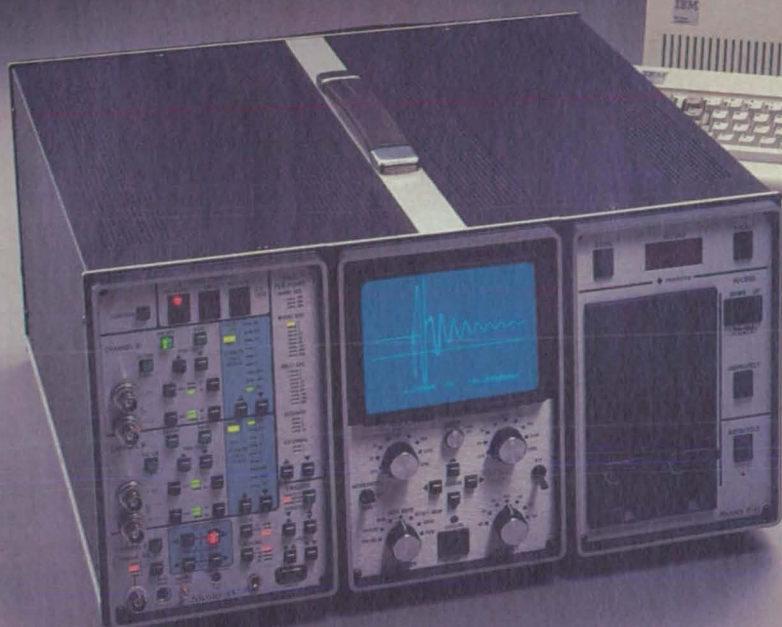
The **Simplified Flux-Gate Magnetometer** is made in part of commercially available integrated circuits.

energy content of the signal. Appreciable time is required in conventional systems for the core magnetization to traverse from one saturation region to the other when the polarity of the magnetizing current is reversed. Since the core in this system is saturated in only one direction, the core may be driven at a much higher frequency,

increasing the energy content of the signal considerably over that obtained when operating in the conventional second-harmonic mode.

In the demodulator, the square wave from the oscillator is used to close an electronic switch, clamping the signal output of the sensing coil to ground during that por-

TEAMWORK.



Combine the waveform capturing abilities of a Nicolet digital oscilloscope with the computing abilities of your IBM PC.

Connected via the RS-232 or the IEEE-488 (GPIB) interface, the power of modern signal analysis can be easily realized.

800/356-3090
or 608/273-5008

Nicolet Digital Oscilloscopes

The Scopes. Nicolet digital oscilloscopes offer ten times the accuracy and as much as one hundred times the resolution of analog oscilloscopes. A wide range of digitizer speeds provide solutions for virtually every measurement problem. Our latest plug-in module, the 4570, has 12-bit resolution at the unprecedented digitizing speed of 10 MHz. Accuracy does not have to be sacrificed for speed! Neither does sweep length. Waveforms composed of up to 16k data points are available regardless of the speed. Cursor readout of measurement values, "zoom" expansion to X256, continuously variable pretrigger data capture, and built-in disk drives all contribute to Nicolet's measurement expertise.

From low cost portables to high performance laboratory systems, Nicolet digital oscilloscopes were the first and are still the best.

Nicolet Software

The Software. Powerful, easy to use software packages are available for every Nicolet scope. Data transfers into the PC as well as mathematical data manipulation (FFT, integration, RMS, multiplication, etc.) can be accomplished without programming or computer expertise. Waveforms can be displayed on the PC screen, stored on the disk drive, and plotted on paper. The powerful new Waveform BASIC program can also operate as a waveform manipulation *language*. Using commands similar to standard BASIC, customized waveform calculations can be written quickly and easily.

Capture, analyze, store, and plot data with the convenience and ease of a Nicolet oscilloscope and Nicolet software.

Nicolet Test Instruments Division
P.O. Box 4288
5225-2 Verona Road
Madison, WI 53711-0288

NTE Nicolet
"Instruments of Discovery"

What do you ex

“Thirty man years—that’s what delivering our first automated design system would have taken using a standard workstation.”



pect for \$36,000?

"Using Symbolics, it took three."

—Patrick O'Keefe, ICAD Inc. Vice President of Technology.



ICAD Inc. is a value-added reseller who has developed one of the most advanced mechanical design systems in the world. Using the ICAD Design Language™, engineers build a knowledge base of the design specifications for complex mechanical products like airplanes and power plants. Alternate designs are then generated and evaluated in a fraction of the time it takes on CAD systems, giving ICAD's customers a strategic competitive advantage.

Three years ago, ICAD® had a concept and a customer. Their mission: to develop a sophisticated, automated design system for complex and semi-custom products. Using a Symbolics 3670™ workstation, they accomplished in three man years what they believe would have taken 30 on any other.

One reason ICAD delivered their product to market so fast was Symbolics' Genera™ software environment. It provides 40 times as many built-in facilities as systems offering just a Common

Lisp compiler. According to Patrick O'Keefe, "Symbolics' facilities are like prewritten programs. Many were essential to developing our design system, and writing them ourselves would've taken years."

ICAD's development time was further reduced by Symbolics' automatic runtime data-type checking, advanced debugging, smart garbage collection, automatic memory management, and the fastest edit-compile-debug loop available.

"These features were invaluable to program development and maintenance," said O'Keefe.

"We had to 'build' assembly configurations for specific products with hundreds of design definitions and thousands of parts. The chance of committing errors was incredibly high. Symbolics provided automatic reliability that would've taken thousands of man hours to assure on our own."

Today, because of technological advances in AI workstation development, ICAD designs similar systems and develops their products further on a

Symbolics 3620™. A low-end workstation, it starts at just \$36,000. But like the more expensive 3670 originally used by ICAD, it can process multiple operations in parallel, compact applications data, and automatically process different datatypes with built-in error detection. With it, ICAD delivers an automated design system with the fastest symbolic processing speeds available. And their customers save thousands of expensive engineering and drafting hours.

What do you expect for \$36,000? ICAD expected faster problem solving, and they got it, from Symbolics. For more information on how Symbolics can do the same for you, give us a call today.

Symbolics, 11 Cambridge Center, Cambridge, MA 02142.

1-800-237-2401, Ext. 15
In Colorado: 1-800-233-6083, Ext. 15

symbolics™

Circle Reader Action No. 446

tion of the cycle in which the core is saturated. In this case it removes the positive pulses, leaving a series of negative pulses, which, when processed by the low-pass filter consisting of R_F and C , are converted into a dc signal of negative polarity, the amplitude of which is proportional to the amplitude of the pulses and, consequently, to the intensity of the external magnetic field parallel to the centerline of the sensing coil. If the magnetometer core assembly were rotated 180° , negative pulses rather than positive pulses would be removed from the signal, resulting in a positive dc

signal.

In order to implement an electronic compass, one can use two orthogonally mounted magnetometers that share the same oscillator but have separate core drivers. Similarly, a single core with a pair of orthogonally mounted sensing coils could be used to achieve the same purpose. When this circuit is equipped with the appropriate northerly turning-error compensation system and with a single-chip microcomputer to perform the necessary computations, it offers a heading reference equivalent to that of conventional

combination of a magnetic compass and a directional gyroscope at great savings in weight, cost, and maintenance.

This work was done by H. Douglas Garner of Langley Research Center. For further information, Circle 61 on the TSP Request Card.

This invention is owned by NASA, and a patent application has been filed. Inquiries concerning nonexclusive or exclusive license for its commercial development should be addressed to the Patent Counsel, Langley Research Center [see page 22]. Refer to LAR-13560.

Self-Stabilizing Storage Loops for Magnetic-Bubble Memories

Adjacent, sinusoidal loops provide defect-tolerant, self-stabilizing structures.

Langley Research Center, Hampton, Virginia

In a self-structured magnetic-bubble memory (SSBM) device, in which magnetic bubbles are placed at small separations and strongly interact, it is necessary to provide position-stabilizing forces on all bubbles so that both propagation and stopping do not disrupt bubble positions and order. The SSBM device requires slippage (propagation) of columns of bubbles past one another with small spacings. The closeness results in strong repulsive forces between the bubbles, tending to disrupt the bubble positions. With the stan-

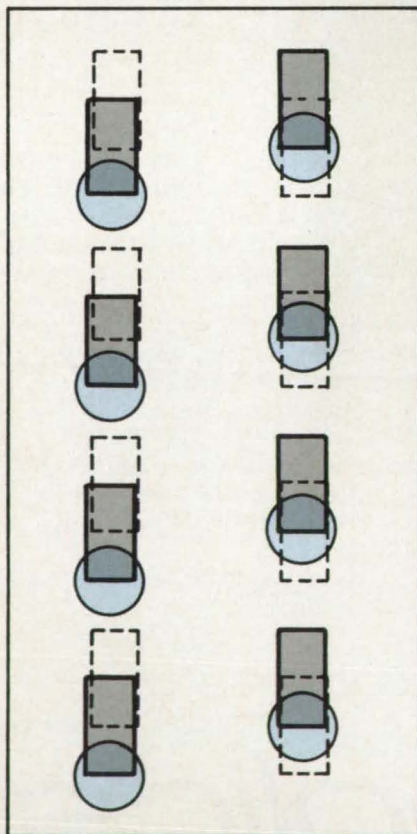


Figure 1. Magnetic Bubbles Are Never at Regular Hexagonal Spacings in the rest position with a conventional aperture.

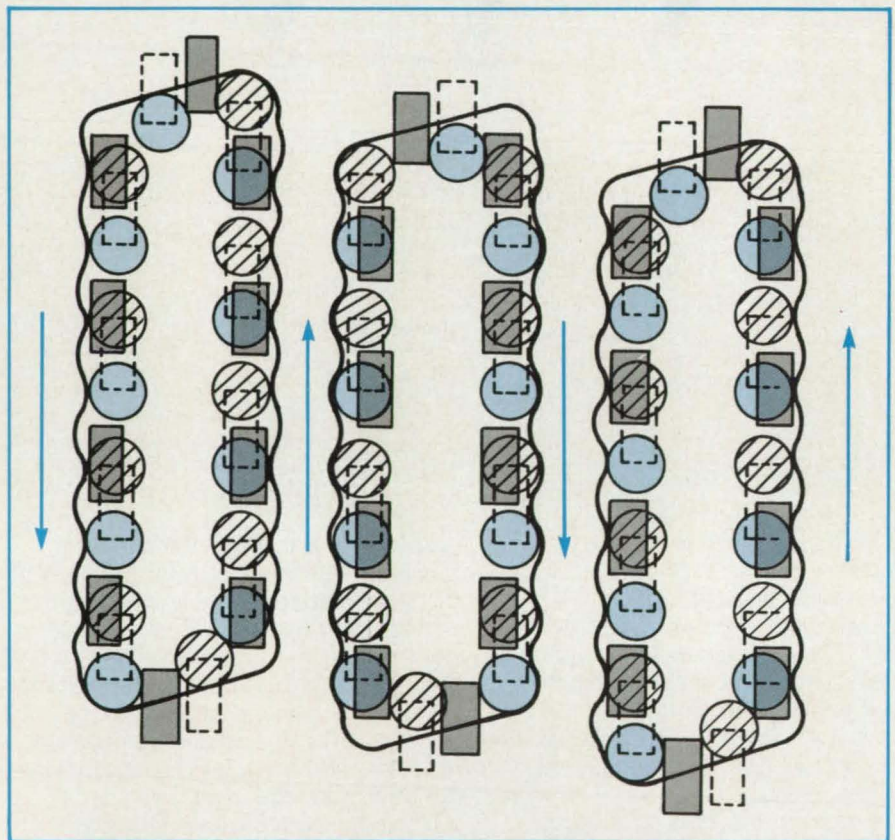


Figure 2. Counterrotating, Properly Phased Storage Loops provide additional stability by maintaining hexagonal relative positioning between adjacent columns in adjacent loops.

dard propagation-aperture positions shown in Figure 1, the bubble-propagation positions never form a hexagonal configuration, which tends to be self-stabilizing. Also, the propagation positions are never directly opposed, in which situation they would also be balanced but metastable. In addition, the repulsive forces on the bubbles tend to push the columns apart.

In an SSBM-device design in which propagation fields are provided by dual-aperture conductors, there are no magnetic features on the surface of the garnet film to position bubbles, as there would be in con-

ventional devices. Therefore, bubble-position and order stability must be provided in the absence of these magnetic features and in the presence of the potentially large destabilizing forces of the close bubbles.

A new technology consists of three components that provide self-stabilizing structures. First, the apertures are positioned so that bubbles propagate alternately into hexagonally related positions (longitudinally stable) and directly opposed positions (longitudinally metastable); the addition of straight barriers by ion milling or implantation of the garnet adds transverse

Never out of uniform.

GAF CARBONYL IRON POWDERS

GAF's Carbonyl Iron Powder particles are spherical in shape and, within any given group, uniform in size distribution, from 2 microns to 10 microns

The only ones that are domestically manufactured, GAF's Carbonyl Iron Powders find ready and broad utility in the aerospace industry in coatings and advanced composites. In addition, their wide range of uniform particle sizes, excellent high frequency absorption, and electromagnetic interference properties recommend them for use in other aerospace applications as well.

GAF's Carbonyl Iron Powders get

along famously with plastic resins, and other metals & alloys, too, like tungsten, copper and bronze. Composites with improved properties are made more easily and economically, usually with no need for additional pre-processing.

If you think GAF's Carbonyl Iron Powders may fit into your plans, our Advanced Technology and Materials Group is available for developmental work on customers' aerospace applications.

All iron powders may look the same. But GAF Carbonyl Iron Powders are always in uniform.

See for yourself. For a free sample and

literature, call or write: GAF Chemicals Corporation, Organometallics and Metals Group, 1361 Alps Road, Wayne, NJ 07470. (201) 628-3000.

©Copyright 1987 GAF Chemicals Corporation

GAF[®]

**Where specialties
are on the move**

Circle Reader Action No. 404

stability but still leaves the longitudinally metastable positions. Second, the modification of the barrier to a sinusoidal shape provides "energy wells" in the longitudinal direction at the opposed positions and eliminates the metastability. Third, the positioning and phasing of counterrotating storage loops, as shown in Figure 2, provide stable hexagonal support between the adjacent loops.

Test devices with bubbles 7 to 8 μm in di-

ameter have been fabricated and tested. Storage loops with 25- μm periodicity were successfully operated at frequencies up to 2.5 MHz, with demonstrated tolerance for fabrication defects in a major-loop/minor-loop design. Defect-tolerant, self-stabilizing behavior was obtained, in that even deliberate defects in the propagation conductors did not upset the behavior.

This work was done by Gary L. Nelson of Sperry Corp. for Langley Research Cen-

ter. Further information may be found in NASA CR-172554 [N85-22525], "Feasibility of Self-Structured Current Accessed Bubble Devices in Spacecraft Recording Systems."

Copies may be purchased [prepayment required] from the National Technical Information Service, Springfield, Virginia 22161, Telephone No. (703) 487-4650. Rush orders may be placed for an extra fee by calling (800) 336-4700. LAR-13625

Diode Structure for Microwave and Infrared Applications

Microwave signals can be switched or modulated optically.

Goddard Space Flight Center,
Greenbelt, Maryland

A planar diode with a transparent cathode can be made in GaAs, Si, and InSb versions. Depending on the specific configuration and material, such a diode could be used for the optical modulation of a microwave signal or as an infrared detector.

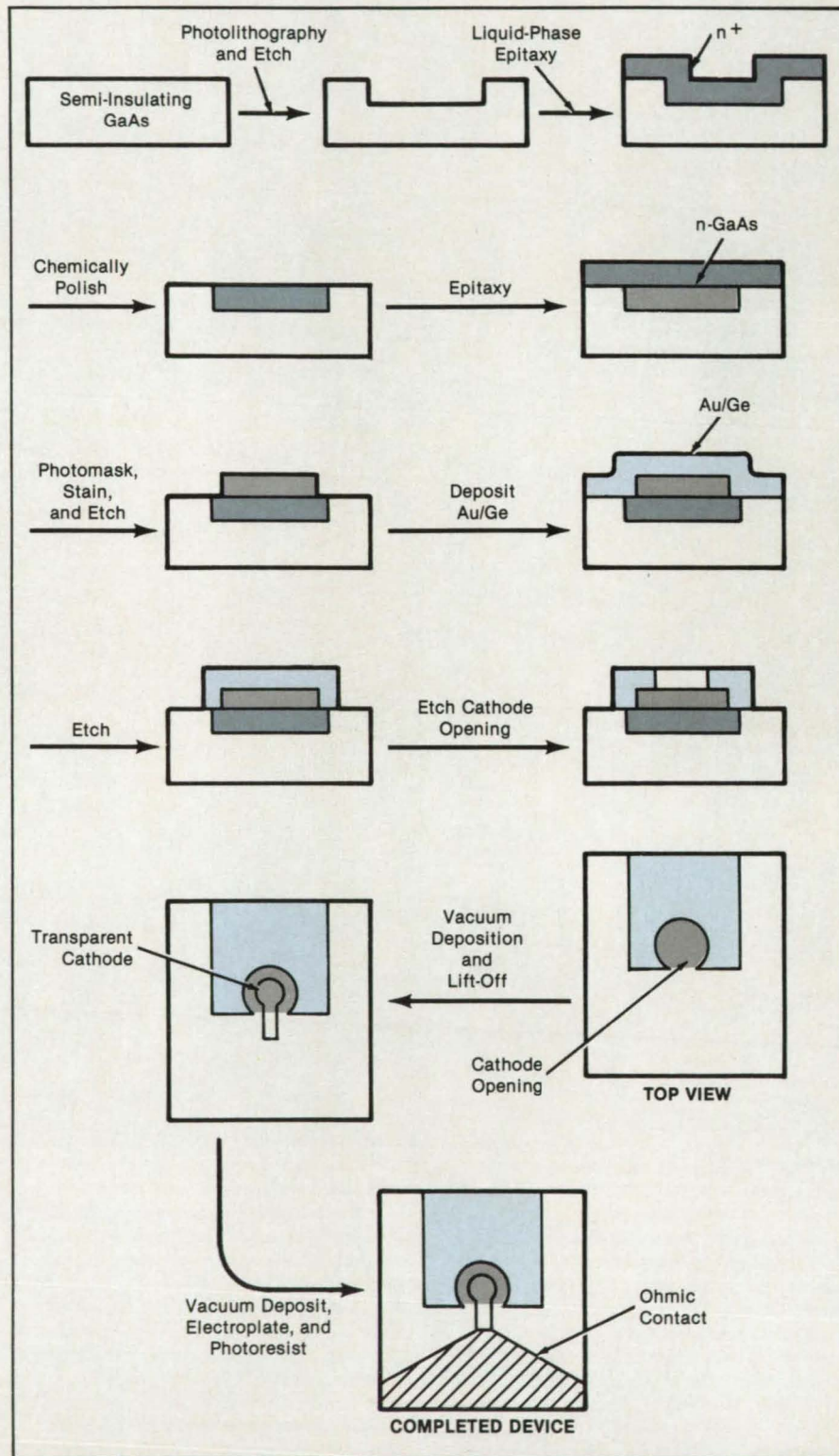
The fabrication of the GaAs version (see figure) begins with the etching of a hole about 10 μm deep into a semi-insulating, Cr-doped substrate having a resistivity of $5 \times 10^8 \Omega\text{-cm}$. An n^+ layer about 15 μm thick is grown by vapor-phase epitaxy, filling the etched hole. The wafer is then chemically polished, leaving the n^+ -filled pocket. An n-type GaAs epitaxial layer is grown on the n^+ . A mesa of n is etched completely inside the n^+ region to form an n/n^+ region.

Au/Ge is evaporated onto the device to form an ohmic contact. The Au/Ge window is etched to open up the area for the transparent cathode, which consists of Ni/Au or Au electroplated to two skin depths at the illuminating wavelength of interest. Lift-off is used to delineate the transparent cathode and the ohmic contact to the cathode.

Similar techniques are used to fabricate InSb version. Because InSb is used primarily in the infrared region, the cathode is made of Si, which is transparent to infrared.

In the Si version, single-crystal n-type Si is grown on a sapphire substrate, and native oxide is available for masking. Photoresist methods are used to open up the oxide to the diffusion of As. A layer of P-doped silicon is then grown over the n^+ pocket. The ohmic contact, cathode, and cathode contact are formed by methods similar to those for the GaAs device.

These processes yield Schottky-barrier



A **Transparent Cathode** is fabricated on a GaAs diode so that the diode can be illuminated to generate and control the short-circuit current.

Abbott Labs ▪ AC Sparkplug ▪ Adapco ▪ ALCOA ▪ Ames Laboratory ▪
 National Laboratory ▪ Ball Aerospace ▪ Bell Labs ▪ Boeing ▪ British Petroleum ▪
 Brookhaven National Laboratory ▪ Burr Brown ▪ Caltech ▪ Cambridge University ▪
 Carleton University ▪ Caterpillar ▪ Chalmers Institute ▪ CIBA-Geigy ▪ Contraves ▪
 Cooper Tire & Rubber Co. ▪ Cornell University ▪ Corning ▪ Daikin ▪ Digital
 Equipment Corporation ▪ Delco Moraine ▪ Dresser ▪ Du Pont ▪ Eastman Kodak ▪
 EDS ▪ Edwards Air Force Base ▪ Fermilab ▪ Ford ▪ Franlab ▪ Garrett Turbine ▪ G
 Aircraft ▪ GE Engine ▪ GenCorp ▪ General Dynamics ▪ General Motors ▪ Grumma
 Data ▪ Gulf Research ▪ Hewlett-Packard ▪ HIRST Research ▪ Honda ▪ Hughes
 IBM ▪ Indiana University ▪ IVECO ▪ JPL ▪ Komatsu ▪ Lawrence Livermore Labs
 Lockheed ▪ Louisiana State University ▪ Lund University ▪ Marconi Space Systems
 Marconi USL ▪ Martin Marietta ▪ Massachusetts General Hospital ▪ MATRA
 Matsushita ▪ McDonnell Douglas ▪ Michigan State University ▪ Michigan Tech
 MIT Lincoln Labs ▪ Mobil ▪ Monsanto ▪ Motorola ▪ NASA ▪ New York University
 Nihon ▪ NORCOMP ▪ Northrop ▪ NRC ▪ Old Dominion University ▪ ONERA
 Prakla Seismos ▪ RCA ▪ Rockwell ▪ Rutgers University ▪ Sandia ▪ Sanyo ▪ SERC
 Stockholm University ▪ Syracuse University
 Sumitomo ▪ TRW ▪ Tinker Air Force Base
 Triangle University ▪ Texas Instruments
 Trinity College ▪ UNOCAL
 ▪ TUCS ▪ VALVO ▪ Volvo

WHEN THESE CUSTOMERS RAN THE NUMBERS ON MINISUPERCOMPUTERS, FPS CAME OUT ON TOP.

To learn why FPS has sold more minisuper-
 computers than all other companies combined,
 call 1-800-635-0938.



Floating Point Systems, Inc., P.O. Box 23489, Portland, OR 97223
 Telex 4742018 FLOATPOIN BEAV.

Real performance.
 The facts speak for themselves.

diodes. When such a diode is operated with reverse bias and no illumination, the space-charge region is depleted of carriers, and the diode acts as an insulator. If placed in a waveguide while operating in this mode, it would thus allow a microwave signal to pass through. However if the diode is illuminated through the transparent cathode, electron/hole pairs gener-

ated by the impinging photons increase the short-circuit current: this causes the diode to present a short circuit to the incident microwave, which is thus prevented from traveling further along the waveguide.

The light can be turned on or off or it can be modulated to switch or modulate the microwave signal at high speeds. Because of the lower mobilities of charge carriers in Si,

the Si version is used at microwave frequencies lower than those of the GaAs version. The InSb device is used mainly for the detection of infrared.

This work was done by George Alcorn, Charles Leinteran, and Bing Chiang of Goddard Space Flight Center. For further information, Circle 42 on the TSP Request Card.
GSC-12962

High-Voltage Switch Containing (DI)² Devices

Series switching diodes are triggered on by passing above the threshold voltage.

Lewis Research Center, Cleveland, Ohio

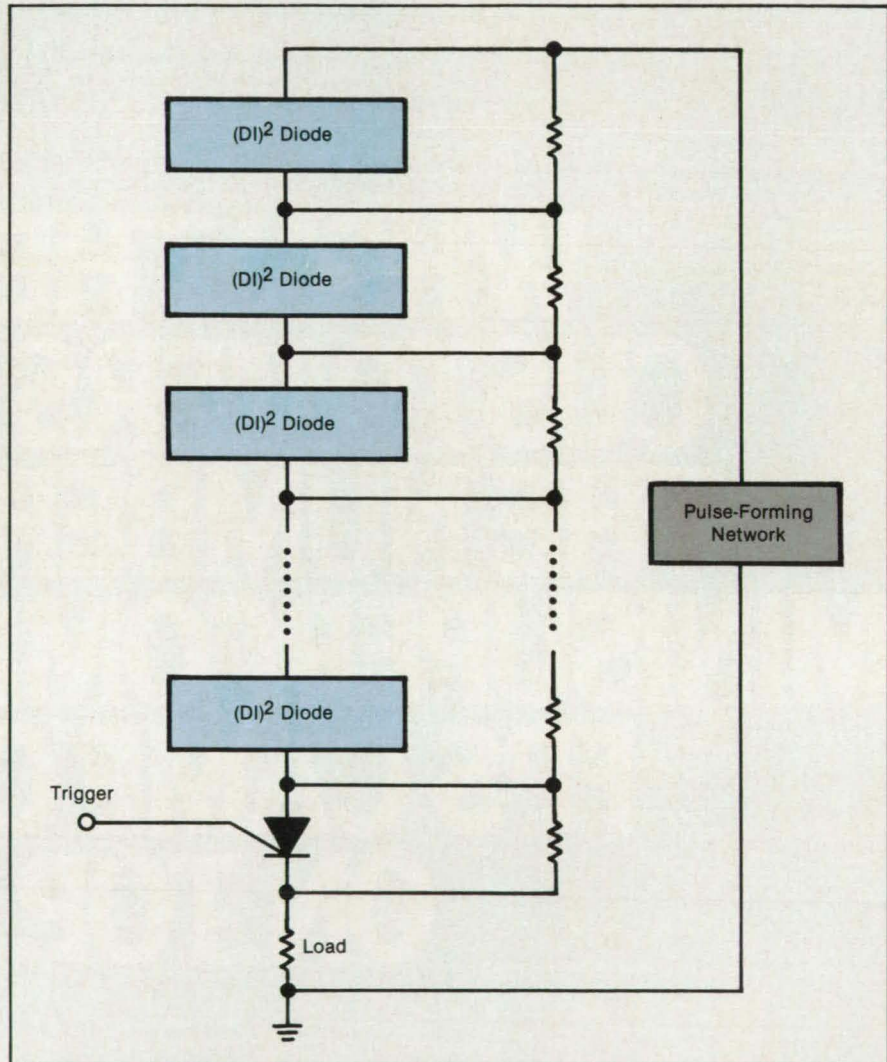
A high-voltage switch is made by connecting a multitude of deep-impurity, double-injection [(DI)²] devices in series with each other and with another, triggerable high-voltage device such as a thyristor (see figure). The triggerable device can be operated near ground potential to avoid insulation problems in the triggering circuit.

In operation, a high voltage from a pulse-forming network or other source would be applied across the high-voltage switch. This voltage would be near, but less than, the combined threshold voltages of the (DI)² devices, so that the current flowing through these devices would be small. Equal voltage sharing among the (DI)² devices and the thyristor can be assured through a resistive network in parallel with the high-voltage devices. Triggering the thyristor on causes the voltage across each of the (DI)² devices to increase to the threshold value, causing them to switch to the high-current, low-voltage mode; the entire string of devices switches to the on condition, sending a high-current pulse through the load.

Because there is no way to turn the switch off, it will continue to conduct current as long as a sufficient voltage is maintained by the voltage source. This is the conventional mode of operation of thyristor circuits.

The advantages of this type of high-voltage switch over conventional high-voltage thyristor strings are the following:

- Since only one of the devices in the series string requires a triggering signal, the difficulties inherent in sending trigger signals to those devices that are at high potentials relative to ground can be avoided.
- Because the switching of one device in a series string automatically causes other devices in the string to switch, it is unnecessary to apply trigger signals simultaneously to each device in the string, and a high degree of switch reliability is obtained.
- (DI)² devices are, at least in principle, easy to fabricate because they do not require high-voltage p/n junctions. As a re-



A High-Voltage Switch is made by cascading deep-impurity, double-injection [(DI)²] devices in series with the load and a thyristor.

sult, they are expected to be less costly to fabricate than voltage thyristors.

- (DI)² devices can be made as lateral devices on a semiconductor wafer; this would avoid the difficulties associated with double-sided diffusions and metallization required with high-voltage thyristors. It would even be possible to connect several (DI)² devices in series on a single wafer instead of separating them for indi-

vidual packages as is required for high-voltage thyristors.

- Other investigators have reported that silicon (DI)² devices are capable of operating at higher temperatures (over 400 °C) than those permissible for thyristor operation (125 °C). This characteristic would permit the use of (DI)² switches in certain high-temperature applications, where conventional silicon devices can-

BAQUS ▪ ADINA ▪ ADLPIPE ▪ AMBER ▪ AMPAC ▪ ANSYS ▪ AOS
 MAGNETIC™ ▪ APTEC IOC ▪ ARC 2D ▪ ARGUS™ ▪ ASAS ▪ ASKA™ ▪
 SKAMESH™ ▪ ASKAVIEW™ ▪ BCSLIB ▪ BEASY™ ▪ CHARMm™ ▪ COMIC
 SPI, CSP1/G™ ▪ CSSL-IV™ ▪ DIS ▪ DISCOVER™ ▪ DISPLAY II ▪ DYNA3D
 EASY 5 ▪ ECLIPSE ▪ EISI-EAL ▪ EISPACK ▪ ENDURE ▪ EOS-PAK ▪ EZBEA
 FE2000 ▪ FIDAP ▪ FIMESH ▪ FIPOST ▪ FIPREP ▪ FL022 ▪ FL052 ▪ FL057
 FL059 ▪ FLODYN ▪ FMSLIB ▪ GAMESS ▪ GAUSSIAN 82 ▪ GTSTRUDL™
 HARWELL SUBROUTINE LIBRARY ▪ HCT ▪ HSPICE ▪ HYDRA ▪ IMSL
 SOCROSS ▪ LINPACK ▪ LUSAS ▪ MARC ▪ MATH PACK ▪ MENTAT™ ▪ MOPA
 MSC/NASTRAN® ▪ NAG LIBRARY ▪ NEKTON ▪ NISAI1 ▪ NISA/FLUID
 NISAOPT ▪ ODEPACK ▪ OMNILOT ▪ PAFEC ▪ PCGPACK64™ ▪ PHOENICS
 PIGS ▪ PISCES™ ▪ POLYDATA ▪ POLYFLOW™ ▪ POLYMESH ▪ POLYPLOT
 PORES ▪ POST NEK ▪ PPLLIB ▪ PREFAS ▪ PRENEK ▪ QSPICE ▪ SACS
 SALE-3D ▪ SAM ▪ SAVFEM ▪ SCORPIO ▪ SEPS ▪ SESAM ▪ SILOS ▪ SIMU
 LATE-E ▪ SINDA ▪ SPICE ▪ SPARSPACK ▪ SPECTRAL6
 SMPACK™ ▪ SOLID ▪ STO ▪ STREAM ▪ SUPREM-3™
 TPS10 ▪ VESPA™ ▪ VIP FAMILY™
 VSAERO ▪ VSPICE

WHEN IT COMES TO MINISUPERCOMPUTER SUPPORT, THE FPS LIBRARY SPEAKS VOLUMES.

To learn what the largest library in minisuper-
 computing has in store for your application, call
 1-800-635-0938.

FPS

Floating Point Systems, Inc., P.O. Box 23489, Portland, OR 97223
 Telex 4742018 FLOATPOIN BEAV.

Real performance.
 The facts speak for themselves.

not be used.

- Other investigators have reported that silicon (DI)² devices continue to operate normally after exposure to high doses of nuclear radiation (in excess of 100 mega-rads total dose). This characteristic would permit the use of (DI)² switches in applications involving nuclear fission or fusion reactors and in military or space

applications.

This work was done by Maurice H. Hanes and Richard J. Fiedor of Westinghouse Electric Corp. for **Lewis Research Center**. Further information may be found in:

NASA TM-86957 [N85-20246/NSP], "A New Very High Voltage Semiconductor Switch" and

NASA CR-174936 [N86-30073/NSP], "Gigard-Tolerant Power Switches and Memory Elements."

Copies may be purchased [prepayment required] from the National Technical Information Service, Springfield, Virginia 22161, Telephone No. (703) 487-4650. Rush orders may be placed for an extra fee by calling (800) 336-4700. LEW-14390

Implantable, Ingestible Electronic Thermometer

The frequency of an oscillator varies with temperature.

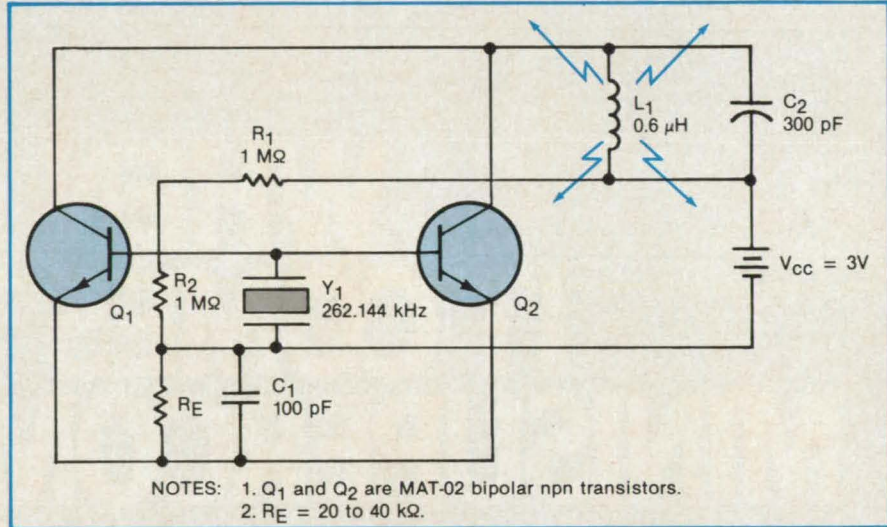
Goddard Space Flight Center, Greenbelt, Maryland

A small quartz-crystal-controlled oscillator would be swallowed or surgically implanted to provide continuous monitoring of a patient's internal temperature. A receiver placed near the patient would measure the oscillator frequency, and the temperature would be inferred from the previously determined variation of frequency with temperature.

The oscillator circuit (see figure) includes a quartz crystal that has a nominal resonant frequency of 262,144 Hz and that is cut in the orientation that gives a large linear coefficient of frequency variation with temperature. In this type of circuit, the oscillation frequency is controlled primarily by the crystal as long as the gain-bandwidth product is at least about 4 times the frequency. In this case, the chosen component values yield a gain-bandwidth product of 1 MHz.

The oscillator frequency is extremely stable, in part because of the way the circuit is biased. Resistors R_1 and R_2 establish the quiescent point at half the power-supply voltage to assure the symmetry of the oscillations. This symmetry combines with a sufficiently low gain to prevent hard limiting of the oscillations, which would otherwise cause noise, frequency instability, and loss of output power.

The output is taken from the combined collector terminals that are connected to L_1 and C_2 , a parallel resonant combination with a high ratio of inductive reactance to resistance (high Q). The inductive current is therefore relatively high and provides



The **Frequency of the Crystal-Controlled Oscillator** varies with temperature. The circuit can be made very small and implanted or ingested to measure internal body temperature.

sufficient signal strength for reception outside the body at typical distances of 1 m or less.

Inductor L_1 can be made very small: 100 to 200 turns with a diameter of 3/16 in. (4.8 mm) and a length of 1/2 in. (12.7 mm). Although the figure shows two transistors in parallel, one could be used (to reduce power consumption) or three could be used (to boost the output). Power for the oscillator can be supplied by lithium cells, which are very small and can last at least 100 hours at a current drain of 0.1 mA.

The general oscillator circuit can be used to measure temperatures from -10 to $+140$ °C. A unit made for use in the hu-

man body from about 30 to 40 °C operates at $262,144 \pm 50$ Hz with a frequency stability of 0.1 Hz and a temperature coefficient of 9 Hz/°C: thus, the temperature readings are accurate within $0.1/9 \approx 0.01$ °C.

This work was done by Leonard Kleinberg of **Goddard Space Flight Center**. For further information, Circle 64 on the TSP Request Card.

This invention is owned by NASA, and a patent application has been filed. Inquiries concerning nonexclusive or exclusive license for its commercial development should be addressed to the Patent Counsel, Goddard Space Flight Center [see page 22]. Refer to GSC-13037.

Waveguide-Horn-to-Waveguide Transition Assembly

A microstrip-to-waveguide transition is integrated with a waveguide-horn antenna element.

Lyndon B. Johnson Space Center, Houston, Texas

The integration of a microstrip-to-waveguide transition and a waveguide-horn antenna element overcomes two major problems of previous systems: (1) the need to assemble two subassemblies dur-

ing manufacture and (2) the need for a mechanical design that overcomes the inherent structural weaknesses associated with joining two subassemblies. The new horn/transition antenna element also

allows for an end launch into the waveguide for easier mechanical and electrical connections. The antenna element operates by coupling electromagnetic energy from the environment through the horn to

MACSYMA

automates symbolic mathematics.
And yields enormous improvements in
speed, accuracy and modeling power.

If you work with quantitative models in scientific or engineering disciplines, MACSYMA can increase your modeling power. MACSYMA combines symbolic and numeric computation. And enables you to accurately manipulate symbolic expressions in a fraction of the time required manually.

Wide range of capabilities

MACSYMA offers the widest range of capabilities for symbolic computations in applied mathematics of any commercially available program. For example:

Algebra: MACSYMA can manipulate large expressions, expand, simplify and factor expressions, handle matrices and arrays, and solve systems of equations.

Calculus: MACSYMA can differentiate, perform definite and indefinite integration, take limits, expand functions in Taylor or Laurent series, solve differential equations, and compute Laplace transforms.

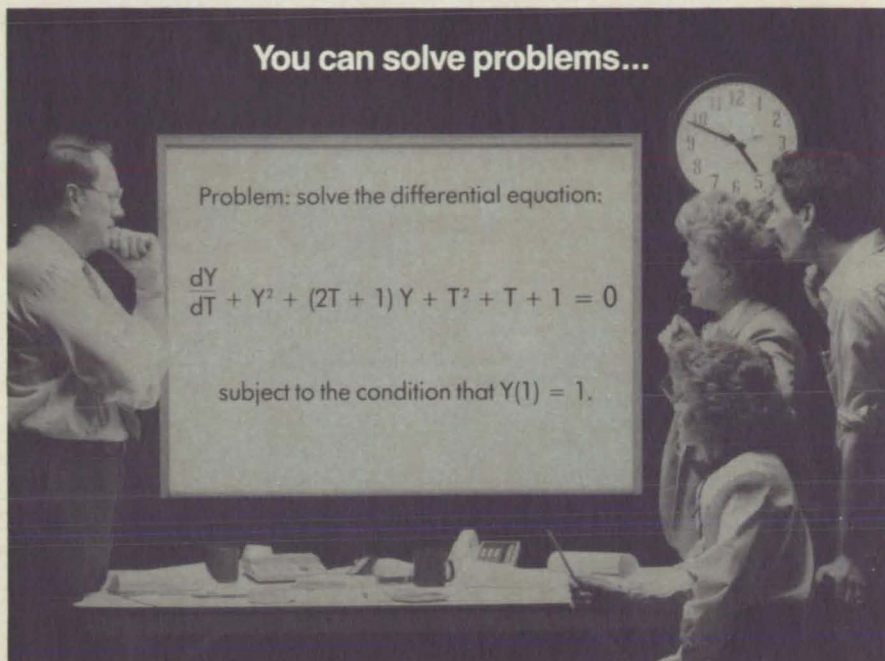
Numerical analysis: You can perform numerical analysis using MACSYMA® language, compute with arbitrary precision arithmetic, use a library of numerical analysis routines, and generate FORTRAN code.

Graphics and interfaces:

MACSYMA can generate report-quality graphics in 2D or 3D, with perspective, hidden line removal, and captions. MACSYMA also interfaces with the mathematical text processors 'TeX' and 'troff'.

Broad base of applications

Throughout the world thousands of scientists, engineers and mathematicians are using MACSYMA in such diverse applications as aeronautical design, structural engineering, fluid mechanics, acoustics, CAD, electronic and VLSI circuit design,



You can solve problems...

Problem: solve the differential equation:

$$\frac{dY}{dT} + Y^2 + (2T + 1)Y + T^2 + T + 1 = 0$$

subject to the condition that $Y(1) = 1$.

Symbolically...

```
(C1) DEPENDS(Y,T)$
(C2) DIFF(Y,T) + Y^2 + (2*T+1)*Y + T^2 + T + 1;
(D2) dY/dT + Y^2 + (2T+1)Y + T^2 + T + 1
(C3) SOLN:ODE(D2,Y,T);
(D3) Y = - (%CT %E^T - T - 1) / (%C %E^T - 1)
(C4) SOLVE(SUBST([Y=1, T=1],D3),%C),NUMER;
(D4) [%C = 0.5518192]
(C5) SPECIFIC SOLN:SUBST(D4,SOLN);
(D5) Y = - 0.5518192 T %E^T - T - 1 / 0.5518192 %E^T - 1
```

and Numerically.

```
(C6) FORTRAN(D5)$
      Y = -(0.5518192*T*EXP(T) - T - 1)
      1 / (0.5518192*EXP(T) - 1)
```

electromagnetic field problems, plasma physics, atomic scattering cross sections, control theory, maximum likelihood estimation, genetic studies, and more.

Available on many computer systems

Current systems include:

- Symbolics 3600™ Series
- VAX & MicroVAX II
- SUN-2 & SUN-3
- Apollo
- Masscomp

Other versions will be following soon.

For an information kit about all the ways MACSYMA can work for you, just call

1-800-MACSYMA.

In Mass., Alaska or Hawaii only, call (617) 621-7770.

Or please write to us at
Computer-Aided Mathematics Group
Dept. M-NA1
Symbolics, Inc.
Eleven Cambridge Center
Cambridge, MA 02142

MACSYMA

The most comprehensive software for
mathematical computing.

symbolics™

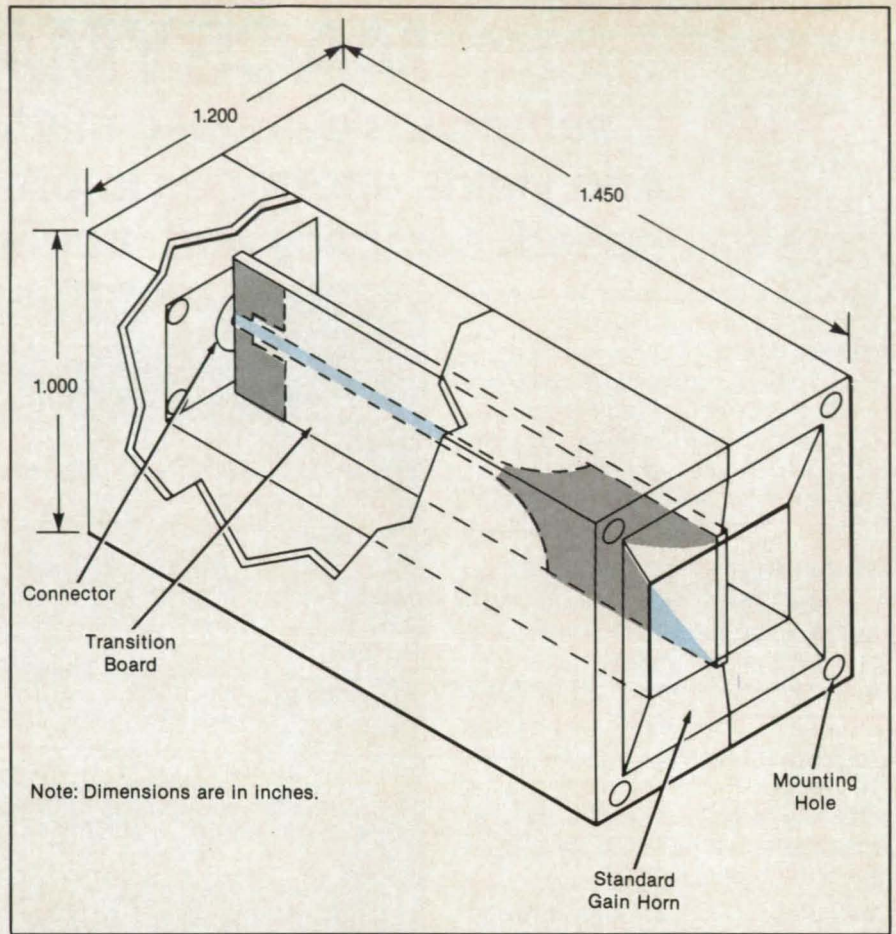
MACSYMA®, Symbolics, Symbolics 3600 are trademarks of Symbolics, Inc. VAX and MicroVAX II are trademarks of the Digital Equipment Corporation. SUN-2 and SUN-3 are trademarks of SUN Microsystems, Inc. Apollo® is a trademark of Apollo Computer, Inc. Masscomp is a trademark of the Massachusetts Computer Corporation. TeX is a trademark of the American Mathematical Society. © Copyright 1987 Symbolics, Inc.

the connector at the other end via the microstrip-to-waveguide transition.

The transition assembly (see figure) includes an inner printed circuit positioned between the halves of an appropriately shaped split metal block. When the block halves and the printed circuit are assembled, one end of the block forms a waveguide-horn antenna element. The other end of the assembly can be joined to a microstrip or coaxial transmission line, depending on the type of connector used.

This work was done by Shayla E. Davidson of **Johnson Space Center** and Roland W. Shaw, Jeffery K. Kovitz, George W. Raffoul, and Larry A. Johnson of Lockheed Corp. No further documentation is available.
MSC-21146

The **Integrated Waveguide-Horn/Microstrip-to-Waveguide Transition Assembly** couples electromagnetic energy through the horn and transition board to the connector.



Diffraction Analysis of Antennas With Mesh Surfaces

A strip-aperture model replaces a wire-grid model.

NASA's Jet Propulsion Laboratory, Pasadena, California

The application of large reflector antennas for satellite communications, such as the third-generation Land Mobile Satellite system concept and ground terminals, has resulted in the use of mesh surfaces, because of their light weight, reduced wind effects, and unfurlability. An accurate performance analysis of these mesh reflectors for various applications demands that the effects of the mesh be properly accounted for in the vector diffraction analysis. This is done by modifying the solid-surface physical-optics-induced current as shown in the block diagram of Figure 1.

The far-field radiation pattern of an antenna with a mesh reflector is calculated more accurately with a new strip-aperture model than with a wire-grid model of the reflector surface. The strip-aperture model is more adaptable than the wire-grid model to a variety of practical configurations and is decidedly superior for reflectors in which

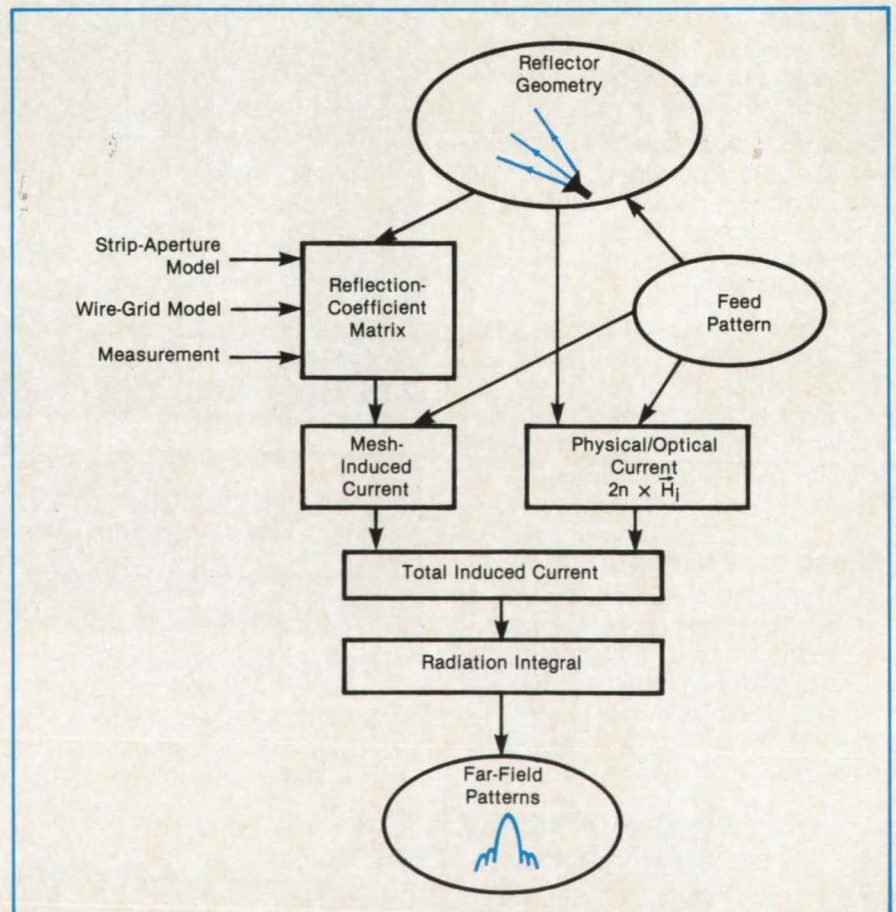


Figure 1. The **Computation of the Far-Field Radiation Pattern** requires the modification of the current previously assumed to be induced on a solid antenna surface, to account for the effects of the mesh.

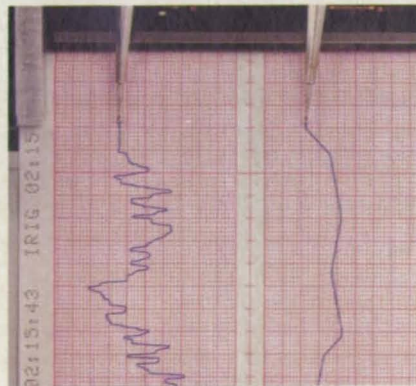
When he goes up to push the envelope, you don't have a split second to waste.



In a test pilot's critical world of action, that split second can mean the difference between life and death. When you're monitoring the parameters that keep test pilots flying, you can't afford the delays inherent to some recording systems.

Gould recording systems, such as the 3000 series and the new MK 200A, show what's happening on board, as it happens. No delay. No questions. A moving pen or video monitor informs you instantaneously about changes in pressure, temperature, pitch, vibration — all the human and mechanical parameters so critical to flight testing.

Highly reliable, rugged Gould strip chart recorders have been the standard in the aerospace industry



for over 40 years. More than 100,000 channels are currently in use.

Fully programmable and remote controllable, both the 3000 and the new MK 200A carry on this tradition, giving you matchless Gould trace

quality, IRIG/NASA time code interfacing, and choice of configurations.

So, before you make a decision on telemetry display equipment, flight test the new MK 200A or the other Gould oscillographic strip chart recorders and emulators. They're built on the premise that you don't have a split second to waste.

For more information on real-time recording systems, call **1-800-GOULD-10**, or write Gould Inc., Test and Measurement, 3631 Perkins Avenue, Cleveland, Ohio 44114.



GOULD
Electronics

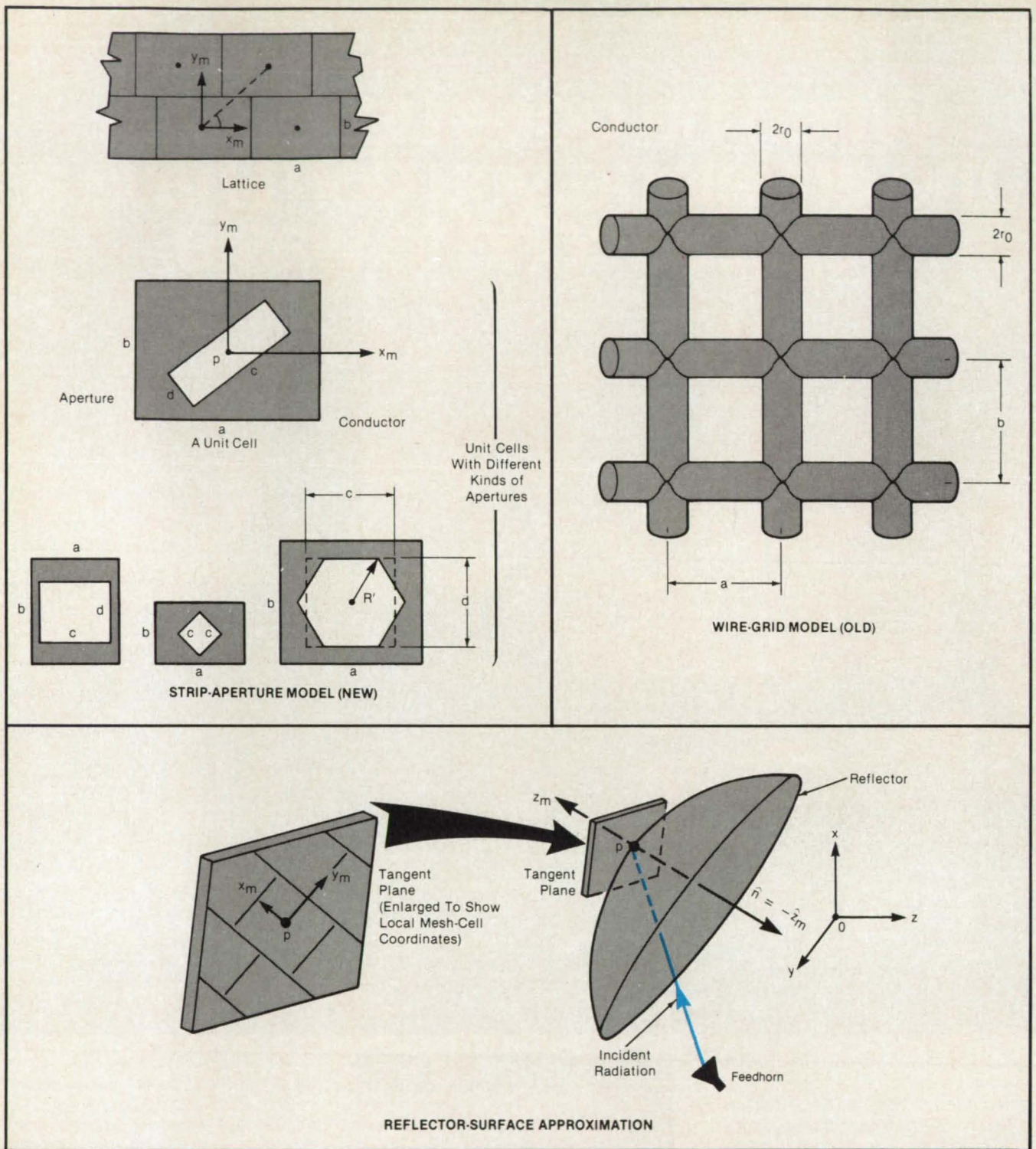


Figure 2. The **Strip-Aperture Model** (top left) of a mesh antenna reflector surface is used in place of the older, wire-grid, model (top right). The strip-aperture model is more easily adapted to a variety of mesh configurations and gives more accurate results for some practical antennas. The reflector surface (bottom) is approximated locally by a tangent plane over which the local aperture structure extends periodically.

the mesh-cell width exceeds the mesh thickness. Unlike the wire-grid model, the strip-aperture model satisfies the reciprocity theorem (relating to the interchangeability of sources and receptors of the electromagnetic field).

The new model (see Figure 2) is applied where the mesh cells are no larger than about a tenth of a wavelength. This small cell size permits the use of the simplifying approximation that the reflector-surface current induced by the electromagnetic

field is present even in the apertures. The approximation is particularly useful in calculating the far field.

Instead of treating the surface-current problem in the full spatial complexity of the mesh, the effect of the apertures is incorporated into the equations for an equivalent current pattern induced on a smooth reflector surface. A matrix of transmission and reflection coefficients is used to calculate the effect of the apertures on the surface current. To obtain the coefficients, the strip-

aperture model is applied in the following way:

- Each point on the reflector surface is treated as an infinitesimal part of a plane tangent to the reflector at that point.
- The incident electromagnetic field is approximated by a plane-wave incident upon the plane along a direction from the antenna feedhorn to that point.
- The local strip-aperture structure is repeated periodically over the entire plane. Because of the periodic nature of the

● *Special Introductory Offer For
Apollo, H-P, and Sun Users*

Ada NOW

New Alsys Toolset For 68000 Ada Builds Unique Project Environment

Organizations serious about the 680X0 architecture, and serious about working with the government, want a lot more than just validated Ada compilers. They want quality solutions; production quality compilers and quality programming tools.

Just what Alsys offers. Alsys' new 68000 Ada Developer's Toolset includes:

- **AdaProbe**, a unique source-level symbolic debugger and program viewer;
- **AdaXref**, an inter-unit cross-referencing utility;
- **AdaReformat**, a pretty printing tool for reformatting source files to selectable conventions; and
- **AdaMake**, an automatic recompilation facility.

Consider, too, all those special Ada "manager tools" that are part of the Alsys Version 3 compilation system: the Family Manager, the Unit Manager, and the Library Manager.

Together, they implement the new

Alsys Multi-Library Environment that allows teams of programmers to share thousands of logically organized compilation units.

Alsys 68000 compilers are in a class by themselves; highest code quality, maturity, reliability, robustness, superior optimization technology, unexcelled error messages... And now, with the new development tools, they are at the core of an Ada project environment unique in the industry.

Here is our special **INTRODUCTORY OFFER**. Between now and October 31, 1987, order any of our 68000 Ada compilers and we will include the complete Toolset **FREE**. AdaProbe, AdaXref, AdaReformat, AdaMake.

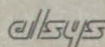
Ada is NOW. Alsys solutions are NOW. Call or Write.



Alsys, Inc. • 1432 Main Street • Waltham, MA 02154 • U.S.A. • Phone: (617) 890-0030
Offer valid in U.S.A. and Canada, only.

NTB 10/87

The Many Facets of
Quality



_____ YES, I'm interested in your Introductory Offer. Send more information on the Toolset and your 68000 compilers.

_____ Send me your free brochure, *The Many Facets of Quality*.

Name _____

Company _____

Address _____

City _____ State _____ Zip _____

Phone _____

Alsys, Inc. • 1432 Main Street • Waltham, MA 02154

mesh, the effect of the surface current on the scattering of the electromagnetic field is expressible in terms of spatial harmonics (aperture modes). Because the apertures are small compared to the wavelength, only a few of the aperture modes need to be calculated to obtain an accurate result.

Like the wire-grid model, the strip-aperture model can be used to study the

performances of many mesh-reflector antennas. In addition, the strip-aperture model can be applied to reflector surfaces perforated with circular holes. Effects that can be investigated include the generation of cross-polarized fields, gain as a function of cell size, the reduction of directivity by surface power dissipation, and other far-field phenomena that are affected by the spati-

ally varying, vector nature of the surface current.

This work was done by Yahya Rahmat-Samii of Caltech for NASA's Jet Propulsion Laboratory. For further information, Circle 9 on the TSP Request Card. NPO-16474

Books and Reports

These reports, studies, handbooks are available from NASA as Technical Support Packages (TSP's) when a Request Card number is cited; otherwise they are available from the National Technical Information Service.

Analysis of a Four-Reflector S/X-Band Antenna

Physical optics accounts for the near field, cross polarization, and higher-order modes.

A report presents a physical-optics analysis of the four-reflector, 64-m antennas of the Deep Space Network. The excellent agreement of the results with the measured properties (e.g., gain, beam shape, and beam offset angle) of the actual antennas is taken as an independent

validation of the algebra and computer code used. This appears to be the first time such a complete and rigorous analysis has been performed on such a complex antenna system.

Because the analysis is thorough and detailed, the report also has instructional value as an example for designers of large microwave dishes with subreflectors and involving reflector surfaces with hyperboloidal, paraboloidal, ellipsoidal, and more complex shapes. The analysis accounts fully for all near-field, cross-polarization, and higher-order-mode-generation effects caused by various asymmetries in the antenna structure and operation. The analysis procedure could be useful in ground-station-antenna design efforts, including the design of high-efficiency shaped reflectors and beam waveguide feeds, and in microwave metrology (holography) applied to the measurements of large reflector surfaces.

The analysis of the four-element, 64-m design proceeds element by element. The far-field diffraction patterns of the feed-horn, ellipsoidal reflector, dichroic mirror, and asymmetric subreflector are computed in turn by physical-optics integrations, using the results from each element as input for the next element. Finally, the far-field diffraction pattern of the symmetric main reflector is computed. The near-field diffraction patterns are calculated from the far fields with the help of a spherical-wave expansion.

In view of the success with the 64-m system, the analysis will be extended to designs that upgrade the antennas to 70-m diameter.

This work was done by Alan G. Cha of Caltech for NASA's Jet Propulsion Laboratory. To obtain a copy of the report, "Physical Optics Analysis of Four-Reflector Antenna," Circle 124 on the TSP Request Card. NPO-16839

LIXI[®] MICROFOCUS — over 100X magnification on CCTV.



Detecting solder voids and solder balls under leadless carrier in a surface mount device.

Find even the smallest defects before they find you.

Lixi's real-time X-ray and portability mean instant inspection on line. You can adjust your processes before bad products fill the pipeline. More than a quality control tool, LIXI MICROFOCUS is your competitive edge in a tough market.

Send us a defective sample - we'll return a picture of the defect.



Better than a fixed cabinet type X-ray system - better image, greater magnification and lower cost. (Model shown LX-85-708 with optional accessories.)

Lixi, Inc.
1438 Brook Drive
Downers Grove, IL 60515, USA
(312) 620-4646
Telex: 6871077 DKROB
Telefax: (312) 620-7776



©1987 Lixi, Inc.
LIXI is a trademark of Lixi, Inc.

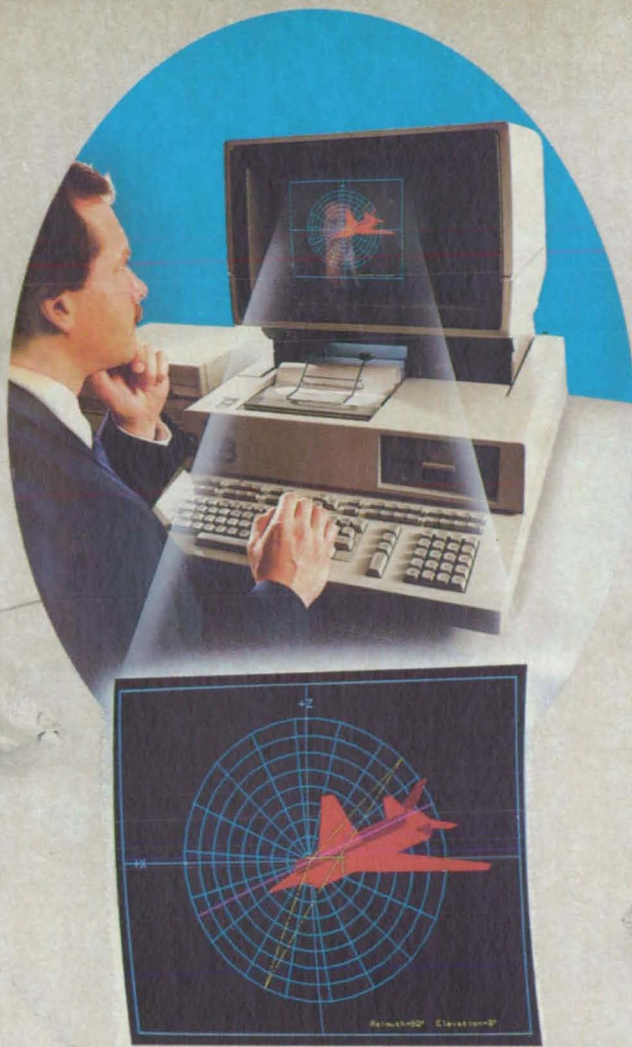
New Products

A new technology for producing light-control thin films has been developed by the **GM Research Laboratories (GMR)**, Warren, MI. This new class of films, the GMR version of which is known as Varilux, consists of submicron liquid crystal droplets dispersed in a polymer. The potential usefulness of these polymer-dispersed liquid crystal films stems from their ability to electrically switch from an opaque "off state" to a transparent "on state." They also can be fabricated in various sizes and shapes, and thus are candidates for a wide variety of electro-optic applications. **Circle Reader Service Number 599.**

Designed for robotics applications and other machine vision analysis systems where high-speed parts recognition is crucial, the T123A compact CCD camera from **NEC America** (Wood Dale, IL) includes a two-step selectable electronic shutter that can freeze action at 1/60th or 1/1000 of a second. The monochrome camera provides 512 horizontal by 492 vertical pixels for high quality images. Resolution is 380 horizontal TV lines and 350 vertical lines. It measures 1-3/4 inches wide, 1-3/4 inches high and 4-5/8 inches deep. **Circle Reader Service Number 598.**

A solid state camera system, suitable for machine vision applications, has been introduced by **Newport Coporation**, Fountain Valley, CA. The V-SSC-37 system is based on a CCD camera that detects light through an array of silicon photodiodes integrated into a solid state circuit substrate. Individual photodiodes are accurately positioned by the manufacturing process, eliminating geometric drift and distortion. The system monitor includes capability for switchable underscan, allowing the operator to view all pixels in the field of view. **Circle Reader Service Number 597.**

A new quick-connect fitting from **Gates Rubber Company** (Denver, CO) simplifies installation of fuel, transmission and other hose lines on engine configurations with limited access. The push-on female connection has a steel spring retainer that interlocks with the formed end of the male tube. Fluoroelastomer O-rings in the retainer provide a tight seal, and the push-on connector is interchangeable with industry standard male ends. The entire assembly is highly resistant to chemical, temperature and vibration extremes. **Circle Reader Service Number 583.**



THE CHOICE for Software Engineering

Vitro assures the best value for your program by providing innovative technical and management approaches at a reasonable cost. These features have made us the choice since 1948.

Technical

- Structured Methodology
- Innovative Approaches
- Experienced
- Reliability

Management

- Responsive
- Project Control
- Quality Assurance
- Management Tools

Cost

- On Schedule
- On Budget
- Efficient
- Actual Cost Tracking

Vitro, the choice again and again. We stand ready to deliver for you. Ask us how we can meet your needs. Call our Business Development Office at (301) 231-1300 or write: Vitro Corporation, 14000 Georgia Avenue, Silver Spring, MD 20906-2972.

Systems Engineering



Software Engineering

The Art of Management / The Science of Engineering

A Unit of the Penn Central Federal Systems Company

Circle Reader Action No. 394



Electronic Systems

Hardware, Techniques, and Processes

- 42 Interface Circuit for Laser Doppler Velocimeters
- 44 Ultrasonic Ranging System With Increased Resolution
- 46 Binary-Symmetry Detection

- 47 Optical Design and Signal Processing for Edge Detection
- 47 Central Processor Acts as High-Speed DMA Controller

Books and Reports

- 48 Predicting False Lock in Phase-Locked Loops

Interface Circuit for Laser Doppler Velocimeters

A new circuit displays more information to the user and provides higher data-collection rates.

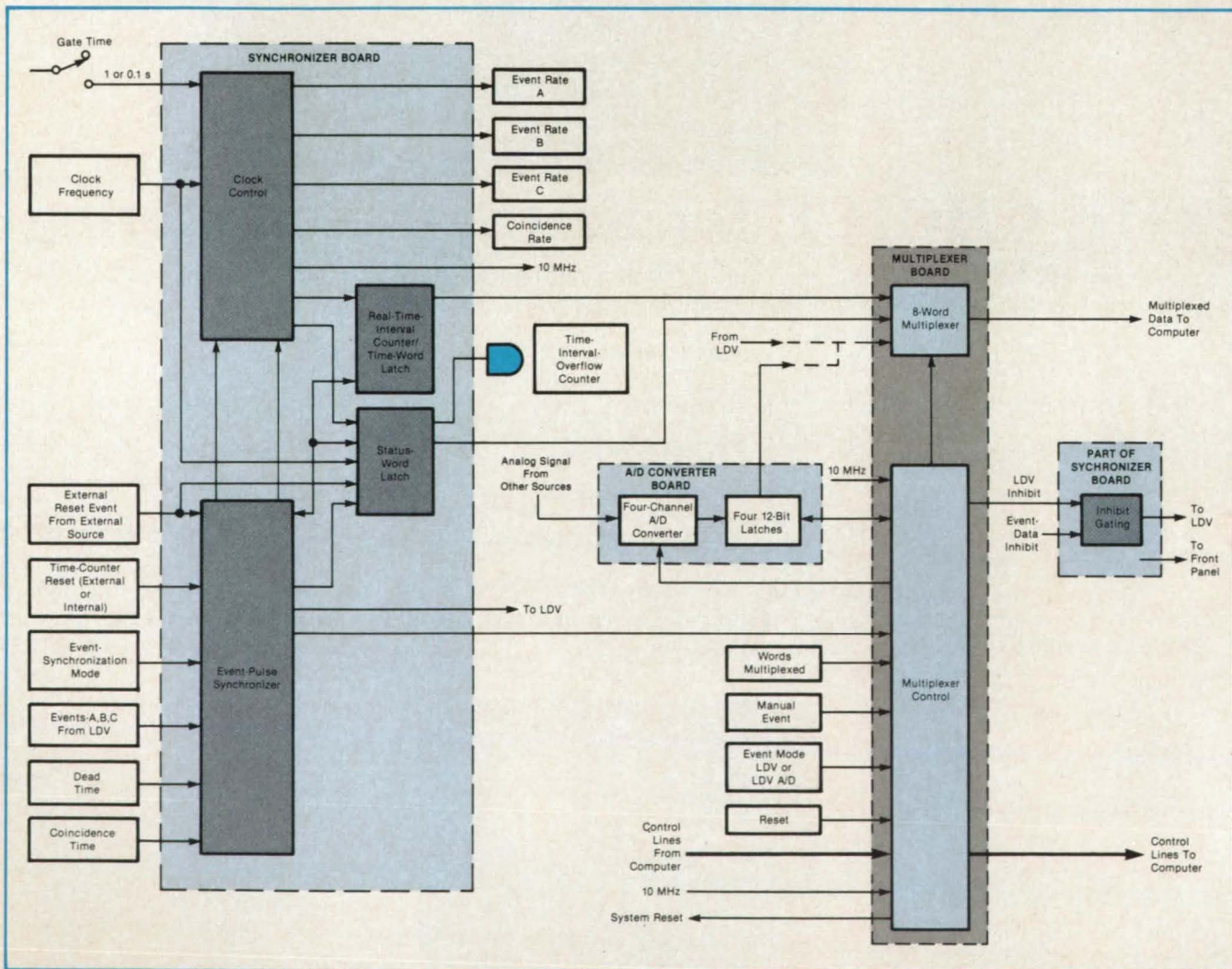
Ames Research Center, Moffett Field, California

The laser-Doppler-velocimeter (LDV) interface circuit shown in the figure provides higher data-collection rates and more detailed display of status information than do commercially-available LDV interfaces. The displays and user controls facilitate adjustments of measurement parameters during measurements. Syn-

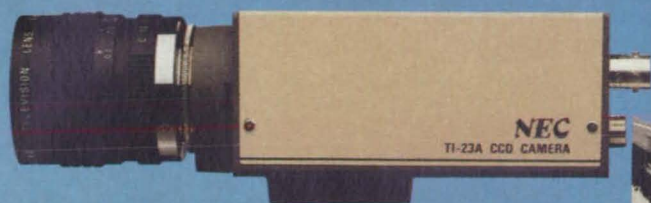
chronizing circuits control the processing of LDV signals arriving at random times on different inputs. The interface can provide data to a minicomputer in a variety of formats. Improved data-transfer control ("handshaking") logic increases the rate of data transfer to the computer.

LDV's are used to measure velocity

components of airstreams in wind tunnels without perturbing the flows with mechanical probes. In an LDV, an interference-fringe pattern is created in a small measuring region in the flow by two intersecting laser beams. Light is scattered from dust particles entrained in the flow as they pass across the fringes. The



This **Interface Circuit** facilitates the coupling of laser-Doppler-velocimeter outputs to a computer for analysis. The interface circuit enables the user to select a variety of intermediate data-processing options, including clock frequency, coincidence channel combinations, coincidence times, dead times, digital or analog output, and channels to be analyzed.



The first ultra-compact CCD camera with high-speed electronic shutter.

*Sharpen your image at 1/1000th
of a second.*

The TI-23A captures clear images of fast moving objects with its 250,000 image-sensing elements and its 1/1000th of a second electronic shutter.

By providing high-quality images for computer input, the TI-23A raises the efficiency of entire image processing systems.

And it's small enough

(1-3/4" x 1-3/4" x 4-3/4" long) to fit right into your machine vision or surveillance application.

The CCD chip contains 512(H) x 492(V) pixels. There is no burn-in, no geometric distortion, and minimal lag. Non-interlace scanning facilitates image processing. Features include an external sync input, auxiliary pulse output and switchable gain/gamma characteristics.

The rugged TI-23A monochrome CCD camera is at home in industrial environments. It resists shock and vibration, and is immune to electromagnetic interference. The CCD sensor, unlike tubes, requires no periodic maintenance.

Efficient image processing starts with high-quality input. Sharpen your image right now. Get clarity at 1/1000th of a second with the TI-23A.



For further information, please contact:

NEC America, Inc.
Broadcast Equipment Division.
1255 Michael Drive, Wood Dale, Illinois 60191
Tel: 312-860-7600

NEC

Circle Reader Action No. 369

scattered light is detected by a photomultiplier. The repetition rate of the photomultiplier-output pulses is therefore a measure of the velocity component of the particles across the fringes.

It is often desirable to process several LDV signals simultaneously to give a more complete description of the flow field being studied. The new interface can process three analog or digital LDV inputs simultaneously, each producing pulses at arbitrary intervals.

The interface circuit includes a multiplexer section and a synchronizer section, both of which include switches and indicators located on the front panel. The multiplexer board holds a multiplexer-control circuit and an 8-word multiplexer. The synchronizer board includes an

event-pulse synchronizer, a clock control, a real-time interval/time-word latch, and a status-word latch.

The front panel has three six-digit displays for indicating the pulse-rate data for three input channels from an LDV. A fourth display indicates coincidence rates among the inputs. Potentiometers enable the user to control the timing intervals used in defining coincidences.

The user can also select clock frequencies in multiples of 10, from 100 Hz to 10 MHz. A time-interval-counter overflow indicator lights up if the interval counter reaches its limit before an event is detected. This warning assists the user in selecting the clock frequency that gives the best resolution.

The multiplexer receives Doppler

pulses from the three LDV channels and rate data from the clock control. The multiplexer converts these inputs to a single 16-bit output, which is fed to the input terminals of the computer. The user can select the particular Doppler-event and rate data to be transmitted to the computer.

This work was done by Dean R. Harrison and James L. Brown of Ames Research Center. For further information, Circle 102 on the TSP Request Card.

Inquiries concerning rights for the commercial use of this invention should be addressed to the Patent Counsel, Ames Research Center [see page 22]. Refer to ARC-11536.

Ultrasonic Ranging System With Increased Resolution

The master-oscillator frequency is increased.

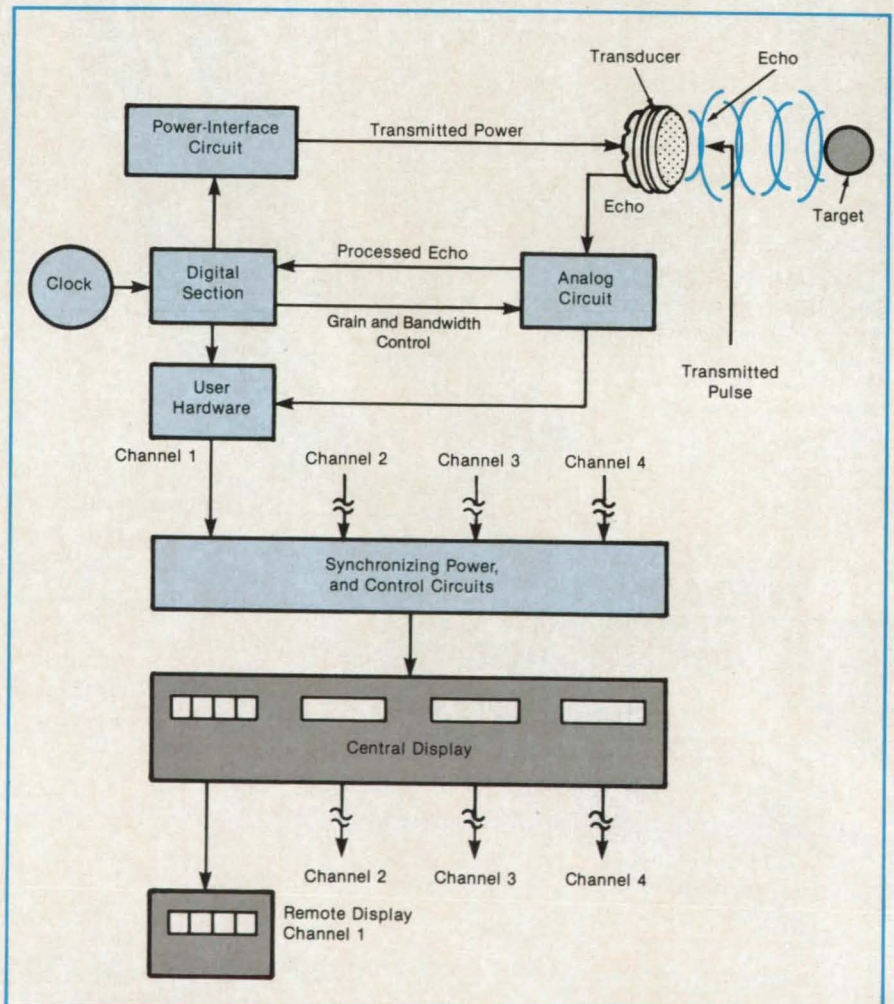
Lyndon B. Johnson Space Center, Houston, Texas

An ultrasonic range-measuring system (see figure) with 0.1-in. (2.5-mm) resolution provides a continuous digital display of four distance readings, each updated four times per second. The four rangefinder modules in the system are modified versions of the rangefinders used for automatic focusing in a commercial series of cameras. The ultrasonic pulses emitted by the system are innocuous to both people and equipment.

Each rangefinder module includes a capacitive transducer that both emits and detects ultrasonic pulses. The distance from the transducer to the target is determined by counting the number of cycles of an oscillator that occur between the emission of a pulse and the detection of its echo. The resolution of the rangefinder was increased by increasing the oscillator frequency so that each cycle corresponds to a range increment of 0.1 in. (2.5 mm) rather than the original 0.1 ft (30.5 mm). The basic characteristics of the measuring circuits as manufactured would permit the improvement of resolution to about 0.01 in. (0.25 mm) by increasing the oscillator frequency further. Temperature compensation could be applied to the oscillator circuit to make the range measurements independent of the variation of the speed of sound with temperature.

Synchronizing circuits gate the operation of the rangefinder transducers so that each transducer channel responds only to its own emitted pulses. The transducers are mounted in machined enclosures to protect them from physical damage and to narrow their beams to prevent the inadvertent returns of signals from other objects near the intended beam.

The system was developed to speed



The **Ultrasonic Range-Measuring System** includes four commercially available rangefinder modules that have been modified to provide higher range resolution and an increased measurement-repetition rate.

payload installation in the Space Shuttle. Installed on the payload-handling mechan-

ism, it provides continuous remote monitoring of the payload position without con-

X-ray...
our only
business

Rigaku's

Thin Film Diffractometer Attachment

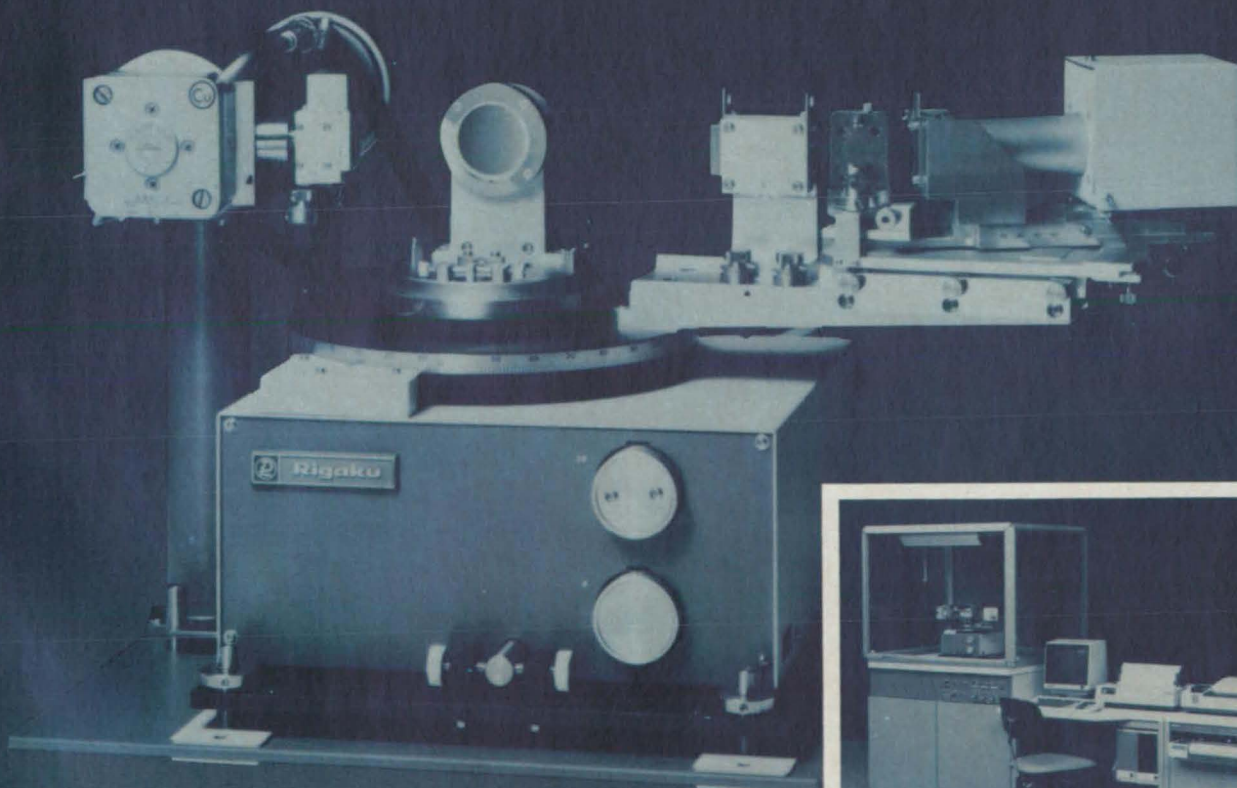
...Throwing light
on 100Å film.

X-ray diffractometry of thin films, which has so far been exceedingly difficult, is now possible with Rigaku's Thin Film Attachment.

Up to now, obtaining a sharp X-ray diffraction profile of a thin film has been a problem; the extremely thin sample weakens the intensity of the diffracted rays, resulting in relatively low signals and high backgrounds. Moreover, since the conventional diffractometer is designed for a θ - 2θ coupled scan, intense diffracted rays from the substrate material overwhelm the diffracted rays from the thin film sample, making it difficult to obtain reliable data.

The dilemma has now been solved by newly developed optics from Rigaku (pat. pend.). Used in conjunction with our wide angle diffractometer, the Thin Film Attachment employs a low-angle incidence method with parallel beam optics that increase the diffraction intensities of thin film samples. A scan system for 2θ alone and an intraplane sample rotation mechanism enhance efficiency. Rigaku has thus made thin film measurement feasible with only the X-ray flux available from a conventional sealed-off X-ray tube.

Throwing light on 100Å... only Rigaku has the technology to make it happen!



D/Max-B Wide Angle Diffraction System

 **Rigaku**

For information write or call: Rigaku/U.S.A., Inc.,
3 Electronics Ave., Danvers, Mass., 01923, U.S.A.
Telephone: (617) 777-2446

Circle Reader Action No. 513

tact with either the payload or the vehicle. Previously, cargo installation was a slow, iterative process requiring repeated small movements alternating with manual position measurements. In addition to use in other cargo-handling situations, the sys-

tem could provide economical solutions to such distance-measurement problems as those posed by a boat approaching a dock, a truck backing toward a loading platform, runway-clearance readout for the tail of an airplane with a high angle of attack, or a

burglar alarm.

This work was done by William E. Meyer and William G. Johnson of Rockwell International Corp. for **Johnson Space Center**. For further information, Circle 135 on the TSP Request Card. MSC-21090

Binary-Symmetry Detection

Transmission errors for zeros and ones are tabulated separately.

Goddard Space Flight Center, Greenbelt, Maryland

When dealing with a digital binary data-transmission system, a priori assumption is made of the existence of a binary symmetrical channel for most calculations. The prediction and computation of the probabilistic bit-error performance of a given system is based on this assumption and on the postulate of equal probability for the transmitted logical ones and zeroes. The present bit-error measurements provided by commercially available test sets simply lump or totalize all errors, masking a wealth of information about the performance of a system.

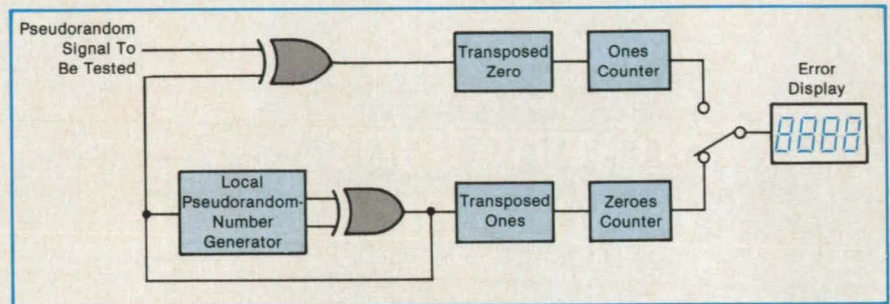


Figure 1. An **Early Test Set** correlated errors by exclusive-or gating with the bit-delayed version of the test signal.

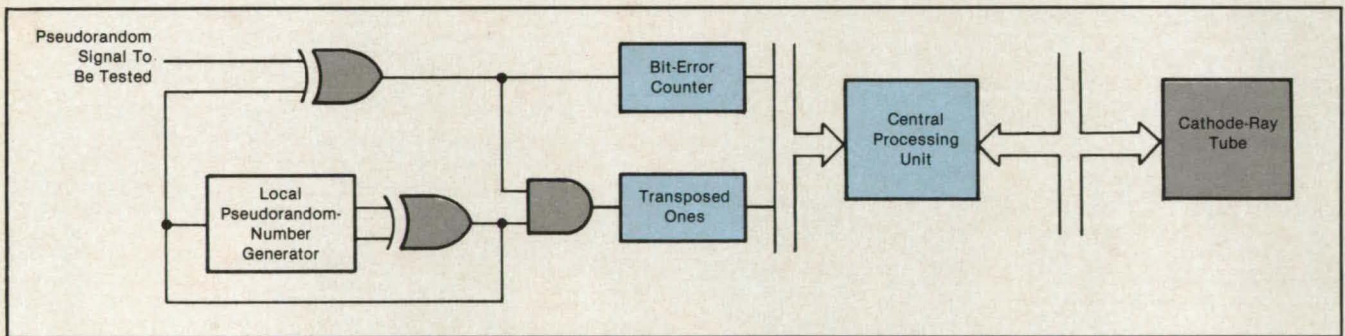


Figure 2. A **Bit-Error-Rate Tester** of the new type includes the symmetry feature.

The probability of error in digital transmission systems can be calculated by $P_e = (1/2) \operatorname{erfc} [(E_b/N_0)^{1/2}]$, (where E_b is the energy per bit, and N_0 is the noise energy during a bit period) for a memoryless uncoded channel in the presence of additive white Gaussian noise, with the corollary assumption that the channel is binary symmetrical. The errors that result when binary data are sent through the noisy channel are in fact logical transpositions (inversions) of the transmitted logical elements sent. For example, each transposition with an equal probability of occurrence for the well-behaved, model channel is depicted by the binary-symmetry model.

The judicious examination of the detected errors and whether the logical ones were transposed into zeroes and, conversely, the zeroes transposed into ones can reveal the nature of the system impairment. It follows that any binary asymmetry thus detected can be correlated to equipment imbalances or inability to match the channel.

The binary-symmetry detector employs the pseudo-random data pattern used as a

test message coming through the channel, which message is then modulo-2 added to the locally generated and synchronized version of the test data pattern in much the same manner found in the manufactured test sets of today. In the early Nascom test-set version, the errors thus detected were correlated by exclusive-or gating with the bit-delayed version of the pattern to resolve the ambiguity of the error (see Figure 1). Steering flip-flops are then used to route the detected ones or transposed zeroes to a separate counter from the zeroes or transposed ones. A binary symmetrical channel will show nearly a 50-percent ones to 50-percent zeroes correspondence. The degree of the asymmetry represents imbalances due to either the modulation, transmission, or demodulation processes of the system when perturbed by noise.

The advent of microprocessors has made this binary-symmetry detection easier to depict by graphing the asymmetry on a cathode-ray tube. This measurement is normally made such that a dynamic channel performance can be viewed without disturbing the basic bit-error performance

computation.

Asymmetry-anomaly-characterization and -detection circuits are not commercially available in off-the-shelf test sets. A typical bit-error-rate tester (BERT, as they are commonly denoted) was built by Nascom with symmetry-detection circuitry as depicted in Figure 2. The new test-set model 610, developed by the NASA Communications Division under contract with Astrotronics, Inc., includes all features found in commercially available BERT's, plus the symmetry feature. Moreover, the symmetry detection is displayed on the self-contained 5-in. (12.7-cm) cathode-ray tube. The display scrolls the channel symmetry as a function of test time. It is envisioned that this method be included as a feature in all commercial test sets to aid in the troubleshooting of digital binary transmission systems.

This work was done by Hiram Lopez of **Goddard Space Flight Center**. For further information, Circle 51 on the TSP Request Card. GSC-12985

Optical Design and Signal Processing for Edge Detection

The number of edge-detection computations is reduced by a factor of 100.

Langley Research Center, Hampton, Virginia

As in human vision, most current approaches to machine vision include edge detection as an initial processing step. The optimal edge-detection response for machine vision closely approximates the spatial response of human vision and is given by the difference-of-Gaussian (DOG) function.

Spatial filtering in the computer requires large (up to 31-by-31) filter masks to approximate the DOG function satisfactorily. This technique offers a design approach to approximate this function closely with only a 3-by-3 element mask, thereby reducing the number of required computations by as much as a factor of 100. This is accomplished by properly combining optical design, including lens apodization, with the signal-processing algorithm as depicted in Figure 1. Figure 2 demonstrates that the resultant response $\tau(x,y)$ closely approximates the DOG-function response.

The desired response can be obtained either by parallel processing of signals from a large number of neighboring photo-sensor elements (i.e., a large mask) or, with a minimal amount of processing, by appropriately shaping the spatial-frequency response of the objective lens. Various combinations of optical design and signal processing algorithms can be used. For example, to increase sensitivity, it may become necessary to increase the lens aperture diameter beyond the diameter (and hence beyond the cutoff frequency) that provides the best realizable spatial response. It would then be advantageous to defocus the optical system.

The importance of this concept lies in the realization that the optical design and the signal-processing algorithm can be combined to approximate closely the optimal edge-detection response with a minimal amount of processing. The processing can be done either in the computer or in the focal plane of the sensor-array image-gathering system. If the processing is done

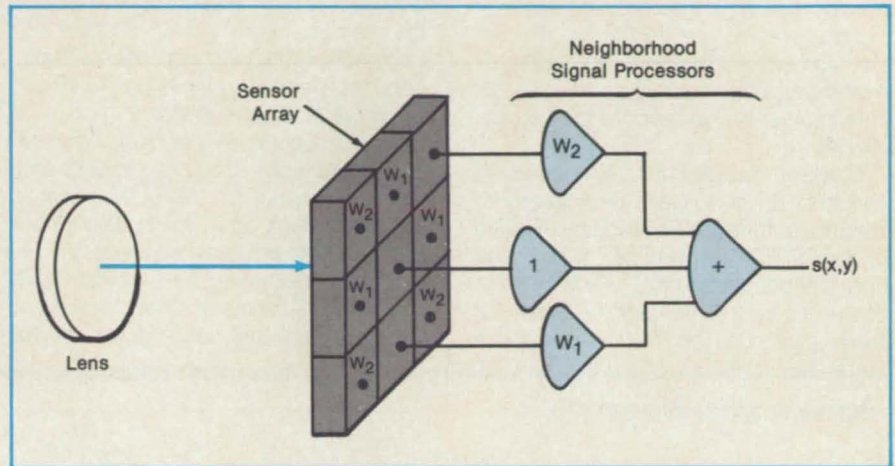


Figure 1. Properly combining the optical design with a 3-by-3 Element Mask reduces the number of required computations by a factor of as much as 100.

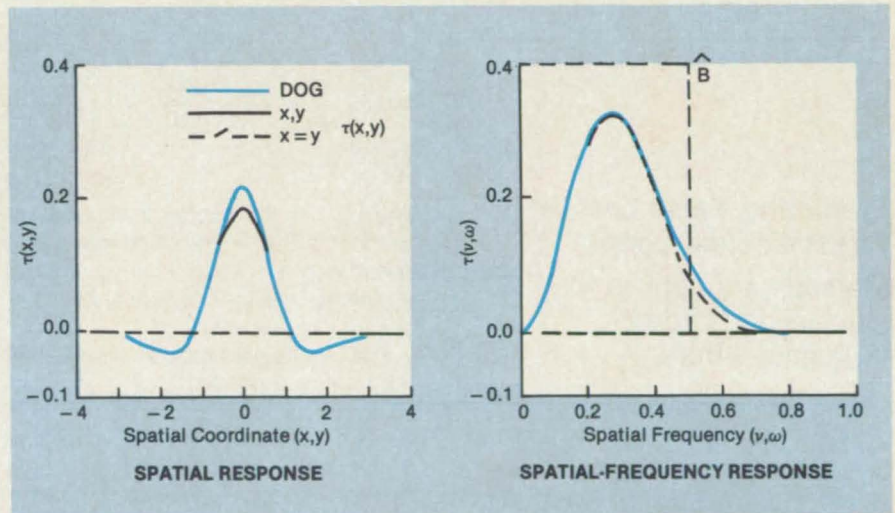


Figure 2. These Spatial and Spatial-Frequency Responses are obtained in the system of Figure 1 by the combination of the optical design and the signal-processing algorithm. These curves closely approximate difference-of-Gaussian-function response.

in the focal plane, then the dynamic range required for analog-to-digital conversion, and the amount of data that must be transmitted are both substantially reduced.

This work was done by Friedrich O.

Huck of Langley Research Center and Kathryn Stacy of Computer Sciences Corp. For further information, Circle 146 on the TSP Request Card. LAR-13416

Central Processor Acts as High-Speed DMA Controller

Maximum transfer rates are achieved with a reduction in cost and complexity.

Langley Research Center, Hampton, Virginia

A computer-system architecture enables the system host central processor (CP) to make high-speed, direct-memory-access (DMA) data transfers without the cost and complexity of adding a dedicated DMA controller. Typically, to obtain maxi-

imum rates of data transfer, a dedicated DMA controller is used. In a typical non-DMA transfer, the CP performs at least two bus cycles to move the data word and another bus cycle to read the status word (which indicates that another data word is

ready to be transferred). As a result, the transfer rate is far lower than that provided by a DMA-type transfer. The new design is a hybrid of these two former methods that eliminates the disadvantages of both.

With the new system, the CP is used as

the DMA controller, obviating the need for a dedicated DMA controller; yet the maximum transfer rates are equivalent to those obtained with a dedicated DMA controller. The CP has access to the memory, as in a conventional configuration. The CP address bus addresses the memory, and the read/write (R/W) line controls the direction of data flow both at the RAM and through the bidirectional buffers. The buffer is enabled and the memory transaction occurs through the activation of the CP data strobe.

Similarly, the CP has direct access to peripheral devices. Again, the bidirectional data-bus buffers are enabled and directed by the CP R/W line, and data flow to and from the peripheral device. The transaction at the peripheral device is a normal read or write as controlled by R/W, ad-

dress, select, and data strobe. Thus, the CP has access to the peripheral device for initialization or for use in the non-DMA mode.

A bidirectional bus buffer is inserted into the data bus between the CP and the local bus. This arrangement enables data to flow directly between the peripheral device and the memory, while the CP supplies the necessary addresses and control signals. This is conveniently done with a MOVE and autoincrement instruction.

The concept is fairly general in nature, and applications should be widespread. This system may be useful wherever a dedicated DMA controller is desired because of required data-transfer rates but is impractical because of cost and complexity or where it is not necessary to perform DMA transfers and concurrently use the

CP for other tasks. A typical application would be where it is desirable to absorb incoming data at a rate that is greater than the CP could otherwise handle. The CP would place the data by DMA into its local memory for later use, enabling the system to connect to high-speed external equipment that otherwise would require the addition of a dedicated DMA controller.

This work was done by Matthew S. Blaha of The Charles Stark Draper Laboratory, Inc. for Langley Research Center. For further information, Circle 1 on the TSP Request Card.

Inquiries concerning rights for the commercial use of this invention should be addressed to the Patent Counsel, Langley Research Center [see page 22]. Refer to LAR-13497.

Books and Reports

These reports, studies, handbooks are available from NASA as Technical Support Packages (TSP's) when a Request Card number is cited; otherwise they are available from the National Technical Information Service.

Predicting False Lock in Phase-Locked Loops

Methods are derived for calculating false-lock frequency errors.

A theoretical paper discusses advances in the mathematical analysis of phase-locked loops. It presents new results in the prediction of false locking; that is, locking to a frequency other than the intended one. The paper should be of interest to users of phase-lock circuits and to researchers seeking ways to detect or avoid false lock.

The analysis is based on a classical model of a phase-locked loop. An input signal proportional to $\sin(\omega_i t)$, where ω_i is angular frequency and t is time, and a voltage-controlled oscillator signal proportional to $\cos(\omega_o t - \psi)$ with unknown phase factor ψ are fed to a mixer. The mixer output passes through a filter, the response of which is characterized by

$$F(S) = \frac{SM + a_{M-1}S^{M-1} + \dots + a_0}{SN + b_{N-1}S^{N-1} + \dots + b_0}$$

where S is the Laplace-transform complex-frequency variable and the a_i and b_i are constants. The filter output is the control voltage for the oscillator.

The nonlinear differential equation governing the evolution of the unknown phase factor ψ is

$$\left[\frac{d^N}{dt^N} + b_{N-1} \frac{d^{N-1}}{dt^{N-1}} + \dots + b_0 \right] \times \left[\omega_1 - \omega_0 - \frac{d\psi}{dt} \right] = \delta \left[\frac{d^M}{dt^M} + a_{M-1} \frac{d^{M-1}}{dt^{M-1}} + \dots + a_0 \right] \times \sin(\omega_f t + \psi)$$

where ω_0 is the oscillator angular frequency at zero control voltage, δ is a closed-loop gain factor, and $\omega_f = \omega_i - \omega_o$; that is, ω_f is the negative of the false-lock angular-frequency error.

The differential equation is written in state-vector form, with ψ and its derivatives constituting the components of the vector. To find the false lock, the derivative of the state vector is postulated to be periodic, repeating at intervals $T = 2\pi/\omega_f$.

The equation is solved with the help of a perturbation expansion in which δ serves as the smallness parameter. Starting from the previous observation that only discrete false-lock frequencies are possible and from the assumption that false lock occurs for all values of δ near zero, a necessary condition for false lock is derived, which is expressed as a relationship among the multipliers of the perturbation equation.

For the first variation in the perturbation expansion of a system with $F(S) = (S + a)/(S + b)$, the necessary condition yields series expansions for the periodic state vector and for ω_f^{-1} . Another algorithm for calculating ω_f^{-1} involves a system of nonlinear algebraic equations derived from the necessary condition and the dynamic-loop equations. These equations are solved numerically by the Newton-Raphson technique, with the Jacobian computed by a finite-difference scheme. This algorithm produces results

that are limited only by the precision of the computer on which it is executed.

The paper gives computational results for a system with $a = 5$, $b = 1$, and $\omega_i - \omega_o = 35$ rad/s. For example, at a loop gain of $\delta = 10$, the perturbation method yields $\omega_f = 29.05173$ rad/s to second order in δ , and 27.02784 rad/s to fourth order in δ . At the same value of loop gain, the algebraic method yields $\omega_f = 25.5071$ rad/s.

This work was done by Bill Reed of Marshall Space Flight Center and John L. Stensby of the University of Alabama. To obtain a copy of the report, "New Results on the PLL False Lock Phenomenon," Circle 109 on the TSP Request Card. MFS-27110

New Products

The new ES2000 system from **Gould Inc., Test and Measurement** (Cleveland, OH) provides the aerospace user with a fully programmable, high speed recording system that supports up to 40 analog or 80 digital and event channels. ES2000 has a 68000-based acquisition and control unit linked to a high speed electrostatic recorder. It can record analog signals up to 35 kHz and transients as fast as 25 microseconds. System setups of over 100,000 characters each of text can be stored using a built-in 3.5 inch disk drive. A single keystroke freezes the display and automatically generates an identical hard copy at chart speeds up to 500 mm/s. **Circle Reader Service Number 590.**

To test surface roughness for optics, silicon wafers, disks and magnetic tape, **Photographic Sciences Corp.**, Webster NY, manufactures a quality non-contacting surface profiler that measures surface heights to an accuracy of one Angstrom (0.004 microns) and a vertical measurement range of over five microns. Measurements can be made up to a length of 100 millimeters with a lateral resolution of approximately one micron. **Circle Reader Service Number 596.**



LP4000 with
Multi-pen Changer

Here's what to look for when you want great value

IOLINE plotters are designed to give you more flexibility and features for less cost than any other machine of their kind.

For example, our plotters draw not only on A through E sizes of media, but also plot on hundreds of in-between sizes from 1.5" x 1.5" up to 37" wide roll stock. This saves you time and money by allowing you to make "check plots" on small, low-cost paper before committing to full-size media for final work.

It's easy also to set paper size, pen speed, micro-calibration, plot rotation—everything exactly as you want—by just tapping a few keys on the plotter's intelligent keypad. Plus, up to 3 sets of personalized defaults can be saved in its non-volatile memory.

They're fast, too. Our high-

performance LP4000™ draws at speeds selectable up to 20 inches per second (ips) axially with .001" resolution. For less demanding applications, our economical LP3700™ plots up to 10 ips axially with .0025" resolution.

Another feature is compatibility. IOLINE plotters emulate both HP-GL and DM/PL plotter languages so they work with a host of software like AutoCAD, VersaCAD, and CADKEY, to name a few.

Furthermore, our Multi-pen Changer™ option holds up to 20

pens and, with our hyper-BUFFER™ option, you can dramatically increase plotting throughput with intelligent vector sorting and compression buffering of up to 1MB of plot data.

Now here's the clincher: Our top-gun LP4000 costs just \$5,495* less options. And there are other models priced even lower!

Why wait? Call us now at 1-206-775-7861. Or, circle our reader service number and we'll gladly send you our brochure.

Remember, getting your money's worth—that's what IOLINE plotters are all about.

IOLINE™

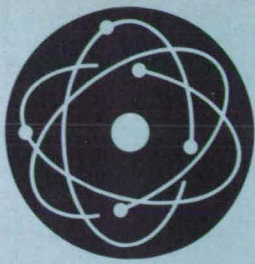
LARGE-FORMAT PEN PLOTTERS

Circle Reader Action No. 472

IOLINE CORPORATION 19417-36TH AVE. W LYNNWOOD, WASH. 98036 (206) 775-7861 TELEX 4949856 IC UI FAX (206) 775-2818

LP4000, LP3700, Multi-pen Changer, and hyperBUFFER are trademarks of Ioline Corporation. AutoCAD is a registered trademark of Auto Desk Inc. VersaCAD is a registered trademark of T&W Systems. CADKEY is a registered trademark of MicroControl Systems, Inc. *Suggested U.S. List price.

See us at COMDEX Fall '87 Booth #R8122 and AUTOFACT '87 Booth #5010



Physical Sciences

Hardware, Techniques, and Processes

- 50 Dual-Mode Laser Velocimeter
- 52 Concentrating Trace Gases at Low Pressures
- 53 Approximate Simulation of Turbulence
- 53 Measuring Gases With Laser-Induced Fluorescence

- 54 Measuring Electrostatic Discharge
- 55 Coating a Hydrogen-Maser Chamber With CF_4
- 56 Measuring Contact Thermal Conductances at Low Temperatures
- 57 High-Rydberg Xenon Submillimeter-Wave Detector

Dual-Mode Laser Velocimeter

A reversible lens system provides two velocity ranges.

Ames Research Center, Moffett Field, California

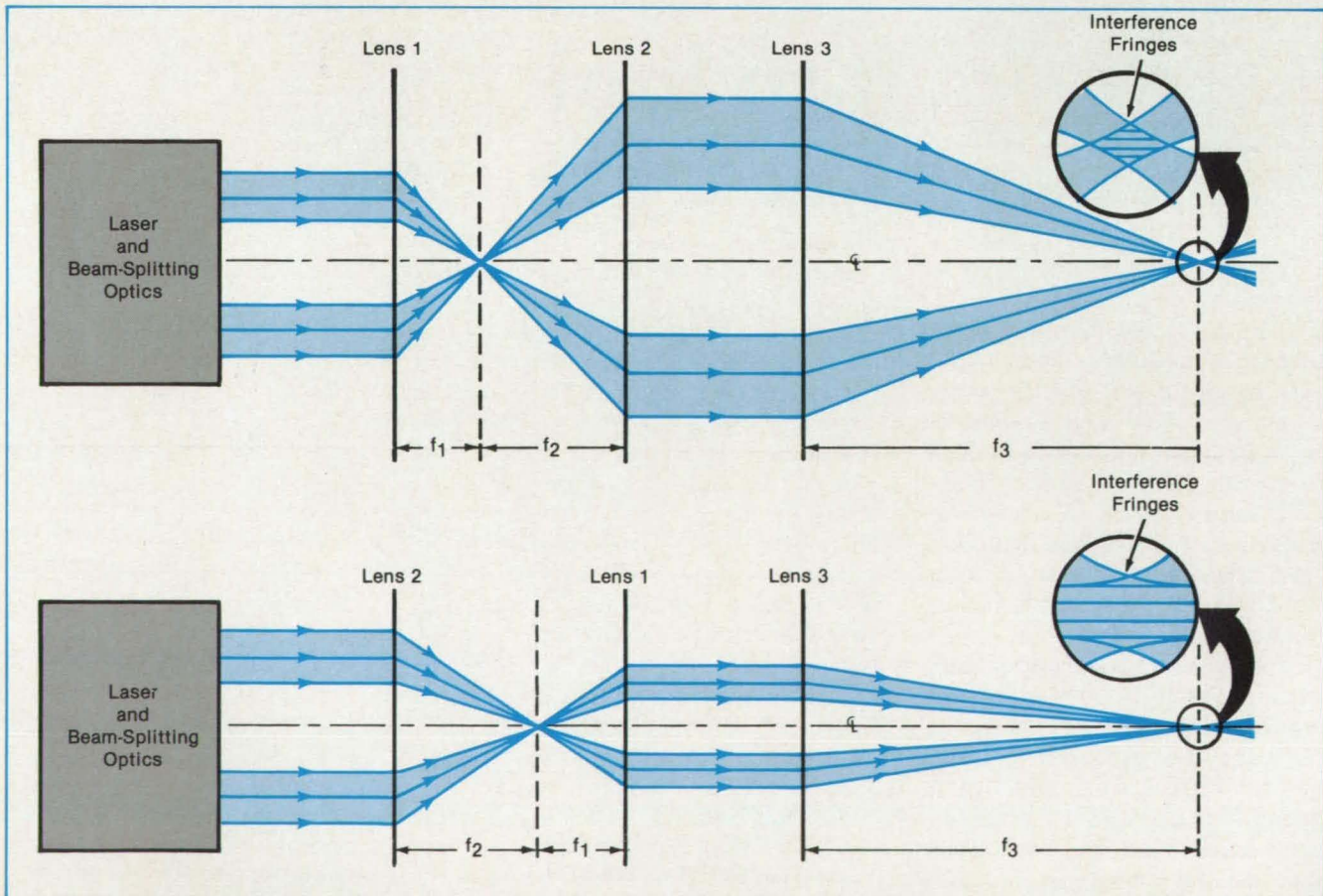
A proposed version of a laser velocimeter for measuring airflows in wind tunnels uses a reversible, two-lens assembly to provide two velocity ranges without changing the location of the measuring region in the airstream. Since the measuring region would remain fixed, a pair of the new velocimeters could be fixed to a single rigid support and aimed at the region from different directions to form a velocimeter for measuring all three velocity components. The velocity range covered by previous velocimeters of this general

type could not be changed easily because realignment of the entire system was required.

A laser velocimeter uses two coherent laser beams aimed at the same point to produce a set of interference fringes in the beam-intersection region. The fringes form on parallel planes that bisect the angle between the two beams. As a dust particle carried by the air stream passes through the fringes, the intensity of the light scattered from it fluctuates at a frequency equal to the number of fringes it

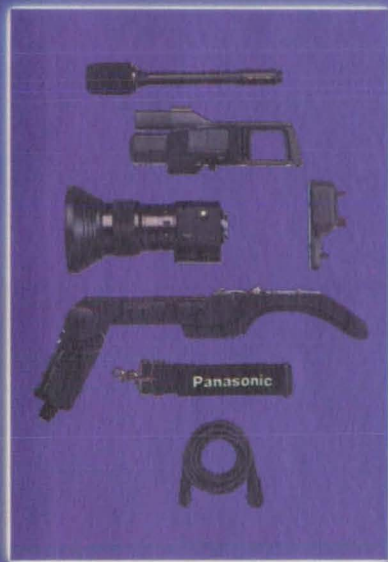
passes through per unit time. Thus the frequency is proportional to the velocity component of the dust particle perpendicular to the planes of the fringes. The scattered light is detected by a photomultiplier. When many dust particles are crossing simultaneously, the frequency can be determined by taking the Fourier transform of the light signal with a spectrum analyzer.

For high velocity resolution and spatial resolution at low velocities, the fringes should be closely spaced and confined to



A **Laser Velocimeter** could be modified to provide two velocity ranges by adding a rotatable assembly containing two lenses. In one orientation (top), the beam waists are narrow, and the two beams intersect at a relatively large angle, providing a low velocity range with high spatial resolution. In the reversed orientation (bottom), the beam waists are wider, and the beams intersect at a smaller angle to produce more widely-spaced fringes in a larger region, thus providing a high velocity range with lower spatial resolution.

Only one video camera can be any video camera you want it to be.
Available on GSA Contract GSOOK87AGS0101.



Imagine being able to design a camera to suit your every need. You can with the Panasonic® WV-D5000 because it's totally modular. Just choose the ENG, EFP, or studio configuration that's right for you.

The WV-D5000 is even more versatile. You can use some of the world's finest photographic lenses. Lenses you may already own. Lenses from Canon, Pentax, Minolta, Olympus and Nikon. Wide angle lenses. Long lenses. Lenses for telescoping and microscopy.

And if that isn't impressive enough, the WV-D5000 has a strobe-effect shutter speed of $1/1000$ th of a second. That means you can shoot high-speed action like a roller coaster and during VCR playback actually see the excitement on a child's face.

But whether the action is fast or slow,

the WV-D5000's CCD pickup element provides clear, stable video images with a minimum of blooming and burn-in. Horizontal resolution is a hefty 380 lines while S/N is a quiet 46dB. And when it comes to light, you need only 0.7 footcandles at f1.4.

You'd expect a camera of this caliber to be fully flexible, and the WV-D5000 fulfills your every expectation. With auto-tracing white balance, intermittent recording as well as audio and video fade-in and fade-out.

The Panasonic WV-D5000. It's the one video camera you can customize to be any video camera.

Panasonic
Professional/Industrial Video



For more information and your copy of the Authorized Communications Schedule Price List contact your local Panasonic Industrial Video dealer or call (703) 486-5533 (FTS: (202) 486-5533) or write to Government Marketing Dept., Panasonic AVSG, Suite 901, 1215 Jefferson Davis Highway, Arlington, VA 22202-4302.

a small region. This requires that the two beams have narrow beam waists at the intersection and that they intersect at a fairly large angle.

Conversely, the measurement of higher velocities requires a larger sensitive region so that each scattering particle spends enough time there to generate an adequate signal. This necessitates larger beam waists and therefore entails lower spatial resolution. In this case, the beams must be made to intersect at a smaller angle so that the fringes occur over a larger volume and are more widely spaced.

To provide two velocity ranges, the proposed velocimeter would change the sizes of the beam waists and angle at which the beams intersect by reversing

the order of two lenses added to the optical system (see figure). The two lenses would be mounted on a single rotatable assembly to provide quick selection of velocity range.

Two velocity components can be measured by using a single laser-velocimeter optical system with two pairs of laser beams lying in perpendicular planes and operating on different wavelengths to form two sets of interference-fringe planes that intersect at right angles.

To determine the remaining velocity component, another velocimeter is aimed at the same measurement point from a different direction. The velocity component measured by that velocimeter will have a component perpendicular

to the two components measured by the first velocimeter, thus providing enough information for an algebraic solution for the third velocity component. The entire velocimeter is translated to scan the measurement point over the region of interest.

This work was done by William D. Gunter, Jr., Ralph W. Donaldson, and Alma G. Anderson, Jr., of Ames Research Center. For further information, Circle 101 on the TSP Request Card.

Inquiries concerning rights for the commercial use of this invention should be addressed to the Patent Counsel, Ames Research Center [see page 22]. Refer to ARC-11634.

Concentrating Trace Gases at Low Pressures

An open adsorption tube enables the measurement of gases at parts-per-trillion-by-volume concentrations.

Ames Research Center, Moffett Field, California

Trace constituents of low-pressure air are collected and concentrated for analysis by a multistage open-tube trap. The trap was developed for collecting samples at high altitudes, at pressure as low as about 6.6 kPa, but can also be used on the ground to collect samples from gas flows at pressures of up to 27 kPa (about one-quarter of 1 atmosphere).

Ordinarily, traps consist of tubes densely packed with adsorbent particles and often cryogenically cooled. As a gas flows through these tubes, constituents are adsorbed by the particles. The adsorbed constituents are later released as enriched samples for analysis. At pressures below about 100 kPa, adsorbent particles impede the flow of the gas and thereby increase the sampling time.

The trap described therefore employs an open tube. It consists of a coil of stainless-steel tubing with each loop, or stage, partly immersed in liquid nitrogen (see figure). After the tube has been evacuated and cooled, a measured volume of low-pressure gas flows through the tube. The trace constituents are adsorbed on the cryogenically cooled tube wall. The open tube allows a flow rate more than an order of magnitude greater than that of a packed tube for gas samples of about 13 kPa. After the enrichment of the sample, the six-part valve is rotated part way to isolate the trace constituents in the trap.

Next, the liquid-nitrogen bath is replaced by a water bath at 50 °C. As the coils warm up to the temperature of the water, the concentrated trace constituents are desorbed. The six-port valve is further rotated to admit a flow of helium gas to the tube. The flow carries the trace constituents to a gas

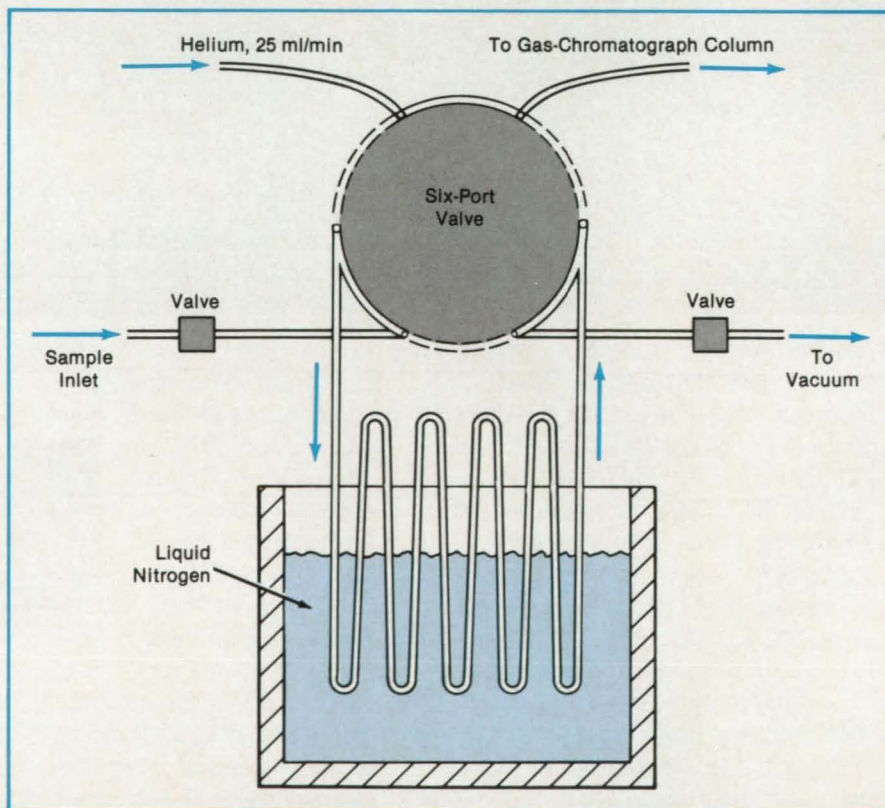
chromatograph for quantitative analysis.

In a demonstration of the multistage open-tube trap, samples containing 200 to 2,500 parts per trillion by volume of ethane and of ethene were enriched. The trapping efficiency (the ratio of the found concentration to the known concentration of a trace

constituent) was 100 ± 4 percent. Total immersion of the coils in the cryogen results in an efficiency of 85 ± 8 percent under similar conditions.

This work was done by James F. Vedder of Ames Research Center, Dean O'Hara of San Jose State University Foundation, and Tuyen Vo of San Jose State University. For further information, Circle 60 on the TSP Request Card.

Inquiries concerning rights for the commercial use of this invention should be addressed to the Patent Counsel, Ames Research Center [see page 22]. Refer to ARC-11671.



An Open Tube Traps Trace Materials in a flowing gas. A variety of configurations is possible; the tube may consist of a single long coil instead of several short ones, and the tube may be made of materials other than stainless steel. The partial immersion of the coil in the cryogen results in 100% trapping rather than a typical 85% for total immersion.

Approximate Simulation of Turbulence

Computed spectra resemble von Kármán spectra of frequencies of interest.

Marshall Space Flight Center, Alabama

A numerical technique yields simulated atmospheric-turbulence spectra that closely approximate von Kármán spectra within the frequency ranges of interest for aircraft response. The technique uses approximate spectra that are especially suitable for computation in that they represent stable systems and roll off as f^{-2} (where f = frequency) at high frequencies outside the range of interest.

Real atmospheric turbulence tends to follow the von Kármán model, with spectral density proportional to $f^{-5/3}$. A simulated turbulence signal can be generated by a system like that of Figure 1, provided that the transfer function of the filter gives the required $f^{-5/3}$ dependence. For purposes of numerical simulation of the instantaneous turbulence signal, the filter transfer function is replaced by its corresponding differential equation, which is then approximated by a finite-time-step difference equation. As a result, the turbulence at the present time step is expressed as a function of the present input noise and the turbulence and input noise at the previous time steps.

Because it is computationally more efficient to simulate a rational rather than an irrational spectrum, the transfer function $(1+S)^{-5/6}$ that represents the exact $f^{-5/3}$ spectral dependence is approximated by the rational expression. For the longitudinal turbulence, this is $(1+S)^{-5/6} \approx [60 + 52S + (91/12)S^2] / [60 + 102S + (561/12)S^2 + (935/216)S^3]$, where S is the Laplace-transform complex frequency. Because all the poles of this function lie in the left half of the complex S plane, the system that it represents is unconditionally stable.

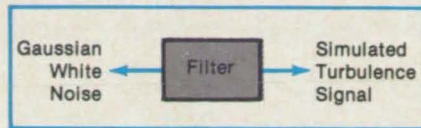


Figure 1. Monte Carlo Simulation of Turbulence can be done with digital or analog equipment by passing Gaussian white noise through a filter that has a transfer function corresponding to the turbulence spectrum.

The transfer function for transverse turbulence is obtained by multiplying the longitudinal transfer function by $[1 + (8/3)^{1/2}S] / [1 + S]$. This function also represents a stable system. In both the longitudinal and transverse cases, the spectral density is found by multiplying the transfer functions by their complex conjugates.

Longitudinal turbulence and transverse turbulence have been simulated by difference equations based on these transfer functions, using a sampling frequency of 5 Hz, an aircraft speed of 100 m/s, a turbulence length scale of 500 m, and a root-mean square turbulent velocity of 1 m/s. As shown in Figure 2, the spectra of the simulated turbulence closely approximate the corresponding von Kármán spectra. In fact, the statistical scatter is greater than the difference between the simulated and von Kármán spectra.

This work was done by C. W. Campbell of the American Institute of Aeronautics and Astronautics for Marshall Space Flight Center. For further information, Circle 125 on the TSP Request Card. MFS-28172

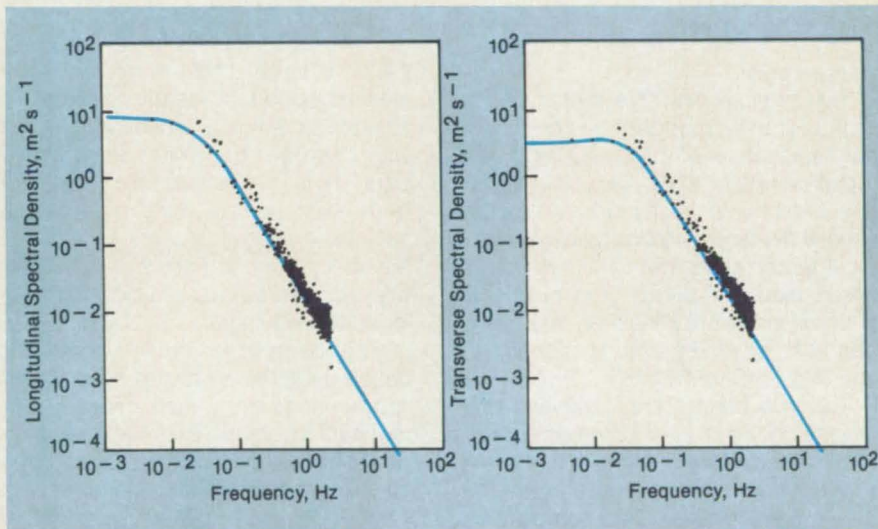


Figure 2. Spectra of Simulated Turbulence (dots) are plotted with the corresponding von Kármán spectra (lines).

Measuring Gases With Laser-Induced Fluorescence

The temperature, density, and pressure are measured simultaneously in supersonic, turbulent flow.

Ames Research Center, Moffett Field, California

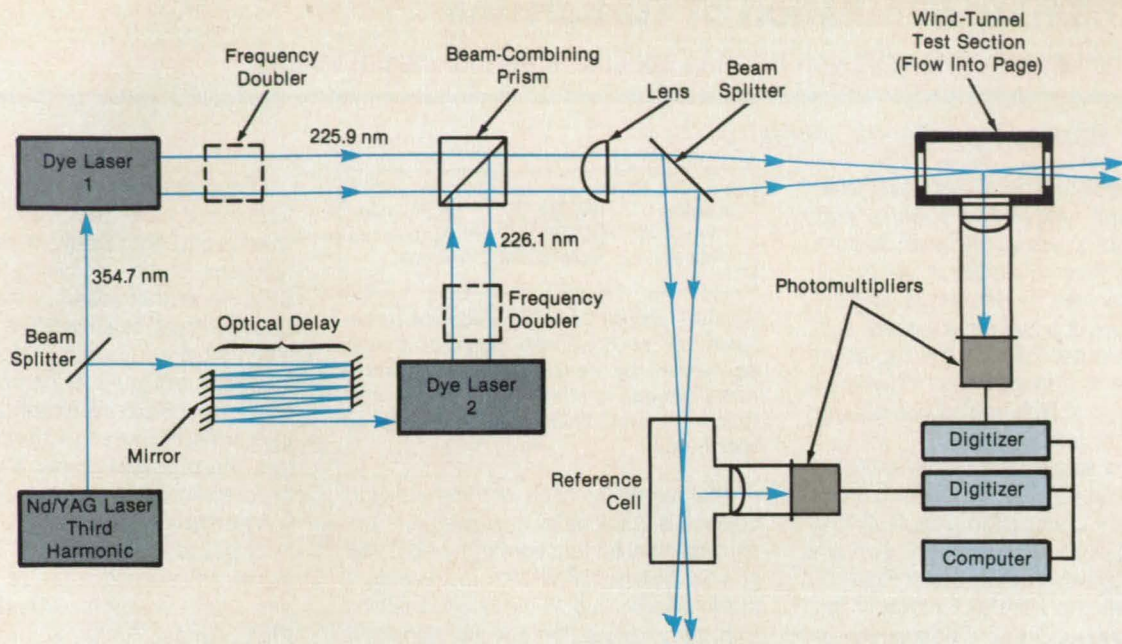
The temperature, density, and pressure at a selected point in a low-temperature, turbulent gaseous flow are measured simultaneously by pulsed laser-induced fluorescence (LIF). The measurements are made with spatial and temporal resolution comparable to those obtained with modern laser-anemometer techniques used for research on turbulent boundary layers. These LIF measurements are unique in that they are noninvasive and constitute the first alternative means of measuring turbulent fluctua-

tions in temperature and density that can be compared with conventional hot-wire-anemometer data.

The LIF technique involves seeding a bulk nitrogen flow with a low concentration (up to 100 parts per million) of nitric oxide (NO) and relies on the ultraviolet fluorescence following single-photon excitation of two rotational/vibrational electronic transitions in the NO gamma band. The test section of the small wind tunnel used for these experiments is a rectangular mach-2 nozzle with a 25-by

64-mm exit, followed by a slightly diverging channel, 762 mm in length from the nozzle throat to the optical ports.

The optical arrangement is illustrated in the figure. The laser beam is admitted through either of two 50-mm-diameter quartz windows on opposite sides of the channel. Fluorescence is observed through a similar window on a third side of the channel. The volume observed is spatially limited by the collection optics and field-stop arrangement to a 1-mm segment of the laser beam centered on



Laser Beams Focused to Small Spots in the wind tunnel and reference cell induce fluorescence in nitric oxide, a small amount of which is mixed with the main gas flow. The fluorescence radiation depends on the main-gas temperature, pressure, and density and is measured to deduce these quantities.

its focal point.

Two grating-tuned dye lasers are simultaneously pumped by the third-harmonic output of a Nd:YAG laser at a repetition rate of 10 Hz. The portion of the 354.7-nm pump beam directed to the second dye laser is optically delayed, giving a temporal separation of 125 ns between dye-laser pulses. The beams of both dye lasers are doubled in frequency, and each second harmonic is tuned to one of the NO transitions.

The two beams are combined collinearly, focused by a common lens of 500-mm focal length and partitioned into the wind-tunnel and reference paths. The reference path contains the same gas as does the wind tunnel, but the gas does not flow and is maintained at a known temperature and pressure. The focal-spot sizes were less than 0.5 mm.

The broad-band fluorescences from

the wind tunnel and the reference cell were collected by nearly identical f/1 fused-silica optics and nominally filtered with ultraviolet-transmitting shortwave-pass filters. The fluorescence waveforms from each source were detected by solar-blind photomultipliers sensitive to the spectral range from 225 to 330 nm and recorded by transient digitizers interfaced to a computer.

The computer deconvolved the double-pulse waveforms to separate the contributions from each excitation, integrated to obtain the relative fluorescence energy associated with each excitation, and compared wind-tunnel with reference values to obtain normalized wind-tunnel data.

The ratio of fluorescence energies from both transitions is related to the rotational temperature of the ground-state NO molecule, with account taken of the

effects of collisional quenching and transition spectral broadening. The rotational temperature, in turn, is assumed to be closely coupled to the kinetic temperature of the gas mixture. The density and pressure are obtained from the measured temperature, together with the combined use of the fluorescence energy from one excitation and the equation of state for the gas mixture.

This work was done by Robert L. McKenzie of Ames Research Center and Kenneth P. Gross of Polyatomics Research Institute and Pamela Logan of Stanford University. For further information, Circle 81 on the TSP Request Card.

Inquiries concerning rights for the commercial use of this invention should be addressed to the Patent Counsel, Ames Research Center [see page 22]. Refer to ARC-11678.

Measuring Electrostatic Discharge

A variety of materials can be tested together under controlled conditions.

Lyndon B. Johnson Space Center, Houston, Texas

An apparatus measures the electrostatic-discharge properties of several materials at once. It allows the samples to be charged either by friction or by exposure to a corona. By testing several samples simultaneously, the apparatus eliminates errors introduced by variations among test conditions.

The samples are placed on a turntable and rotated beneath a charging arm and a diametrically opposed noncontacting volt-

meter probe (see figure). Positioned 6 millimeters above the turntable, the probe registers the voltage on each sample as it passes. The voltmeter output is displayed on a fast-responding chart recorder.

When the corona-charging arm is selected, it is extended to the radius of the samples; the pointed electrode of the arm is held 15 millimeters above the surface of the samples. When frictional charging is required, the corona arm is retracted and

the frictional, or tribocharging, arm is extended; the abrasive tip of this arm is held against the surfaces of the samples.

As the turntable rotates, the samples are repeatedly charged by the selected arm. After about 150 seconds at a turntable speed of 8 radians per second, the charges on the samples build up to equilibrium levels. At this point, charging is stopped, and the voltmeter readings are started. The readings thus indicate the

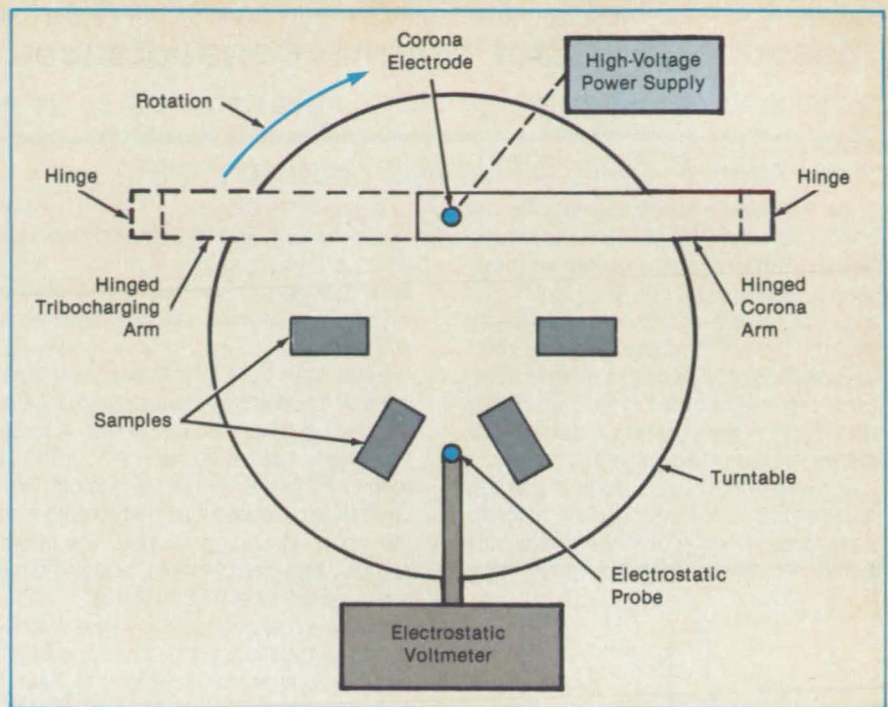
rates at which various materials dissipate the charge imposed on them.

The apparatus has been used to measure the electrical-discharge characteristics of paints. The measurements showed that the maximum charge on a sample increases with the sample thickness and decreases with the discharge rate of the sample material. The charge-versus-time curve for each paint is fit approximately by a sum of two exponentials, indicating that several discharge mechanisms operate simultaneously.

Electrostatic properties of materials can be compared under identical, controlled conditions with the apparatus. The results of such comparisons are immediately available. In addition, samples can be compared with reference materials also on the turntable — for example, with polytetrafluoroethylene, which holds a charge for a long time, or with antistatic polyethylene film ("pink poly"), which loses a charge within 5 seconds.

Generally, the corona arm is preferable to the tribocharging arm. It gives more consistent results from measurement to measurement, is more sensitive to variations in material composition, and is non-destructive.

This work was done by William C. Smith of Lockheed Engineering and Management Services Co. for **Johnson Space Center**. For further information, Circle 95



Samples Are Spaced so that they pass at intervals under either of two retractable arms. The samples are 2 inches (5 centimeters) wide along the circular path. The arm tips and the voltmeter probe are 6 inches (15 centimeters) from the turntable center. The servocontrolled turntable speed is constant within 0.1 percent.

on the TSP Request Card.

Inquiries concerning rights for the commercial use of this invention should be ad-

ressed to the Patent Counsel, Johnson Space Center [see page 22]. Refer to MSC-21094.

Coating a Hydrogran-Master Chamber With CF_4

Sprayed gas forms a smooth frozen surface.

NASA's Jet Propulsion Laboratory, Pasadena, California

A coating of carbon tetrafluoride (CF_4) has been formed on the interior surface of an atomic-hydrogen maser by allowing CF_4 gas to freeze on the surface. The new coating enables the maser to oscillate down to 26 K; the most effective previous coating, a fluorinated ethylene/polypropylene (FEP) copolymer allowed oscillation down to about 50 K.

The key to maintaining maser stability while lowering the operating temperature is to find a surface coating that reflects hydrogen atoms without disturbing the phase of the oscillating magnetic dipole moment of the hyperfine interaction between the electron and proton in each atom. The CF_4 coating performs this function better than does FEP because CF_4 is a tetrahedral molecule with no polymer end groups to harbor impurities and because the surface formed is smoother.

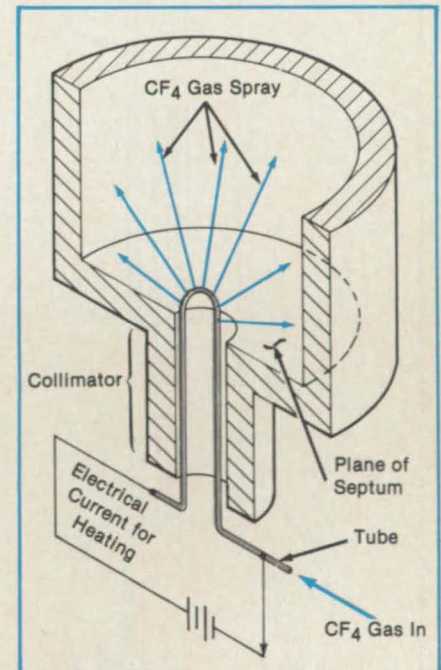
The CF_4 gas is sprayed into the cooled, evacuated chamber using a pair of opposed nozzles, one on each side of the maser septum (see figure). Pulses of electric current are passed through the nozzles to heat them enough to prevent the gas

The **Coating Nozzle** used to spray the CF_4 into half of the TE_{111} -mode maser chamber is formed from 0.020-inch (0.5-mm) diameter nonmagnetic metal tubing. The nozzle for each half is placed on one side of the septum in the chamber. Several small holes are drilled on the outside of the bend to distribute the gas evenly. The nozzle is electrically insulated from ground and thermally isolated, except for contact with the septum.

from condensing and freezing in them. The coating obtained with the nozzles is more uniform than the one that results from simply introducing the gas via the existing hydrogen-beam collimator.

Since the electronic structure of the bound fluorine atom is similar to that of the inert gas neon, the use of the latter gas as a maser-chamber coating has been proposed. It should be possible to hold neon in place at a reasonably low vapor pressure of 10^{-5} torr (about 10^{-3} Pa) at a temperature of about 10 K.

This work was done by Robert F. C. Vessot and Edward Mattison of the Smithsonian Institution for **NASA's Jet Propul-**



sion Laboratory. For further information, Circle 66 on the TSP Request Card. NPO-16380 and NPO-16381

Measuring Contact Thermal Conductances at Low Temperatures

An apparatus applies controlled force to metal samples at controlled heat flows.

Ames Research Center, Moffett Field, California

An instrument measures the thermal conductance of pressed contacts in liquid helium. The instrument makes its measurements automatically as a function of the force on pairs of brass samples having various surface finishes. The instrument was developed as part of an effort to determine the heat-transfer characteristics of bolted joints on cryogenically cooled focal planes in infrared equipment.

A rocker arm presses a pair of samples together in a fixture. A small gear motor applies force to an end of the rocker arm

through a wire extending through a stainless-steel tube into the vacuum cylinder, which is immersed in liquid helium. A second tube carries electrical wiring into the cylinder, and a third is used to evacuate the cylinder.

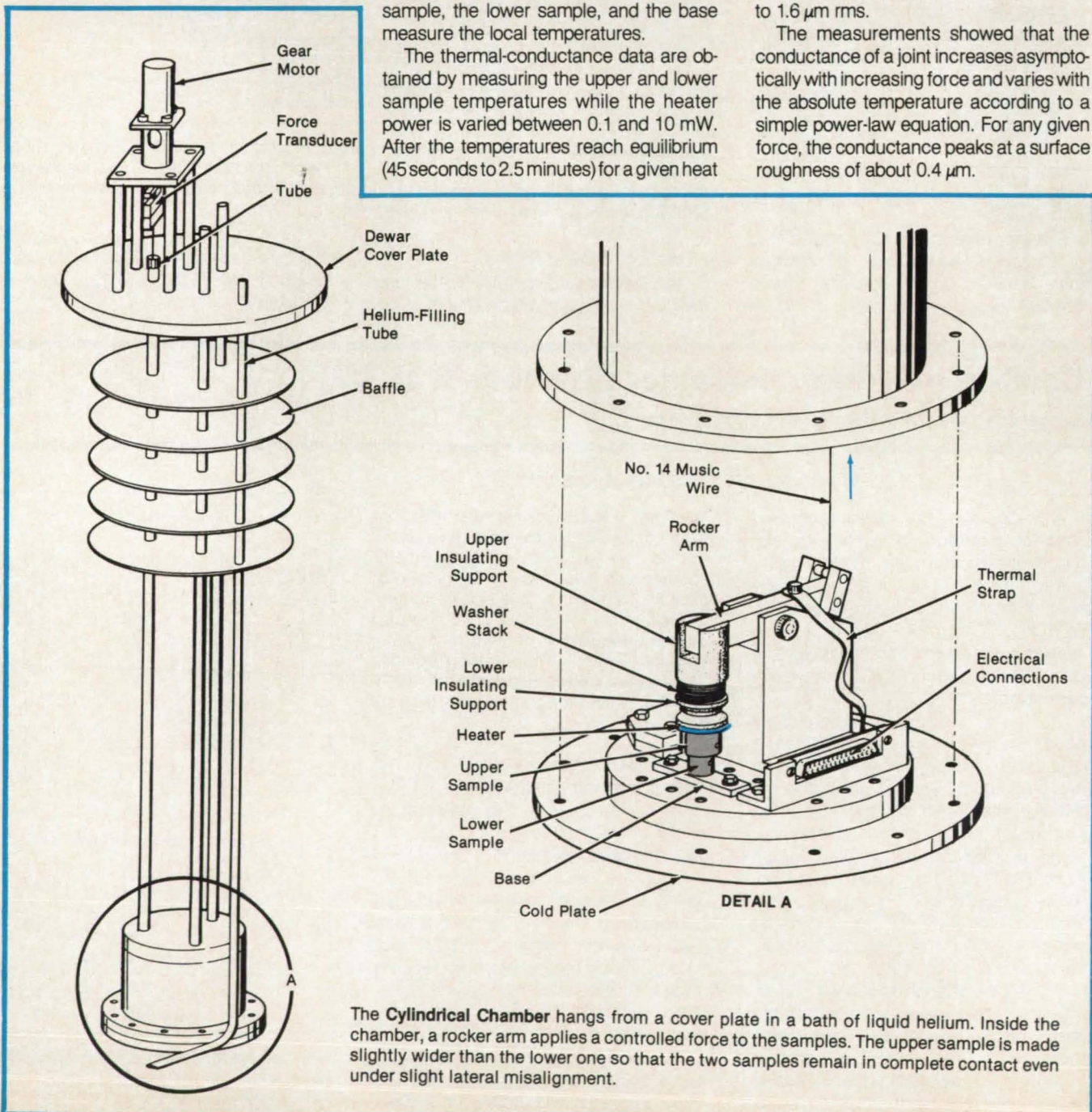
Heat flows from a small electrical heating disk through the upper and lower samples to the base of the fixture. A force transducer calibrated from 0 to 1,100 N measures the force on the sample pair. Germanium resistance thermometers in the upper insulating support, the upper sample, the lower sample, and the base measure the local temperatures.

The thermal-conductance data are obtained by measuring the upper and lower sample temperatures while the heater power is varied between 0.1 and 10 mW. After the temperatures reach equilibrium (45 seconds to 2.5 minutes) for a given heat

load, the data are recorded. The force is raised to the next value, the system is allowed to equilibrate, and the data are logged. The procedure is repeated for other heater powers and for other values of surface roughness.

The sequence is completely automated, under the control of a calculator that controls temperatures, heat loads, and applied forces. The temperature can be set at 1.5 to 6.5 K. The force on the contacts can be set at values up to 700 N. The samples tested had surface roughness ranging from 0.1 to 1.6 $\mu\text{m rms}$.

The measurements showed that the conductance of a joint increases asymptotically with increasing force and varies with the absolute temperature according to a simple power-law equation. For any given force, the conductance peaks at a surface roughness of about 0.4 μm .



The **Cylindrical Chamber** hangs from a cover plate in a bath of liquid helium. Inside the chamber, a rocker arm applies a controlled force to the samples. The upper sample is made slightly wider than the lower one so that the two samples remain in complete contact even under slight lateral misalignment.

This work was done by Louis J. Salerno, Peter Kittel, and Walter Brooks of **Ames Research Center**; Alan L. Spivak of **Trans-Bay Electronics, Inc.**; and William G.

Marks, Jr., of **Lockheed Missiles and Space Co.** For further information, Circle 82 on the TSP Request Card. Inquiries concerning rights for the com-

mercial use of this invention should be addressed to the Patent Counsel, **Ames Research Center** [see page 22]. Refer to ARC-11693.

High-Rydberg Xenon Submillimeter-Wave Detector

The use of reactive alkali metals is avoided.

NASA's Jet Propulsion Laboratory, Pasadena, California

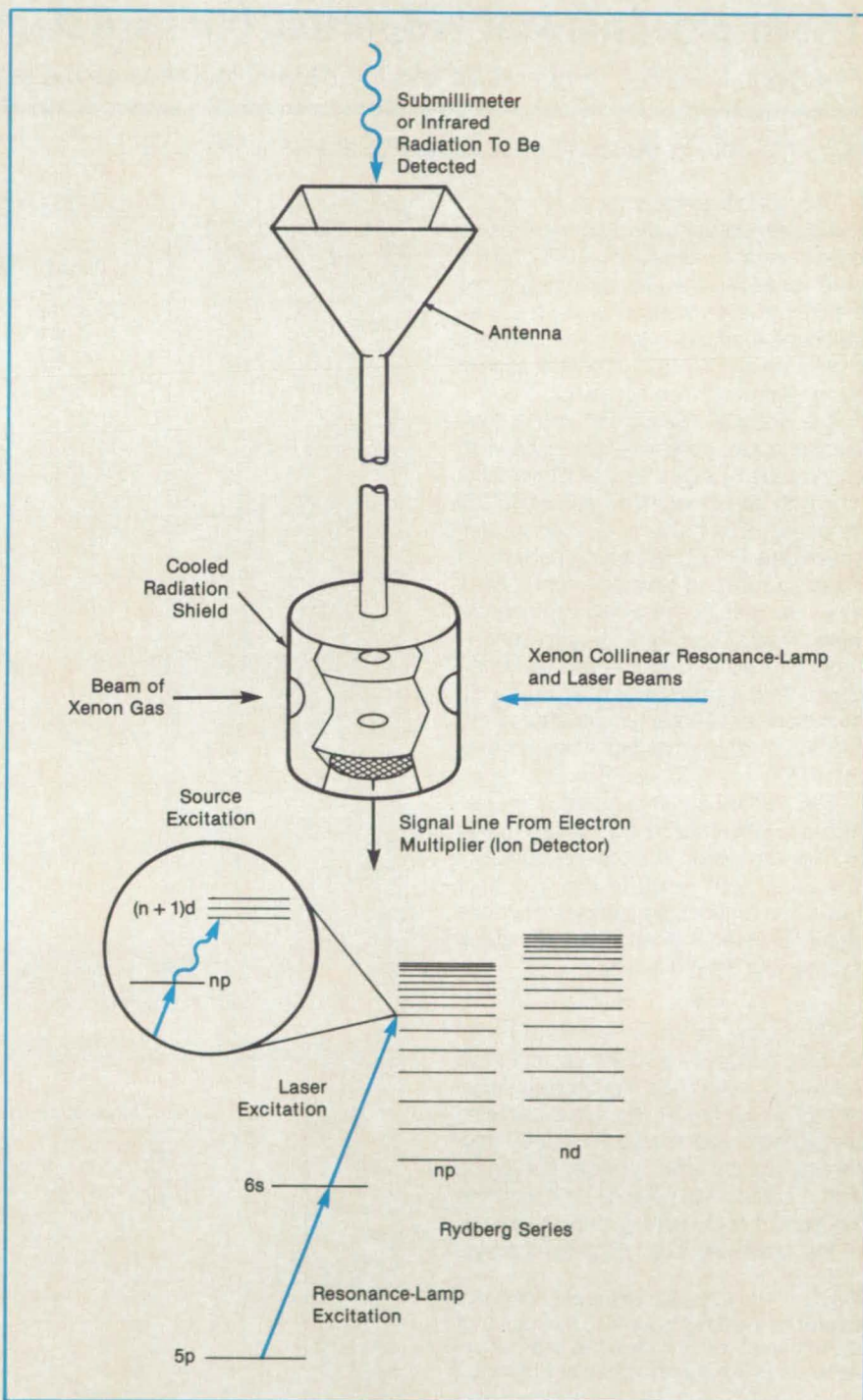
A proposed detector for infrared and submillimeter-wavelength radiation would use excited xenon atoms as Rydberg sensors instead of the customary beams of sodium, potassium, or cesium. The chemically inert xenon is easily stored in (and released from) pressurized containers, whereas beams of the dangerously reactive alkali metals must be generated in cumbersome, unreliable ovens. The xenon-based detector has potential for infrared astronomy and for the Earth-orbiter detection of terrestrial radiation sources.

The Rydberg-sensor concept is based on the excitation of one of the electrons in each detector atom to a high energy state. In the xenon-based detector, the excitation would be performed in two stages (see figure). First, one of the six electrons in the highest level, (5p), of each ground-state xenon atom would be raised to the 6s level by radiation from a xenon resonance lamp. Next, a tunable laser emitting light of about 400 nm would raise the electron to an np ($n > 6$) energy level.

The excited xenon atoms would absorb infrared radiation, causing the already twice-excited electron to be excited to the $(n + 1)d$ level. The frequency of the absorbed infrared radiation would correspond to the energy spacing between the np and $(n + 1)d$ levels, which would depend on the value of n and hence on the wavelength of the laser light used to excite the electron to the np level; alternatively, the wavelength sensitivity of the device could be tuned by shifting a given $(n + 1)d$ level via the Stark effect. In either case, the atoms in the $(n + 1)d$ level would be field ionized; the intensity of the incident infrared radiation would be determined by counting the resulting positive xenon ions using a microchannel-plate detector and standard particle-counting circuitry.

As in the case of other infrared detectors, this device would have to be cooled to very low temperatures to reduce interfering black-body radiation from the device walls. In terms of the noise-equivalent power, the device is expected to be competitive with, or even to exceed, bolometers, point-contact Josephson junctions, and Schottky diodes.

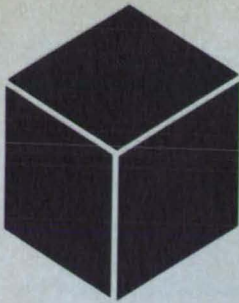
This work was done by Ara Chutjian of **Caltech** for **NASA's Jet Propulsion Laboratory**. For further information, Circle 92



Xenon Atoms Would Be Excited to high energy states in two stages. The doubly excited atoms, which are sensitive to photons in the submillimeter wavelength range, would be further excited by these photons, then ionized and counted.

on the TSP Request Card. Inquiries concerning rights for the commercial use of this invention should

be addressed to the Patent Counsel, **NASA's Jet Propulsion Laboratory** [see page 22]. Refer to NPO-16372.



Materials

Hardware, Techniques, and Processes

- 58 Thermomechanical Properties Indicate Degree of Epoxy Cure
- 59 Fluidized-Bed Cleaning of Silicon Particles
- 60 Bismaleimide Copolymer Matrix Resins

Books and Reports

- 61 Design of Fiber Composites for Structural Durability
- 61 Protective Coatings for Spacecraft Polymers
- 64 Tribological Properties of Structural Ceramics

- 64 Amorphous Insulator Films With Controllable Properties
- 65 Radiation Resistances of Dielectric Liquids

Thermomechanical Properties Indicate Degree of Epoxy Cure

The glass-transition temperature and the density increase as the reaction proceeds.

NASA's Jet Propulsion Laboratory, Pasadena, California

The glass-transition temperature (T_g) and the density of a cured epoxy resin have been found to be related to the extent of the cure. In addition to providing insight into the chemical reactions of curing, these relationships show potential for process monitoring and control in the fabrication of strong, lightweight composite parts.

The material investigated was a commercial epoxy containing tetraglycidyl diaminodiphenyl methane (TGDDM) monomer with diaminodiphenyl sulfone (DDS) hardener. This material is used in non-stoichiometric, epoxy-rich proportions of about 2.1 moles of resin per mole of hardener. Samples of these two components were mixed at 120 °C in an N_2 atmosphere, then poured into aluminum weighing dishes and partially cured in an N_2 atmosphere at various temperatures from 140 to 201 °C and various times from 15 min to 6 h.

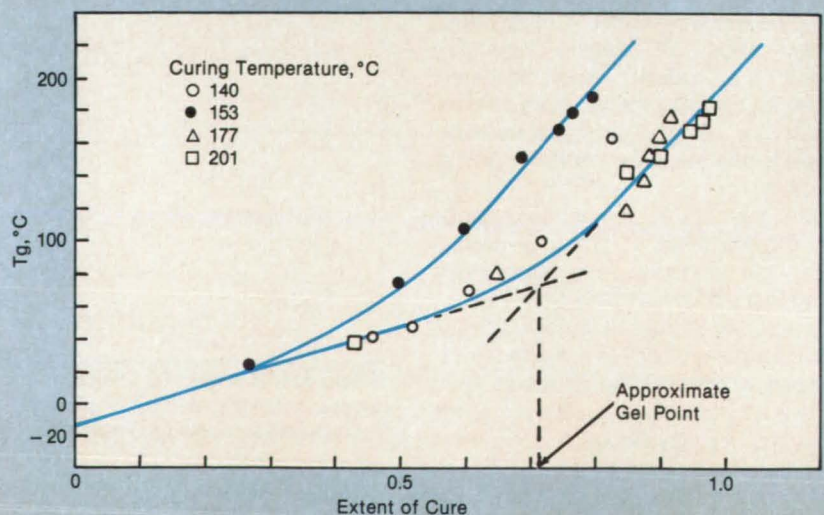
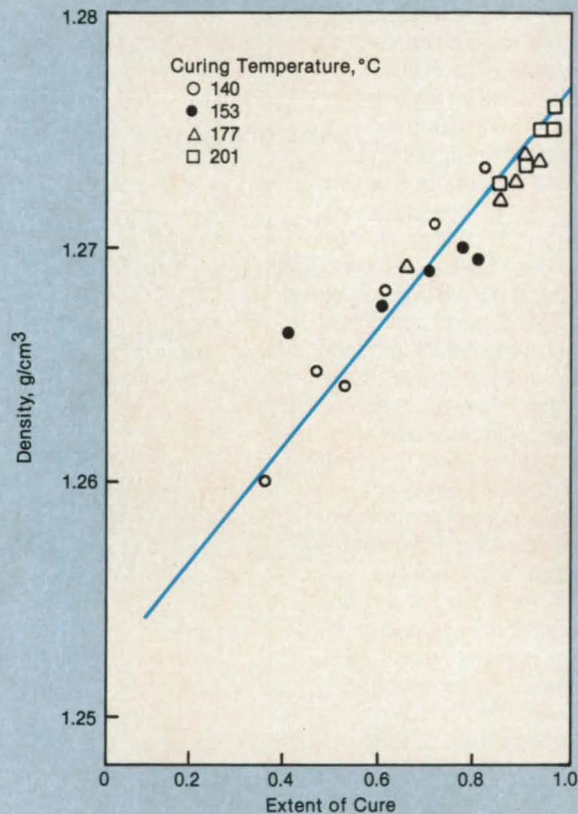
The partially cured samples were subjected to differential scanning calorimetry to measure the residual heat of cure, H_R . The total heat of cure, H_T , was also measured on uncured samples. Then the extent of cure, α , of each partially cured sample was determined from

$$\alpha = (H_T - H_R)/H_T$$

The sample densities were measured in an 80-cm density-gradient column filled with K_2CO_3 solution having a density range of 1.21 to 1.3 g/cm³. The glass-transition temperature was measured in a thermomechanical analyzer: an expansion probe with a contact diameter of 2.54 mm was loaded to 1 g against 2-mm-thick samples of the same diameter. Each sample was

Figure 1. The **Increase of Density With the Extent of Cure** is believed to indicate that the free volume in the resin has been reduced by cross-linking of molecular segments.

Figure 2. The **Glass-Transition Temperature** increases with the molecular weight below the gel point. Above the gel point, T_g also increases with the degree of cross-linking, making the rate of increase larger. The anomaly of the curve for 153 °C is not understood.



heated at 10°C/min. The glass-transition temperature was taken to be the temperature at which the two tangent lines to the thermal-expansion curves intersected.

As shown in Figure 1, the measurements yielded a linear relationship between the density and the extent of cure; this relationship appears to be independent of the curing temperature. As shown

in Figure 2, the glass-transition temperature was found to depend on the extent of cure and to be independent of the curing temperature for three of the four curing temperatures used. At present, the divergence of the data for the 153°C cure is not understood. Overall, the data seem consistent with a theory of gelation that takes into account the functionalities of the react-

ants, the degree of cross-linking, and the molecular distribution.

This work was done by Muzaffer Cizmecioglu, Amitava Gupta, and Robert F. Fedors of Caltech for NASA's Jet Propulsion Laboratory. For further information, Circle 120 on the TSP Request Card. NPO-16903

Fluidized-Bed Cleaning of Silicon Particles

Metallic impurities are removed by acids.

NASA's Jet Propulsion Laboratory, Pasadena, California

A fluidized-bed chemical cleaning process is developed to remove metallic impurities from small silicon particles. These particles (250 µm in size) are utilized as a seed material in a silane pyrolysis process for production of 1-mm-size silicon. The product silicon (1 mm in size) is used as a raw material for fabrication of solar cells and other semiconductor devices. The principal cleaning step is a wash in a mixture of hydrochloric and nitric acids, which leaches out the metals and carries them away as soluble chlorides. The particles are fluidized by the cleaning solution to assure good mixing and uniform wetting.

Typically, the silicon particles as purchased contain significant impurities and range in size up to 2 mm. These particles are jet-milled down to sizes of 111 to 400 µm, with an average size of about 250 µm. A batch of about 500 g of milled particles is placed in each of three bottles in a fluidized-bed apparatus (see figure), restrained at the bottom by a screen with 50-µm pores and at the top by a screen with 75-µm pores.

A pump forces the cleaning fluid into each bottle through its bottom screen and a distributor that provides a tangential flow, for good mixing. The solution passes through and fluidizes the bed of particles, flows out through the top screen, then falls

Impurity Elements	Impurity Levels, Atoms Per Million Atoms of Silicon	
	In Raw Particles	In Cleaned Particles
P	0.2	0.2
Fe	20	<0.6
Cr	0.05	0.03
Ni	10	<0.5
Cu	0.06	<0.02
Zn	<0.02	<0.04
Co	<0.1	<0.1
Mn	0.5	<0.02
Na	<0.1	<0.1
Mg	<1	<1
Al	2	0.05
S	<1	<1
K	<0.07	<0.1
Ca	0.6	0.1

The Concentrations of Metallic Impurities are reduced by the acid cleaning process.

NASA Tech Briefs, October 1987

See us at The ISA Show—Anaheim, CA 10/5-8 Booth #s 1436-37
Wescon Show—San Francisco, CA 11/17-19 Booth #s 2138-42

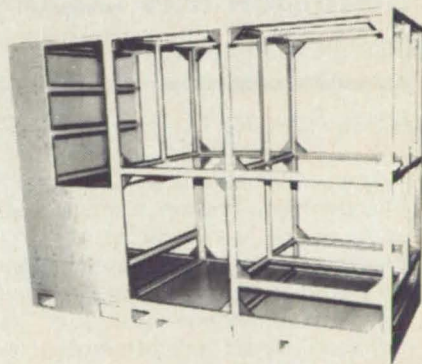
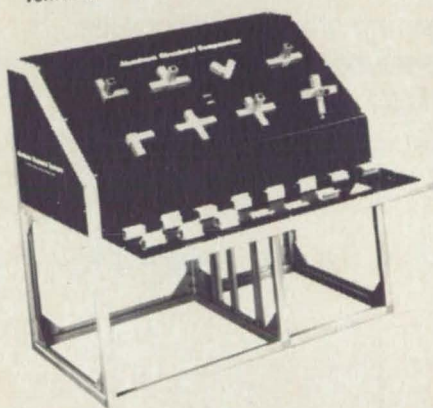
• STRENGTH • DESIGN VERSATILITY

ALUMINUM... HEAVY DUTY STRUCTURAL SYSTEMS

More and more equipment manufacturers, government and industrial project leaders are finding solutions to their unique structural needs at Amco... military and industrial enclosures of complex structural design and strength are often readily resolved with the Amco Aluminum Structural System. Here's why:

You can eliminate expensive welding and inherent stress relieving because Amco bolted assembly techniques exceed welded strength.

Application testimonials include Sentinel Program enclosures, Army mobile communications vehicles, military ground support and shipboard, Airforce and NASA airborne applications.



The Simple Solution For Complex Shock, Vibration And Environmental Requirements

- Simple assembly without special tools
- Greater structural stability and strength **without welding**
- Saves labor, time and materials cost
- Maintains tight tolerances — no distortion in the finished structure
- Eliminates magnetic properties
- Design and build even the most intricate structures
- Ideal for electronics, computer, communications, scientific instrumentation and experimentation, military and industrial equipment

- 11 different extrusions with or without integral flanges for assembly; flush or recessed panel mounting; 1 1/2 inch OD
- 8 versatile corner castings includes 0 to 120 degree hinged corner
- All extrusions (6061-T6) and corner castings (356-T6) provide high-strength structural integrity
- Assembled with locking or non-locking clips, as needed
- Standard gusseting for heavy duty applications adds extra strength where needed

Call for Amco's FREE Aluminum Catalog #203
CALL TOLL FREE 1-800-833-3156 In Illinois Call (312) 671-6670

AMCO Engineering Co.
3801 North Rose St. • Schiller Park, IL 60176-2190
TWX: 910-227-3152
FAX: 312-671-9496

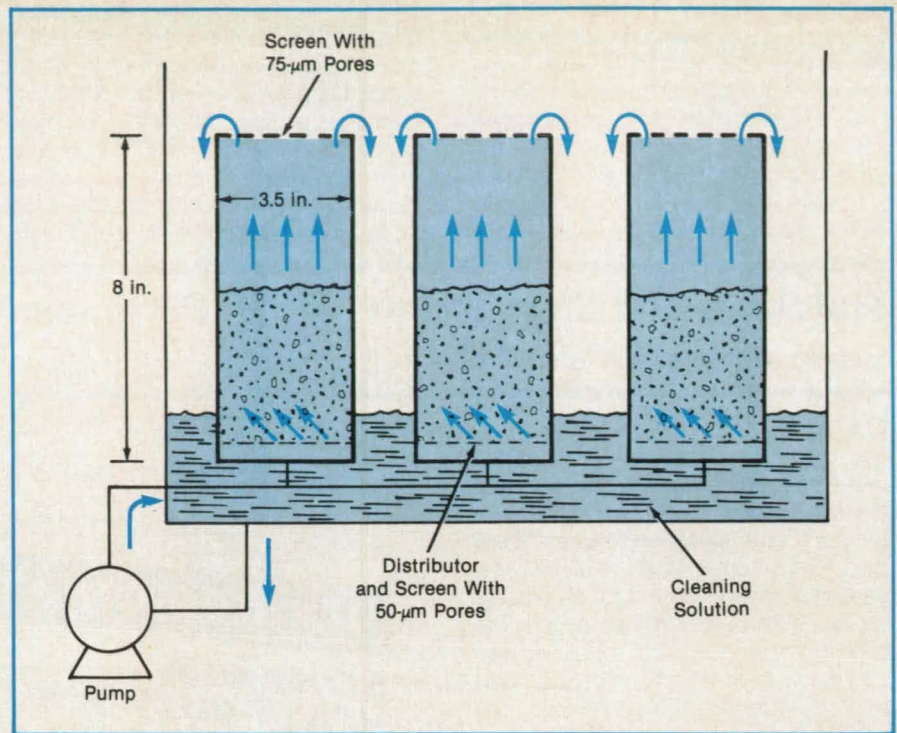


Circle Reader Action No. 498

back into the tank and is recirculated by the pump. The tank is usually filled with about 2 gallons (7.6 liters) of solution. All parts in contact with the silicon or cleaning fluid (including the pump) are made of polyethylene and polypropylene.

In the first washing step, the particle beds are flushed with deionized water to remove silicon particles smaller than $75\ \mu\text{m}$. This is followed by the main 20-minute wash in a mixture of two parts 12N HCl and one part 16N HNO_3 , then by a rinse in deionized water. The oxide layer on the silicon particles is then removed by washing for 20 minutes in 48-percent HF. After a final rinse in deionized water, the particles are removed from the fluidized beds, dried in a quartz diffusion furnace at 150°C under a nitrogen blanket, and sealed in a plastic bag. The concentrations of the principal metallic impurities (Fe, Cr, Ni, Cu, Mn, and Al) are reduced significantly by this cleaning process — in most cases, below the detection limits of spark-source mass spectroscopy (see table).

This work was done by Naresh K. Rohatgi and George C. Hsu of Caltech for NASA's Jet Propulsion Laboratory. For further information, Circle 99 on the TSP Request Card. NPO-16935



Beds of Silicon Particles are fluidized and washed by recirculating an acid cleaning solution.

Bismaleimide Copolymer Matrix Resins

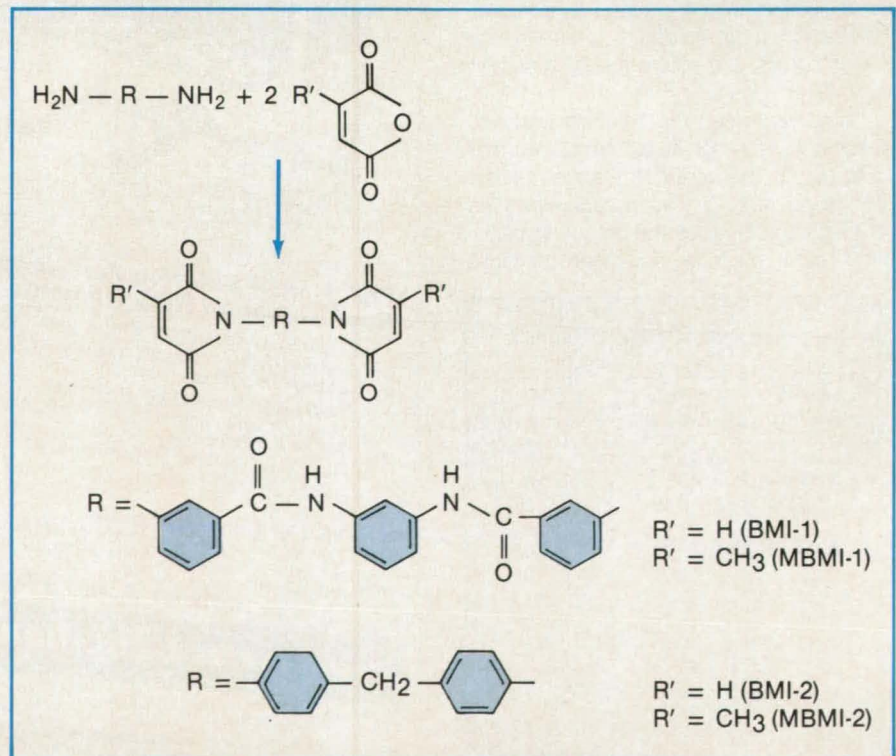
Bismaleimide copolymers yield strong graphite composites.

Ames Research Center, Moffett Field, California

Graphite composites, prepared from a 1:1 copolymer of two new bismaleimides based on the N,N' - m -phenylene-bis(m -amino-benzamide) structure have mechanical properties superior to those prepared from other bismaleimide-type resins. The new heat-resistant composites could replace metal in some structural applications.

The bismaleimide monomer (BMI-1) and the methyl-substituted monomer (MBMI-1) are prepared by the reaction of N,N' - m -phenylene-bis(m -amino-benzamide) (MMAB) with maleic anhydride or citraconic anhydride in N,N -dimethylformamide (DMF) at room temperature, followed by the elimination of water by use of sodium acetate and acetic anhydride at room temperature (see figure). After 3 to 4 h of stirring, the DMF solutions are poured into water, yielding the solid monomers.

The monomers are collected, washed with water, and dried in vacuum at 60°C . For BMI-1 the melting point is 235°C , and the curing temperature is 244°C . For MBMI-1 the melting point is 147°C , and the curing temperature is 217°C . A 1:1 (molar) mixture of BMI-1 and MBMI-1 melts and cures at 142°C and 213°C , respectively.



The **Monomers** used to form copolymers with superior mechanical properties are prepared by the reaction of MMAB with maleic or citraconic anhydride.

The composite prepregs are prepared by coating graphite cloth with a DMF or DMF/acetone (1:1) solution of the resin, then drying them in a vacuum oven at 100 °C for 1 h. The dried prepreg is stacked and pressed between aluminum plates covered with polytetrafluoroethylene film. The laminate is then cured in a flat-plate press at 200° to 240 °C at a pressure of 100 psi (690 kN/m²) for 5 to 6 h.

These composite mixtures of the two resins exhibit better handling, processing, mechanical, and thermal properties

than do the individual resins. The strongest composites are made from a 1:1 copolymer of the two resins; these possess excellent mechanical strength at both ambient and elevated temperatures. They are stronger than composites made of epoxy. They are also stronger than composites made from BMI-2 and MBMI-2 resins (which are similar except that they are formed from the popular methylenedianiline). Even in the case of BMI-2 and MBMI-2, however, copolymers show better properties than do the indi-

vidual resins.

This work was done by John A. Parker and Alvin H. Heimbuch of the Ames Research Center and Ming-Ta S. Hsu and Timothy S. Chen of HC Chem Research & Service Corp. For further information, Circle 126 on the TSP Request Card.

Inquiries concerning rights for the commercial use of this invention should be addressed to the Patent Counsel, Ames Research Center [see page 22]. Refer to ARC-11599.

Books and Reports

These reports, studies, handbooks are available from NASA as Technical Support Packages (TSP's) when a Request Card number is cited; otherwise they are available from the National Technical Information Service.

Design of Fiber Composites for Structural Durability

Hygrothermomechanical effects can be analyzed by computers.

A computational methodology has been developed and is available at NASA Lewis Research Center to design and analyze fiber-composite structures subjected to complex hygrothermomechanical environments. This methodology includes composite mechanics and advanced finite-element structural-analysis methods. Methodology can be applied to such problems as the progressive fracture of a composite material, the design of a composite material for cycle fatigue combined with hot and wet conditions, and general composite-laminate configurations.

A major concern in the fiber-composite community has been the prediction, or even a reasonable approximation, of the structural durability of fiber-composite structures in service environments. Fiber-composite structures need to be designed to resist such service conditions as mechanical load (static, cyclic, or impact), heat, moisture, and combinations of these; i.e., hygrothermomechanical (HTM) conditions.

The general procedure for designing a fiber-composite part that will be exposed to HTM environments begins with the use of empirical data to select laminate configurations for the part, followed by the validation of these data through the preliminary design phase. Subsequently, a variety of tests are conducted in the specified HTM environments. The results of these tests are then used to reconfigure the laminates to meet the design requirements in these HTM environments. This procedure, though successful, is cumbersome

because it is costly, time consuming, and needs to be repeated for each new design. It can be circumvented to a large extent by a methodology for predicting the structural durabilities and, therefore, the service lives of fiber composites in HTM environments. The computational methodology developed accurately predicts the HTM effects on fiber-composite stiffness and strength and, therefore, can be used to design fiber-composite structural components for structural durability.

This computational methodology has evolved over the past seven years. It began with the development of an integrated theory for predicting the hygrothermal effects on fiber composites and has culminated in three major computer programs: (1) CODSTRAN (Composite Durability Structural Analysis), (2) INHYD (Intrapy Hybrid-Composite Design), and (3) ICAN (Integrated Composite Analyzer). These programs collectively provide analyses required for the design of structures durable in HTM service environments.

This work was done by Christos C. Chamis of Lewis Research Center. Further information may be found in NASA TM-87045 [N85-27978/NSP] "Designing for Fiber Composite Structural Durability in Hygrothermomechanical Environments."

Copies may be purchased [prepayment required] from the National Technical Information Service, Springfield, Virginia 22161, Telephone No. (703) 487-4650. Rush orders may be placed for an extra fee by calling (800) 336-4700. LEW-14385

Protective Coatings for Spacecraft Polymers

Thin films of metal-oxide/polymer are applied by ion-beam sputtering.

A report describes experiments in the development of coatings to protect polymers from bombardment by atomic oxygen. Anticipated space systems like the space station, which must operate in low orbits around the Earth for many years, will require materials that are durable in their environment. Early Space Shuttle flights have demonstrated that many materials,

such as polyimide (Kapton® or equivalent), carbon coatings, and some paints, are gradually eroded and suffer changes in optical properties when exposed in low orbit. The observed rates of material loss may be sufficiently high to compromise the long-term durability of polymers typically used in solar arrays or thermal blankets in low Earth orbit. The postulated mechanism for the material loss is oxidation by ram impact (at approximately 4.5 eV) of the geosynchronous atomic oxygen, which is the predominant environmental species at altitudes between 180 km (97 nmi) and 650 km (351 nmi).

One approach to prevent oxidation of materials in low Earth orbits is to provide a protective coating over the oxidizable material. In addition to being unaffected by atomic-oxygen bombardment, such a coating should be flexible, thin, lightweight, adherent, tolerant of ultraviolet light, resistant to abrasion, and susceptible to adhesive bonding; it must not alter the optical properties of the substrate if it is to be used for protecting such polymers as polyimide. Finally, oxidation-preventing coatings must be sufficiently elastic to allow the typical flexure and handling required for a specific polymer application.

Oxidation-preventing, flexible coatings consisting predominantly of metal oxide with small amounts of fluoropolymer have been produced by ion-beam sputter co-deposition. The use of mixed metal-oxide and fluoropolymer ingredients results in protective films of increased flexibility, but additional film thickness may be required to assure long-term (>10 yr) protection against oxidation.

The ground-laboratory tests used thin-film-sensing techniques and radio-frequency-plasma ashers to assess thin-film performance. The space-flight test consisted of a 41.17-h exposure of four samples to the ram atomic oxygen in a low orbit around the Earth on Space Shuttle flight STS-8. Characterizations of the sample exposed to space were performed to address two general questions: (1) What are the changes in properties of the protected Kapton® (or equivalent) as a result of the exposure to atomic oxygen in orbit and (2) how effective is the coating in pro-



Technology that breaks design barriers.

THORNEL® Carbon Fibers

New solutions. Whether you are developing aerospace designs for the next century or aircraft designs for the near future we can help you like no other carbon fiber supplier can.

Technological superiority. Our state-of-the-art production facilities are computer controlled to provide materials with demonstrated low coefficients of variation. You can design closer to the limit and use our materials with more confidence and efficiency.

Domestic security. Our THORNEL fibers are made in fully integrated facilities right here in the U.S.A. Our Greenville, South Carolina plant has been on-line since 1982 producing fiber for a range of application requirements. If domestic fiber is as important to you as it is to us, you can qualify it now for that major program.

Accessible experience. We have been on the leading edge of carbon fiber technology since the early 1960's. That experience enables us to offer you unmatched research and development, and superior technological support. We are, in fact, uniquely qualified to work with you in solving your individual materials problems because our fully integrated plants are here in the States.

Talk to us. Ask us questions. The earlier you involve us in the development process, the more we can help you. Call Amoco Performance Products, Customer Service at 1-800-222-2448.

Because there should be no barriers to design freedom.

THE ALL AMERICAN SOLUTION



Amoco Performance Products

Circle Reader Action No. 336

viding long-term durability to the underlying Kapton® (or equivalent)?

Ion-beam sputter-deposited thin films of Al_2O_3 , SiO_2 , and SiO_2 /polytetrafluoroethylene molecular mixtures are effective in preventing oxidation of such underlying materials as Kapton® (or equivalent), as demonstrated in both ground-based-laboratory and flight tests. The addition of small amounts (<15 percent by volume) of codeposited polytetrafluoroethylene to SiO_2 can be used to increase, by a factor of 3, the strain that the film can withstand without fracture.

However the ground-based radio-frequency-plasma ashing tests, in conjunction with the optical detection of the protective films, indicate that the minimum protective film thickness required for permanent protection from oxidation is increased by an order of magnitude (from 50 to 600 Å) if one adds 15 percent polytetrafluoroethylene. The application of protective films of Al_2O_3 , SiO_2 , and >96 percent SiO_2 with <4 percent polytetrafluoroethylene did not alter the optical properties of Kapton® (or equivalent) over the wavelengths from 0.33 to 50 μm . In addition, no change occurred in optical properties of the protected Kapton® (or equivalent) over the wavelengths from 0.33 to 2.2 μm . Postflight analysis indicates that the three protective coatings remained intact and functional throughout the 41.17-h orbital ram exposure to environmental atomic oxygen.

This work was done by Bruce A. Banks, Michael J. Mirtich, Jr., Sharon K. Rutledge, Henry K. Nahra, and Diane Swec of Lewis Research Center. Further information may be found in NASA TM-87051 [N85-3017/NSP], "Ion Beam Sputter-Deposited Thin Film Coatings for Protection of Spacecraft Polymers in Low Earth Orbit."

Copies may be purchased [prepayment required] from the National Technical Information Service, Springfield, Virginia 22161, Telephone No. (703) 487-4650. Rush orders may be placed for an extra fee by calling (800) 336-4700.

This invention has been patented by NASA (U.S. Patent No. 4,560,577). Inquiries concerning nonexclusive or exclusive license for its commercial development should be addressed to the Patent Counsel, Lewis Research Center [see page 22]. Refer to LEW-14384.

Tribological Properties of Structural Ceramics

Studies of wear and lubrication promote longer component lives.

A paper discusses the tribological properties of structural ceramics. Tribology is the study of the adhesion, friction, wear, and lubricated behavior of solid materials in contact. The function of tribological

research is to bring about a reduction in the adhesion, friction, and wear of mechanical components; to prevent their failure; and to provide long, reliable component life — through the judicious selection of materials, operating parameters, and lubricants.

The paper reviews the adhesion, friction, wear, and lubrication of ceramics; their anisotropic friction and wear behavior; and the effects of surface films and of interactions between ceramics and metals. Analogies with metals are made. Both oxide and nonoxide ceramics, including ceramics used as high temperature lubricants, are discussed.

Mechanical systems like bearings, gears, and seals are examples of components amenable to tribology. Whenever there is relative motion between two or more solid surfaces in contact, tribology is involved. Such mundane activities as shaving involve both friction and corrosive wear, and considerable tribological research has gone into increasing blade life and reducing friction and shaving discomfort. With more complex tribological systems such as gyroscope bearings and instrumentation gears, attention must be directed to many elements.

With a notable amount of research effort already having been put into fundamental studies of the tribological behavior of metals, attention is focused on ceramics because of their increasing potential as components in mechanical systems. Tribological studies have been conducted to gain increased understanding of those physical and chemical properties of ceramic parts that will affect their behavior when they are in contact with parts either of the same material or of other ceramics or metals.

Whereas metals readily deform plastically, ceramics, while having high strength, are normally brittle and fracture with little or no evidence of plastic flow. However, plastic flow has been observed in the surface layers of a number of ceramics, at the interface between two ceramics in contact under load and relative motion. Plastic flow has been observed with magnesium oxide, aluminum oxide, and silicon carbide, under relatively modest conditions of rubbing contact.

Factors like dislocations, vacancies, stacking faults, and crystal structure, which influence the mechanical behavior of materials when plastic flow occurs, also influence the friction and wear behavior of ceramics. Comparisons can be made between the anisotropic friction behaviors of ceramics and of metals. Surface films such as adsorbates markedly influence the adhesion, friction and wear behavior of ceramics. Further, with ceramics and other ionic solids, the presence of such surface films as water and surface-active organics can influence adhesion, friction, and wear by altering the amount of plastic

deformation that will occur during sliding or rubbing.

Ceramic compositions can be used both as coatings and in composites for the high-temperature lubrication of both alloys and ceramics.

This work was done by Donald H. Buckley and Kazuhisa Miyoshi of Lewis Research Center. Further information may be found in NASA TM-87105 [N86-10341/NSP], "Tribological Properties of Structural Ceramics."

Copies may be purchased [prepayment required] from the National Technical Information Service, Springfield, Virginia 22161, Telephone No. (703) 487-4650. Rush orders may be placed for an extra fee by calling (800) 336-4700. LEW-14387

Amorphous Insulator Films With Controllable Properties

These films have potential for optical, electronic, magnetic, and mechanical applications.

In experiments described in a report, amorphous hydrogenated carbon (a-C:H) films were grown at room temperature by low-frequency plasma deposition, using methane or butane gas. These films have a unique array of useful properties: (a) they adhere to a wide variety of materials (including quartz insulators, semiconductors, and metals); (b) they contain only carbon and hydrogen; (c) they are very smooth and free of pinholes; (d) they are resistant to attack by moisture and chemicals; and (e) they have high electric-breakdown strength and electrical resistivity. Two of the optical properties (refractive index and absorption coefficient) and the hardness of this film can be controlled by the deposition conditions.

In this work, the film thickness of the a-C:H varied from 2 to 30 μm . (0.05 to 0.76 μm), and the deposition time was kept at or below 30 min. The films were smooth [better than 0.1 μm . (0.0025 μm)], uniform (better than ± 2 percent), and without an overlayer or interface layer. Some deposition conditions resulted in a-C:H films so hard that they were not easily scratched by a sharp carbide edge.

In an application where the transparency edge (the light frequency or wavelength corresponding to 1 percent absorption) is required to be in the deep ultraviolet [down to a wavelength of 10 μm . (0.25 μm)], another amorphous insulator film can be used; namely, boron nitride (BN). The BN films are generally similar to the a-C:H films. Deposition techniques for BN are different from those for a-C:H. The amorphous a-C:H and BN films are expected to be used for the hermetic sealing and protection of optical, electronic, magnetic, or delicate mechanical systems, and for semiconductor field dielectrics.

This work was done by Samuel A. Alterovitz, Joseph D. Warner, David C. Liu, and John J. Pouch of **Lewis Research Center**. Further information may be found in NASA TM-87135 [N86-12134/NSP], "Ellipsometric and Optical Study of Some Uncommon Insulator Films on III-V Semiconductors."

Copies may be purchased [prepayment required] from the National Technical Information Service, Springfield, Virginia 22161, Telephone No. (703) 487-4650. Rush orders may be placed for an extra fee by calling (800) 336-4700. LEW-14370

Radiation Resistances of Dielectric Liquids

Although data are sparse for some liquids, polyphenyls appear to be particularly stable.

A report presents data on the effects of ionizing radiation on dielectric liquids for high-energy-density, pulsed-power capacitors. The report is based on Jet Propulsion Laboratory test results, a search of NASA and Department of Energy computer files, a survey of the open literature, and contacts with manufacturers and suppliers. The report covers 22 organic liquids, although detailed data were found for only one compound, polydimethyl siloxane. Generic data on the effects of radiation on compounds with similar chemical structures are provided where data on specific compounds are lacking.

Some organic liquids are much more radiation-resistant than others, according to the report; the polyphenyls are particularly stable. For reasons of economy and viscosity, the diphenyls and triphenyls are preferred. When irradiated in a nuclear reactor, these materials lose some hydrogen atoms and gradually polymerize to higher polyphenyls. The polyphenyls become useless as liquid insulators after exposure to a thermal-neutron fluence of 10^{19} neutrons per square centimeter because they polymerize excessively and form solids.

A radiation exposure of 10^7 to 10^9 rads causes observable degradation in organic dielectric liquids. The liquids are less stable than are plastic dielectric films, and the stability of a given liquid depends strongly on the film with which it is combined.

This work was done by Frank L. Bouquet and Robert B. Somoano of Caltech for NASA's Jet Propulsion Laboratory. To obtain a copy of the report, "Radiation Effects Data on Dielectric Liquids for Capacitor Applications," Circle 107 on the TSP Request Card. NPO-16891

HIGH PERFORMANCE SUPERMATERIALS IN PLASMA SPRAYED OR SOLID FORM

At Last—here's a convenient way for engineers, scientists and researchers to analyze and test characteristics of hundreds of ceramic and metal materials. Need "white" ceramics? Need "black" ceramics? Need corrosion resistant coatings? Need metals that won't oxidize at 1000°C ? Need thermal barrier coatings? How about experimenting with electrically conductive coatings?:

We'll supply coupons in your size needs, such as 1 inch diameter. We will plasma coat the ends or diameter of small cylinders to any thickness desired, from .0004 inch (.01 mm) to .120 inch (3 mm). We will coat small flat plates of metal on one or both sides to these thicknesses. We will not fuse your powders by sintering in a hot furnace (too unpredictable!) Plates can be steel, copper, aluminum or any other non-precious metal. We fuse powders at gun temperatures up to $17,000^\circ\text{K}$ with no dopants or matrix needed to cement particles together. Multi-layer material coupons available.

SPECIAL OFFER: We will supply 6 round coupons in a set, up to 2 inch diameter, or flat plates, "mix or match" coated on surfaces desired. We will not polish, leaving surface structure unchanged. We will throw in 1 pound of commercial purity powder metal or ceramic, for your further analysis. We will supply a data sheet describing the powder material at no extra charge.

Specify if coatings are to be oxidized, such coupons should usually be coated all over. If you have oddly shaped parts to coat we can supply engineering applications advice from our affiliate company, Carboride Corporation, the world's leading high tech product development group, specializing in high performance material applications from ceramic rocket nozzles to ceramic coated diesel engine pistons.

Price per coupon set as described above \$990 plus UPS shipping charge of \$5.00. Delivery can be made usually in 1 to 2 weeks for commonly used materials, and up to 8 weeks for relatively rare materials (Superconducting experimental materials require a special quotation.)

Many powders are only a few dollars a pound. Many are far more expensive. (Minimum powder order any one material \$100.) Upon receipt of your purchase order, we will invoice you 70% of your order amount, which we must collect in advance before shipment because of the danger of cancellation.

LIST OF MATERIALS AVAILABLE IN POWDER AND ROD FORM

The following is a partial listing of our high temperature materials, high purity metals and powders, rare earths, metal borides, nitrides, silicides, carbides, oxides, submicron powders, plasma spray powders, exotic metal powders, spherical powders, rods, wire, foils, Superconductor materials, and alloy materials. Commercial purities are much less costly than laboratory purities.

Aluminum	Cobalt	Indium	Palladium	Thallium
Antimony	Columbium	Iron	Platinum	Thulium
Barium	Copper	Lanthanum	Praseodymium	Tin
Beryllium	Dysprosium	Lead	Samarium	Titanium
Bismuth	Erbium	Lutetium	Scandium	Tungsten
Boron	Europium	Magnesium	Selenium	Vanadium
Brass	Gadolinium	Manganese	Silicon	Ytterbium
Cadmium	Gallium	Molybdenum	Silver	Yttrium
Calcium	Germanium	Neodymium	Strontium	Zinc
Cerium	Gold	Nickel	Tantalum	Zirconium
Cesium	Hafnium	Niobium	Tellurium	
Chromium	Holmium	Osmium	Terbium	

SUPERMATERIALS COMPANY

Suite 356 Statler Office Tower
1127 Euclid Avenue, Cleveland, Ohio 44115
Telephone (216) 861-0724

(An Affiliate of Carboride Corporation—world leaders in high performance ceramic composites)



Computer Programs

- 66 **Calculating Wave Drag on an Aircraft**
- 66 **Computer Program for Flow in a Combustor**
- 66 **Program for Analysis and Enhancement of Images**
- 68 **Program for Development of Artificial Intelligence**
- 68 **Assessing the Reliability of NDE**

COSMIC: Transferring NASA Software

COSMIC, NASA's Computer Software Management and Information Center, distributes software developed with NASA funding to industry, other government agencies and academia.

COSMIC's inventory is updated regularly; new programs are reported in *Tech Briefs*. For additional information on any of the programs described here, circle the appropriate TSP number.

If you don't find a program in this issue that meets your needs, call COSMIC directly for a free review of programs in your area of interest. You can also purchase the 1986 *COSMIC Software Catalog*, containing descriptions and ordering information for available software.

COSMIC is part of NASA's Technology Utilization Network.

COSMIC® — John A. Gibson, Director, (404) 542-3265

Computer Services Annex, University of Georgia, Athens, GA 30602

Computer Programs

These programs may be obtained at a very reasonable cost from COSMIC, a facility sponsored by NASA to make raw programs available to the public. For information on program price, size, and availability, circle the reference number on the TSP and COSMIC Request Card in this issue.



Mechanics

Calculating Wave Drag on an Aircraft

An improved program is based on a more-accurate mathematical model.

WDRAG2 calculates the supersonic zero-lift wave drag of complex aircraft configurations. WDRAG2 incorporates extended capabilities for geometric input to enable the use of a more-accurate mathematical model. With WDRAG2, the engineer can define aircraft components as fusiform or non-fusiform by the use of traditional parallel contours.

The geometrical construction can include any combination of the following components: wings, body, pods, fins, and canards. The body can consist of arbitrary contours, while such other fusiform components as pods or nacelles must be axisymmetric. The wing can include camber and twist. This program allows only laterally symmetrical configurations. (The WAV-DRAG program, available separately from COSMIC, can handle laterally asymmetrical configurations but requires much greater time and computational resources.)

The calculations in WDRAG2 are based on Whitcomb's area-rule computation of equivalent bodies, with modifications for supersonic speed using the von Kármán slender-body formula. Instead of using a single equivalent body, WDRAG2 calculates a series of equivalent bodies, one for each roll angle. The total wave drag on the aircraft of the specified configuration is the integrated average of the equivalent-body wave drags through the full roll range of 360°.

The input consists of user-defined components, the mach number, the desired numbers of longitudinal computation stations and roll angles, and optional constraint and optimization inputs. The program warns of body-line segments having slopes larger than the mach angle. WDRAG2 calculates the wave drag of the specified aircraft configuration as well as an optimum wave drag for specified constraints.

WDRAG2 is written in FORTRAN IV for batch execution and has been implemented on a CDC CYBER 170 computer under NOS with a central-memory requirement of approximately 61K (octal) of 60-bit words. The program was developed in 1976.

This program was written by Samuel M. Dollyhigh and Charlotte B. Craidon of Langley Research Center. For further information, Circle 154 on the TSP Request Card. LAR-13634

Computer Program for Flow in a Combustor

This program simulates subsonic, swirling, reacting, turbulent flow about a bluff body.

A new version of the TEACH computer program has been developed specifically for use in the analysis of the subsonic, swirling, reacting, turbulent flow in a cylindrical bluff-body research combustor. This combustor design is widely used as a research tool for the mathematical modeling of gas turbines and for the development of diagnostic instrumentation.

The flow field of interest is developed in the open-ended, cylindrical chamber downstream of the base of the bluff body that houses the fuel injector. Such flows can be described by the fully-elliptic, steady-state equations of motion. This version of TEACH solves these equations using an improved finite-difference procedure, the B rounded skew upwind differencing (BSUD) method. The axisymmetric pressure distribution is estimated by means of a new algorithm, the pressure-implicit split-operation (PISO) predictor/corrector technique.

Sections of the computer program have been reorganized in an attempt to minimize the changes necessary to install the

program in different computer systems. The input format has been extensively revised to permit more flexibility in setting up and running cases. Additional options include the analysis of two-dimensional planar flow and the selection of the more-conventional hybrid differencing scheme.

This program was written by Louis M. Chiappetta of United Technologies Corp. for Lewis Research Center. For further information, Circle 20 on the TSP Request Card.

LEW-14271



Mathematics and Information Sciences

Program for Analysis and Enhancement of Images

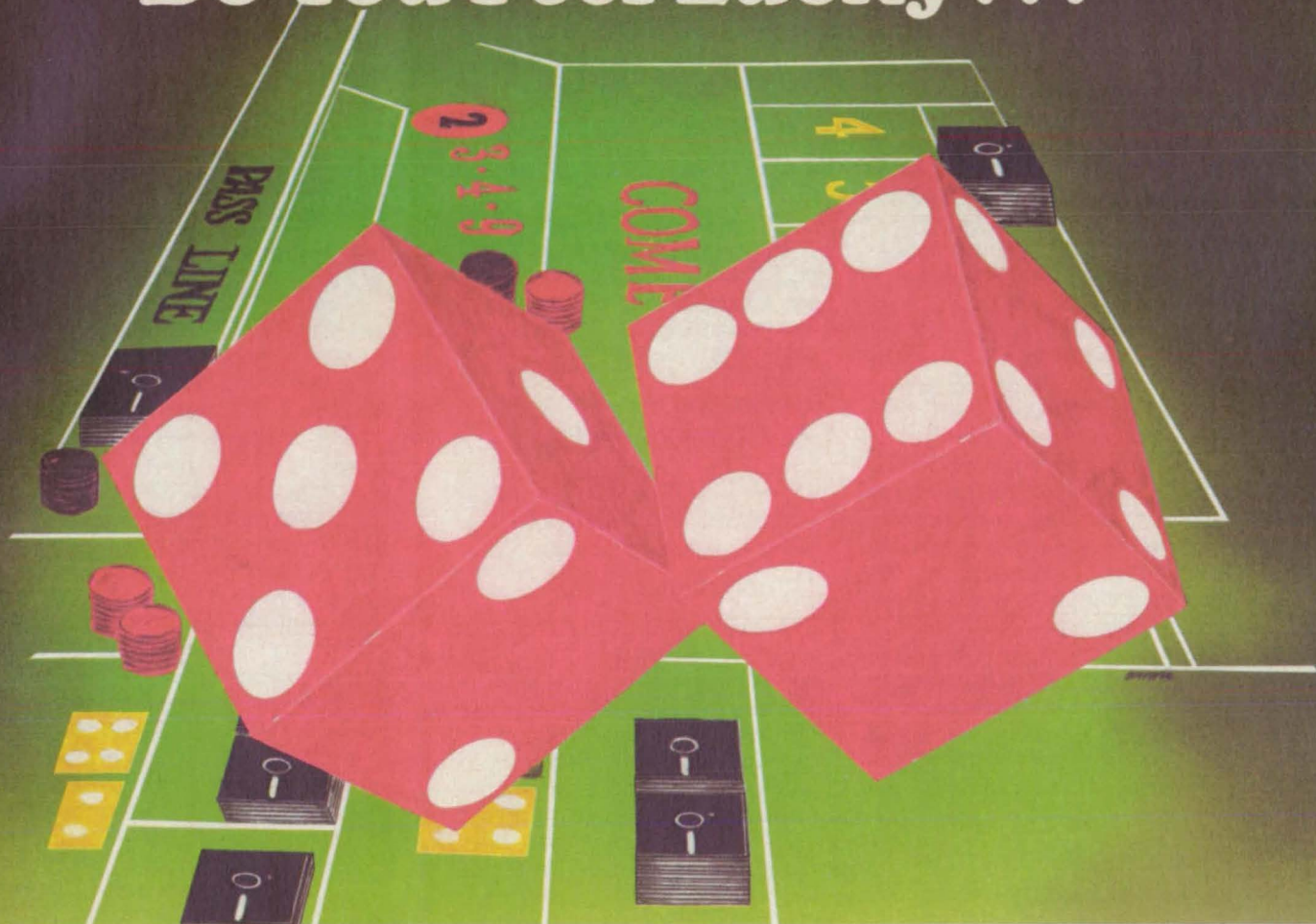
Image data can be manipulated from and to a variety of forms.

The Land Analysis System (LAS) is a collection of image-analysis computer programs designed to manipulate and analyze multispectral image data. It provides the user with functions ingesting various sensor data, radiometric and geometric corrections, image registration, training site selection, supervised and unsupervised classification, Fourier domain filtering, and image enhancement.

The package is sufficiently modular and includes an extensive library of subroutines to permit inclusion of new algorithmic programs. Included are routines for image input/output from tape and disk, statistical data handling, pixel manipulations, geometric transformations, and general utility routines. The commercial package International Mathematical & Statistical Library (IMSL) is required for full implementation of the LAS.

The LAS is integrated with the Transportable Applications Executive (TAE). TAE has four modes of user interaction: (1) menu, (2) direct command, (3) tutor (or help), and (4) dynamic tutor. This allows new users to select LAS functions from the menus and to obtain online help information. It also allows experienced users the efficiency of issuing direct commands.

Do You Feel Lucky???



Good programming isn't a matter of luck. It requires skill, perseverance and good programming tools. You already have the skill and perseverance; **Janus/Ada** provides the programming tools. Tools you can rely on in any project, in almost any MS DOS environment, with full portability to any other Ada system. With **Janus/Ada**, you get lucky in all the right ways:

- SYSTEM REQUIREMENTS:** Any Intel 86 family processor with 512K RAM, two floppy disk drives or a hard disk and DOS 2.0 or higher.
- COMPILATION SPEEDS:** 8086/6MHZ: 300 lines per minute; 80186/8MHZ: 500 lines per minute; 80286/8MHZ: 900 lines per minute (DOS 3.0)
- PRODUCT SUPPORT:** Quarterly newsletters, 24 hour Bulletin Board, and a staff with over 20 man years of actual Ada programming experience.
- APPLICATIONS AND TOOLS:** Assemblers, disassemblers, Ada source code, a Pascal to Ada translator, 8087 support, tutorials and more!
- AFFORDABILITY:** Our **Janus/Ada "C" Pak** is available for \$99.95 and contains the **Janus/Ada** Compiler and Linker, designed specifically for microcomputers and consumer tested since 1981. Our customers can upgrade to our development and embedded systems "paks" with 100% credit for this starter package. Our **Janus/Ada** Extended Tutorial is available for the same low price. We feature commercial and educational "site" licensing for all of our packages.
- ADA STANDARDIZATION:** **Janus/Ada** source code can be ported to any validated Ada system and compiled. We offer a variety of tools and consultations to assist you in this process, if needed.
- JANUS/ADA USERS:** Over 5,000 separate sites use the **Janus/Ada** compiler for training, embedded systems and applications each day. We supply our tools to the U.S. Armed Forces, Fortune 500 companies and over 400 educational institutions, as well as to individuals like you.

We've been making programmers lucky with our tools for over 5 years; isn't it about time you changed your luck? We'll even pay for the call! To place an order or receive our informative brochure, please call 1-800-722-3248. It'll make your day!!!



SOFTWARE, INC.

P.O. Box 1512 Madison, Wisconsin 53701
(608) 244-6436 TELEX 4998168

specialists in state of the art programming

1-800-722-3248

Circle Reader Action No. 467

CP/M, CP/M-86, CCP/M-86 are trademarks of Digital Research, Inc.
*ADA is a trademark of the U.S. Department of Defense
MS-DOS is a trademark of Microsoft

© Copyright 1986 RR Software

TAE also provides the ability for users to create sequences of LAS functions to be executed as a single command.

A Catalog Manager (CM) package provides users with the ability to assign names for data files and to organize the cataloged set of names in a structure suitable for the user's application.

The next release of LAS, scheduled for summer 1987, will include a Display Management Subsystem (DMS) which facilitates the ability to interface LAS with image analysis and display devices. The LAS will include an interface to the International Imaging Systems Inc. (IIS) model 75 image processor. Other display devices are expected to be available as they are implemented by the LAS user community.

The LAS package (including TAE, CM, and DMS) is available by license for a period of ten years to approved domestic licensees. It includes the source code and one complete set of documentation. Additional copies of the documentation can be purchased separately at any time.

LAS is written in VAX FORTRAN 77, C, and Macro assembler for a DEC VAX operating under VMS 4.0.

This program was written by Yun-Chi Lu of Goddard Space Flight Center. For further information, Circle 147 on the TSP Request Card. GSC-13075

Program for Development of Artificial Intelligence

CLIPS surpasses other programs in its category.

The C Language Integrated Production System (CLIPS) computer program is a shell for developing expert systems. It was designed to enable research, development, and delivery of artificial intelligence on conventional computers. The primary design goals for CLIPS were portability, efficiency, and functionality. For these reasons, the program was written in C. CLIPS meets or out-performs most microcomputer- and minicomputer-based artificial-intelligence tools.

CLIPS is a forward-chaining-rule-based language. The program contains an inference engine and a language syntax that provide a framework for the construction of an expert system. CLIPS is based on the Rete algorithm, which enables very efficient pattern matching. The collection of conditions, and, the actions to be taken if the conditions are met, is constructed into a rule network. As facts are asserted either prior to or during a session, CLIPS pattern-matches the number of fields. Wild cards and variables are supported for both single and multiple fields. CLIPS syntax allows the inclusion of externally defined functions (outside functions written in a language other than CLIPS). CLIPS itself can be embedded in a program in such a way that the

expert system is available as a simple sub-routine call.

CLIPS is written in C for interactive execution and has been implemented on an IBM PC computer operating under DOS with a central-memory requirement of approximately 256K of 8-bit bytes. It should run on any computer system that supports a full (Kernighan and Ritchie) C compiler. CLIPS was developed in 1986.

This program was written by Gary Riley, Chris Culbert, and Frank Lopez of Johnson Space Center. For further information, Circle 157 on the TSP Request Card. MSC-21208

Assessing the Reliability of NDE

A computer program assesses the ability of inspection techniques to find structural flaws.

A versatile FORTRAN computer algorithm has been developed for calculating and plotting the reliability of a nondestructive evaluation (NDE) technique for the inspection of flaws. The algorithm was developed specifically to determine the reliability of radiographic and ultrasonic methods for the detection of critical flaws in structural ceramic materials. Reliability is displayed in the form of a plot of the probability of detection (at a selected confidence level) versus the flaw size.

NDE methods are used in such applications as diagnostic medicine, quality control in industrial production, and the prediction of failure in structural components. In the latter application, sensitive, reliable NDE techniques are needed to (1) detect flaws and reject parts containing critical flaws or concentrated flaw populations and (2) aid in the optimization of processes by identifying the stages of fabrication during which flaws are introduced.

The reliability of an NDE inspection technique is a quantitative measure of the ability of that technique to detect flaws of a specific type and size in a particular material. In experiments to determine reliability, specially prepared specimens containing a known number of accurately characterized flaws are inspected. Data are gathered on the number and size of flaws detected. Applying binomial-distribution statistical theory to these data, reliability is then calculated in terms of the probabilities of detection at specific confidence levels for various flaw sizes. This calculation requires great computational effort.

This new FORTRAN program calculates and plots the reliability of flaw inspection by NDE. The program was written for a Digital PDP 11/45 minicomputer interfaced with Control/Grinnell 274 image processor. Its task file requires 64 kilobytes (125 blocks) of memory.

Initially, flaw-inspection data are entered into the computer and stored in files. These data are arranged in intervals using the options of equal flaw-size interval, overlapping flaw-size interval, or optimized probability methods. The user selects the interval sizes and method of data grouping, and a record of the number and size of flaws examined and detected per interval is stored. The probability of detection is then calculated over the range of flaw-size data using any preselected confidence level.

Two types of plots displaying quantitative flaw-detectability results are generated on a video monitor by use of the image-processor software routines. One plot shows the number of flaws examined and detected versus the flaw size or flaw size/part thickness. The second plot shows the probability of detection (at the selected confidence level) versus the flaw size or flaw size/part thickness.

An application of the technique includes the determination of the reliability of an NDE inspection technique for detecting such critical flaws as voids, cracks, foreign impurity particles, and delaminations in metal, ceramic, polymeric, and composite structural components. Industrial interests might include developers of NDE inspection equipment who wish to evaluate the reliability of the equipment for flaw detection and producers and users of structural components who use NDE methods to detect flaws deemed critical to component integrity.

This program was written by Don J. Roth of Lewis Research Center. For further information, Circle 47 on the TSP Request Card.

LEW-14286

New Products

A wet/wet bidirectional and unidirectional differential pressure transducer with a four active-arm diffused, media isolated semiconductor bridge is now available from **CEC Instruments Division, Pasadena, CA**. The Model 6600 has high accuracy, small size and media isolation, and has a corrosion resistance comparable to stainless steel. Useful throughout the aerospace, industrial and chemical industries, the 6600 is available in standard pressure ranges from 10 to 500 psid and has a rated excitation of 10 VDC. **Circle Reader Service Number 589.**

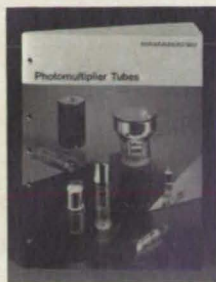
National Instruments (Austin, TX) has announced the GPIB-PRL, an 8-bit microcomputer based interface tailored for use as an IEEE-488 bus (GPIB) to parallel (Centronics) bus converter. It offers a low cost method for connecting a device with a Centronics type parallel interface to IEEE-488 instruments and controllers. GPIB-PRL includes an integrated DMA controller that transfers data directly to a 64K byte memory buffer, thus allowing data transfer rates as high as 900K bytes/second. Buffered data is then output to the parallel device at its own rate. **Circle Reader Service Number 586**

GREAT BOOKS IN PHOTONICS...

EVERYTHING YOU NEED TO KNOW TO SELECT THE RIGHT PHOTSENSITIVE DEVICES — SEND FOR THEM TODAY!

Send today for the compendium of photosensitivity knowledge. Described in detail is the world's most complete line of photosensitive devices — Hamamatsu's! You'll have

at your fingertips the precise information you need to specify the right device for each application!



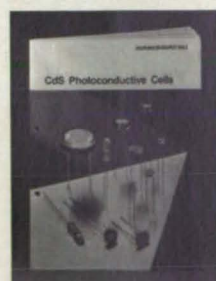
PHOTOMULTIPLIER TUBES FOR EVERY NEED This 68-page catalog details 18 PMT characteristics including spectral response, luminous sensitivity, ground polarity, dark current and hysteresis for the most complete line of head-on and side-on types, $\frac{3}{8}$ "-20 inch diameter. Selection guide with specifications and dimensional outlines help you make the best choice.



PHOTOTUBES — This 18-page catalog includes a selection guide, spectral response charts, dimensional outlines and specification charts for more than 40 head-on and side-on phototubes, UV detectors, vacuum phototubes, gas-filled and biplanar phototubes.



PHOTODIODES — Silicon, PIN Silicon, GaAsP, GaP, Avalanche This 44-page catalog provides spectral range, response time, temperature characteristics, linearity and specifications for UV to IR silicon, visible to IR silicon, GaAsP and GaP photodiodes.



PHOTOCONDUCTIVE CELLS CdS, CdSe This 16-page catalog describes performance characteristics and specifications of various photoconductive cells used in exposure meters, auto dimmers, musical instruments, flame monitors, street light controls and other applications.



OPTOISOLATORS Single and multi-element LED-CdS optoisolators, LED phototransistors, Lamp CdS and optointerrupters are described. Photos and diagrams illustrating physical characteristics and complete specifications are provided in this 18-page catalog.

Call or write to receive one or all ten catalogs.



LIGHT SOURCES — Deuterium, Xenon, Mercury-Xenon, Hollow Cathode, etc. This 24-page catalog provides information about the most complete line of light sources for scientific instruments. Specifications are provided which define the high stability and dependability. Super-quiet xenon lamps are among the special light sources described.



PHOTOMULTIPLIER TUBES FOR SCINTILLATION COUNTING AND HIGH ENERGY PHYSICS This 30-page catalog provides a quick reference of PMTs with special performance characteristics. Energy resolution, pulse linearity, response time and application information are included.



VIDICONS — Visible, IR, UV, X-Ray This 24-page catalog provides a cross-reference of vidicon types and typical applications in addition to dimensional outlines, application photos and complete specifications.



SPECIALTY IMAGING TUBES — This 25-page catalog contains a number of new types of photonic devices for capturing static and transit images. An ideal source of ideas for new types of instrumentation.



INFRARED DETECTORS — PbS, PbSe Cells; Ge, InAs, InSb Cells; Photon Drag Detector; Pyroelectric Detectors & More This 36-page catalog describes IR detectors with various elements and configurations. Extensive diagrams, characteristic graphs and glossary accompany performance specifications.

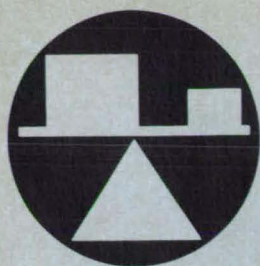
OTHER CATALOGS AVAILABLE:
Accessories for Photomultiplier Tubes,
Image Intensifier Tubes, PCD Linear
Image Sensors

© Copyright 1986, Hamamatsu Corporation

HAMAMATSU

HAMAMATSU CORPORATION • 360 Foothill Road, P.O. Box 6910, Bridgewater, NJ 08807 • Phone: 201/231-0960
International Offices in Major Countries of Europe and Asia.

Circle Reader Action No. 471



Hardware, Techniques, and Processes

- 70 Determining Directions of Ultrasound in Solids
- 71 High-Differential-Pressure Heat Exchanger

- 72 Measuring Viscosities of Gases at Atmospheric Pressure
- 74 Fiber-Optic Temperature Sensor
- 74 Gamma-Ray Fuel Gauges for Airplanes
- 79 Thermally Insulating Support for Cryogenic Tanks
- 80 Analyzing Wakes From Hovering-Helicopter Rotor Blades

- 83 Measuring and Plotting Surface-Contour Deviations
- 84 Color-Video Thermal Maps
- 84 Stiffening Heat-Exchanger Tubes Against Vibrations
- 85 Lead Scales for X-Radiographs
- Books and Reports
- 85 Experiments in Boundary-Layer Turbulence
- 85 Preliminary-Design Software for Composite Structures

- 86 Structural-Dynamics of Filament-Wound Booster Rockets
- 86 Calculations of Wall Effects on Propeller Noise
- 86 Water-Tunnel Flow Visualization with a Laser
- 87 Control and Simulation of Space-Station Vibrations
- Computer Programs
- 66 Calculating Wave Drag on an Aircraft
- 66 Computer Program for Flow in a Combustor

Determining Directions of Ultrasound in Solids

Ultrasound shadows are cast by grooves.

Lewis Research Center, Cleveland, Ohio

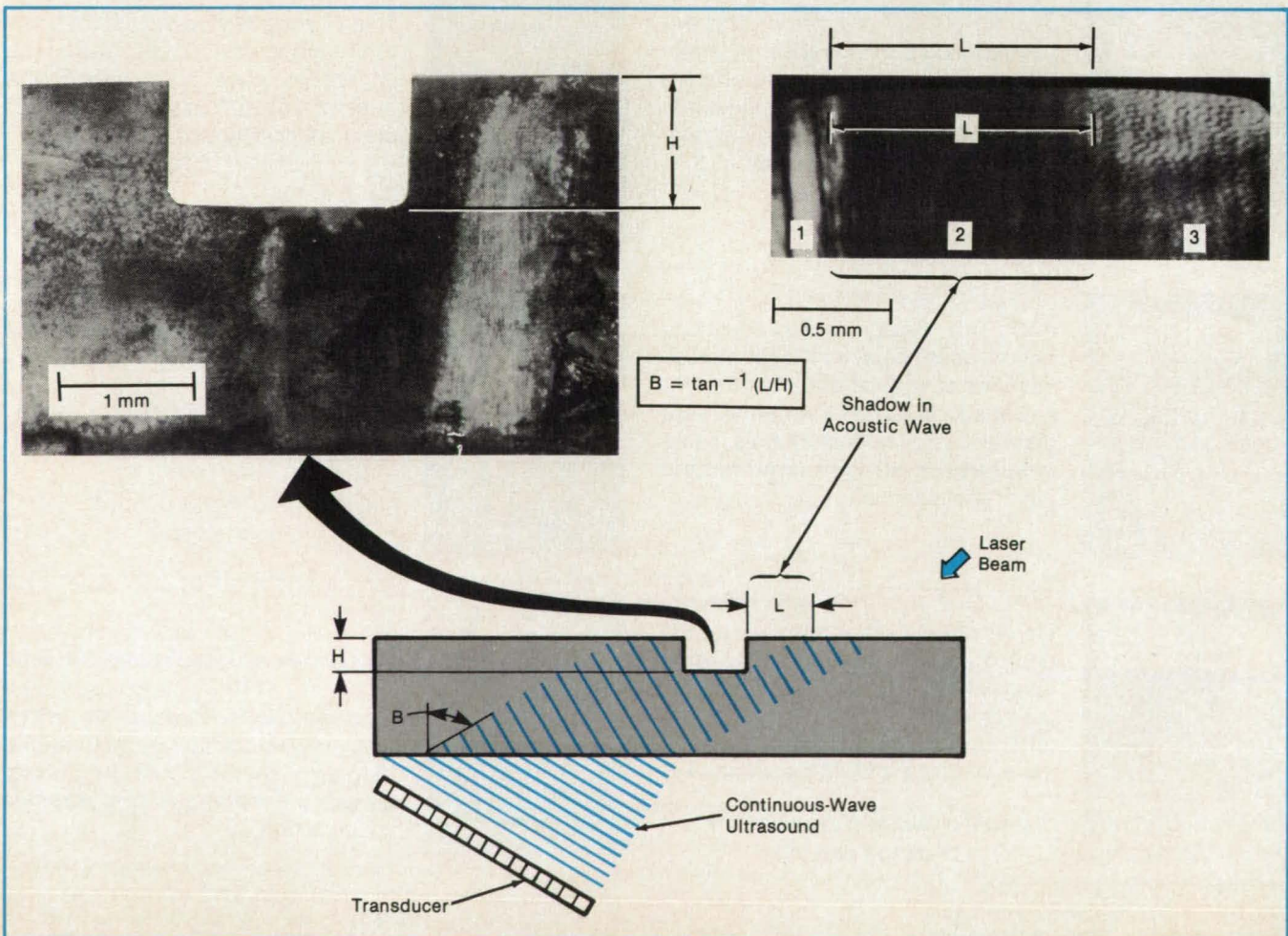
Defects or flaws within a structural material can effectively weaken a component or degrade its toughness to the point of catastrophic failure. For example, ceramics being investigated as replacements for metal components in automobile engines exhibit both low toughness and wide variability in strength. This combination of undesirable properties is generally attributed to impurities, voids, or microcracks introduced during processing. Pin-

pointing the locations of such flaws is important in determining whether a manufactured component is fit for service.

Scanning laser acoustic microscopy (SLAM) uses high-frequency ultrasound in conjunction with a laser to produce acoustic images of specimens on a video monitor. These acoustic images are analogous to optical images. Depths of flaws within opaque specimens can be predicted using a stereoscopic method with SLAM. The ac-

curate determination of flaw depth requires accurate knowledge of the direction at which ultrasound travels within the specimen. This direction can be calculated from Snell's relation if the velocity of ultrasound in the material is known and if the specimen surface is acoustically flat and smooth.

An improved method for determining the direction of ultrasound in materials is the shadow method using SLAM. The



In the **Shadow Method**, the direction of ultrasound is calculated from the dimensions of a groove and the portion of the surface that the groove shields from the ultrasound.

shadow method is applicable to a wide range of surface roughnesses. The configuration for the shadow method is shown in the figure. A rectangular groove cut into the surface of a specimen blocks the ultrasound signal from reaching a limited area of the surface. On the video screen, this area shows up as an extremely dark (low-sound-intensity) region compared to adjacent areas in the acoustic image and is defined as the shadow region.

The direction of ultrasound, as denoted by the angle B, is determined by the simple trigonometric relationship shown in the figure. Despite the uncertainty in the measurements of the channel height and of the shadow length, the maximum uncertainty

is 10 percent for channels approximately 1 mm high with B equal to approximately 25° to 45°. This shadow method has been used to determine the directions of ultrasound accurately in ceramic, glass, and plastic specimens having surface finishes ranging from highly polished to as-fired. From these directions, the stereoscopic method has been used to predict the depths of flaws in these specimens accurately. This method may have a variety of applications in nontraditional quality-control applications.

This work was done by Edward R. Generazio and Don J. Roth of **Lewis Research Center**. Further information may be found in:

NASA CP-2383 [N86-22962/NSP], "Analysis Ultrasonics in Materials Research and Testing" (Reprinted as "Quantitative Flaw Characterization with Scanning Laser Acoustic Microscopy" and NASA TM-88797 [N86-31913/NSP] "Quantitative Void Characterization in Structural Ceramics Using Scanning Laser Acoustic Microscopy."

Copies may be purchased [prepayment required] from the National Technical Information Service Springfield, VA 22161, Telephone No. (703) 487-4650. Rush orders can be placed for an extra fee by calling (800) 336-4700. LEW-14473.

High-Differential-Pressure Heat Exchanger

All critical joints are full-penetration welds inspectable with x rays.

NASA's Jet Propulsion Laboratory, Pasadena, California

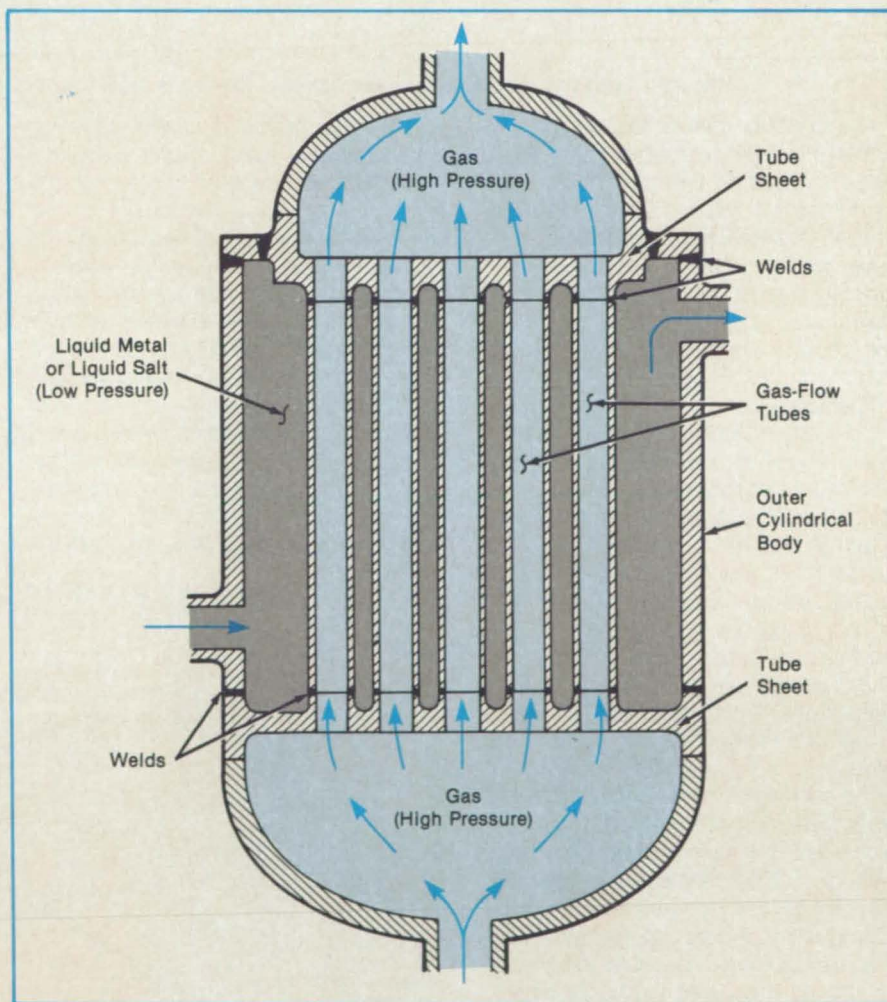
A heat exchanger accommodates a large pressure difference between the heat-transfer fluids. It is designed so that all its welded joints can be inspected with x rays to ensure leak-free operation over many years. Joints between the fluids and between each fluid and the environment are radiographically inspectable.

The low-pressure medium can be a liquid; for example, a molten metal or salt. The high-pressure medium can be a gas. The heat-exchanger design can be used in Stirling-cycle engines, including those in proposed nuclear and solar powerplants.

The heat-exchange tubes through which the pressurized gas flows are butt-welded to the tube sheets from inside the tubes (see figure). Nipples machined on the tube sheets help to position the tubes for welding. After welding, the tube-to-sheet joints are inspected radiographically. The tube-to-sheet joints are the only ones at boundaries between the two fluids: all other joints are at boundaries between one of the fluids and the environment.

If the tube welds are found to be satisfactory, stuffers are inserted in the tubes. These tubelike structures slow the flow of gas through the tubes to a speed optimum for heat transfer. This minimizes the number of tubes required. The gas manifolds are then welded to the tube sheets, and the outer cylindrical heat-exchanger body is welded to the sheets on the faces opposite the manifolds (see figure). A ring or a flange or both may have to be welded to close the liquid side. These welds are then subjected to x-ray inspection.

This work was done by Edward C. Hylin of Rockwell International Corp. for **NASA's Jet Propulsion Laboratory**. For further information, Circle 88 on the TSP Request Card.



Gas in Tubes Exchanges Heat With Liquid in the spaces between the tubes. The gas is at a pressure of about 150 atm (15 MPa), while the liquid pressure is about 2 atm (0.2 MPa).

Inquiries concerning rights for the commercial use of this invention should be ad-

ressed to the Patent Counsel, NASA's JPL [see page 22]. Refer to NPO-16947.

Measuring Viscosities of Gases at Atmospheric Pressure

A thermal mass flowmeter provides a capillary section for differential-pressure measurement.

Langley Research Center, Hampton, Virginia

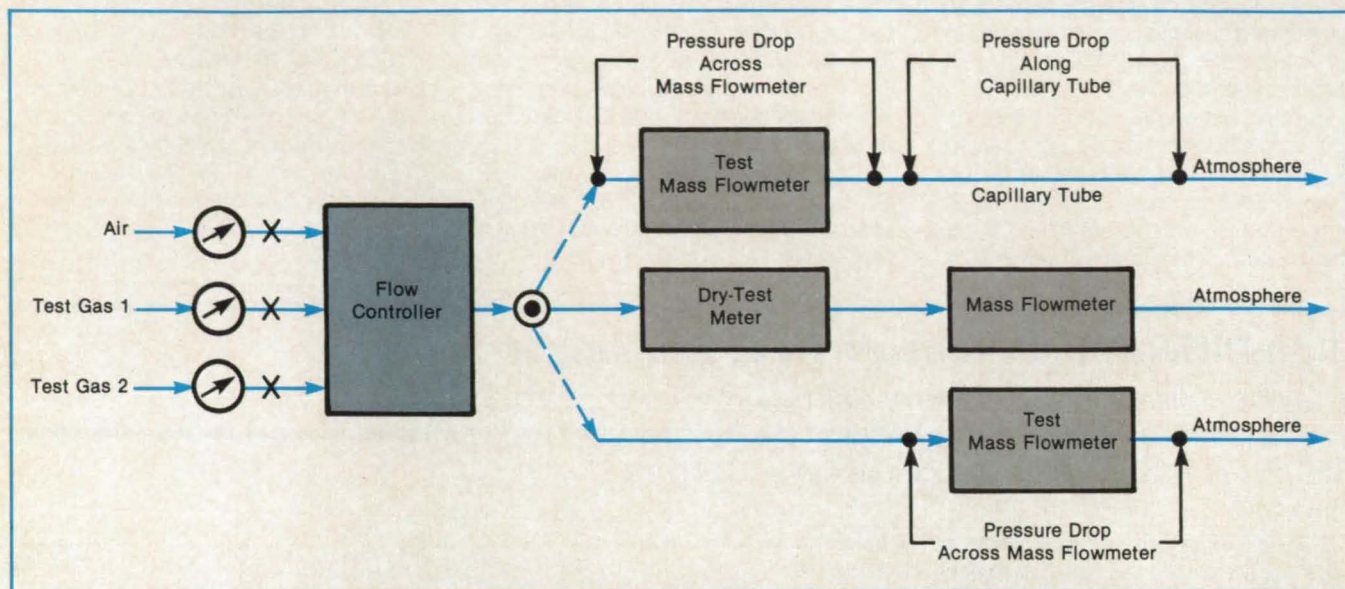


Figure 1. The Pressure Drop Along the Capillary Section is measured first in air, then in the test gas.

A variant of the general capillary method for measuring the viscosities of unknown gases is based on the use of a thermal mass-flowmeter section for direct measurement of pressure drops. In this technique, the flowmeter serves a dual role, providing data for determining the volume flow rates and serving as a well-characterized capillary-tube section for the measurement of differential pressures across it.

Coefficients of viscosity of various types of gas mixtures, including simulated natural gas, have been measured at atmospheric pressure and room temperature by the use of this technique. Pressure differences across the capillary-tube section of the thermal mass flowmeter were measured at small, well-defined, volume flow rates in the test gases and in standard air. Care was exercised to ensure that the flow rates for the air and test gas were such as to maintain the laminarity of the gas flows through the capillary section of the flowmeter.

The coefficients of viscosity of the test gases were calculated using the reported value of 185.6 micropoises for the viscosity of dry air at 300 K. The coefficients of viscosity for the test mixtures were also calculated using Wilke's approximation of Chapman-Enskog (C-E) theory. The experimental and calculated values for binary mixtures were in agreement within the reported accuracy of Wilke's approximation of C-E theory, but agreement for multicomponent gases was less satisfactory, presumably because of the limitations of Wilke's approximations of the classical dilute-gas state model.

The new method is simple, sensitive, and adaptable for absolute or relative viscosity measurements of low-pressure gases. Figure 1 is a diagram of the experimental system. Figure 2 shows the linear correlation between the pressure difference across the capillary-tube section of the thermal mass flowmeter and the flow rate through it. This technique is particularly suited for very complex hydrocarbon mixtures where the limitations of classical theory and compositional errors make theoretical calculations less reliable. The results for pure gases indicate that the technique is accurate to within ± 1 percent. In fact, the only limiting factors ap-

pear to be the accuracies with which volume flow rates and differential pressures can be measured.

This work was done by Jag J. Singh of Langley Research Center, Gerald H. Mall of Computer Sciences Corp., and Chegini Hoshang of Old Dominion University. Further information may found in NASA TP-2582 [N86-24962/NSP], "Measurement of Viscosity of Gaseous Mixtures at Atmospheric Pressure."

Copies may be purchased [prepayment required] from the National Technical Information Service, Springfield, Virginia 22161, Telephone No. (703) 487-4650. Rush orders may be placed for an extra fee

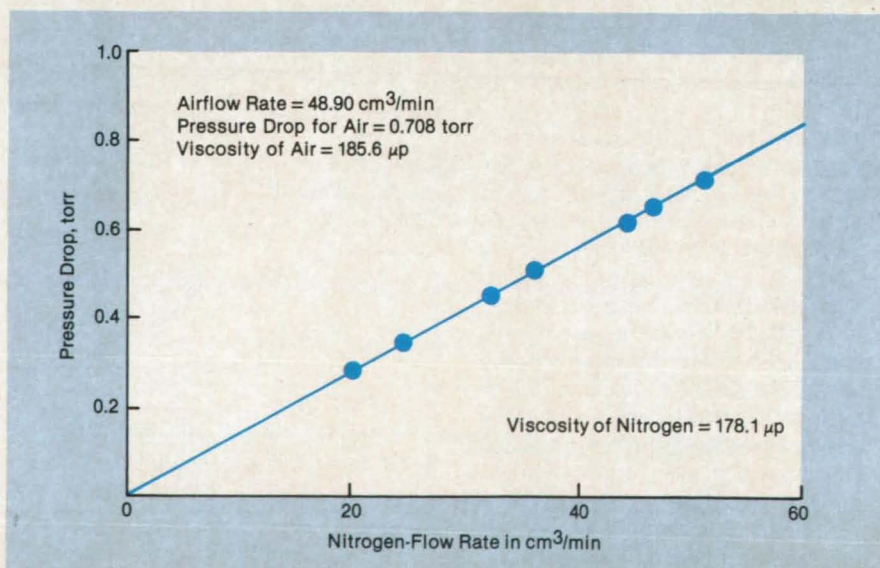


Figure 2. A Linear Relationship exists between the flow rates and the pressure drops along the capillary section.

THE X-30 IS KID STUFF.

To build higher and stronger. To shape an idea into reality that reaches the sky. For a kid, that's the stuff dreams are made of.

Kid stuff, because it's your kids, and ours, who will gain most from the advances in materials technology required to build the X-30 National AeroSpace Plane, forerunner of the Orient Express.

New materials will be needed to withstand the enormous heat and stress of X-30 flight. They'll be stronger materials, much lighter than those available today, with uses far beyond space flight.

The X-30 is kid stuff, because it is our children who will move from Earth to space and back at far less cost than we do today. And who will one day fly from Los Angeles to Tokyo in two hours aboard an Orient Express.

It is our children who will have—
or not have—world leadership in
aerospace as a result of our decisions today.

We can do no less than begin the task.

MCDONNELL DOUGLAS



by calling (800) 336-4700.

This invention is owned by NASA, and a patent application has been filed. In-

quiries concerning nonexclusive or exclusive license for its commercial development should be addressed to the Pa-

tent Counsel, Langley Research Center [see page 22]. Refer to LAR-13591.

Fiber-Optic Temperature Sensor

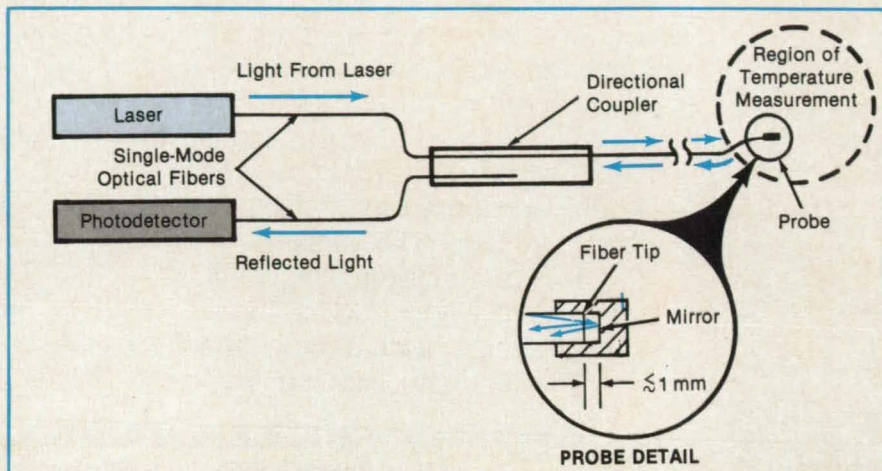
A remote thermometer would be small, lightweight, and immune to electrical noise.

Marshall Space Flight Center, Alabama

A proposed sensor would measure temperatures over a wide range — from those of cryogenic liquids to those of burning gases. Made in part of optical fibers, the sensor would be lighter in weight than a thermocouple and immune to electromagnetic interference. Unlike some other fiber-optic temperature sensors, the new device would not respond to temperatures elsewhere than at its sensing tip.

The probe consists of the polished tip of a fiber and a small mirror mounted on it (see figure). The fiber carries light from a laser to the tip. The inside surface of the fiber end reflects part of the light back into the fiber. The mirror reflects the remaining light transmitted through the tip back into the fiber.

The two reflected light beams interfere. The intensity of the light returning through the fiber therefore varies with the phase difference between the reflected beams, which in turn varies with the distance between the fiber end and the mirror surface. The gap changes with temperature as a result of the thermal expansion and contraction of the probe.



The Thermal Expansion and Contraction of the distance between fiber end and the mirror would alter the interference between the light reflected from those two surfaces, thereby giving an interferometric indication of temperatures.

A directional coupler extracts part of the returned light from the fiber, feeding it into a second fiber. A photodetector converts the extracted light into an electrical signal indicative of the probe temperature.

This work was done by Jonathan M.

Maram of Rockwell International Corp. for Marshall Space Flight Center. No further documentation is available. MFS-29164

Gamma-Ray Fuel Gauges for Airplanes

An accurate system overcomes problems of capacitance gauges.

Langley Research Center, Hampton, Virginia

Capacitance fuel gauges have served as the basis for fuel-quantity-indicating systems in aircraft for decades. However, there have been persistent reports by the airlines that these gauges often give faulty indications because of microbial growth and other contaminants in the fuel tanks. A feasibility study has been conducted on the use of attenuation of gamma rays to measure the quantities of fuel in the tanks. Studies with a weak Am^{241} 59.5-keV radiation source indicate that it is possible to monitor continuously the fuel quantity in the tanks to an accuracy of better than 1 percent. These measurements also indicate that there are easily measurable differences in the physical properties and resultant attenuation characteristics of JP-4, JP-5, and Jet A fuels.

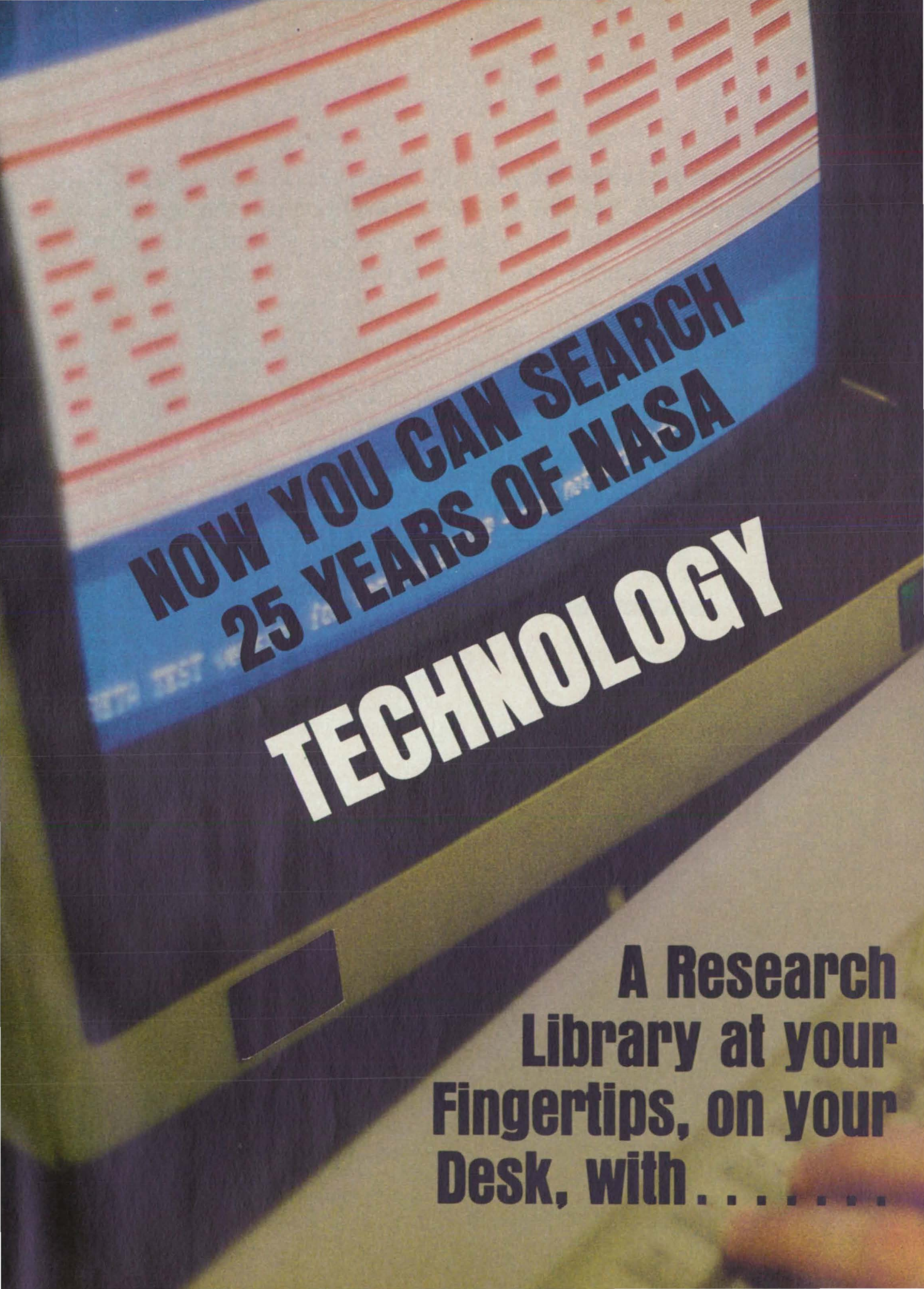
The operation of a nuclear gauge is based on the attenuation of gamma rays passing through matter. As a result of interaction of gamma rays with the atoms in

the test medium, the number of unaffected primary photons arriving at the detector is a function of the path length in the test medium. Such a gauge will be more sensitive if the attenuation coefficient is large for the incident photons. This dictates the choice of sources of low photon energy (less than 100 keV). Two candidate sources that meet the requirements of low photon energy, long source life, and well-resolved photon spectrum are Am^{241} (458 years) and Cd^{109} (453 days).

Since the exact compositions of aviation fuels are seldom known, it was not possible to calculate their attenuation coefficients for Am^{241} and Cd^{109} gamma rays. Therefore, the attenuation coefficients were measured experimentally for water, JP-4, JP-5, Jet A, and leaded and unleaded automobile gasoline. The nominal radioactive source strengths readily available were of the order of 10 microcuries (Am^{241}) and 100 microcuries (Cd^{109}). They pro-

vided good counting statistics for all test fluids over a period of 10 minutes. Measurements were made with and without the source in each case to subtract out the counts due to cosmic rays and other background radiation sources.

After the attenuation coefficients of the test fluids were measured, the wing-tank geometry for a Boeing 737 aircraft was selected for the computer model to test the sensitivity of attenuation of low-energy photons as the basis for fuel-gauging systems aboard aircraft. For purposes of the model, the fuel tank was divided into 14 compartments. Each of the 14 compartments in the fuel tank was approximated by a rectangular box. Any similar wing tank can be modeled by this technique by simply adjusting the number of compartments and the dimensions of each rectangular box. Once the tank geometry was defined, the computer program stepped through fixed percentages of tank capacity. For



**NOW YOU CAN SEARCH
25 YEARS OF NASA**

TECHNOLOGY

**A Research
Library at your
Fingertips, on your
Desk, with**

12,000+ Solutions

In minutes you can search 25 years of NASA Tech Briefs to find briefs related to your current project. NASA may have already found a solution or NASA may suggest other ways of resolving the problem. On the way to space NASA has had to solve thousands of unique problems in all engineering fields; electronics, mechanics, materials, fabrication, etc. under the most extreme conditions. Each issue of NASA Tech Briefs has about 50 to 70 briefs. Now with NTB:BASE you can examine over 12,000 briefs for a new slant on a down-to-earth problem.

NTB:BASE

from NASA Tech Briefs

NTB:BASE, a PC-compatible database of all NASA Tech Briefs for the past 25 years, containing proven solutions developed by working engineers like you—from NASA's Research Laboratories.

NOT JUST AEROSPACE!

NASA's research covers the entire spectrum of technology. From mechanics to matrix calculations, from chemistry to computer science. . . and most everything in between.

SEARCH TWO DECADES IN TWO MINUTES!

Sold by category and grouped by the year published, you will be able to repeatedly search the entire 25 year file of abstracts of *NASA Tech Briefs* and then call up for display on your desktop any one you feel appropriate. Searching by *subject title* or by *key word or phrase* will allow you to scan more than two decades of NASA technology and change the most arduous week or month-long task into a research project that literally takes seconds.

Then, after perusing the Tech Brief abstract, if interested, you will be able to order the complete brief with illustrations for a nominal charge.

NTB:BASE IS A ONE-TIME ONLY COST.

You can access NTB:BASE as often as you like. No online time clock to consider. With over 12,000 abstracts at your fingertips, NTB:BASE puts over one billion dollars of NASA technology on your desk.

NTB:BASE can be used on an IBM PC/XT/AT or any IBM compatible equipped with: 256k-available memory or more; DOS 2.0 or higher; one double sided disk drive (a hard drive will enhance program performance).

Q.

How is the material categorized?

A.

You can subscribe to any or all of the six (6) categories offered.

- A. **ELECTRONICS** (includes: Electronic Systems; Electrical; Electronic Components and Circuits)
- B. **PHYSICAL SCIENCES** (includes: Energy Sources)
- C. **MECHANICS** (includes: Machinery; Equipment and Tools)
- D. **MATERIALS** (includes: Chemistry)
- E. **FABRICATION TECHNOLOGY**
- F. **3-IN-1** (includes: Mathematics & Information Sciences; Life Sciences; and Pre-1976 Computer Programs. After 1975, Computer Programs have been grouped under one of the appropriate categories above.)

Q.

How do I initiate a search?

A.

You can search by:

- 1. **SUBJECT TITLE**
- 2. **AUTHOR**
- 3. **TECH BRIEF NUMBER** or by
- 4. **KEY WORD** or **PHRASE**.

You can review the abstract of any brief on your computer. The year in which the brief was published will be displayed with the abstract. You may order the complete briefs for as little as \$2.00 each, subject to ordering procedure.

Q.

How much does it cost to subscribe to NTB:BASE?

A.

Each category subscription costs \$100.00. **All six (6) for \$500.** That is a one time charge for 25 years of NASA Tech Briefs abstracts. Annual updates are \$20.00 per category. **All six (6) for \$100.00.**

Q.

What are the Tech Brief ordering procedures?

A.

You may telephone or mail in your request. For your convenience, you can choose among several different methods of payment:

- 1. **DEPOSIT ACCOUNT**

\$5.00 minimum order. The complete brief will be mailed within 24 hours of your request. A **DEPOSIT ACCOUNT** requires a minimum \$100.00 deposit. The cost for ordering briefs will be deducted from your balance. Your statement/invoice will show your purchases and current balance. Accounts must maintain a positive balance to remain on **DEPOSIT** status.

- 2. **OPEN ACCOUNT**

\$10.00 minimum order. The complete brief will be mailed within 48 hours of your request. An **OPEN ACCOUNT** must be kept current (30 days).

Depending on how you order, complete briefs can cost as little as \$2.00!

BONUS—

Technical Support Packages (TSP), in-depth descriptions of the technology covered by the briefs, are available from NASA for most published Tech Briefs. A TSP request form included with your Tech Brief allows you to obtain most TSP's, when available, at no additional cost.

NTBM-RESEARCH CENTER™

The answer to your hi-tech questions

SPECIAL
NASA Tech Briefs subscribers'
PRE-ORDER

- 25 Years of NASA Technology
 —On your desk
 —At your fingertips
- Searching with only a Key Word or Phrase.
- A one time cost for access. No online timeclock. Use and re-use at no additional cost.
- **NO CHARGE** for Technical Support Packages (TSPs), when available.
- Transferable to hard disk drive for faster access and convenience.

NASA Tech Briefs'

NTB:BASE

Pre-Order Form for **NASA** Tech Briefs Subscribers

Yes, I want the following **NTB:BASE** categories.

- | | |
|---|--|
| <input type="checkbox"/> ★ All Categories | <input type="checkbox"/> D Materials |
| <input type="checkbox"/> A Electronics | <input type="checkbox"/> E Fabrication Technology |
| <input type="checkbox"/> B Physical Sciences | <input type="checkbox"/> F 3-in-1 (Mathematics & Information Sciences, Life Sciences and Computer Programs) |
| <input type="checkbox"/> C Mechanics | |

Each Category is \$100.00—All 6 for \$500.00 \$ _____

Tech Briefs Ordering Procedure

Deposit Account. Yes, I want the economy, speed and convenience of a Deposit Account.

I'm enclosing an additional \$100. \$ _____

Please ship **NTB:BASE** Diskettes in the following format: (check one)

- 360K DS/DD(PC or XT) or
 1.2M DS/HD (AT)

Sub Total \$ _____
 N.Y. Residents Add 8 1/4 % Sales Tax \$ _____
 Total \$ _____

ORDERS WILL BE FILLED ACCORDING TO POSTMARK, ALLOW 30 DAYS FOR DELIVERY.

Check Enclosed Payable to: NTBM Research Center

Bill Me Purchase Order # _____

Name _____ Title _____

Company _____ Div./Branch _____

Address _____ P.O. Box _____ M/S _____

City _____ State _____ Zip _____

Authorizing Signature _____ Telephone () _____

Special Instructions _____

each amount of fuel, the fuel level was computed assuming a level fuel surface. With the fuel level known, the path length between each source/detector pair occupied by fuel or air was determined. From these path lengths, the number of counts was determined.

The results show that the counting rate is constant at all 14 stations when the tank is full. A 1-percent reduction in tank fuel content causes a large jump (about 57 percent) in the counting rate at the wing-tip detector. As fuel is expended, the counting rates change first in those compartments near the wing tip. After approximately 35 percent of the fuel has been expended, the compartment nearest the tip is empty and shows no further change in the counting rate. When the tank is nearly empty, the counting rates in the outer-station detectors have stabilized, but the counting rates at the stations near the fuselage are changing rapidly.

It is apparent that a suitably designed nuclear gauge should enable continuous

monitoring of the fuel-tank contents to an accuracy of better than 1 percent. The nuclear gauge is not expected to be susceptible to the fouling/corrosion problems experienced by the conventional capacitance gauges since both the source and radiation detector are sealed. Any algae or microbial growth on the source and detector windows can be easily removed during scheduled periodic maintenance checks of the gauging system. An added advantage of the nuclear gauge is its inherent capability to detect water buildup in the tank. Also, it is a self-calibrating system with a high degree of cross-checking capability, rendering the system independent of any changes in the background count rate with altitude.

It should be noted that despite the large flux of low-energy photons obtainable with a Cd^{109} source, an Am^{241} source would be more economical since it would be safer to handle and/or shield because of its lower energy. In fact, Am^{241} -based densitometers are currently in use aboard some air-

craft, and licensing requirements for Am^{241} -based fuel-quality-measurement systems should be no different from what they are for these aircraft. It is estimated that a complete system, including a micro-processor and associated display devices, can be assembled at a cost of less than \$10,000 per fuel tank.

This work was done by Jag J. Singh and Danny R. Sprinkle of Langley Research Center, Gerald H. Mall of Computer Sciences Corporation, and Hoshang Chegini of Old Dominion University. Further information may be found in NASA TM-87706 [N86-28385/NSP], "Feasibility of a Nuclear Gauge for Fuel Quantity Measurement Aboard Aircraft."

Copies may be purchased [prepayment required] from the National Technical Information Service, Springfield, Virginia 22161, Telephone No. (703) 487-4650. Rush orders may be placed for an extra fee by calling (800) 336-4700. LAR-13604

Thermally Insulating Support for Cryogenic Tanks

A passive alternate-load-path support scheme keeps weight low while conserving cryogenic liquid.

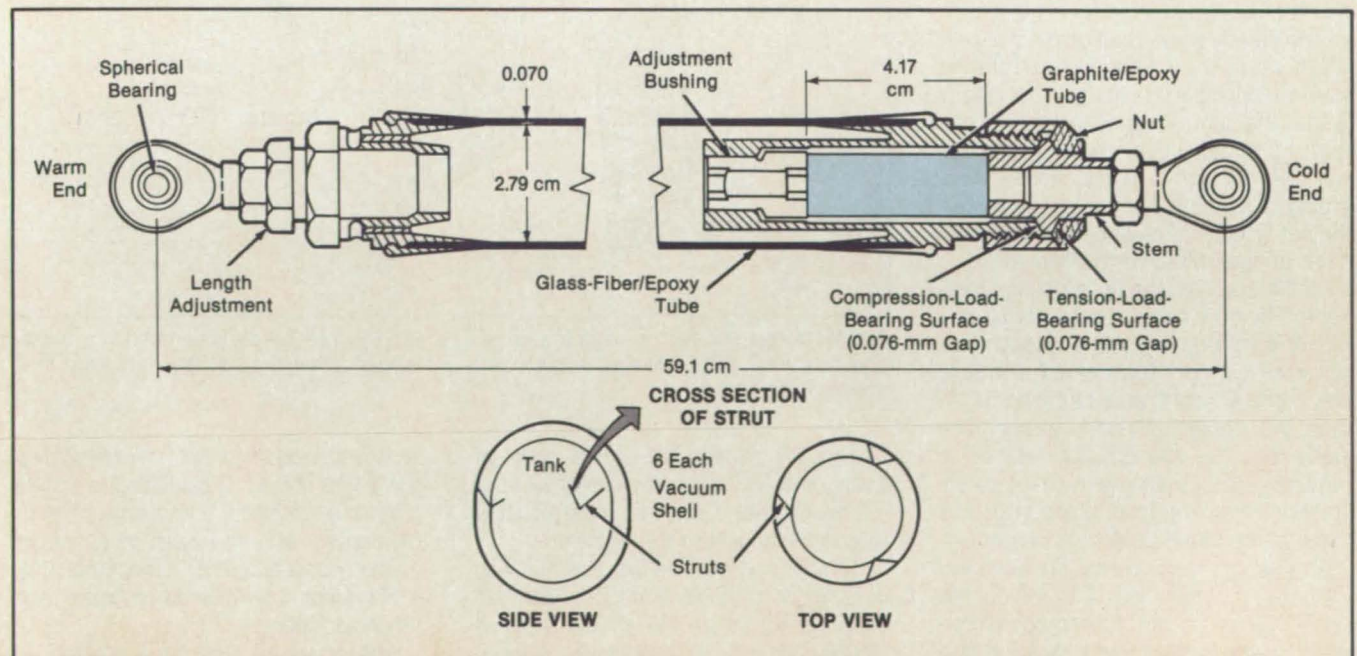
Ames Research Center, Moffett Field, California

A method of supporting the inner vessel of a large Dewar container minimizes heat conductance and weight but ensures high strength and impact resistance. The support method also accommodates thermal expansion and contraction of the vessel while introducing minimal stresses in the structure.

The inner vessel, which may contain liquid helium at 4 K, for example, hangs from three pairs of struts extending from the outer vessel (see figure). A strut consists of two concentric tubes in series with end fittings. The outer tube, made of a fiberglass-reinforced epoxy, is the stronger but has a higher thermal conductivity. The inner thin

wall tube is made of low conductance graphite-reinforced epoxy.

The outer tube connects solidly to the outer vessel (the warm end) and connects in series to the inner tube to the inner vessel (the cold end). When a low thrust is transmitted through the strut, both tubes carry the full load in series. However, when



The Inner Vessel Hangs From Struts in the outer vessel. The thin wall graphite/epoxy tube is protected from high loads by close tolerance stops.

the load increases to a large value in tension or in compression, the conical surface of the stem on the inner tube reaches a stop and bypasses the load around the thin wall inner tube. When the load drops, the stem returns to its original position, and the inner tube again takes up the full load.

The struts are free to swivel at the outer-vessel pins and at the paired joints at the inner vessel. As the diameter of the inner vessel changes with temperature and pressure, the angle between the struts in each pair grows or shrinks slightly to adjust to the new dimensions.

The support method was developed for cryogenic tanks on spacecraft. It allows a tank to withstand the loads imposed on it

during launching and maneuvering but keeps heat gain extremely low when the craft is in orbit or on earth. It is expected to reduce thermal conductance by a factor of 10 or more and weight by a factor of 2 in a 3-year-lifetime, superfluid-helium Dewar container. Struts have been fatigue tested up to 500,000 cycles and subjected to tension and compression tests and simulated temperature change tests and have met their design goals. Possible terrestrial applications include transportation of cryogenic liquids. The struts might also be used to support large supercooled magnets that are designed for earthquake loads.

This work was done by Richard T. Parmley of Lockheed Missiles & Space

Co., Inc., for Ames Research Center. Further information may be found in NASA CR-177325 [N85-17020/NSP], "Passive Orbital Disconnect Strut (PODS III) Structural Test Program."

Copies may be purchased [prepayment required] from the National Technical Information Service, Springfield, Virginia 22161, Telephone No. (703) 487-4650. Rush orders may be placed for an extra fee by calling (800) 336-4700.

Inquiries concerning rights for the commercial use of this invention should be addressed to the Patent Counsel, Ames Research Center [see page 22]. Refer to ARC-11608.

Analyzing Wakes From Hovering-Helicopter Rotor Blades

An analytical method and computer program yield realistic results quickly.

Ames Research Center, Moffett Field, California

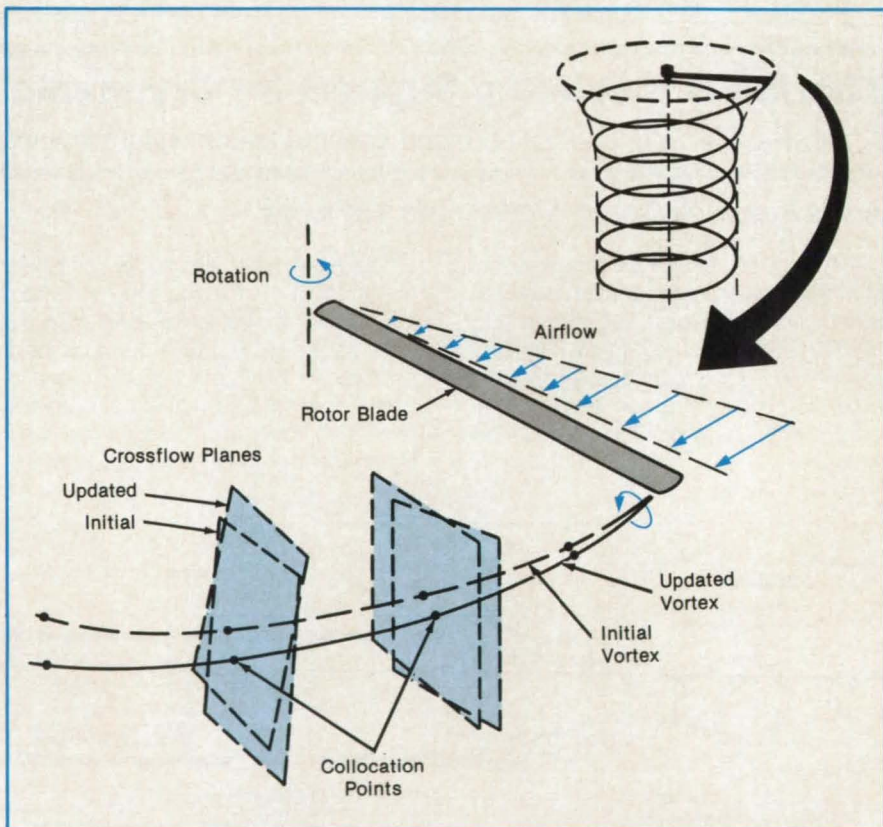
A new method for analyzing the free wake of a hovering-helicopter rotor produces more reliable results and requires less computer time than do previous methods. The new method copes with wake instabilities — both physical and numerical — that afflict the usual time-stepping analysis methods.

The new method is based on the newly recognized fact that among the solutions of the wake-airflow equations for a hovering-helicopter rotor is one that appears steady when it is viewed in a coordinate frame that rotates with the blades. Although steady, this solution is unstable; that is, it is disrupted when subjected to temporal disturbances. Nevertheless, this solution allows prediction of some average performance characteristics of the rotor.

The steady wake solution must satisfy equilibrium conditions in the rotating frame: a principal one of these conditions is that the sum of velocity contributions from all effects must be such that the wake is not convected to a new size, shape, or location. For the free-tip vortex, the net velocity at each point must be locally tangent to the vortex filament.

In the analysis, the tip vortex is represented by new basic curved vortex elements developed in another aerodynamic research project. The curved elements are more efficient and more accurate than the traditionally-used straight-line elements. The new solution method is naturally compatible with the curved-vortex-element method, since both use many of the same geometric properties.

The velocity components are analyzed in crossflow planes normal to the curved vortex filament in the rotating coordinate plane. These planes are located at the wake collocation points through which the curved vortex elements pass (see figure).



The Tip-Vortex Position, in coordinates moving with the rotor blade, is updated in a relaxation procedure. The wake-airflow solution is reached when the updates converge to a steady wake shape.

The steady solution is reached when, at every crossflow plane, the crossflow velocity is zero; that is, when the local resultant velocity is tangent to the filament.

The method involves the determination of influence-coefficient matrices. Given an initial configuration, the effects of small displacements on the collocation points on the rest of the wake are determined. The matrices are constructed from these ef-

fects and used to predict how the collocation points should be displaced to null the crossflow velocities. The calculation is implemented with the help of a special mathematical-relaxation procedure. Only a few steps are required to obtain converged solutions.

The computer time for a solution depends roughly on the square of the number of free-wake points. The traditional

Multiple Pages Intentionally Left
Blank

time-stepping method, in contrast, depends on the cube of the number of points and therefore is much more time consuming.

This work was done by D. B. Bliss, D. A.

Measuring and Plotting Surface-Contour Deviations

An electromechanical apparatus provides along-track and across-track displacement information to a plotter.

Lyndon B. Johnson Space Center, Houston, Texas

A hand-held device measures the deviation of the contour of a surface from a desired contour and provides an output to an x-y plotter. A carriage on the device is rolled along a track that represents the desired contour, while a spring-loaded stylus on the device deflects perpendicularly to the track to follow the surface (see Figure 1).

The stylus is connected by a pivot-arm

Wachspress, T. R. Quackenbush, and A. J. Bilanin of Continuum Dynamics, Inc., for Ames Research Center. For further information, Circle 96 on the TSP Request Card.

Inquiries concerning rights for the commercial use of this invention should be addressed to the Patent Counsel, Ames Research Center [see page 22]. Refer to ARC-11675.



Figure 1. An Operator Moves the Carriage of the contour-measuring device on a beamlike track. A stylus on the carriage traces the contour of the surface above it.

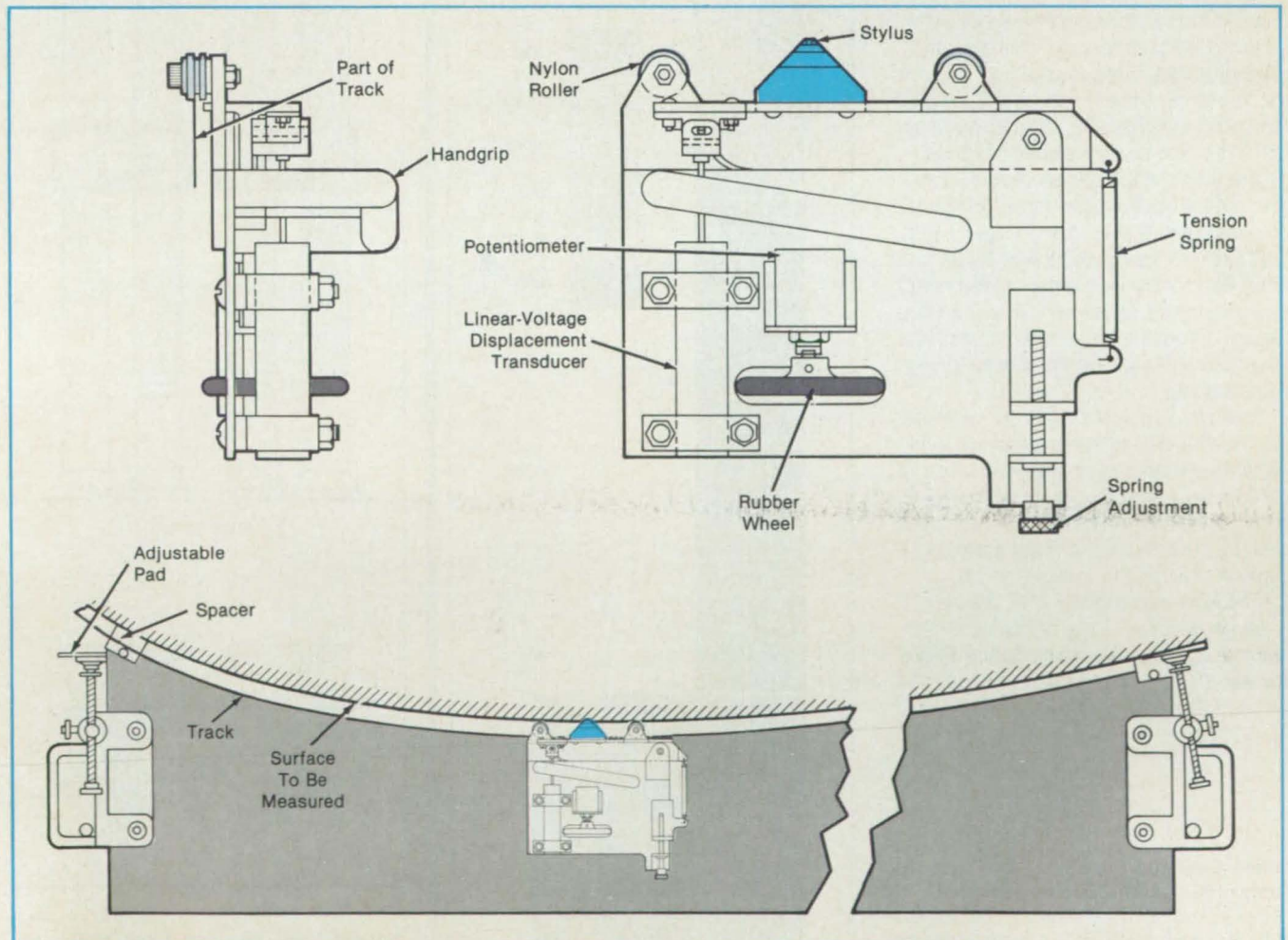


Figure 2. The Carriage of the Measuring Device holds a transducer that measures the cross-track displacement of the surface from the desired contour, and a multiple-turn potentiometer that measures the position along the track.

mechanism to a linear-voltage displacement transducer (see Figure 2). Displacements of the stylus as it follows the contour are thus transformed into an electrical signal that is applied to the y-axis input of the plotter.

Two nylon rollers ride on the track, which is 5 ft (1.5 m) long and made of aluminum. The track is maintained at a 0.75-in. (1.9-cm) offset from the desired surface. The track is equipped with pads and handholds for manual placement and adjustment. The carriage also has a handgrip so that the operator can move it easily.

A rubber wheel protrudes through a cut-

out in the device carriage and bears against the side of the track. As the operator moves the carriage on the track, the wheel turns a potentiometer shaft. The potentiometer resistance thus changes continuously as the stylus moves along the contour, providing a signal for the x input of the x-y plotter. The wheel and the two rollers provide three-point support for the carriage.

This work was done by Lino A. Aragon, Thomas Shuck, and Leroy K. Crockett of Rockwell International Corp. for Johnson Space Center. For further information, Circle 33 on the TSP Request Card. MSC-21163

Color-Video Thermal Maps

Temperatures appear in time-varying color.

Marshall Space Flight Center, Alabama

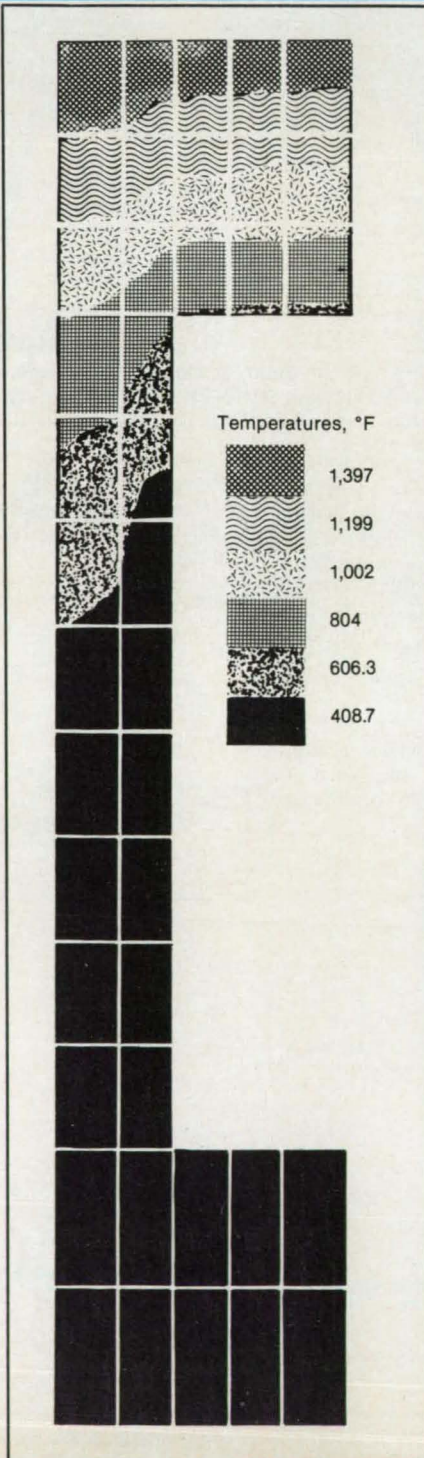
A computer-simulation method produces a color-video representation of the temperatures in a combustion-chamber wall. Until now, simulators have been limited to modeling temperature behavior at individual points. The new method displays the two-dimensional or three-dimensional temperature variation — that is, across a plane or volume of the coolant channel.

The colors in the display represent specific temperature ranges (see figure). The colors change to show the changes in temperature with flow, pressure, heat flux, and other factors during startup, steady-state operation, and shutdown. The data are used to determine whether the fatigue and structural limits of the combustor design are adequate.

The simulator solves for the temperature by the finite-difference method, making a timewise step-by-step evaluation of the fuel flow, heat flux, and cooling conditions. It converts its digital temperature data to a color-graphic map, changing it either in real time or in slow motion.

This work was done by W. R. Wagner, C. A. Laren, and W. T. Tonis of Rockwell International Corp. for Marshall Space Flight Center. For further information, Circle 104 on the TSP Request Card. MFS-29223

Colors (Depicted Here by Textures) Show Temperatures in a cross section of a coolant channel in the wall of a combustor. Many such cross sections are combined to give a three-dimensional view of temperatures in the channel.

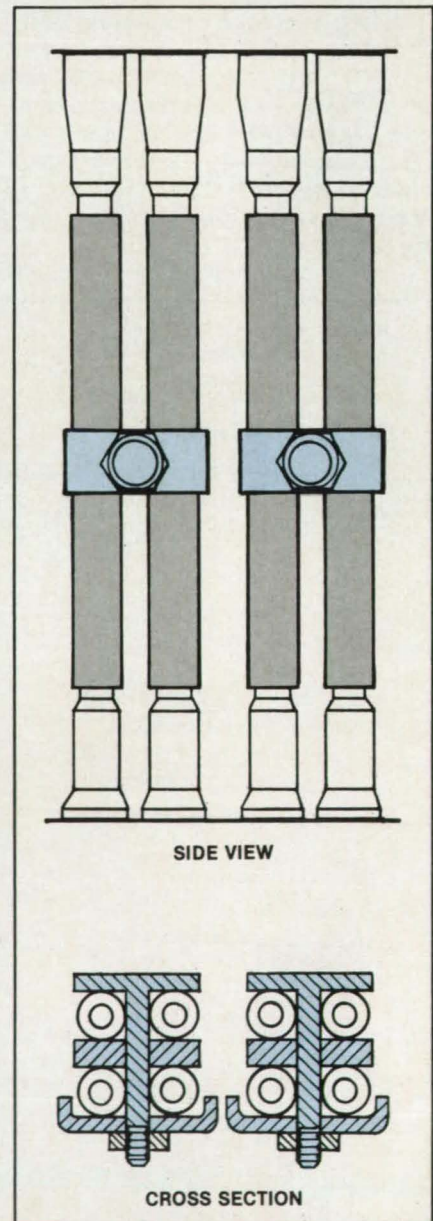


Stiffening Heat-Exchanger Tubes Against Vibrations

Midsection clamps reduce the harmful effects of crossflow.

Marshall Space Flight Center, Alabama

Arrays of parallel tubes in a strong crossflow can be protected from excessive vibration by simple braces. When the velocity of transverse fluid flow rises to a high level, tube arrays (in nuclear-reactor heat exchangers and in rocket-engine



A Clamp Bolts Onto Four Tubes, increasing their stiffness and natural frequency. Unstable vibrations are thereby suppressed.

fuel injectors, for example) can vibrate unstably.

An effective solution is to brace the tubes in bundles of four near their midpoints (see figure). The stiffness and,

therefore, the natural vibrational frequency of the tubes is thereby increased. The tubes are less likely to resonate in response to high crossflow velocities.

This work was done by G. V. R. Rao of

Rockwell International Corp. for Marshall Space Flight Center. No further documentation is available.
MFS-19907

Lead Scales for X-Radiographs

Indentations are made by typing on lead tape.

Marshall Space Flight Center, Alabama

Lead scales for inclusion in x-radiographs as length and position references can be created by repeatedly imprinting a character like upper-case I, L, or V, or lower-case L into lead tape with a typewriter. The character pitch of the typewriter serves as a length reference for the scale. The thinning of the tape caused by the impacts of the type shows up dark in the radi-

ograph.

The typed lead-tape scales are more accurate and convenient to use than are the hand-cut sawtooth shapes or manually stamped scales that were often used on radiographs of weld defects and the like. Other information can also be typed on the lead tape for inclusion in the radiograph for purposes of identification or explanation.

The typewriter ribbon should not be used for typing on the lead tape.

This work was done by Richard K. Burley and James F. Adams of Rockwell International Corp. for Marshall Space Flight Center. No further documentation is available.
MFS-29247

Books and Reports

These reports, studies, handbooks are available from NASA as Technical Support Packages (TSP's) when a Request Card number is cited; otherwise they are available from the National Technical Information Service.

Experiments in Boundary-Layer Turbulence

Motion in the layer is highly three-dimensional.

A report describes experimental studies of the disturbances induced by weak free-stream turbulence in a pre-transitional Blasius boundary layer. The report asks and partially answers some fundamental questions concerning these large-amplitude, low-frequency disturbances, including the following:

- What causes the low-frequency mode of the layer?
- Does the low-frequency mode excite Tollmien-Schlichting (T-S) waves?
- Does the low-frequency mode render existing T-S waves oblique, preventing them from remaining two-dimensional for maximum growth?
- Are T-S waves important in the transition from laminar to turbulent flow, or does the ingested turbulence cause sufficient mixing to ensure transition?

The experiments were performed in a wind-tunnel test section of 0.6 by 0.6 m cross section and 2.5 m long, at free-stream speeds up to 19.8 m/s. Upstream of the test section, six turbulence-damping screens 1.8 m square and a 3:1-by-3:1 contraction section provided a freestream turbulence level of 0.07, measured at frequencies above 0.3 Hz. The test model was a flat glass plate 1.8 m long and 6.5 mm thick, with a semi-elliptical leading edge, oriented horizontally and lengthwise

in the test section. Attached to the plate was a small earphone to generate T-S waves on the underside.

The freestream turbulence in the test section could be increased deliberately by installing a comb of vertical rods of either 6.35 or 4.8 mm diameter, or a comb of 4.8 mm horizontal rods. All flow measurements were taken on the underside of the plate. A three-axis translation stage under computer control carried hot-wire anemometers or anemometer arrays. Notable among the sensors was an eight-wire rake for simultaneous observation at eight stations across the flow at 1.25-cm intervals. The flow was visualized by oil emitted from the surface of an electrically heated 0.07-mm wire. A timing circuit controlled both the heating of the wire and a flash-lamp for photography.

For grid-produced freestream turbulence near 0.15 percent and a lateral scale similar to that of the pre-transitional Blasius-layer thickness, the following conclusions were reached:

- The root-mean-square fluctuation amplitude in the layer grew to more than 6.0 percent.
- The motion was highly three-dimensional, with a lateral scale similar to that of the freestream.
- The large-amplitude disturbances altered the mean velocity within the profile by about 1.5 percent.
- Evidence of streamwise vorticity was found.
- At the highest Reynolds numbers tested (1.6×10^6), the naturally occurring T-S waves were weak in comparison with the large-amplitude background motion.
- Forced T-S waves were strongly amplitude- and phase-modulated by the large-amplitude motion, but the time-average amplitude was not greatly different in the absence of the grid.
- With the finer grid, sharp velocity gra-

dients appeared locally and randomly. With the coarser grid, there arose turbulent spots wider than the coherence scale of the background motion.

This work was done by James M. Kendall, Jr., of Caltech for NASA's Jet Propulsion Laboratory. To obtain a copy of the report, "Experimental Study of Disturbances Produced in a Pre-Transitional Laminar Boundary Layer by Weak Freestream Turbulence," Circle 123 on the TSP Request Card.
NPO-16754

Preliminary-Design Software for Composite Structures

An easy-to-use program enables fast analysis and evaluation of rough designs.

A report describes an interactive program for the preliminary approximate stress analysis of structures made of fiber-reinforced composite materials. The program, intended for a personal computer, helps the designer select or confirm the sizes of composite structural members. It is useful in evaluating conceptual designs.

Called COMPSIZE, the program uses classical lamination theory to predict an effective elastic modulus for a laminate of arbitrary material and ply orientation. It then uses the elastic modulus in a family of subroutines that incorporate the familiar basic methods of the structural analysis of isotropic materials. Other subroutines calculate the coefficient of thermal expansion of the laminate and the ply-by-ply strains within the laminate.

The procedure is simple and convenient for the user. Its approximate results can later be refined by more detailed and precise methods as the design progresses.

COMPSIZE is written in Basic, a language that proved to be more than ade-

quate for providing an easy-to-use format and for setting up solutions to the equations. It is designed so that a user can initiate the program and solve a problem even without reading the user manual. Its main menu lists 15 major types of problems for selection by the user. Examples include the estimation of the properties of a composite material, axial tension or compression without buckling, shear induced by bending, and section area and moment of inertia. Several of the major problems have submenus of up to five further specialized problems.

For each problem, input and output units are specified. After the solution of a problem, COMPSIZE asks the user whether the results should be printed and whether any additional problems are to be solved.

This work was done by Charles N. Eastlake of Embry-Riddle University for Marshall Space Flight Center. To obtain a copy of the report, "Preliminary Design Methods for Fiber Reinforced Composite Structures Employing a Personal Computer," Circle 17 on the TSP Request Card. MFS-27153

Structural Dynamics of Filament-Wound Booster Rockets

A mathematical model agrees closely with measurements.

A report summarizes a program of measurements and calculations of vibrations in filament-wound composite models of the Space Shuttle solid-rocket boosters. The vibrational behavior predicted by a finite-element computer model of the structural dynamics correlates well with data from tests on full- and quarter-scale models.

The quarter-scale booster case includes five cylindrical composite segments, formed by winding graphite filaments in $\pm 29^\circ$ helices alternating with 90° hoop layers. There are 15 layers, including a glass-cloth layer at the inner surface. The case is intended as a replacement for a heavier steel version.

The computer model was developed with the NASTRAN general-purpose structural-analysis computer code. It employs a grid spacing nearly identical to that of full-scale cases. The segments are modeled with quadrilateral membrane and bending elements having orthotropic material properties. Joints and other metal parts are modeled with triangular and quadrilateral elements. Bar elements are used to represent stiffener rings and stringers in the forward and aft skirts and to provide most of the ring bending stiffnesses at tang and clevis joints. The model takes into account both the stiffening and the vibrating-mass effects of the propellant content and the decrease thereof after lift-off.

The early versions of the mathematical model correlated poorly with test data: stiffness discrepancies ranged from 10 to 25 percent. However, load and deflection data from full-scale equipment showed that the tang and clevis joints between case segments have low stiffnesses at the interfaces between steel parts and the composite material. When the mathematical-model joints were modified to match the measured joint stiffness, excellent correlations with vibration-mode shapes and frequencies resulted.

This work was done by F. M. Bugg of Marshall Space Flight Center. To obtain a copy of the report, "Structural Dynamics of Filament Wound Space Shuttle Booster Rockets," Circle 31 on the TSP Request Card. MFS-28155

Calculations of Wall Effects on Propeller Noise

Reverberations affect sound levels in wind tunnels.

A report describes calculations of the acoustic field of a propeller in a wind tunnel that has walls of various degrees of softness. The understanding provided by this and related studies is necessary for the correct interpretation of wind-tunnel measurements of the noise generated by high-speed, highly loaded, multiple-blade turbopropellers: such measurements are becoming increasingly important because considerations of fuel economy have renewed interest in propeller-driven airplanes.

The mathematical model of the propeller and wind tunnel is a set of acoustical dipoles on a disk that rotates on the axis of a duct of circular cross section. Although a typical wind tunnel has a rectangular cross section, the circular model involves less calculation, and the results should be qualitatively similar to those of a rectangular model. The convected-wave equation for the acoustic field is written in cylindrical coordinates in steady-state, nondimensional form, scaled by the reference values of the air density, speed of sound, mean flow speed, wind-tunnel radius, propeller radius, number of blades, and rotational speed. The wind-tunnel boundary layer is ignored in this analysis.

The duct-wall boundary condition is characterized by an acoustical impedance or admittance. The hard-wall (purely reflecting) boundary condition is represented by zero admittance and a zero perpendicular pressure gradient, while a soft-wall (partly reflecting, partly absorbing) boundary condition is represented by a finite admittance and a perpendicular pressure gradient related to the continuity of the air-particle displacement. The soft-wall boundary conditions are manipulated to investigate the relative effectiveness of

various wall linings in creating an acoustic field more nearly representative of the open atmosphere.

The wave equation was integrated numerically by the finite-element method, using a number of different combinations of the acoustic impedance and the scaling parameters. For comparison, the acoustic field of the same propeller in free space was also computed.

The calculations show that at flow speeds much less than that of sound, the wall must be lined with acoustical absorbers to make the free-field and ducted-propeller models agree in acoustic-pressure levels and directionality. The best agreement would occur where the ratio of wall radius to propeller radius is large and the measurements are made away from the walls.

At a flow speed half that of sound, the acoustic-pressure magnitude and directivity along the duct wall near the propeller are similar for a hard wall and for a variety of soft walls. However, the hard-wall results may be fortuitous, and additional studies are needed.

Upstream or downstream from the propeller, soft wall liners having suitable admittances can suppress the usual duct acoustic modes. In this case, the duct and free-field acoustic characteristics can agree over greater sideline distances. At high flow speeds, different upstream and downstream wall admittances are necessary for the equal suppression of duct modes on both sides of the propeller.

This work was done by Kenneth J. Baumeister of Lewis Research Center and Walter Eversman of the University of Missouri. Further information may be found in NASA TM-87333 [N86-29630/NSP], "Modeling the Effects of Wind Tunnel Wall Absorption on the Acoustic Radiation Characteristics of Propellers."

Copies may be purchased [prepayment required] from the National Technical Information Service, Springfield, Virginia 22161, Telephone No. (703) 487-4650. Rush orders may be placed for an extra fee by calling (800) 336-4700. LEW-14516

Water-Tunnel Flow Visualization With a Laser

Experimental conditions for effective visualization are determined.

A NASA Technical memorandum describes preliminary experiments in laser-enhanced flow visualization in a water tunnel. Aspects of the study include the required laser power, flow seeding, model preparation, and photographic techniques. The results of the study can assist potential users in the design and construction of similar equipment.

The optical components were assem-

bled around and in a water tunnel with a vertical test section of 0.61 by 0.41 m. The flow channel was enclosed by transparent poly(methylmethacrylate). The light from a 4-W argon laser was passed through a glass rod that served as a cylindrical lens to expand the beam into a fan of light 1.6 mm thick.

By the horizontal or vertical alignment of the glass rod, the plane of the light fan could be oriented parallel to the channel axis for the visualization of longitudinal flow or perpendicular to the axis to give a cross-sectional view of the flow. The fan was scanned along or across the model in the test section by moving the box containing the laser and its associated optics.

Various flow-seeding media were tried, including dyes that fluoresce under the laser radiation, the particles that naturally accumulate in the system, diatomaceous earth, glitter, and aluminum dust. Three test models were used: one of the Space Shuttle orbiter, one of the AV-8 Harrier airplane, and an ogive/cylinder/trailing-disk body. The Harrier engine intake was simulated by suction into the inlets, and the exhaust was represented by the ejection of water and dye through the outlets. The models were painted and marked in different ways to find which color scheme was most easily observable.

The illuminated, seeded flow was recorded by video techniques and by a 35-mm camera on color film. Some experiments were also conducted with black-and-white film, but color film was used predominantly because color prints were regarded as the most useful for documentation.

The experiments led to the following conclusions regarding the conditions that contribute to effective flow visualization:

- Of the dyes tested, the best is fluorescein sodium at a concentration of about 250 mg/L.
- With only the naturally occurring particles entrained, the flow could be seen by eye, but not enough light was reflected for good photography. Most of the deliberately entrained particulates formed clumps, but aluminum powder dispersed well when liquid soap was added to reduce the surface tension.
- Though particles degrade the pumps and filters, they give a more accurate visualization than do jets of dye, which can distort the flow.
- The models and flow are best seen when the models are painted medium gray with a matte finish. Reference marks on the models should be drawn with a grease pencil for high visibility and for ease of application and erasure.
- The laser power should be about 270 mW.
- With ASA 1,000 color film and a lens of aperture $f/1.2$, the shutter time should be $1/250$ s for streamwise flow and $1/80$ to

$1/60$ s for crossplane flow.

- Both $f/1.6$ and $f/1.4$ lenses work well for video recording.

This work was done by Christine Beckner and Robert E. Curry of Ames Research Center. Further information may be found in NASA TM-86743 [N86-11206/NSP], "Water Tunnel Flow Visualization Using a Laser."

A copy may be purchased [prepayment required] from the National Technical Information Service, Springfield, Virginia 22161, Telephone No. (703) 487-4650. Rush orders may be placed for an extra fee by calling (800) 336-4700.

Inquiries concerning rights for the commercial use of this invention should be addressed to the Patent Counsel, Ames Research Center [see page 22]. Refer to ARC-11698.

Control and Simulation of Space-Station Vibrations

An adaptive control system can reduce the effects of model uncertainties.

A report outlines a method for the finite-element dynamic analysis of a space station. The purposes are to determine the periods and modes of oscillation of the structure and to analyze the effect of a proposed adaptive control system to damp out unwanted vibrations. With the simplifications proposed by the authors, the finite-element simulations could be performed during a dynamic event, like docking of the Space Shuttle, and used to control the vibration-damping actuators. The general technique, known as direct model reference adaptive control, is used to make the output of an unknown or poorly known system asymptotically track that of a reference model that specifies the desired performance of the system. The technique is also applicable to robotics, seismic control of large buildings, electromechanical systems, metallurgical processes, and large oil tankers.

Two basic space-station configurations were considered. One has two large solar panels at one end of the inhabited module and is asymmetric. The second has four solar panels, two at each end of the inhabited module, and is symmetric. The authors provide a detailed development of the stiffness matrices for these two structures.

With the finite-element technique, the authors perform analyses to determine the natural frequencies and the vibrational modes of the structures. Based on these results, they propose several adaptive control systems to aid in removing the unwanted oscillations. The vibrations would be sensed by accelerometers. The proposed control mechanisms include thrusters, active hinges, control-moment gyroscopes,

and reaction wheels at critical points in the structures. Analyses of the behaviors of the structures with the adaptive controls showed that the controls can minimize the motions.

The adaptive control system is augmented by an inner control loop that eliminates the instabilities caused by zero-frequency rigid-body modes. An inner-loop control-gain matrix can be chosen to give the rigid-body modes non-zero frequencies, thereby making it possible to implement a stable, adaptive control system. The inner-loop controller can be made robust — that is, relatively insensitive to dynamic-model errors — by placing the loop only at the location where the rigid-body modes are most controllable.

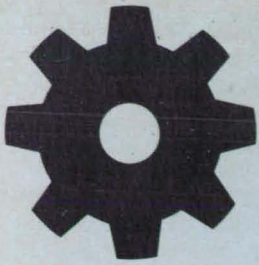
The system as a whole is robust in the presence of unmodeled dynamics caused by truncation of the mathematical model, poor knowledge of the dynamics of the structure, and instantaneous changes of system mass and mass distribution by more than 100 percent (as in docking of the Space Shuttle). The system has good convergence even under such severe dynamic conditions as high initial elastic deformations and attitude errors, and sudden impact of docking or pushoff.

The high gain required by an ideal adaptive controller will far exceed practical equipment limitations. Gain limitation can be applied to set a practical limit on the control effort and to maintain stability of the system, entailing the penalties of slightly higher transient vibrations and longer settling time. Model switching and disturbance modeling provide means for the reduction of output errors and, therefore, to reduce control demand. To compensate for incomplete knowledge of the structure, some simulation would have to be done for fine tuning.

This work was done by Che-Hang Charles Ih, Shyh Jong Wang, and Yu-Hwan Lin of Caltech for NASA's Jet Propulsion Laboratory. To obtain a copy of the report "Space Station Dynamic Modeling, Control and Simulation," Circle 84 on the TSP Request Card. NPO-16852

New Products

A new software program called Hi-Scan Raster Graphics Toolkit has been recently announced by **Houston Instrument**, Austin TX. The program enables users to edit and manipulate drawings scanned into a computer using the company's Scan-CAD Plotter Accessory. An icon-driven package, the software allows users to input and edit up to an "E" size raster image file created with Scan-CAD. Users can edit a raster image either before output to a raster device or before the automatic vectorization needed for computer aided design applications. The package will also let users manually convert the raster file into a vector file. **Circle Reader Service Number 585**



Machinery

Hardware, Techniques, and Processes

- 88 Steam Reformer With Fibrous Catalytic Combustor
- 89 Hanging Windmills From Cables
- 90 Unducted-Fan Engine

Books and Reports

- 90 Fatigue Lives of Materials Cut by Lasers
- 95 Flight Research on a Forward-Swept Wing Airplane

Steam Reformer With Fibrous Catalytic Combustor

Heat transfer would be more controllable.

NASA's Jet Propulsion Laboratory, Pasadena, California

A proposed steam-reforming reactor would derive its heat from internal combustion on a fibrous catalyst. The supplies of fuel and air to the combustor could be controlled to meet the demand for heat for the steam-reforming reaction. Such control could also enable the use of less expensive reactor-tube material by limiting the temperature to a value that is safe for the material yet not so low as to reduce the reactor efficiency.

The new reactor concept combines the catalytic combustor with an annular steam reformer (see figure) to enhance the transfer of heat into the steam-reforming catalyst and thereby raise the efficiency. The combustor catalyst is applied to the outer portion of a shell of fibrous alumina, silica, or other suitable oxide material.

A gaseous fuel, fuel/air premix, or air is

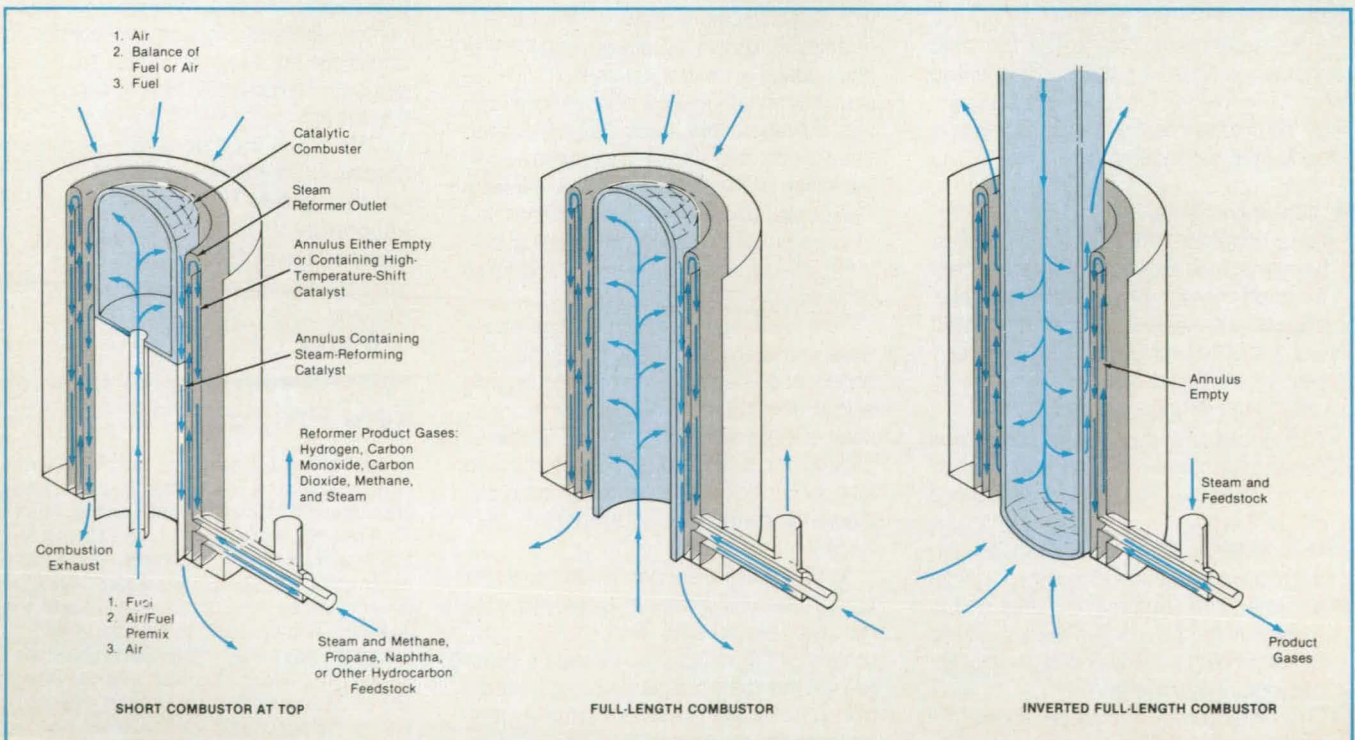
fed to the hollow inside of the combustor and diffuses out through the fibrous material. To maintain the fuel/air ratio necessary for combustion and to meet the heat-flow requirement, a flow of air, air/fuel premix, or fuel, respectively, is directed over the outer surface of the combustor. The inside and outside gas flows meet and react on the combustor wall, and the resulting heat is radiated onto the inside wall of the steam reformer.

The hot combustion exhaust gas flows through the space between the combustor and the reformer, convectively transferring additional heat to the reformer. The space between the combustor and the reformer can be filled with fins or with porous or fibrous metal or ceramic to enhance the heat transfer. The size of this space and the precise nature of the packing can be

chosen to meet the heat-transfer and pressure-drop requirements.

The relative sizes of the combustor and reformer are also chosen according to the heat-transfer requirement. Typically, the outlet end of the steam-reformer catalyst bed requires less heat per unit area than does the inlet end, but the temperature of the steam-reforming product gases must be raised into the range of 1,500 to 1,700 °F (800 to 900 °C) to increase the degree of conversion in the reactor. The combustor design is compatible with the gas flows at the exit end of the steam reformer to provide the necessary temperature rise without overheating the reformer tube or any of the surrounding materials.

Refinements of the design could distribute the heat flux in a manner that increases the degree of conversion and the effi-



The **Steam-Reforming Reactor** is made of concentric tubes, with the steam-reforming catalyst in the innermost annular segment. Heated by the catalytic combustor, the reactor converts steam and a feedstock gas into a product-gas mixture. Such a reactor could be used to produce hydrogen or synthesis-gas mixtures.

ciency in the particular system in which the reformer is incorporated. For example, the combustor could be segmented for different air/fuel flows to its upper and lower ends. This would make it possible to concentrate the heat flux at the lower end of the combustor, where the steam-reforming reactor requires the most heat. For another example, the air could be added at the top at more than the stoichiometric ratio, so that not all of the oxygen would be consumed at the top. A secondary flow of

fuel through the lower part of the fiber catalytic combustor would provide the additional heat needed below by the steam reformer.

In another version, the combustor would occupy the entire length of the reactor, and the flows of fuel and air would be distributed along the length in a pattern designed to give the required temperature and heat-flow distributions. In yet another version, the combustor would be turned upside down and the direction of flow in the

inner reformer annulus would be reversed.

This work was done by Gerald E. Voecks of Caltech for NASA's Jet Propulsion Laboratory. For further information, Circle 132 on the TSP Request Card.

Inquiries concerning rights for the commercial use of this invention should be addressed to the Patent Counsel, NASA Resident Office-JPL [see page 22]. Refer to NPO-16971.

Hanging Windmills From Cables

A relatively inexpensive structure would enable the raising and lowering of windmills.

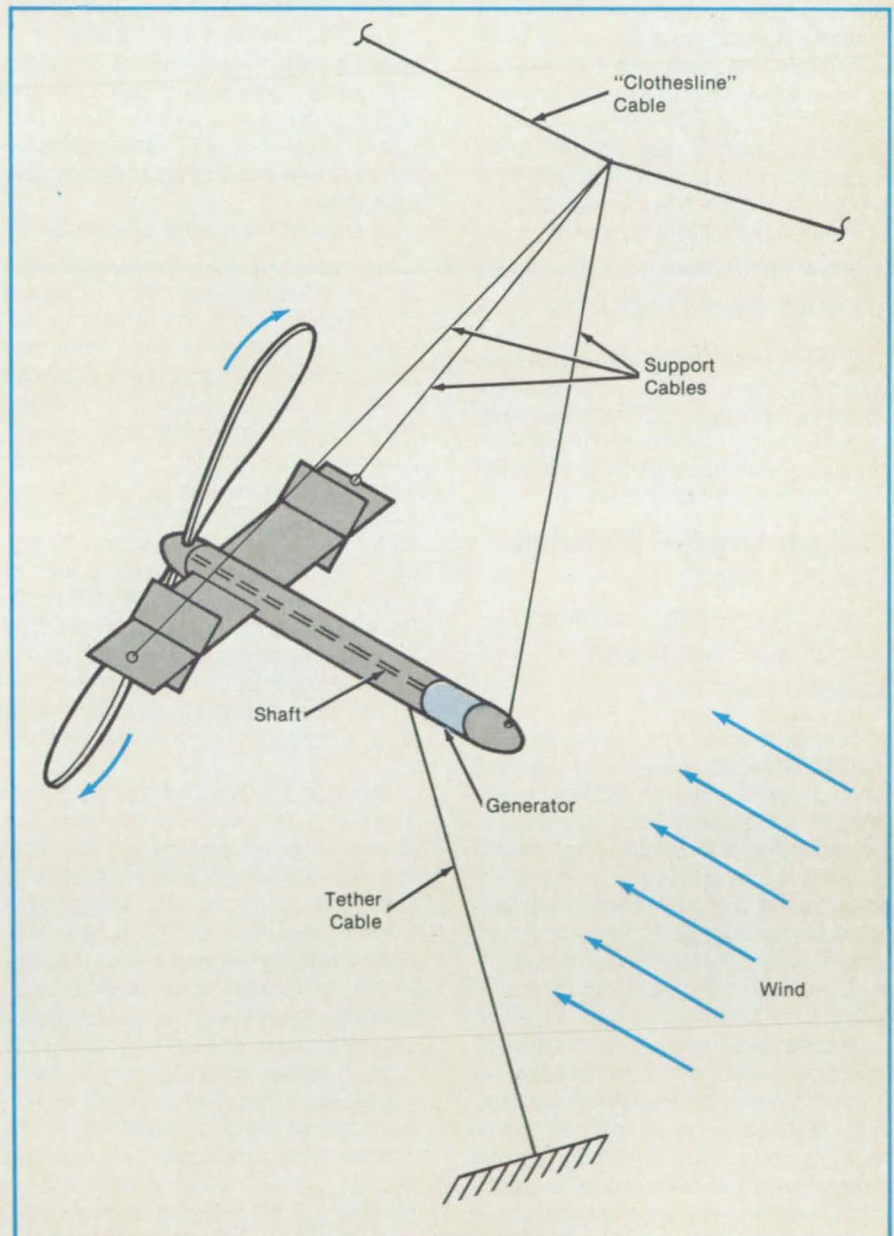
Langley Research Center, Hampton, Virginia

Windmills would be supported, according to a new concept, by hanging them from cables. There are two primary reasons why this concept may have practical applications. First, it would be possible to raise and lower windmills easily for maintenance and to lower them to avoid excessive windspeeds. Second, because much of the supporting structure would consist of tension members, the structure may be relatively inexpensive. In addition, it may be practical to hang windmills in canyons or other natural wind tunnels where tower structures would be impractical.

The concept is illustrated in the figure. The airframe consists of a fuselage and an empennage. The windmill turns a shaft that drives an electrical generator. The device is aerodynamically stable so that it will rotate in yaw to maintain the windmill in a downwind position as the wind direction changes.

The device is suspended by three cables, two of which are attached to the horizontal stabilizer and the third to the fuselage. The suspension cables are attached to a common point on a "clothesline" cable so that the device swings as a pendulum. The "clothesline" cable spans the space between two poles, trees, or other strong, rigid structures, which may be strengthened by guy wires. A tether cable from the ground is attached to the device to carry the aerodynamic drag force. The electrical cables may be brought down to the ground by attaching them to the tether cable.

In a geographical area where the average wind velocity is at least 20 ft/s (6.1 m/s), one such device with a 14-ft (4.3-m) rotor diameter and a 25-percent energy-conversion factor could produce a significant amount of the power required by a typical household. It may be feasible for an array of several devices or multirotor devices to supply power for a small factory



A Simple, Lightweight Windmill and Generator can be raised, lowered, and suspended in an optimal position.

or village. An array of several devices could be suspended from a multidevice rig. The devices could be positioned at different heights above the ground to reduce downwind interference effects. The devices could even be lowered to change the

pitch of the rotor blades for maximum efficiency when the average wind velocity changes.

This work was done by Moses G. Farmer of Langley Research Center. No further documentation is available.

Inquiries concerning rights for the commercial use of this invention should be addressed to the Patent Counsel, Langley Research Center [see page 22]. Refer to LAR-13434.

Unducted-Fan Engine

Counterrotating propellers are directly connected to turbines.

Lewis Research Center, Cleveland, Ohio

The unducted-fan (UDF™) engine is an advanced counterrotating-pusher-propeller propulsion system for high-subsonic (mach 0.7 to 0.85) aircraft. The UDF combines a modern high-pressure-ratio gas-turbine engine with a multistage counterrotating power turbine that is directly coupled to counterrotating, advanced high-speed propellers called "unducted fans." A key feature of the system is the unique direct turbine drive that eliminates the need for a gearbox to transmit power to the propeller blades.

The two highly loaded, multiple-bladed, counterrotating propeller stages have swept, variable-pitch blades with thin, advanced airfoil sections for good high-speed

performance. Counterrotation reduces propeller and turbine flow losses and, along with the large number of highly loaded blades, allows a relatively small propeller diameter.

First operated in August, 1985, this engine has achieved its design thrust of 25,000 lb (0.11 MN). Its measured specific fuel consumption (SFC) of 0.24 lb of fuel per hour per pound of thrust (6.8×10^{-6} kg/sN) is lower than the SFC of any previous turboprop-type engine. UDF-powered aircraft should consume 30 to 50 percent less fuel than do aircraft powered by conventional turboprop engines at comparable flight speeds.

This work was done by Edward T.

Meleason of Lewis Research Center and K. O. Johnson of General Electric Co. Further information may be found in AIAA Paper 85-3061, "Propulsion for Advanced Commercial Transports."

Copies may be purchased [prepayment required] from AIAA Technical Information Service Library 555 West 57th Street New York, New York 10019, Telephone No. (212) 247-6500.

Inquiries concerning rights for the commercial use of this invention should be addressed to the Patent Counsel, Lewis Research Center [see page 22]. Refer to LEW-14429.

Books and Reports

These reports, studies, handbooks are available from NASA as Technical Support Packages (TSP's) when a Request Card number is cited; otherwise they are available from the National Technical Information Service.

Fatigue Lives of Materials Cut by Lasers

Laser machining may help to balance high-speed rotating machinery.

A report describes continuing studies of the fatigue lives of materials cut by lasers. One of the long-term objectives of such studies is the use of laser machining to balance rotors that operate at high speeds. To achieve this objective, it is necessary to know the relationship between the effects of conventional and laser machining on the fatigue lives of the machined materials.

The evolution of rotating machinery has given rise to the need for multiplane and multispeed balancing. Research in balancing at high speeds performed by Lewis Research Center has shown that the exceedingly flexible high-speed shafts employed in advanced machines do not respond adequately to balancing procedures commonly used in the past. Operating above one or more critical speeds, these shafts require a sophisticated approach to balancing if increased reliability is to be

achieved. This requirement has an impact on the design of entire machines in that access to the shafts at multiple planes may be necessary for an acceptable balance.

The ultimate success of any balancing procedure depends on the ability to apply balance correlations precisely and in optimum balance planes. The use of laser machining to apply these balance correlations holds promise for solving two problems: accessibility to balance planes in assembled machines and reliance on such labor-intensive balance corrections as hand grinding and bolt-on weights. The removal of material by lasers requires access to balancing areas only along lines of sight, and the process is readily automated.

The use of a laser for the removal of material in the balancing of a rotor has several important advantages. The most important advantage is that the material can be removed in an extremely accurate manner while the machine is operating, thus eliminating the need to stop the rotor to add or remove material after each balancing run. Much time can be saved, especially when working with high-inertia rotors. Another advantage is that many machines can be balanced inside their normal housings without disassembly. Rotors can be balanced accurately on their production supports under actual dynamic conditions. Ports designed into the balancing planes of the machine housings can support lenses or adjustable-focus lens tubes. The lenses would then be in position

to converge the laser beam on the surface from which the material is to be removed.

Using this method, rotors could be balanced to a much finer degree than they could from outside the machine, causing a reduction of the dynamic loads and, in turn, a relaxation in the design constraints needed to withstand these loads. There would be a consequent reduction in the time needed to balance each unit and in manufacturing costs. Developments in the technology of laser and multiplane balancing of flexible rotors indicate that influence-coefficient balancing methodology has considerable promise as a practical, cost-effective procedure for the manufacture and overhaul of gas turbines, especially when it is combined with laser machining for the precise removal of metal.

An investigation into the removal of material by lasers showed that laser burns act in a manner typical of mechanical stress raisers, causing a reduction in fatigue strength; the fatigue strength is decreased relative to that of a smooth specimen. Laser-burn zones were studied in four materials: alloy steel 4340, stainless steel 17-4 PH, Inconel* 718, and aluminum alloy 6061-T6. Calculations were made of stress-concentration factors for laser-burn grooves of each material type. A comparison was then made to determine experimentally the fatigue-strength-reduction factors. No attempt was made to optimize the laser cuts to maximize fatigue lives nor to compare the effects of laser machining with those of the more-conventional hand-

Multiple Pages Intentionally Left
Blank

grinding method of removing material.

To qualify laser machining for eventual use in the balancing of gas-turbine rotors, it will be necessary to determine the reduction in fatigue life due to currently used hand grinding and compare it with the results of an optimized laser-machining procedure.

*Inconel is a registered trademark of the Inco family of companies.

This work was done by Michael R. Martin of Mechanical Technology Inc., for Lewis Research Center. Further information may be found in NASA CR-179501 [N87-11158/NSP], "Fatigue Life of Laser Cut Metals."

Copies may be purchased [prepayment required] from the National Technical Information Service, Springfield, Virginia 22161, Telephone No. (703) 487-4650. Rush orders may be placed for an extra fee by calling (800) 336-4700. LEW-14532

Flight Research on a Forward-Swept-Wing Airplane

Tests yield information relating to design, safety, and performance.

A report gives an overview of the flight-research program on the X-29A experimental airplane. The X-29A features forward-swept wings, which offer the following potential advantages:

- Improved lateral control at high angles of attack;
- A 13-percent reduction in total drag;
- A decrease in wing-structural-box weight;
- Aft placement of the wing support, permitting fuselage contours that are more effective in the minimization of drag; and
- Reduced wing twist, with consequent reduction of manufacturing complexity and cost.

To maximize the useful information yielded by the research program, the airplane incorporates a variety of advanced technologies including graphite/epoxy wing covers, aeroelastically tailored wings, automatic wing-camber control, and digital fly-by-wire control.

A typical test flight is preceded by a technical briefing 1 week in advance. This is followed by a flight-test simulation on a computer, a mission briefing, the actual flight, and a mission debriefing. The facilities involved in a flight include an aeronautical-test range, a mission-control center, spectral-analysis equipment, and a satellite data link.

The airplane is highly instrumented with rate gyroscopes, accelerometers, strain

gauges, aerodynamic-pressure taps, temperature and pressure monitors, and position indicators for surface positions and movements. Measurement data and control signals are integrated into a single pulse-code modulation stream. Flight data and the pilot's voice are transmitted to a ground station.

The research program is providing the data needed to improve the design, fabrication, and testing procedures for the airplane. Data on aerodynamics, structures, and controls correlate well with predictions, and the flight systems are performing as expected.

This work was done by Walter J. Sefic and Cleo M. Maxwell of Ames Research Center. Further information may be found in NASA TM-86809 [N86-26328/NSP], "X-29A Technology Demonstrator Flight Test Program Overview."

Copies may be purchased [prepayment required] from the National Technical Information Service, Springfield, Virginia 22161, Telephone No. (703) 487-4650. Rush orders may be placed for an extra fee by calling (800) 336-4700.

Inquiries concerning rights for the commercial use of this invention should be addressed to the Patent Counsel, Ames Research Center [see page 22]. Refer to ARC-11740.

SPACE COMMERCE '88

2nd INTERNATIONAL CONFERENCE & EXHIBITION ON THE COMMERCIAL AND INDUSTRIAL USES OF OUTER SPACE
MONTREUX, SWITZERLAND
21 to 25 FEBRUARY 1988

A TRULY INTERNATIONAL CONFERENCE AND EXHIBITION for all those seriously involved in developing or contemplating the vast business opportunities in outer space:

- launch vehicles, satellites, space station/platforms, materials processing, earth observation, spinoff technologies, financing, etc.

Pioneer in this field, Space Commerce '88 will provide a unique opportunity for established space industry to meet new clients and potential users from the emerging non-space sector:

- financial/insurance circles, governmental planning and R+D organisations, potential user industry, agencies interested in the financing and applications of space programmes.

IT WILL COMBINE:

- A Conference
- Commercial/academic exhibits
- Seminars
- Visual presentations
- Panel and round-table discussions

TO ILLUSTRATE PRESENT AND FUTURE POSSIBILITIES IN THIS EXCITING INDUSTRY

OFFICIAL ENDORSEMENT and PARTICIPATION by ESA, NASA, NOAA, EUROSPACE, the US Department of Commerce and the National Space Agencies and/or industry of Canada, Great Britain, Federal Republic of Germany (DFVLR), France (CNES), Italy (PSN) and Japan (NASDA), among others.

CONFERENCE TOPICS

- Setting the commercial space scene
- New space business opportunities
- Legal and financial aspects
- Industrial prospects in the microgravity environment
- Space communications and TV broadcasting business
- Facilities for space industrialisation
- Space-based earth observation business
- New technical support services for industrial space operations
- Spinoff business from space
- The new commercial and industrial realities of space

COMMERCIAL EXHIBITION

Leading international companies and agencies seeking business counterparts and contacts will present commercial displays:

- Communications satellites, remote sensing, spacecraft
- Launch vehicles and services
- Materials processing in space - equipment, systems products and services
- Computer and communications systems
- How industry works with agencies

ORGANISERS

SPACE COMMERCE '88
2, Rue de la Gare
PO Box 122
CH-1820 Montreux 1
Switzerland
Tel: +41 21 63 48 48
Telex 453254 mtx ch
Telefax: +41 21 63 80 65

Exhibition Representative for North America:
ACCESS MANAGEMENT CORP.
George A. Suter, President
7 Woodlawn Green, Suite 102
Charlotte, NC 28217 U.S.A.
Phone: +1 (704) 525-7030
Telex: 910240 1552 access cha
Telefax: +1 (704) 527-3768

REPLY COUPON

Return to one of the above mentioned addresses
Business card may be attached

NAME: _____

TITLE: _____

COMPANY: _____

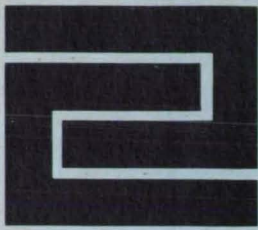
ADDRESS: _____

TEL: _____ TELEX: _____ TELEFAX: _____

YES! I wish to be kept informed about SPACE COMMERCE '88.

- PLEASE SEND ME: Conference programme when available
 Information on how to exhibit
 Pre-register me as delegate to the SPACE COMMERCE '88 Conference

Date: _____ Signature: _____



Hardware, Techniques, and Processes

- 96 Single-Axis Acoustic Levitator With Rotation Control
- 97 Preset Electrodes for Electrical-Discharge Machining

- 97 Higher-Quality Weld Joints for Tube Sections
- 98 Pressure-Localizing Inserts for Bagging Laminations
- 99 Repairing Holes in Pressure Walls
- 99 Growing II/VI Semiconductors With Double Decantation

- 100 Ceramic Adhesive for High Temperatures
- 101 Contamination-Free Electrical-Discharge Machining
- 101 Glass-Bead Blasting Alters Antenna Surface
- 102 Pin Inserts for Plug Welds

Single-Axis Acoustic Levitator With Rotation Control

Rotation-control equipment is simplified.

NASA's Jet Propulsion Laboratory, Pasadena, California

An acoustic levitator with rotation control handles liquid and solid specimens as dense as steel in both low gravity and normal Earth gravity. Unlike conventional acoustic levitators that rotate samples in a controlled manner, this one does not require three acoustic drivers in a chamber of square cross section nor does it depend on the maintenance of a precise phase relationship between the two acoustic drivers associated with the two axes of the square.

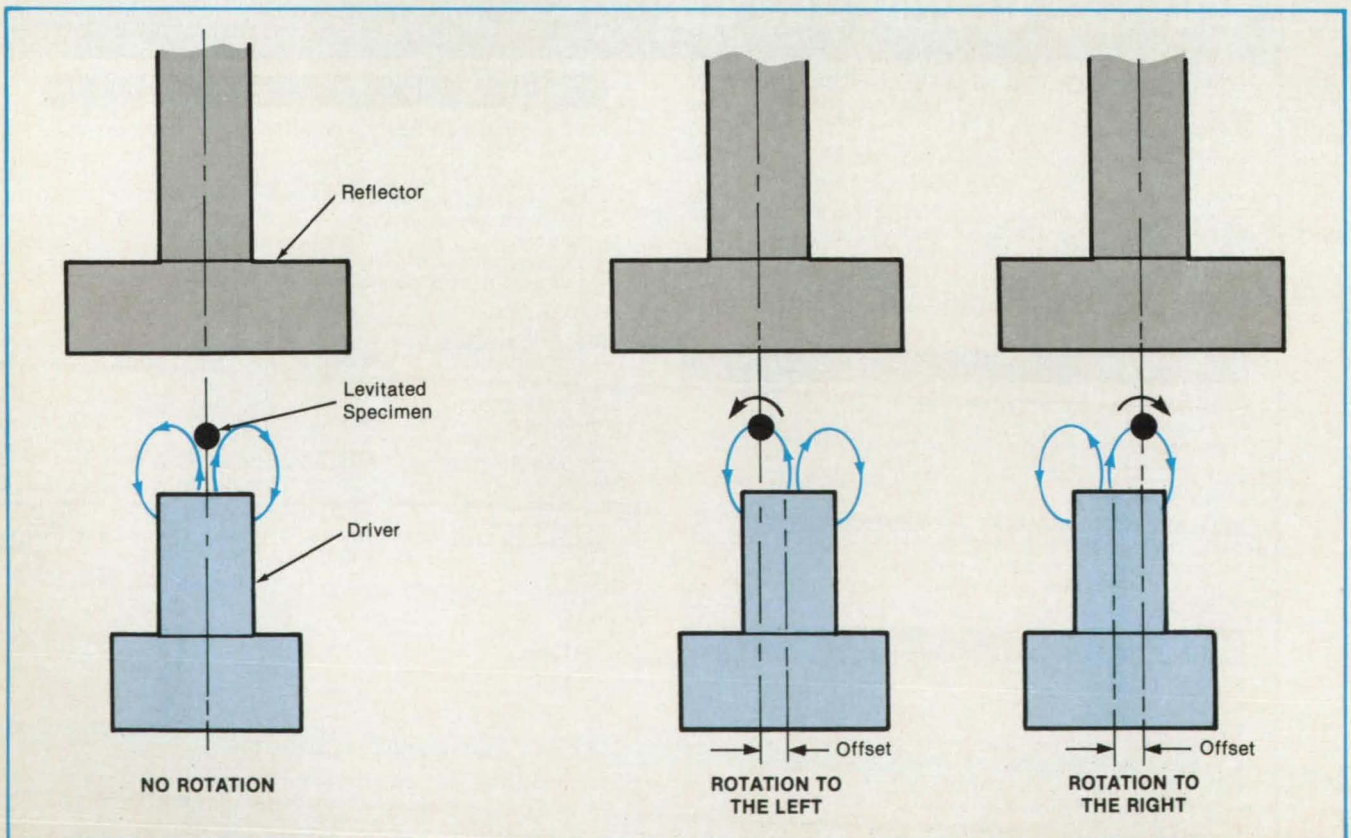
The new levitator is of the single-axis type. A circularly symmetrical acoustic driver excites a standing acoustic wave under a circularly symmetrical reflector,

which is wider than the driver. The specimen is suspended at a point between the driver and the reflector. Operating at a frequency above 10 kHz, the levitator can handle specimens ranging in size from 8 mm to 0.1 mm. The exact resonance frequency of the chamber is adjusted to accommodate the size of the specimen.

When the driver and reflector are coaxial, the levitating acoustic field exerts no torque on the specimen. When the reflector is moved aside, however, (see figure) the specimen translates with the reflector into the off-axis region of the airflow field induced by the acoustic driver. In this region, the flow exerts a torque about a rotation

axis perpendicular to the driver axis and to the direction of offset. Thus, by offsetting the reflector in a chosen direction, the specimen can be made to rotate about any axis in a plane perpendicular to the axis of the driver. The torque, and therefore the speed of rotation, can be adjusted by the choice of the offset distance or of the acoustic pressure. In experiments, solid spheres have been rotated as fast as 50 revolutions per second.

This work was done by E. H. Trinh and E. E. Olli of Caltech for NASA's Jet Propulsion Laboratory. For further information, Circle 98 on the TSP Request Card. NPO-16924



The Acoustic Reflector Can Be Translated perpendicularly to the axis of the acoustic driver to move the specimen to different parts of the levitating acoustic field. When the reflector and driver are not coaxial, the acoustic field makes the specimen rotate.

Preset Electrodes for Electrical-Discharge Machining

Time-consuming loading and setting are eliminated.

Marshall Space Flight Center, Alabama

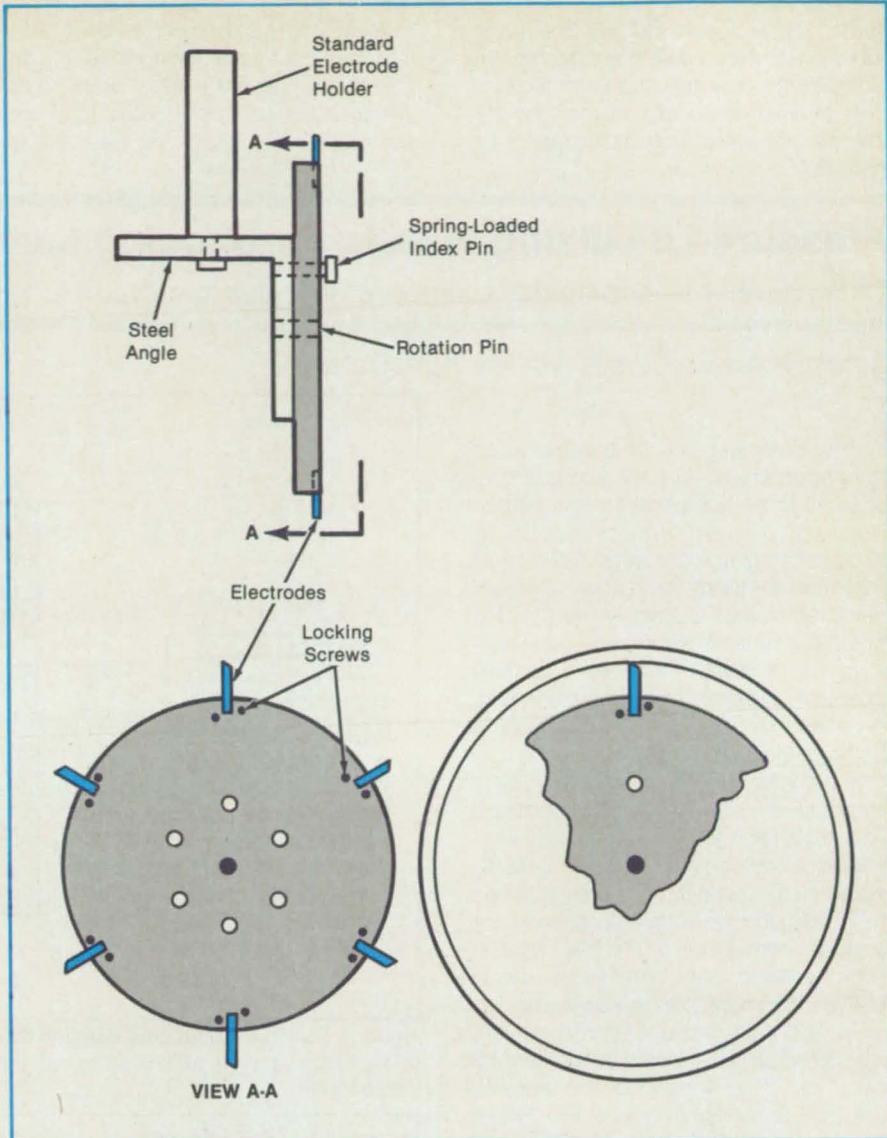
A new electrode holder for electrical-discharge machining (EDM) provides for the repeatable loading and setting of many electrodes. With the previous holder, each time an electrode was replaced, it had to be carefully set with respect to a master part.

The new holder is a rotating-index tool carrying six, eight, or possibly more electrodes. Before use, all of the electrodes are set with the aid of a ring that surrounds the tool, and are locked in position with screws.

When an electrode is to be replaced, the EDM operator pulls a spring-loaded pin on the tool so that it can be rotated about a center pin. A fresh electrode is thus rotated into position against the workpiece.

This work was done by Bill E. Coker of Rockwell International Corp. for Marshall Space Flight Center. For further information, Circle 152 on the TSP Request Card.

Inquiries concerning rights for the commercial use of this invention should be addressed to the Patent Counsel, Marshall Space Flight Center [see page 22]. Refer to MFS-29198.



Any One of Six Electrodes on a Disk can be rotated into position for electrical-discharge machining. All the electrodes are set by contact with a ring.

Higher-Quality Weld Joints for Tube Sections

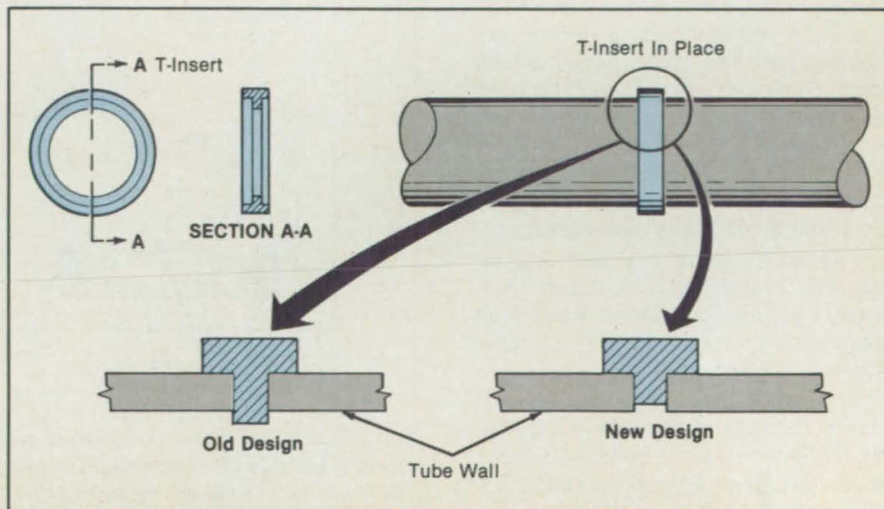
Less material in weld inserts results in better fusion.

Marshall Space Flight Center, Alabama

A redesigned insert for joining tubes by welding improves the quality of the weld. Like its predecessor, the insert is a ring with a T-shaped cross section. In the new insert, however, the leg of the T is shorter so that it does not protrude into the tube cavity.

Occasionally, the old version was not fully consumed in the welding process because of its length. It therefore did not fuse completely with the tube sections. The new, short-leg insert is more easily con-

The New Welding Insert Does Not Protrude into the tube channel, whereas the old insert, with its longer-legged T-section, protruded significantly. The excess material sometimes prevented complete consumption of the insert and fusion with the tube section.



sumed and decreases the chances of poor fusion on the inside wall. Its shorter leg also facilitates the detection of defects because the unconsumed edges of the tube become apparent during radiographic inspection.

A further advantage of the new insert is that it exhibits a small sag or droptrough, if it has been properly welded. Droptrough indicates full weld penetration, total consumption of the insert, and adequate fusion on the inside wall.

This work was done by John T. Olszewski of Rockwell International Corp. for Marshall Space Flight Center. No further documentation is available.
MFS-29190

Pressure-Localizing Inserts for Bagging Laminations

These devices can compress composite laminates to conform to tight inside corners of the molds.

Ames Research Center, Moffett Field, California

The proposed use of a pressure-localizing insert would allow composite laminates to be compacted into tight corners by conventional pressure- or vacuum-bagging techniques. Because of this manufacturing technique, a larger selection of part shapes would become amenable to lamination.

In conventional bagging, a uniform pressure is applied to all areas of the part; consequently, the laminates often fail to conform to tight inside curves or corners. One technique for avoiding this problem is the use of a staggered array of laminas, with expansion joints between adjacent pieces in the same layer (see Figure 1). However, the applied pressure load often produces enough friction to prevent the laminas from slipping into the corners, with the result that corner voids remain between the mold and the laminate.

In the proposed technique, the staggered laminas would be bridged by an insert that localizes the applied pressure at the tight corners (see Figure 2). Consisting of a rigid bar connecting rubber or silicone "rope" pieces that conform to the corners, the insert would provide high compaction force to the corners, while allowing the laminas to slip into the corners. Following compaction of the tight corners, these inserts could be removed to allow conventional compaction to complete the lamination.

A modification of this technique would require only a single bagging operation. The insert would include a flexible connecting bar. The insert would deliver localized pressures to begin corner compaction at a relatively low bagging pressure. However, at the customary bagging pressure of 50 psi ($3.4 \times 10^5 \text{ N/m}^2$), the connecting bar would yield so that its entire length would press on the laminas.

This work was done by Dave Schmalzing and Donald Carter of United Technologies Corp. for Ames Research Center. No further documentation is available.

Inquiries concerning rights for the commercial use of this invention should be addressed to the Patent Counsel, Ames Research Center [see page 22]. Refer to ARC-11673.

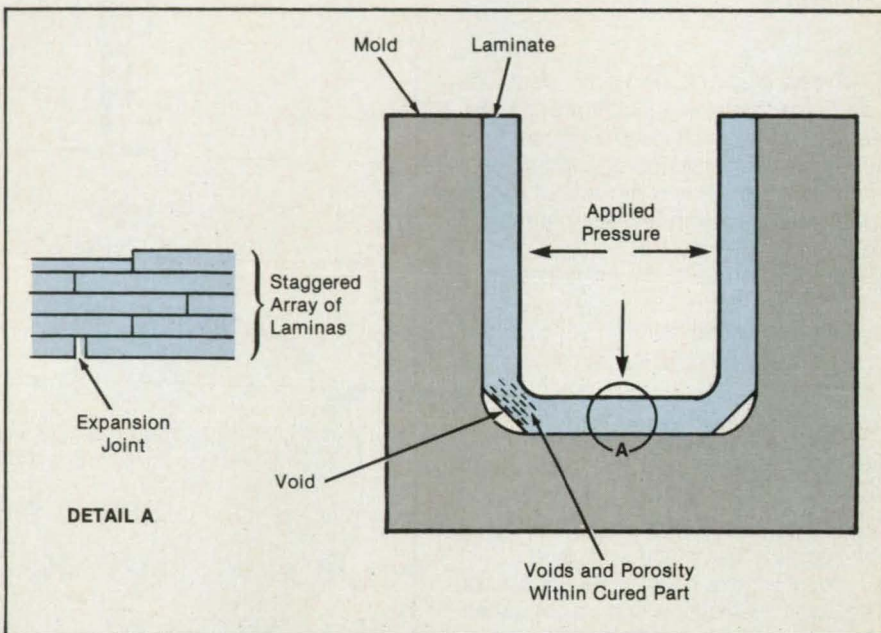


Figure 1. During **Conventional Bagging** the applied pressure can give rise to friction that prevents the laminate from slipping into tight corners, leaving voids between the mold and the laminate.

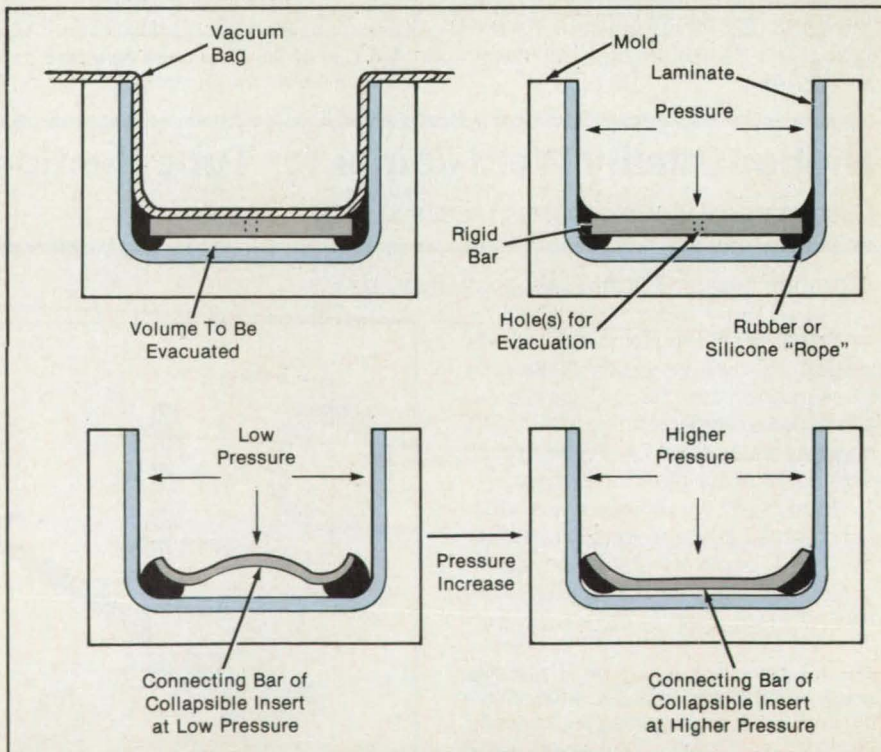


Figure 2. **Localized Pressure** might insure conformity of the mold and the laminate in tight corners. A rigid insert (above) would require a second bagging step. Only one bagging step would be required if the insert is collapsible (below).

Repairing Holes in Pressure Walls

Patches and easy-to-use tools yield a pressure-tight seal.

Marshall Space Flight Center, Alabama

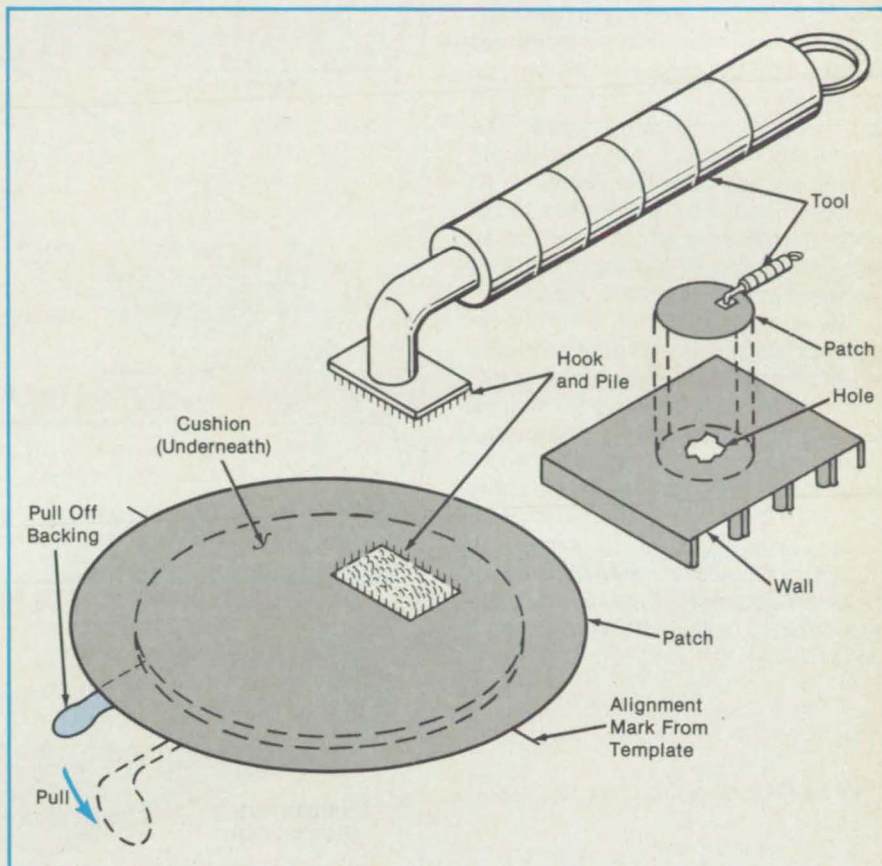
A method of repairing punctures in pressure walls is straightforward, neat, and fast. Developed for closing holes caused by the impact of orbiting debris or micro-meteoroids on spacecraft, the method employs a patch precoated with adhesive.

The patch (see figure) includes a disk of soft aluminum about 8 mils (0.2 mm) thick. A backing sheet on the cushion covers the adhesive until the patch is used. A Kevlar® aramid cushion in the central portion of the patch protects the aluminum from the sharp, ragged edges of the puncture. The patch is thin enough to conform to surface irregularities. Nevertheless, it can be handled — and the cover on the adhesive can be removed — by an operator wearing heavy gloves.

The repairer first uses a tool with an abrasive pad to smooth the sharp edges of the hole and to remove paint and loose material. With a cleaning pad on the same tool, the repairer collects dust and chips on the surface (the cleaning pad is layered so that the user can discard a dirty layer and expose a fresh one as necessary).

The repairer places an alignment template over the puncture, positioning the template crosshairs over the center of the hole. With a marker, the repairer draws locator lines at three or more places on the wall at the periphery of the template, then removes the template.

The repairer picks up the patch with a hook-and-pile tool and tears off the backing. With the adhesive side of the patch toward the wall, the repairer aligns the patch with the locator lines. The repairer presses the patch edge firmly against the wall and then uses a tool to burnish bubbles, folds, and creased edges on the



A Repairer Lifts a Patch from a repair kit with a hook-and-pile-tipped tool and positions it over a puncture hole. With the tool, even a gloved repairer can easily manipulate the patch without damaging it.

patch.

This work was done by Paul Bruce Y. Mori, Laurie J. Capriolo, Alexander R. Corocado, Martin N. Gibbins, and Robert B. Horne of the Boeing Co. for Marshall Space Flight Center. For further informa-

tion, Circle 151 on the TSP Request Card.

Inquiries concerning rights for the commercial use of this invention should be addressed to the Patent Counsel, Marshall Space Flight Center [see page 22]. Refer to MFS-28179.

Growing II/VI Semiconductors With Double Decantation

A concept for growing single crystals combines sheet solidification with controlled cooling.

NASA's Jet Propulsion Laboratory, Pasadena, California

A proposed crystal-growth method for II/VI semiconductor compounds would cool a newly solidified crystal gradually and nearly isothermally so that few defects are formed. At the same time, the method would obtain the maximum amount of crystal from the minimum amount of melt.

Only a small amount of a II/VI melt is usable for crystal growth. In growing a binary crystal, impurities build up in the melt, and so the crystal must be withdrawn well before the melt is used up. A ternary

crystal must similarly be withdrawn because the composition of the melt changes as solidification proceeds. In the new technique, the crystalline material would be solidified in a sheet so that as much of the melt as possible would be utilized before the impurity content rises excessively or the composition changes too much. In addition, the crystal would be cooled in a liquid that would remove heat gradually and evenly at a controlled rate. Thermal stresses and the consequent defects in-

duced by uneven cooling would thus be reduced.

In one version of the proposed technique, the molten semiconductor would be contained by baffles in a horizontally oriented vessel (see figure). A layer of molten encapsulant having a freezing temperature much lower than that of the semiconductor would float on top of the semiconductor melt.

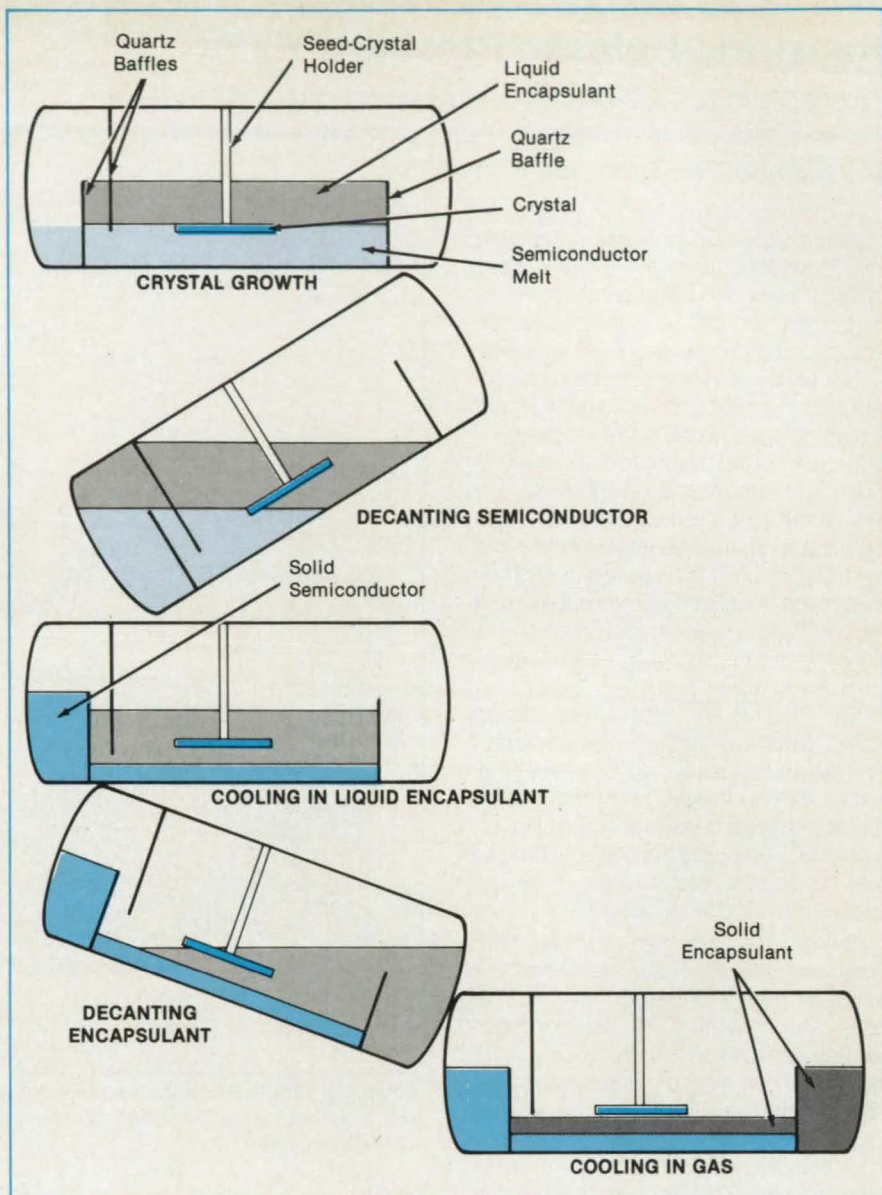
A seed crystal would be introduced into the melt, just below the layer of encapsu-

lant. The crystal would grow in a horizontal sheet along the semiconductor/encapsulant interface. When the crystal reaches its optimum size, the vessel would be tilted to raise the crystal into the encapsulant. The melt would run through a pair of end baffles into the space at the lower end of the vessel. When the vessel is returned to its horizontal position, much of the melt would remain in the end space, and the balance of the melt would form a shallow layer on the bottom of the growth chamber. The crystal would remain immersed in the molten encapsulant. The vessel would then be cooled at a controlled rate to just above the melting point of the encapsulating liquid. During this cooling, the molten semiconductor would turn to a solid.

The vessel would then be tilted in the opposite direction to pour much of encapsulant into the unfilled space at the other end. The vessel would be cooled further, and the encapsulant would solidify. The crystal would undergo a final cooling to room temperature in the gas that fills the upper part of the vessel.

This work was done by Andrew D. Morrison of Caltech for NASA's Jet Propulsion Laboratory. For further information, Circle 91 on the TSP Request Card. NPO-16808

Double Decantation causes a sheet crystal to cool first in a liquid, then in a gas. The vessel is tilted to pour off molten semiconductor material. A second tilt, in the opposite direction, pours off the encapsulant.



Ceramic Adhesive for High Temperatures

The fused-silica/magnesium-phosphate adhesive resists high temperatures and vibrations.

Lyndon B. Johnson Space Center, Houston, Texas

Developed to bond gap fillers to low-density ceramic insulating tiles used in the thermal-protection system of the Space Shuttle, a ceramic adhesive can be used in aerospace, metallurgical, ceramic, electronic, and other applications where conventional adhesives cannot meet requirements for service at high temperatures. The adhesive consists of a base material of fused silica and a bonding agent of magnesium phosphate.

An older procedure for filling unacceptably large gaps between the tiles involved room-temperature-vulcanizing silicone-rubber adhesives, which could not tolerate

temperatures above 550 °F (288 °C) and therefore had to be replaced after each mission. The new adhesive, which has a coefficient of expansion compatible with that of the tiles, is unaffected by extreme temperatures and by vibrations. Assuring direct bonding of the gap fillers to the tile sidewalls, the new adhesive obviates the expensive and time-consuming task of the removal, treatment, and replacement of tiles.

The process for filling tile gaps is as follows:

- Water and colloidal silica are added to the ceramic adhesive powder, and the mix-

ture is stirred to a homogenous paste.

- The surfaces of the shim and the tile to be joined are wetted thoroughly.
- The ceramic adhesive is applied to the surface of the shim.
- The shim is installed against the tile sidewall, which has been diamond-abraded, and pressure is applied to assure full contact.
- The adhesive is cured for 24 hours in air.

This work was done by Everett G. Stevens of Rockwell International Corp. for Johnson Space Center. For further information, Circle 25 on the TSP Request Card. MSC-21085

Contamination-Free Electrical-Discharge Machining

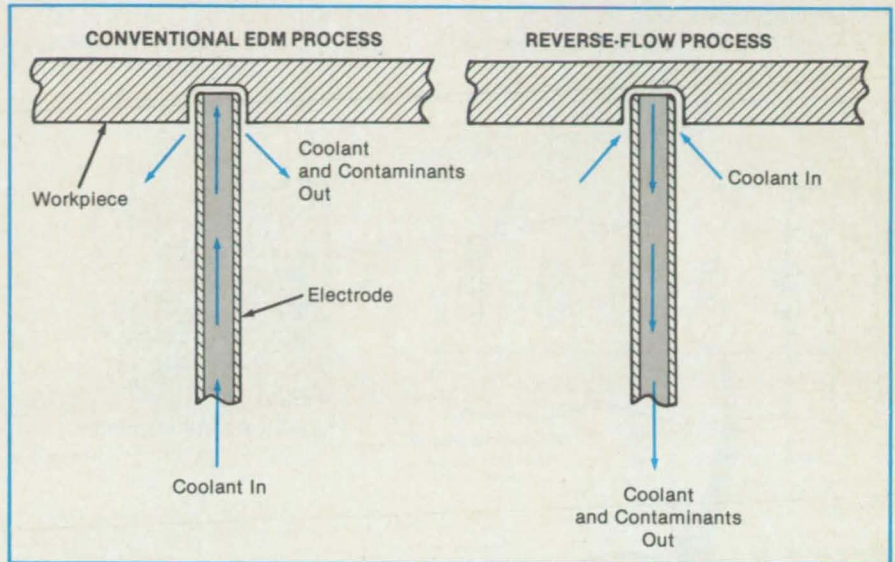
Debris are swept into the electrode by the flow of coolant.

Marshall Space Flight Center, Alabama

The contamination of parts by electrical-discharge machining (EDM) can be almost completely eliminated by reversing the flow of coolant. EDM normally produces contamination from electrode wear and workpiece erosion. When the direction of flow of coolant in the electrode is away from the workpiece instead of toward it (see figure), contaminant particles are whisked away through the hollow EDM electrode.

Use of CCl_2F_2 as the coolant instead of the usual water or oil further reduces contamination. The CCl_2F_2 efficiently cools the electrode and electrically insulates it from the workpiece until a sufficiently high voltage is reached. Unlike water or oil, however, the CCl_2F_2 is completely volatile and leaves no contaminating residue on the workpiece. The CCl_2F_2 is used in the saturated-vapor state.

In a demonstration of the reverse-flow process, holes of 0.050 in. (1.27 mm) in diameter were drilled through Inconel* 718 samples 0.125 in. (3.18 mm) thick. Four sets of samples were machined with repeatable results. The vapor pressure of the CCl_2F_2 varied from 40 to 90 psig (283 to 627 kPa). The brass EDM electrode had a 0.045-in. (1.14-mm) outside diameter and a 0.030-in. (0.76-mm) inside diameter. No



The Flow Is Reversed from the usual direction so that the coolant carries contaminants out through the passage in the electrode. The coolant for reverse flow is pressurized dichlorodifluoromethane vapor.

contamination was visible.

*Inconel is a registered trademark of the Inco family of companies.

This work was done by Mark G. Schmidt of Rockwell International Corp. for Marshall Space Flight Center. For further information, Circle 155 on the TSP Request

Card.

Inquiries concerning rights for the commercial use of this invention should be addressed to the Patent Counsel, Marshall Space Flight Center [see page 22]. Refer to MFS-29197.

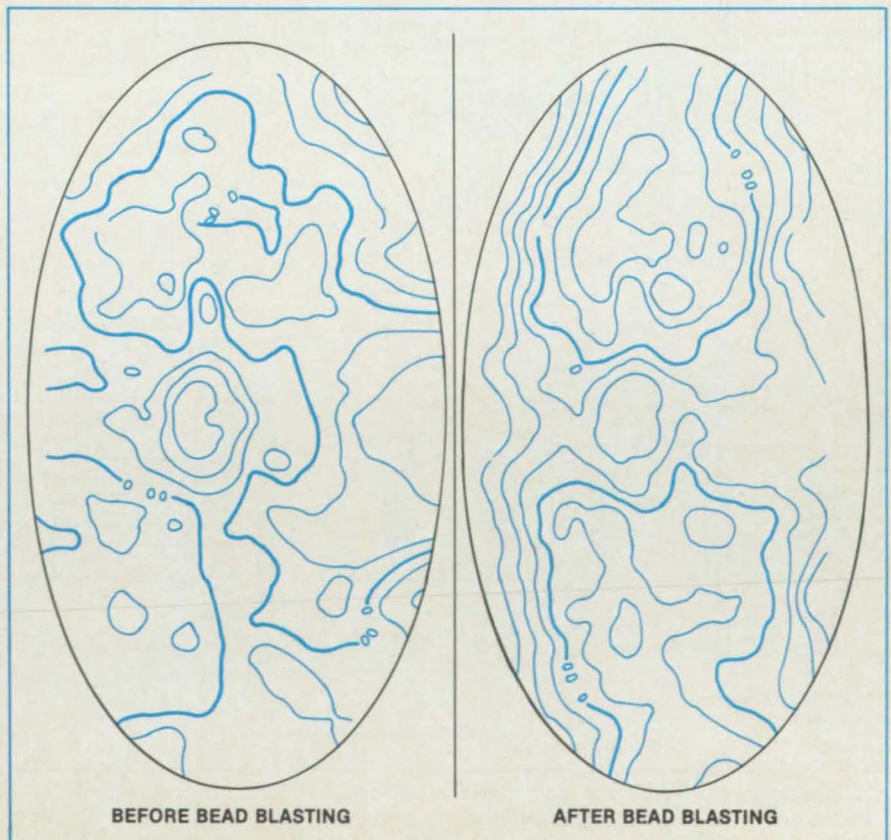
Glass-Bead Blasting Alters Antenna Surface

Thermal-emissivity properties are improved, and focal length is adjusted.

NASA's Jet Propulsion Laboratory, Pasadena, California

Experiments have shown that gentle blasting with glass beads can produce beneficial changes in the macroscopic surface shapes and in the microscopic surface features (textures or finishes) of lightweight microwave reflectors made of thin metal reflective surfaces on deformable substrates of aluminum honeycomb. Until now, it has been difficult to make microwave reflectors from metal honeycomb stock because fabrication techniques that adjust surface shapes to desired contours

Surface-Contour Maps show the shape of an aluminum-honeycomb reflector before and after blasting with glass beads.



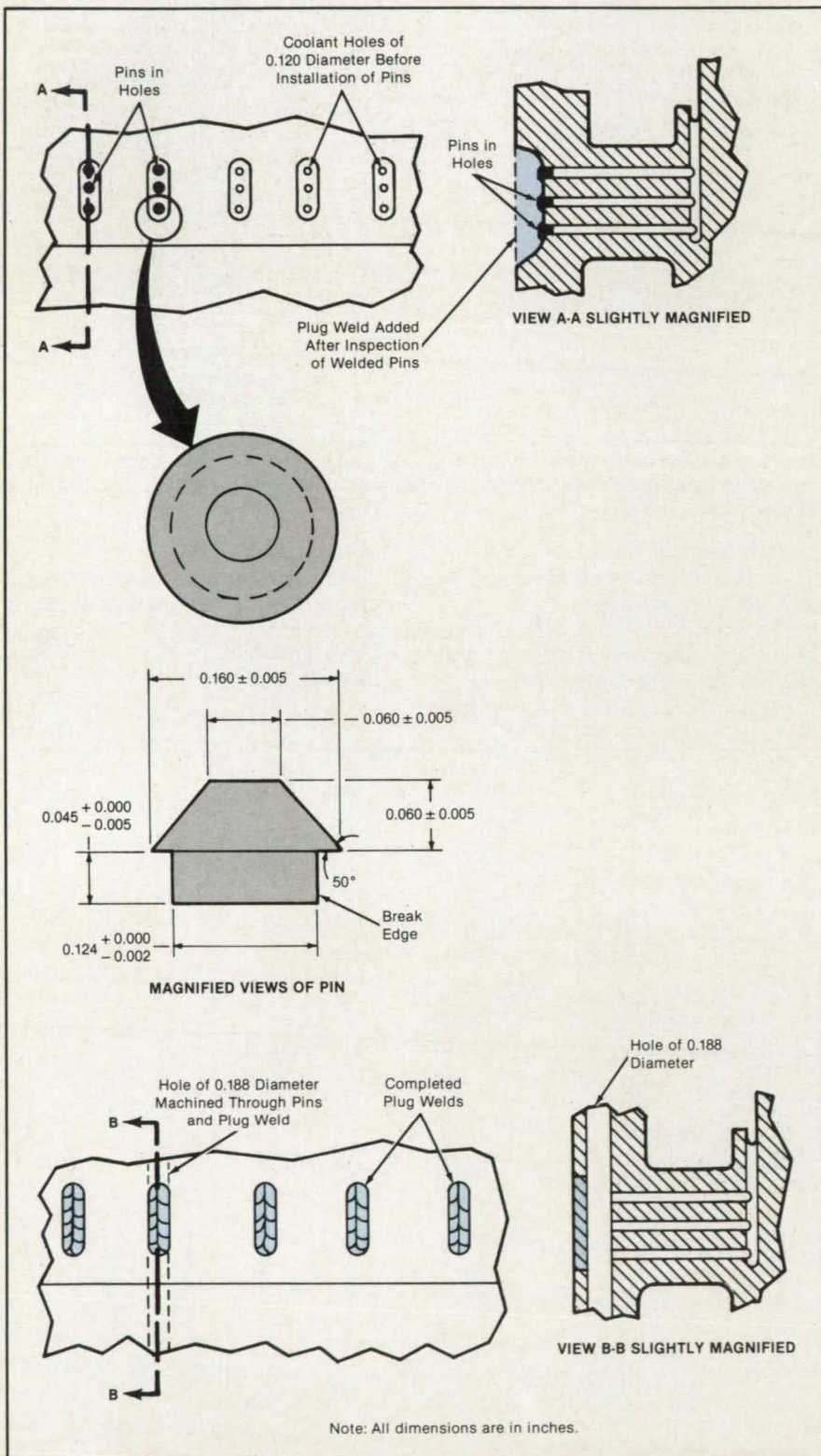
can also remove metal and cause unwanted changes in the thermal emissivity/absorptivity of the surfaces, while techniques that achieve the desired thermal-radiative properties can also change surface contours undesirably.

In a typical fabrication experiment, 50- μm glass beads were sprayed by hand at about 15 psi (100 kPa) on a concave

reflector surface. This treatment did not remove metal or damage the surface but did change the surface finish and appearance to flat gray. The altered surface finish satisfied the thermal-radiative specification. The bead blasting also changed the surface contour (see figure), increasing the focal length by about 0.080 in. (2 mm).

This work was done by James W.

Fortenberry, Richard L. Jilka, Boyce Kimmel, Ramon D. Garcia, Richard E. Cofield, Gerhardt J. Klose, and Thomas O'Toole of Caltech for NASA's Jet Propulsion Laboratory. For further information, Circle 103 on the TSP Request Card. NPO-16898



Pin Inserts for Plug Welds

Leakage through minute cracks is eliminated.

Marshall Space Flight Center, Alabama

Expendable pin inserts solve a chronic problem of cracking in and near plug welds. Previously, machined coolant holes in Inconel* were sealed by gas/tungsten arc welding. However, the welded parts frequently contained cracks that became evident in radiographic inspection. The parts had to be reworked and sometimes discarded.

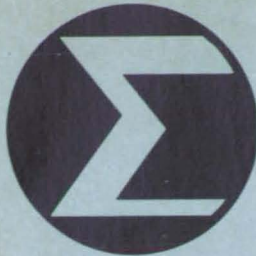
With the expendable-pin method, cracks are nearly eliminated. Inconel* 718 pins are machined to press-fit into the coolant holes, which are 0.120 in. (3 mm) in diameter and arranged in slots in groups of three. The pins are electron-beam-welded in place. (The welding parameters are determined by experimenting on scrap material.)

The quality of the pin welds is checked by liquid-penetrant and radiographic inspection. If the welds pass these tests, the pins are ground flush to the adjacent surfaces. The slots are then filled by gas/tungsten arc welding. The welds are subjected once more to liquid-penetrant and radiographic inspection, which shows that the slots are 90 to 100 percent free of defects. Finally, a hole 0.188 in. (4.78 mm) in diameter and perpendicular to the coolant holes is machined along the slot, removing the pins.

*Inconel is a registered trademark of the Inco family of companies.

This work was done by Michael Penninger of Rockwell International Corp. for Marshall Space Flight Center. No further documentation is available. MFS-29193

Electron-Beam-Welded Pins reinforce the material around the coolant holes during plug welding and subsequent remachining. The pins are removed in the final machining of the 0.188-in.-diameter hole.



Mathematics and Information Sciences

Hardware, Techniques, and Processes

103 System-Assurance Analysis for Nuclear Powerplants

Books and Reports

104 Effects of Structural Errors on Parameter Estimates

Computer Programs

66 Program for Analysis and Enhancement of Images

68 Program for Development of Artificial Intelligence

68 Assessing the Reliability of NDE

System-Assurance Analysis for Nuclear Powerplants

Rocket-launch reliability techniques could be adapted to benefit powerplants.

John F. Kennedy Space Center, Florida

A system-assurance-analysis (SAA) methodology developed for aerospace launch-support systems has been proposed for nuclear powerplants. Launch-support systems and nuclear powerplants are similar in complexity and share common reliability and safety goals. This similarity prompted a study that showed that it would be feasible and practical to apply SAA methodology to nuclear powerplants.

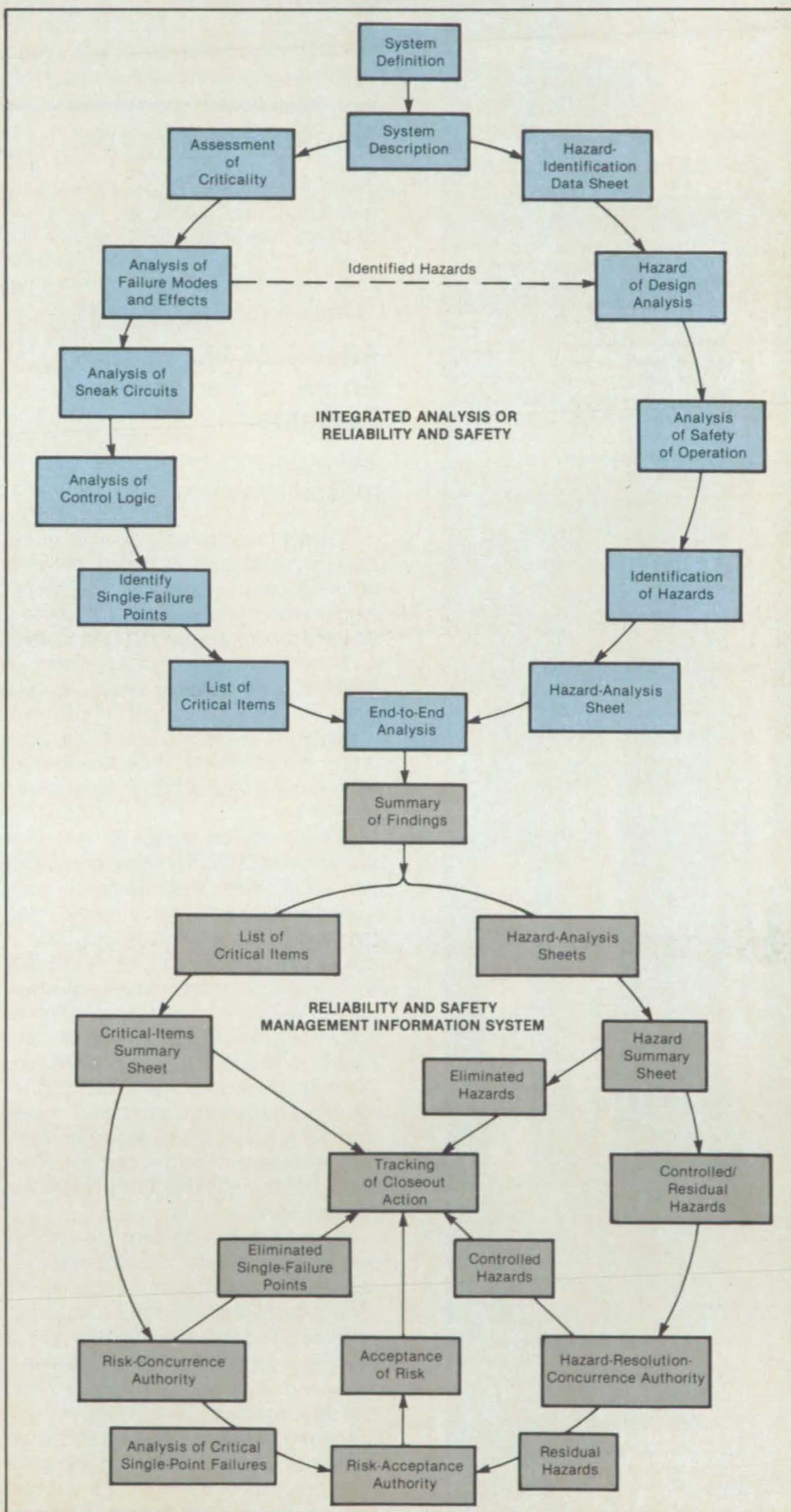
SAA methodology is simply the combination of well-known safety and reliability analytical techniques with new management methods to identify, track, and resolve critical items and hazards (see figure). The SAA examines systems, subsystems, components, control functions, integrated systems, and human/machine operations.

SAA started early in the design-engineering process becomes the foundation for an expanded analysis as design progresses. Tracking of the results of the analysis continues after design is complete and operations and test procedures are defined — in fact, tracking continues as long as the system operates. Future modifications in the system will be analyzed and integrated into the information system for presentation to management.

When a given design is complete, the reviewing agency examines the acceptance rationale for the remaining critical items and residual hazards and evaluates the risks involved. The SAA thus gives management a focal point at which problems can be assessed.

For this methodology to be most useful and attractive to the nuclear-power industry, it should be an integral part of the design and licensing process, not just an

The **SAA Methodology** is essentially a combination of analytical techniques related to safety and reliability with an information system that assists managers in making decisions that affect safety and reliability.



fisher SPACE PEN

**...DEVELOPED FOR
N.A.S.A.
...USED BY
ASTRONAUTS ON
SPACE FLIGHTS**

Probably the world's most dependable pen. The patented pressurized cartridge developed for NASA permit these pens to write at any angle (even upside down) in severe temperatures -50° to +400°F, over glossy or greasy surfaces, under water and up to 3 times longer than ordinary pens.



Chrome Space Pen with flight button point retraction. Refills readily available.

\$10.00



Chrome pocket/purse pen with distinctive Space Shuttle emblem. Unique compact design.

\$15.00

Fisher Space Pens are available wherever better pens are sold. Corporate logos and emblems are available. You may order or request further information by contacting:

FISHER PEN CO.
743 Circle Avenue
Forest Park, IL 60130
(312) 366-5030

additional requirement. A further consideration is that SAA methodology differs somewhat from the present direction of Nuclear Regulatory Agency policy, which relies on safety goals with numerical guidelines. Although SAA methodology does consider the probability of failure in the single-failure-point assessment, this is only one of the many items examined to determine whether a single failure point is an acceptable risk. Other items include design safety margins, qualification testing, man-

datory inspections, training and certification requirements, and operating procedures.

This work was done by Donald W. Page of Kennedy Space Center. To obtain copies of the reports, "Application of NASA Kennedy Space Center System Assurance Analysis Methodology to Nuclear Power Plant Systems Designs," and "System Assurance Analysis Application Handbook," Circle 49 on the TSP Request Card. KSC-11306

Books and Reports

These reports, studies, handbooks are available from NASA as Technical Support Packages (TSP's) when a Request Card number is cited; otherwise they are available from the National Technical Information Service.

Effects of Structural Errors on Parameter Estimates

The information content of a measurement is defined.

A paper introduces the concept of the near equivalence in probability between different parameters or mathematical models of a physical system. It is one in a series of papers, each of which establishes a different part of a rigorous theory of mathematical modeling based on concepts of structural error, identifiability, and equivalence. In this installment, the focus is upon the effects of additive structural errors on the degree of bias in estimates of parameters.

A mathematical model is fitted to a system by adjusting the values of parameters in the model. These values are estimated by fitting solutions computed using the model to the physical system. Thus, a quantitative representation of the information content of a measurement expresses the degree to which the measurement enables one to distinguish between different models or sets of parameter values. For real measurements that are subject to error, the information content of a measurement is related to the degree to which the measurement enables one to narrow the probability distribution of the parameter values.

The information content can be expressed in a matrix form reported by prior authors. The present authors show that the nonsingularity of the information matrix is a necessary and sufficient condition for the near equivalence in probability between a model and a system in the presence of several error sources. The resulting formulation makes it possible to evaluate the effects of modeling errors by comparing the output probability densities of the model and the system. This technique is appli-

cable to both deterministic and stochastic errors.

The problem of identifiability of a model is then approached through the evaluation of the information matrix for nearly equivalent models. For a deterministic modeling error, the covariance of the error of the parameter estimates turns out to be independent of the structural-error term. However, a random modeling error can increase the variance of errors and contribute to considerable bias in the parameter estimates.

In this study, the unknown parameters were assumed to be deterministic constants. In principle, appropriate modifications of the definitions of near equivalence could enable the extension of the theory to models with random parameters. The effects of random parameters and multiplicative modeling errors on the near-equivalence and the parameter-identifiability problems also remain to be investigated.

This work was done by F. Y. Hadaegh and G. A. Bekey of the University of Southern California for NASA's Jet Propulsion Laboratory. To obtain a copy of the report, "Effects of Structural Error on the Estimates of Parameters of Dynamical Systems," Circle 89 on the TSP Request Card.

NPO-16816

New Products

An all-aluminum airborne cooler assembly has been announced by **Lytron Incorporated**, Woburn, MA. Designed for cooling MIL-L-5606 hydraulic fluid on a military helicopter, the integrated assembly includes a reservoir can, fan and housing, heat exchanger, and support structure. The 4.5 lb cooler features high heat transfer efficiency, removing 12,000 BTU/hr from an ambient temperature of 122° F. **Circle Reader Service Number 595.**

A 12 page color brochure from **MTS Systems Corp.** (Minneapolis, MN) describes the firm's capabilities in engine simulation for dynamic drive train testing and design. MTS engine simulation systems allow the engineer to apply oscillating torque or motion to a specimen while it is spinning, thus simulating dynamic operating conditions. **Circle Reader Service Number 596.**



Life Sciences

Hardware, Techniques, and Processes

105 Collector/Compactor for Waste or Debris

Collector/Compactor for Waste or Debris

A stretchable net gathers loose material and compresses it.

Lyndon B. Johnson Space Center, Houston, Texas

A device collects and compacts debris by sweeping through a volume with a net. The device, developed for compacting human waste in 2.7-ft³ (0.076-m³) storage containers in the microgravity of space vehicles, can have such terrestrial applications as cleaning swimming pools and tanks.

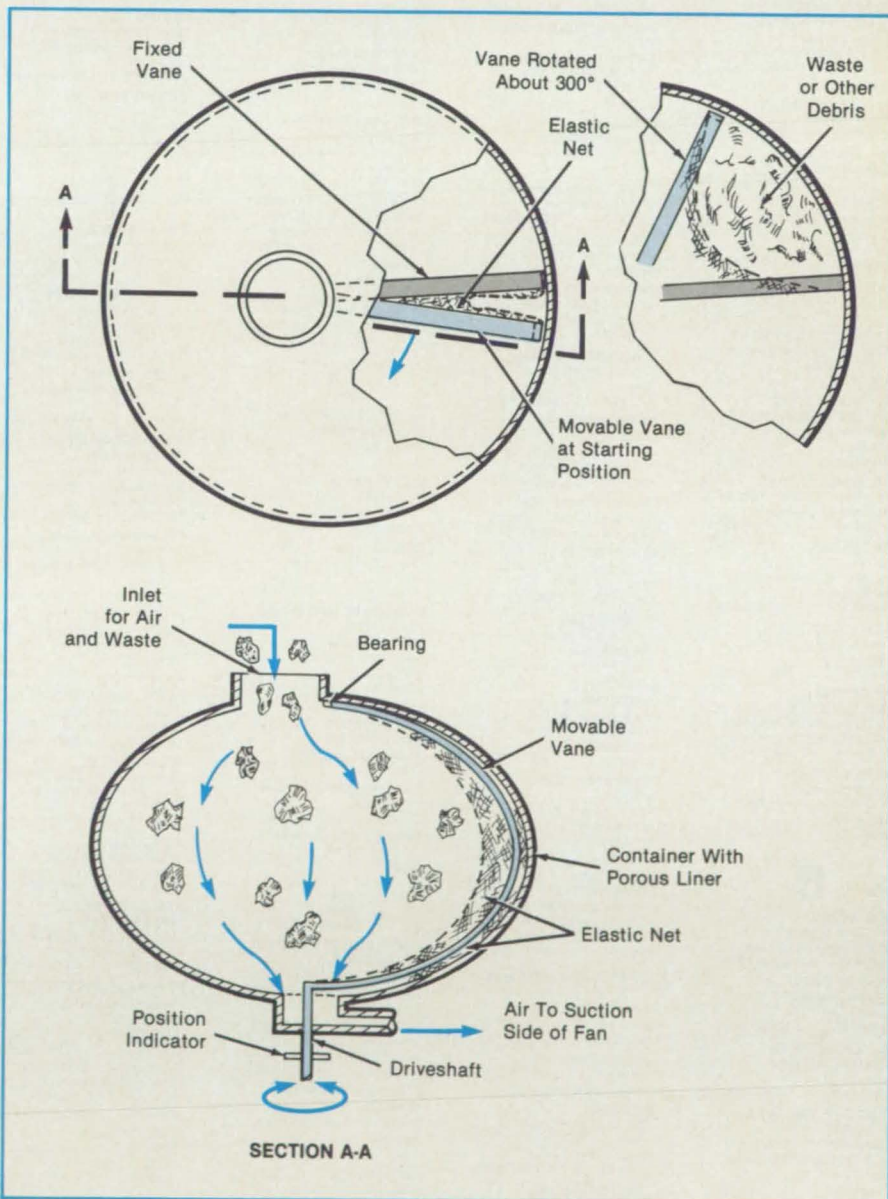
In the space application, a flow of air carries debris into the containers. Without the new device, debris accumulates at the container inlets as the containers become full and the airflow loses effectiveness. By collecting and compacting the debris, the device enables the use of the full volume of the container.

The device consists of a movable vane, a fixed vane, and an elastic net connected to both vanes (see figure). The movable vane is a metal strip curved to follow the general contour of the container but with enough clearance to prevent interference with other parts on the inside wall of the container. One end of the movable vane is mounted in a bearing and the other end is connected to a driveshaft equipped with a handle. When the user rotates the movable vane, the net is stretched and swept through the container. The net captures most of the debris coarser than its mesh as it moves, compressing the debris as it arrives at the fixed vane.

The elasticity of the net accommodates its varying length, which grows as the movable vane rotates to 180° from the fixed vane, then shrinks as it rotates from 180° toward 360°. An external dial on the driveshaft indicates the position of the movable vane.

The elastic net can be made of a stretchable polymer like Spandex (or equivalent) polyurethane, of a combination of extension springs and netting, or of springs alone. The greater the elastic tension, the better will be the retention and compression of waste against the container wall.

The motion of the vane can be reversed after use to collect and compress material in the opposite direction. The device can



Sweeping Through the Container Volume, an elastic net gathers and compresses debris. The container is thus cleared of most loose material, and its useful capacity is increased.

be used many times.

This work was done by John K. Mangialiardi of General Electric Co. for

Johnson Space Center. No further documentation is available.
MSC-21196

Subject Index

A

ACCESS CONTROL
Central processor acts as high-speed DMA controller page 47 LAR-13497

ACCUMULATORS
Collector/compactor for waste or debris page 105 MSC-21196

ACOUSTIC LEVITATION
Single-axis acoustic levitator with rotation control page 96 NPO-16924

ADHESIVES
Ceramic adhesive for high temperatures page 100 MSC-21085

AERODYNAMICS
Interface circuit for laser-Doppler velocimeters page 42 ARC-11536

AIR FLOW
Dual-mode laser velocimeter page 50 ARC-11634

AIR SAMPLING
Concentrating trace gases at low pressures page 52 ARC-11671

AIRCRAFT DESIGN
Calculating wave drag on an aircraft page 66 LAR-13634

AIRCRAFT ENGINES
Unducted-fan engine page 90 LEW-14429

AIRCRAFT EQUIPMENT
Gamma-ray fuel gauges for airplanes page 74 LAR-13604

AIRCRAFT NOISE
Calculations of wall effects on propeller noise page 86 LEW-14516

ANTENNA ARRAYS
Analysis of four-reflector S/X-band antenna page 40 NPO-16839

ANTENNAS
Diffraction analysis of antennas with mesh surfaces page 36 NPO-16474

Waveguide-horn-to-waveguide transition assembly page 34 MSC-21146

ARTIFICIAL INTELLIGENCE
Program for development of artificial intelligence page 68 MSC-21208

ATMOSPHERIC TURBULENCE
Approximate simulation of turbulence page 53 MFS-28172

B

BALANCING
Fatigue lives of materials cut by lasers page 90 LEW-14532

BINARY DATA
Binary-symmetry detection page 46 GSC-12985

BIT ERROR RATE
Binary-symmetry detection page 46 GSC-12985

BOOSTER ROCKET ENGINES
Structural dynamics of filament-wound booster rockets page 86 MFS-28155

BORON NITRIDES
Amorphous insulator films with controllable properties page 64 LEW-14370

BOUNDARY LAYERS
Experiments in boundary-layer turbulence page 85 NPO-16754

BUBBLE MEMORY DEVICES

Self-stabilizing storage loops for magnetic-bubble memories page 28 LAR-13625

C

CAPACITORS
Radiation resistances of dielectric liquids page 65 NPO-16891

CARBON TETRAFLUORIDE
Coating a hydrogen-maser chamber with CF_4 page 55 NPO-16380

CEMENTS
Ceramic adhesive for high temperatures page 100 MSC-21085

CENTRAL PROCESSING UNITS
Central processor acts as high-speed DMA controller page 47 LAR-13497

CERAMICS
Ceramic adhesive for high temperatures page 100 MSC-21085

Determining directions of ultrasound in solids page 70 LEW-14473

TRIBOLOGICAL PROPERTIES OF STRUCTURAL CERAMICS
page 64 LEW-14387

CHEMICAL CLEANING
Fluidized-bed cleaning of silicon particles page 59 NPO-16935

COLOR TELEVISION
Color-video thermal maps page 84 MFS-29223

COMBUSTION CHAMBERS
Computer program for flow in a combustor page 66 LEW-14271

Steam reformer with fibrous catalytic converter page 88 NPO-16971

COMPACTING
Collector/compactor for waste or debris page 105 MSC-21196

COMPASSES
Improved flux-gate magnetometer page 24 LAR-13560

COMPOSITE STRUCTURES
Pressure-localizing inserts for bagging laminations page 98 ARC-11673

COMPUTER AIDED DESIGN
Preliminary-design software for composite structures page 85 MFS-27153

COMPUTER COMPONENTS
Central processor acts as high-speed DMA controller page 47 LAR-13497

COMPUTER PROGRAMS
Computer program for flow in a combustor page 66 LEW-14271

Program for analysis and enhancement of images page 66 GSC-13075

COMPUTER STORAGE DEVICES
Self-stabilizing storage loops for magnetic-bubble memories page 28 LAR-13625

CONCENTRATING
Concentrating trace gases at low pressures page 52 ARC-11671

CONDUCTIVE HEAT TRANSFER
High-differential-pressure heat exchanger page 71 NPO-16947

CONSTRUCTION MATERIALS
Tribological properties of structural ceramics page 64 LEW-14387

CONTOUR SENSORS
Measuring and plotting surface-contour deviations page 83 MSC-21163

CONTOURS
Glass-bead blasting alters antenna surface page 101 NPO-16898

CONTRAROTATING PROPELLERS
Unducted-fan engine page 90 LEW-14429

COOLING SYSTEMS
Contamination-free electrical-discharge machining page 101 MFS-29197

CORONAS
Measuring electrostatic discharge page 54 MSC-21094

CRYOGENIC EQUIPMENT
Thermally insulating support for cryogenic tanks page 79 ARC-11608

CRYOGENICS
Measuring contact thermal conductances at low temperatures page 56 ARC-11693

CRYOTRAPPING
Concentrating trace gases at low pressures page 52 ARC-11671

CRYSTAL GROWTH
Growing II/VI semiconductors with double decantation page 99 NPO-16808

CRYSTAL OSCILLATORS
Implantable, ingestible electronic thermometer page 34 GSC-13037

CURING
Thermomechanical properties indicate degree of epoxy cure page 58 NPO-16903

D

DATA TRANSMISSION
Binary-symmetry detection page 46 GSC-12985

DIELECTRICS
Radiation resistances of dielectric liquids page 65 NPO-16891

DIODES
High-voltage switch containing $(DI)_2^2$ devices page 32 LEW-14390

DIRECTORS (ANTENNA ELEMENTS)
Diffraction analysis of antennas with mesh surfaces page 36 NPO-16474

DURABILITY
Design of fiber composites for structural durability page 61 LEW-14385

DYNAMIC STRUCTURAL ANALYSIS
Structural dynamics of filament-wound booster rockets page 86 MFS-28155

E

EARTH OBSERVATIONS (FROM SPACE)
Program for analysis and enhancement of images page 66 GSC-13075

ELECTRIC DISCHARGES
Measuring electrostatic discharge page 54 MSC-21094

ELECTRIC POWER PLANTS
Hanging windmills from cables page 89 LAR-13434

ELECTRICAL INSULATION
Amorphous insulator films with controllable properties page 64 LEW-14370

ELECTRODES
Contamination-free electrical-discharge machining page 101 MFS-29197

Preset electrodes for electrical-discharge machining page 97 MFS-29198

ELECTROMECHANICAL DEVICES
Measuring and plotting surface-contour deviations page 83 MSC-21163

ELECTRON TRANSITIONS
High-rydberg xenon submillimeter-wave detector page 57 NPO-16372

ELECTROSTATIC CHARGE
Measuring electrostatic discharge page 54 MSC-21094

EPOXY RESINS
Thermomechanical properties indicate degree of epoxy cure page 58 NPO-16903

EQUIVALENCE
Effects of structural errors on parameter estimates page 104 NPO-16816

ERRORS
Effects of structural errors on parameter estimates page 104 NPO-16816

ESTIMATES
Effects of structural errors on parameter estimates page 104 NPO-16816

EXPERT SYSTEMS
Program for development of artificial intelligence page 68 MSC-21208

F

FATIGUE LIFE
Fatigue lives of materials cut by lasers page 90 LEW-14532

FIBER COMPOSITES
Design of fiber composites for structural durability page 61 LEW-14385

FIBER OPTICS
Fiber-optic temperature sensor page 74 MFS-29164

FIBER REINFORCED COMPOSITES
Preliminary-design software for composite structures page 85 MFS-27153

FILAMENT WINDING
Structural dynamics of filament-wound booster rockets page 86 MFS-28155

FLIGHT TESTS
Flight research on a forward-swept-wing airplane page 95 ARC-11740

FLOW VISUALIZATION
Water-tunnel flow visualization with a laser page 86 ARC-11698

FLOWMETERS
Measuring viscosities of gases at atmospheric pressure page 72 LAR-13591

FLUID FLOW
Higher-quality weld joints for tube sections page 97 MFS-29190

FLUIDIZED BED PROCESSORS
Fluidized-bed cleaning of silicon particles page 59 NPO-16935

FLOURESCENCE
Measuring gases with laser-induced fluorescence page 53 ARC-11678

FREQUENCY CONTROL
Predicting false lock in phase-locked loops page 48 MFS-27110

FUEL GAUGES
Gamma-ray fuel gauges for airplanes page 74 LAR-13604

G

GAMMA RAY ABSORPTION
Gamma-ray fuel gauges for airplanes page 74 LAR-13604

GAS DYNAMICS
Measuring gases with laser-induced fluorescence page 53 ARC-11678

GAS FLOW
Computer program for flow in a combustor page 66 LEW-14271

GAS VISCOSITY
Measuring viscosities of gases at atmospheric pressure page 72 LAR-13591

GRAPHITE-EPOXY COMPOSITES
Bismaleimide copolymer matrix resins page 60 ARC-11599

H

HEAT EXCHANGERS
High-differential-pressure heat exchanger page 71 NPO-16947

Stiffening heat-exchanger tubes against vibrations page 84 MFS-19907

HEAT TRANSFER
Steam reformer with fibrous catalytic converter page 88 NPO-16971

HELICOPTER WAKES
Analyzing wakes from hovering-helicopter rotor blades page 80 ARC-11675

HIGH VOLTAGES
High-voltage switch containing $(DI)_2^2$ devices page 32 LEW-14390

HORN ANTENNAS
Waveguide-horn-to-waveguide transition assembly page 34 MSC-21146

HOVERING
Analyzing wakes from hovering-helicopter rotor blades page 80 ARC-11675

HYDROCARBONS
Amorphous insulator films with controllable properties page 64 LEW-14370

HYDROGEN MASERS
Coating a hydrogen-maser chamber with CF_4 page 55 NPO-16380

I

IMAGE PROCESSING
Program for analysis and enhancement of images page 66 GSC-13075

IMAGING TECHNIQUES
Optical design and signal processing for edge detection page 47 LAR-13416

INFRARED DETECTORS
Diode structure for microwave and infrared applications page 30 GSC-12962

High-rydberg xenon submillimeter-wave detector page 57 NPO-16372

INSERTS
Pin inserts for plug welds page 102 MFS-29193

INSPECTION
Assessing the reliability of NDE page 68 LEW-14286

J

JOINTS (JUNCTIONS)
Measuring contact thermal conductances at low temperatures page 56 ARC-11693

L

LAMINATES
Pressure-localizing inserts for bagging laminations page 98 ARC-11673

LANGUAGE PROGRAMMING
Program for development of artificial intelligence page 68 MSC-21208

LASER APPLICATIONS
Water-tunnel flow visualization with a laser page 86 ARC-11698

LASER CUTTING
Fatigue lives of materials cut by lasers page 90 LEW-14532

LASER DOPPLER VELOCIMETERS
Dual-mode laser velocimeter page 50 ARC-11634

Interface circuit for laser-Doppler velocimeters page 42 ARC-11536

LASER SPECTROSCOPY
Measuring gases with laser-induced fluorescence page 53 ARC-11678

LENGTH
Lead scales for x-radiographs page 85 MFS-29247

LEVITATION
Single-axis acoustic levitator with rotation control page 96 NPO-16924

LOOPS
Predicting false lock in phase-locked loops page 48 MFS-27110

M

MACHINE TOOLS
Contamination-free electrical-discharge machining page 101 MFS-29197

Preset electrodes for electrical-discharge machining page 97 MFS-29198

MAGNETIC STORAGE
Self-stabilizing storage loops for magnetic-bubble memories page 28 LAR-13625

MAGNETOMETERS
Improved flux-gate magnetometer page 24 LAR-13560

MARKING
Lead scales for x-radiographs page 85 MFS-29247

MASERS
Coating a hydrogen-maser chamber with CF_4 page 55 NPO-16380

MATHEMATICAL MODELS
Calculating wave drag on an aircraft page 66 LAR-13634

MATRIX MATERIALS
Bismaleimide copolymer matrix resins page 60 ARC-11599

MEASURING INSTRUMENTS
Measuring and plotting surface-contour deviations page 83 MSC-21163

MELTS (CRYSTAL GROWTH)
Growing II/VI semiconductors with double decantation page 99 NPO-16808

MICROWAVE ANTENNAS
Analysis of four-reflector S/X-band antenna page 40 NPO-16839

Glass-bead blasting alters antenna surface page 101 NPO-16898

MICROWAVE FILTERS
Diode structure for microwave and infrared applications page 30 GSC-12962

MONTE CARLO METHOD
Approximate simulation of turbulence page 53 MFS-28172

N

NAVIGATION INSTRUMENTS
Improved flux-gate magnetometer page 24 LAR-13560

NONDESTRUCTIVE TESTS
Assessing the reliability of NDE page 68 LEW-14286

Determining directions of ultrasound in solids page 70 LEW-14473

PROVIDING THE FOUNDATION FOR FUTURE GROWTH

Martin Marietta has been providing technology to the United States Government for over fifty years and now has the most diversified contract portfolio of any major space defense contractor. Martin Marietta Aero & Naval Systems is experiencing tremendous growth applying advanced naval systems technology to a wide variety of projects and programs including the U.S. Navy's Vertical Launch System and the Army's Patriot Air Defense Missile Launcher.

Other current program activity includes work in:

- **Autonomous Underwater Vehicles**
- **Wide Aperture Array**
- **Advanced Lightweight Sonar**
- **Remotely Piloted Air Vehicles**
- **ASW Research & Technology**
- **Surface Weapons Systems**
- **Combat Systems Engineering**
- **MK 50 Torpedo**

Our continuing growth at Aero & Naval Systems has created immediate opportunities for these engineers with a technical MS/PhD or at least one year experience in:

Manufacturing Engineers

- Tool Designers
- Planners
- NC Programmers
- Electronics

Manufacturing Test Engineers

- Software Engineers
- Microprocessor Applications

Robotic Systems

- Telepresence
- Supervisory Vehicles
- Manipulator Design

Electronics Engineering

- Local Area Network
- Power Supply
- Electro/Mech. Pkg
- Microprocessor Applications
- IR/EO Systems Design
- VLSI Design
- Radar Support

Mechanical Engineering

- Thermal Analyst

Logistics Engineering

- Reliability
- Systems Safety

Advanced Manufacturing Technologies

- Materials Engineers
- Test Engineers
- NDT Engineers

We also have opportunities for these professionals:

- **Quality Engineers**
- **Sr. Subcontract Administrators**
- **Configuration & Data Management Specialist**
- **Contract Administrators**
- **Master Program Planners**
- **Finance Administrators**
- **Industrial Engineers**
- **Pricing Analyst**

Please send your resume to:
Martin Marietta Aero & Naval
Systems, Employment Dept.
NASA, 103 Chesapeake
Park Plaza, Baltimore, MD 21220.
Special background investigation
may be required. An equal opportunity employer m/f/h/v.



MASTERMINDING TOMORROW'S TECHNOLOGIES

MARTIN MARIETTA

SCIENTIFIC/ENGINEERING GRAPHIC TOOLS

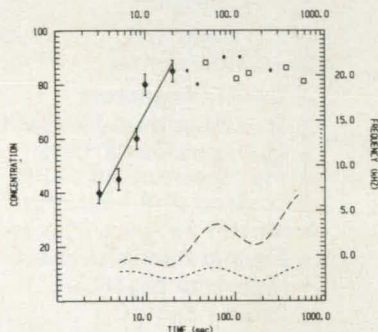
for the IBM PC and compatibles

FORTRAN/Pascal tools: **GRAFATIC** (screen graphics) and **PLOTMATIC** (pen plotter driver)

These packages provide 2D and 3D plotting capabilities for programmers writing in a variety of FORTRAN/Pascal environments. We support MS, R-M, LAHEY FORTRAN and more. PLOTMATIC supports HP or Houston Instrument plotters. Font module available too!

Don't want to program? Just ask for **OMNILOT!** Menu-driven, fully documented integrated scientific graphics. Write or call for complete information and ordering instructions.

GRAFATIC-PLOTMATIC-OMNILOT [S] & [P]



Microcompatibles, 301 Prelude Drive, Silver Spring, MD 20901

(301) 593-0683

Circle Reader Action No. 389

NUCLEAR POWER PLANTS
System-assurance analysis for nuclear powerplants
page 103 KSC-11306

OPTICAL MEASUREMENT
Optical design and signal processing for edge detection
page 47 LAR-13416

OXYGEN ATOMS
Protective coatings for spacecraft polymers
page 61 LEW-14384

PARABOLIC ANTENNAS
Analysis of four-reflector S/X-band antenna
page 40 NPO-16839

PHASE LOCKED SYSTEMS
Predicting false lock in phase-locked loops
page 48 MFS-27110

PIPELINES
Higher-quality weld joints for tube sections
page 97 MFS-29190

PLUGGING
Pin inserts for plug welds
page 102 MFS-29193

POSITIONING DEVICES (MACHINERY)
Fresnel electrodes for electrical-discharge machining
page 97 MFS-29198

PRESSURE VESSELS
Repairing holes in pressure walls
page 99 MFS-28179

PROPELLERS
Calculations of wall effects on propeller noise
page 86 LEW-14516

PROTECTIVE COATINGS
Protective coatings for spacecraft polymers
page 61 LEW-14384

QUARTZ CRYSTALS
Implantable, ingestible electronic thermometer
page 34 GSC-13037

RADAR EQUIPMENT
Ultrasonic ranging system with increased resolution
page 44 MSC-21090

RADIATION TOLERANCE
Radiation resistances of dielectric liquids
page 65 NPO-16891

RANGE FINDERS
Ultrasonic ranging system with increased resolution
page 44 MSC-21090

REACTOR DESIGN
Steam reformer with fibrous catalytic converter
page 88 NPO-16971

REFLECTORS
Diffraction analysis of antennas with mesh surfaces
page 36 NPO-16474

RELIABILITY ANALYSIS
Assessing the reliability of NDE
page 88 LEW-14286

RESIN MATRIX COMPOSITES
System-assurance analysis for nuclear powerplants
page 103 KSC-11306

ROBOTICS
Optical design and signal processing for edge detection
page 47 LAR-13416

ROTATION
Single-axis acoustic levitator with rotation control
page 96 NPO-16924

ROTOR AERODYNAMICS
Analyzing wakes from hovering-helicopter rotor blades
page 80 ARC-11675

SEMICONDUCTOR (MATERIALS)
Growing III/V semiconductors with double decantation
page 99 NPO-16808

SEMICONDUCTOR DIODES
Diode structure for microwave and infrared applications
page 30 GSC-12962

SILICON
Fluidized-bed cleaning of silicon particles
page 59 NPO-16935

SPACE STATIONS
Control and simulation of space-station vibrations
page 87 NPO-16852

SPACECRAFT SHIELDING
Protective coatings for spacecraft polymers
page 61 LEW-14384

STRESS ANALYSIS
Preliminary-design software for composite structures
page 85 MFS-27153

STRUCTURAL DESIGN
Design of fiber composites for structural durability
page 61 LEW-14385

STRUCTURAL VIBRATION
Control and simulation of space-station vibrations
page 87 NPO-16852

SUBMILLIMETER WAVES
High-rydberg xenon submillimeter-wave detector
page 57 NPO-16372

SURFACE FINISHING
Glass-bead blasting alters antenna surface
page 101 NPO-16898

SUSPENDING (HANGING)
Hanging windmills from cables
page 89 LAR-13434

SWEPT FORWARD WINGS
Flight research on a forward-swept-wing airplane
page 95 ARC-11740

SWITCHES
High-voltage switch containing (DI)² devices
page 32 LEW-14390

SYSTEMS ANALYSIS
System-assurance analysis for nuclear powerplants
page 103 KSC-11306

TANKS (CONTAINERS)
Thermally insulating support for cryogenic tanks
page 79 ARC-11608

TEMPERATURE DISTRIBUTION
Color-video thermal maps
page 84 MFS-29223

TEMPERATURE PROBES
Fiber-optic temperature sensor
page 74 MFS-29164

THERMAL CONDUCTIVITY
Measuring contact thermal conductances at low temperatures
page 56 ARC-11693

THERMAL INSULATION
Thermally insulating support for cryogenic tanks
page 79 ARC-11608

THERMAL MAPPING
Color-video thermal maps
page 84 MFS-29223

THERMOMETERS
Fiber-optic temperature sensor
page 74 MFS-29164

THERMOSETTING RESINS
Thermomechanical properties indicate degree of epoxy cure
page 58 NPO-16903

THIN FILMS
Amorphous insulator films with controllable properties
page 64 LEW-14370

TOOLS
Repairing holes in pressure walls
page 99 MFS-28179

TRIBOLOGY
Tribological properties of structural ceramics
page 64 LEW-14387

TUBE HEAT EXCHANGERS
High-differential-pressure heat exchanger
page 71 NPO-16947

TURBOPROP ENGINES
Unducted-fan engine
page 90 LEW-14429

TURBULENT BOUNDARY LAYER
Experiments in boundary-layer turbulence
page 85 NPO-16754

TURBULENT FLOW
Computer program for flow in a combustor
page 66 LEW-14271

ULTRASONICS
Ultrasonic ranging system with increased resolution
page 44 MSC-21090

WAVEGUIDE ANTENNAS
Waveguide-horn-to-waveguide transition assembly
page 34 MSC-21146

WELDING
Higher-quality weld joints for tube sections
page 97 MFS-29190

WIND TUNNEL WALLS
Calculations of wall effects on propeller noise
page 86 LEW-14516

WIND TUNNELS
Dual-mode laser velocimeter
page 50 ARC-11634

INTERFACE CIRCUIT FOR LASER-DOPPLER VELOCIMETERS
page 42 ARC-11536

WINDMILLS (WINDPOWERED MACHINES)
Hanging windmills from cables
page 89 LAR-13434

WASTE DISPOSAL
Collector/compactor for waste or debris
page 105 MSC-21196

WATER TUNNEL TESTS
Water-tunnel flow visualization with a laser
page 86 ARC-11698

WAVE DRAG
Calculating wave drag on an aircraft
page 66 LAR-13634

X RAY IMAGERY
Lead scales for x-radiographs
page 85 MFS-29247

X-29A AIRCRAFT
Flight research on a forward-swept-wing airplane
page 95 ARC-11740

YON KARMAN EQUATION
Approximate simulation of turbulence
page 53 MFS-28172

Z

W

X

WASTE DISPOSAL
Collector/compactor for waste or debris
page 105 MSC-21196

WATER TUNNEL TESTS
Water-tunnel flow visualization with a laser
page 86 ARC-11698

WAVE DRAG
Calculating wave drag on an aircraft
page 66 LAR-13634

New Products

NTR Systems manufactures ultra-sound measuring instruments. The NP1000 Needlepoint Hydrophone is a miniature ultra-sound field measuring sensor for use in liquid media. The NP1000 has a 1/2" mm aperture and a bandwidth of a 1-20 MHz. It comes equipped with a three foot cable that terminates in a standard BNC connector.

Advertiser's Index

Alsys Inc.	(RAC* 341)	39
Amco Engineering Co.	(RAC 498)	59
Amoco Performance Products .	(RAC 336)	62-63
Astro Met Associates, Inc.	(RAC 484)	6
Automation Gages	(RAC 453)	6
Cadre Technologies Inc.	(RAC 300)	13
Data-Control Systems	(RAC 371)	3
E G & G Photon Devices	(RAC 431)	20
Fisher Pen Company	(RAC 451)	104
Floating Point Systems Inc.	(RAC 399, 401)	31, 33
Fluoramics Inc.	(RAC 455)	12
GAF Corporation	(RAC 404)	29
Gould Inc., Recording Systems Division	(RAC 486)	37
Hamamatsu Corporation	(RAC 471)	69
Hewlett Packard	(RAC 416)	14-15
Iolone Corporation	(RAC 472)	49
Keithley Instruments, Inc.	(RAC 525)	11
Klinger Scientific Corp.	(RAC 368)	7
Lixi, Inc.	(RAC 522)	40
MACSYMA	(RAC 524)	35
Martin Marietta	COV II-1
Martin Marietta recruitment ...	(RAC 440)	107
McDonnell Douglas Corp.	(RAC 372, 501) 73, COV IV	108
Microcompatibles, Inc.	(RAC 389)	108
Micromet	(RAC 523)	18
NEC America Inc.	(RAC 369)	43
Nicolet Test Instruments Div. ...	(RAC 350)	25
NTBM-Research Center	75-78
Panasonic Industrial Company	(RAC 380)	51
Racal Recorders, Inc.	(RAC 397)	21
Rigaku/USA, Inc.	(RAC 513)	45
RR Software, Inc.	(RAC 467)	67
Space Commerce '88	(RAC 514)	95
Supermaterials Company	(RAC 515)	65
Symbolics Inc.	(RAC 446)	26-27
Tektronix Logic Analyzers	(RAC 327)	110-COV III
Texas Instruments	4-5
T. F. Associates	(RAC 409)	19
3M Comtal	(RAC 319)	23
United Technologies	(RAC 394)	8-9
Vitro Corporation	(RAC 394)	41

*RAC stands for Reader Action Card. For further information on these advertisers, please circle the RAC number on the Reader Action Card elsewhere in this issue. This index has been compiled as a service to our readers and advertisers. Every precaution is taken to ensure its accuracy, but the publisher assumes no liability for errors or omissions.

On the wings of the new Sunbird airplane rest hopes of a safer future in aviation. The Sunbird, a two-place training and recreational flyer produced by the Verilite Aircraft Company, a subsidiary of the DeVore Corporation, is the first aircraft initially designed with the drooped leading-edge wing technology developed by NASA's Langley Research Center to provide spin resistance and thereby reduce stall/spin accidents.

"Wing stall is a major concern for aviators," said Paul Stough, Assistant Head of Flight Applications at Langley. "You only have to look at the accident records to see why." Last year, according to the National Transportation Safety Board 234 accidents were due to stalls and subsequent spins, resulting in 139 fatalities—nearly one quarter of the general aviation total.

Spinning begins when the wings stall and one wing drops. Normally when a wing drops, increased angle of attack induces lift, which opposes roll. This is called roll damping. But at an already high angle of attack, as the wing drops, it exceeds its stall angle and loses lift abruptly, sending the plane into a helical descent. If the pilot is flying at a low altitude, he may not be able to recover.

Langley began investigating methods of improving stall/spin departure resistance in the mid-1970's. Part of their effort focused on modifying the wing leading-edge since, as Stough explained, "Its effects can overpower the tail, especially on spin entry." Langley engineers developed drooping extensions for the outboard leading edges. By providing attached flow at the wing tips, the droops improve lateral control at higher angles of attack.

An important feature of the drooped design, according to Long Yip, project engineer of the Langley stall/spin program, is the abrupt discontinuity of the inboard leading edge. Explained Mr.

Flight testing of the Sunbird prototype is underway at Roswell Industrial Air Center in New Mexico. "The Sunbird is a replacement for the FAA Certified light aircraft which are no longer in production by the industry's major manufacturers," said Arnold Robinson, Verilite Vice President.

NASA Tech Briefs, October 1987

Mission **A**ccomplished

The 1/6 scale Sunbird underwent more than 200 tests in Langley's 12 foot wind tunnel.

Yip: "This discontinuity generates a vortex which acts as an aerodynamic fence to stop the spanwise flow from the wing's inboard portion as stall progresses. As a result, the ailerons remain effective and the outer panels continue to exert positive roll damping."

Arnold Robinson, Vice President of Verilite, learned of the droop technology in 1983 and asked NASA to adapt the extensions to the Sunbird design. A 1/6 scale model was fabricated for wind tunnel tests at Langley. The results, said Yip, "gave everyone great confidence in the design." He explained: "We performed oscillation tests without the drooped edges and hit wing lock at 15° near stall. But with the edges on we attained 38° angles before locking."

Flight testing of a 1/4 scale radio

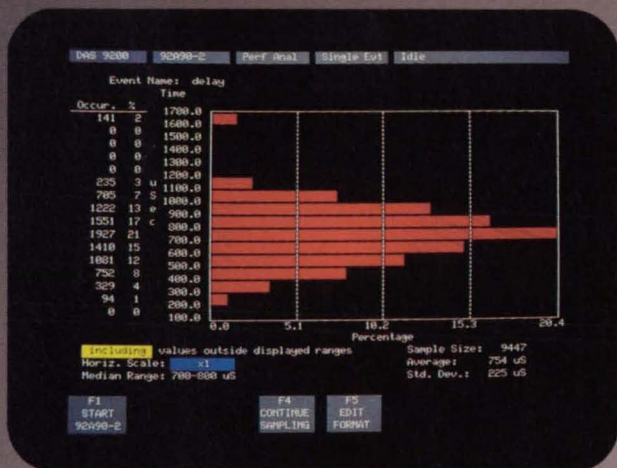
controlled model provided similar success. "With the edges off," stated Yip, "we experienced roll departure near stall. When we put them back on, we were able to do all kinds of maneuvers—recording 28° angles of attack before stall."

The first Sunbird prototype began flying in April of this year. Certification and initial deliveries are slated for early 1989. According to Mr. Robinson, Verilite expects to sell as many as 1000 units per year within the next five years. Target customers include flight schools, small companies, and survey groups.

"Sunbird is just the beginning," stated Yip. "I expect you'll see numerous applications (of the drooped design) on future models. It's an improvement in safety and performance that can't be ignored." □



DAS9200 DIGITAL ANALYSIS: NOW TEK MAKES THE IMPOSSIBLE LOOK EASY.



DAS 9200 92090-2 Display Disasm Idle

Cursor Seq: 14698

Seq	Address	Data	Mnemonic	State
6597	main + 2F7C	4EB9	JSR ser_io	(U)
6791	ser_io + 94	61FC	ESR put_byte	(U)
6871	put_byte + 42	4E75	RTS	(U)
7600	ser_io + 1296	4EB9	JSR delay	(U)
11699	delay + 76	4E75	RTS	(U)
11796	ser_io + 1324	61FC	BSR conn_tst	(U)
11899	conn_tst + 76	4E75	RTS	(U)

DAS 9200 92090-2 Display Disasm Idle

Cursor Seq: 14698

Seq	Address	Data	Mnemonic	State
14697	io_int + 1C0	20FF	MOVL (R7)+,D3	(S)
	0AFB26	0000	(READ)	(S)
	0AFB28	0040	(READ)	(S)
14698	io_int + 1C2	211F	MOVL (R7)+,D4	(S)
	0AFB2A	0000	(READ)	(S)
	0AFB2C	0040	(READ)	(S)
14701	io_int + 1C4	4E75	RTS	(S)

Data: 00000000 00000000 007C0024 00000040 0000000C 00000000 00000000 00000000 00000000 00707C28

Address: 00400006 0020C77B 00000000 00000000 00000000 00000000 00000000 00707C28

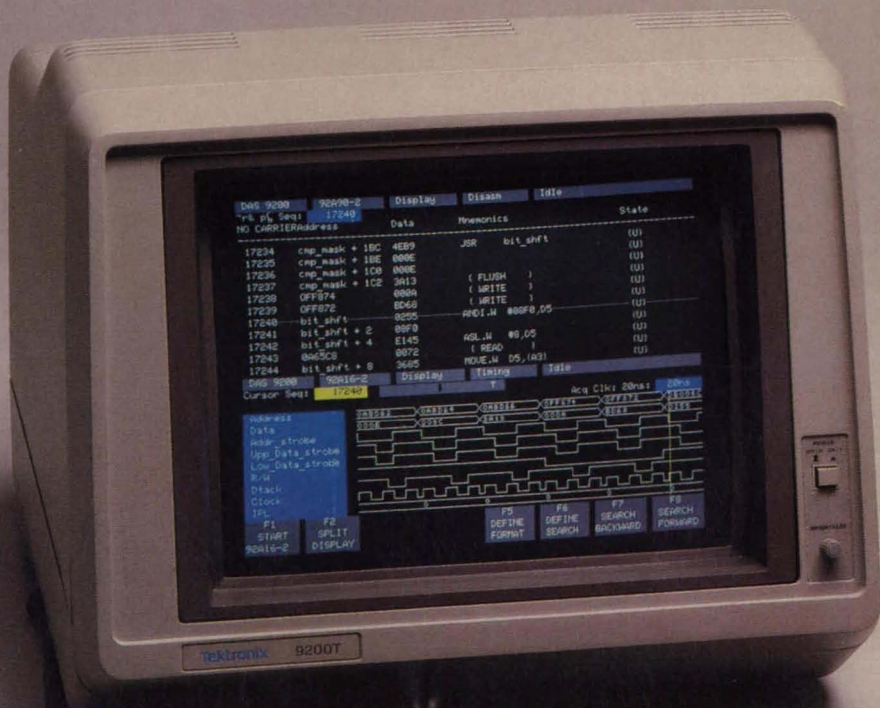
F1 START 92090-2
F2 SPLIT DISPLAY
F5 DEFINE FORMAT
F6 DEFINE SEARCH
F7 SEARCH BACKWARD
F8 SEARCH FORWARD

Software Performance Analysis, like this distribution of a subroutine's execution times, helps you easily understand the activity of your code.

Step backwards through acquired data, including sub-routines, stack and register models, using time-correlated split-screen displays to pinpoint problems.

In every dimension— speed, channel width, memory depth, trigger capability, modularity and ease of use—the DAS9200 dwarfs what's been possible before.

The DAS9200 features a tightly coupled, high-speed architecture in which multiple card modules can act as a single unit. Large color-coded displays, pop-up menus, performance analysis graphs,



multi-tasking and more combine to take logic analysis to levels like these:

1 State-driven triggering at 200 MHz.

You can use up to 384 channels of sync and async data acquisition. You can assure-test high-speed logic at full speed, using 4-level state tracking and high-speed counter/timers. You can monitor and verify all timing measurements in a circuit.

2 Symbolic, real-time software debugging.

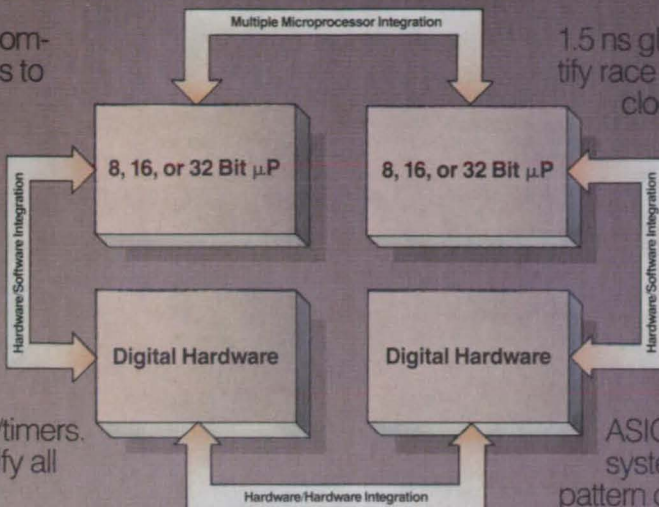
Register deduction and stack simulation let you pinpoint problems like stack overflow or incorrectly restored pointers—without breakpoints or manual notation.

3 Simultaneous integration of up to six microprocessors.

Use the dual timebases and real-time handshaking between system modules to set up split-screens displays that scroll in precise time alignment.

4 160 channels of acquisition at 2 GHz.

Use up to 500 ps sample interval and



1.5 ns glitch detection to identify race conditions, spurious clocks and setup/hold violations in any logic family. System probes feature input capacitance of <1 pf.

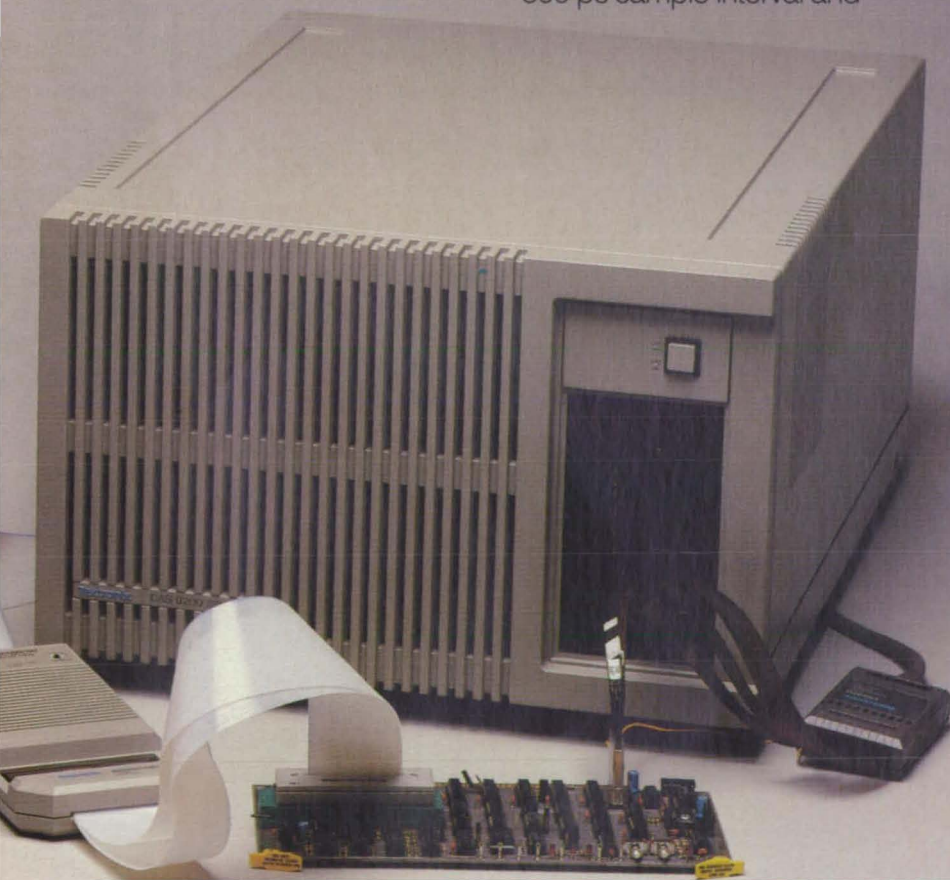
5 Easy ASIC verification at up to 50 MHz.

The DAS9200 is available as a low-cost turnkey ASIC device verification system. Featuring 50 MHz pattern generation, 8K bit vector depth, and 1 ns edge placement, it offers the power, precision and simplicity to be an attractive alternative to centralized systems.

6 Stop wishing for the impossible in digital analysis:

Compare your wish list against the complete list of DAS9200 capabilities. Contact your Tek sales engineer, or call toll-free for more information.

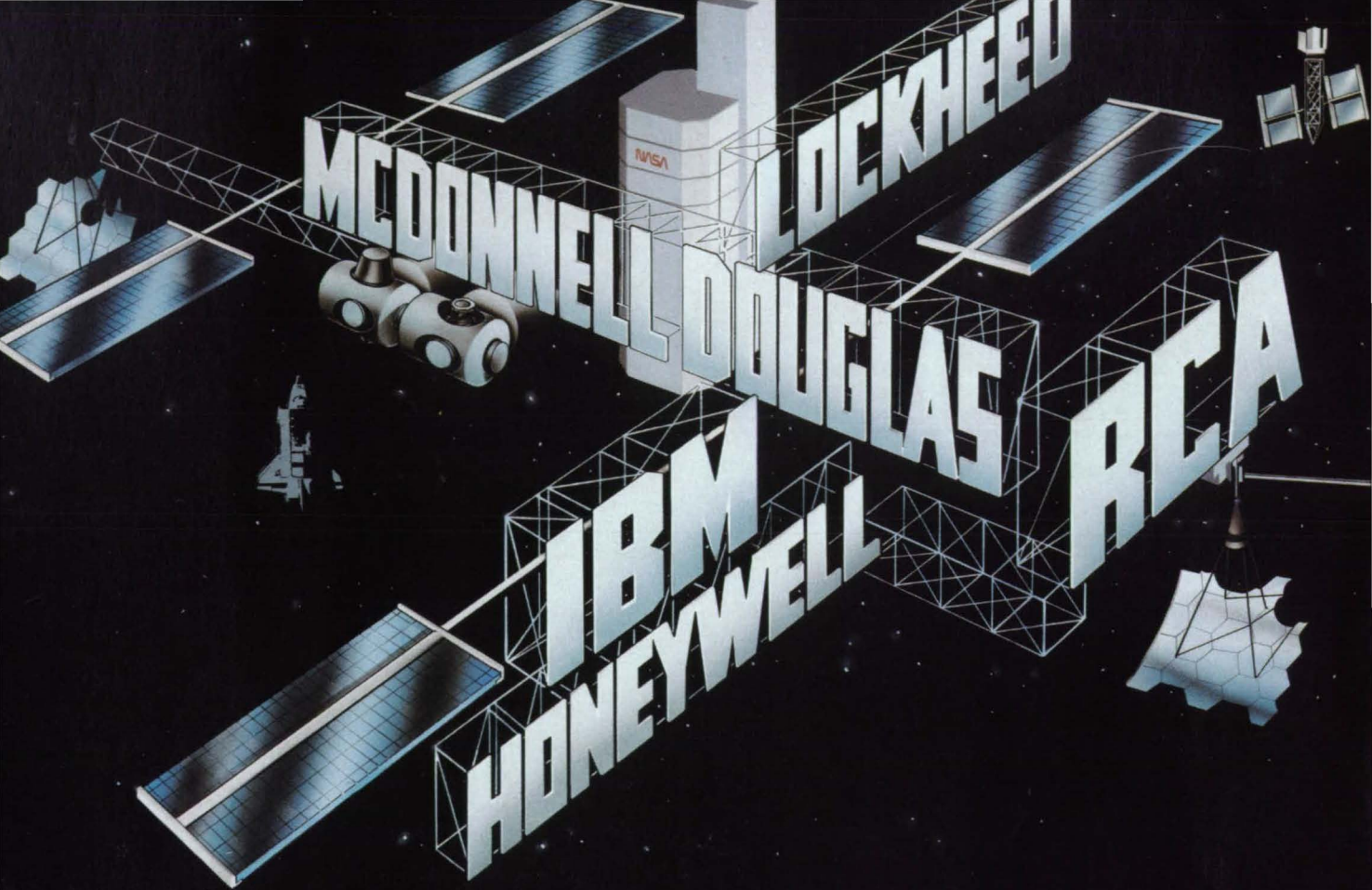
Call 1-800-245-2036.
In Oregon, 231-1220.



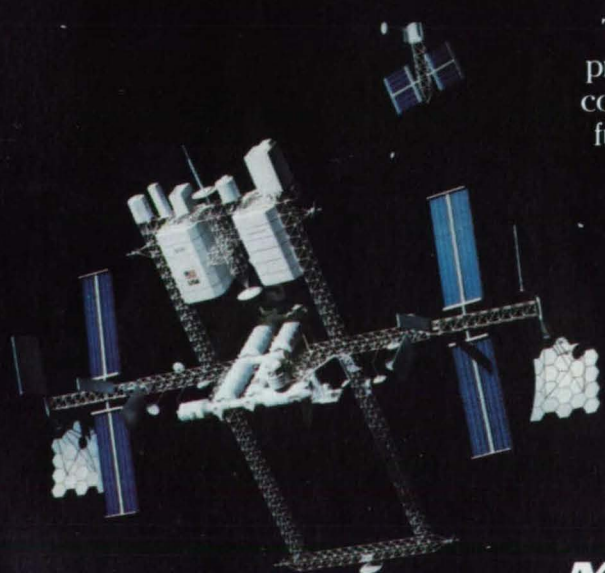
Available in desktop and rack-mount versions, the DAS9200 mainframe can be augmented with up to three expansion mainframes for a total of 28 card slots.

Tektronix
COMMITTED TO EXCELLENCE

Circle Reader Action No. 327



THE FIVE STAR TEAM



To build the best possible space station, you'd probably look for a team of experts to design and coordinate the systems the station would need to function in space. You'd probably want IBM's thinking on computer systems. And Honeywell's solutions on controls. And Lockheed's innovations on EVA and thermal control systems. And RCA's experience with space communications. And you'd want the leadership of McDonnell Douglas to help put your space station together and make it work.

It's easier once you've been there
...and we all have.

MCDONNELL DOUGLAS

Circle Reader Action No. 501